THÈSE DE DOCTORAT DE

L'INSTITUT NATIONAL DES
SCIENCES APPLIQUÉES DE RENNES

ÉCOLE DOCTORALE Nº 601
Mathématiques, Télécommunications, Informatique, Signal, Systèmes, Électronique
Spécialité : *Informatique*

Par
Pierre-Antoine CABARET

Design of multi-actuator haptic devices and rendering methods for navigation and virtual interactions

Thèse présentée et soutenue à Rennes, le 13 décembre 2024
Unité de recherche : IRISA, INSA Rennes
Thèse Nº : 24ISAR 28 / D24 - 28

Rapporteurs avant soutenance :

Jan VAN ERP	Full Professor, University of Twente, Pays-Bas
Thomas PIETRZAK	Professeur des Universités, Université de Lille, France

Composition du Jury :

Président :	Christophe JOUFFRAIS	Directeur de Recherche CNRS, France
Examinateurs :	Jan VAN ERP	Full Professor, University of Twente, Pays-Bas
	Thomas PIETRZAK	Professeur des Universités, Université de Lille, France
Directrice de thèse :	Maud MARCHAL	Professeure des Universités, INSA Rennes, IUF
Co-directrice de thèse :	Marie BABEL	Professeure des Universités, INSA Rennes
Co-encadrant de thèse :	Claudio PACCHIEROTTI	Chargé de recherche CNRS, IRISA, Rennes

REMERCIEMENTS

Tout d'abord, je souhaiterais remercier mes encadrants, qui m'ont donné cette opportunité et m'ont accompagné tout au long de cette thèse. Merci à Maud pour m'avoir poussé du côté de la recherche, à Marie pour avoir toujours été disponible pour discuter, à Claudio pour tous ses conseils.

Merci aussi aux membres du jury d'être venus jusqu'à Rennes et pour leurs nombreuses questions et les discussions qui en ont découlé, et tout particulièrement aux rapporteurs pour avoir pris le temps de relire ce manuscript.

Vient le tour des nombreuses personnes que j'ai pu côtoyer, que ce soit à l'Irisa ou à l'INSA. Merci à Thomas pour toute son aide sur les premiers papiers et expériences, avant et pendant le début de la thèse. Merci aussi à Guillaume pour son aide sur la partie technique.

Un grand merci à Lendy et Erwan, pour toutes les discussions dans nos bureaux, pour toutes les fois où l'on a pu râler ensemble, et puis pour tous ces projets Unity d'Erwan sans qui de nombreuses expériences n'auraient pas été ce qu'elles sont.

Merci à toute la troupe Dornell à l'INSA, à Thomas pour m'avoir fait plonger dans l'impression 3D, à Louise, François, Sébastien, Fabien pour leur aide précieuse dans la conception des nombreux prototypes et expériences. Je pense aussi à toute l'équipe du Lab au pôle Saint-Hélier, grâce à qui on a pu tester ces travaux avec les usagers. Merci aussi à Inès, Antoine, Maxime, Sylvain pour leur aide dans la réalisation de certaines des expériences, et à tous les autres doctorants avec qui j'ai pu partager un bureau.

Je souhaite aussi remercier mes parents, qui m'ont donné les moyens de suivre ma curiosité scientifique tout au long de mes études, et m'ont ainsi permis d'arriver jusqu'ici. Enfin, merci à toi, Emilie, pour ton soutien quand c'était difficile, et pour tout le reste. On l'a fait !

TABLE OF CONTENTS

INTRODUCTION

This manuscript presents the research conducted as part of the PhD thesis entitled “Design of multi-actuator haptic devices and rendering methods for navigation and virtual interactions“. The PhD aims to investigate the use of haptics in handheld interfaces as a mean of providing users with richer and more informative sensations. In particular, our work focuses on multi-actuator vibrotactile interfaces, designed to provide localized sensations. These can benefit users in applications such as haptic navigation and virtual reality interactions.

Context

Haptic navigation assistance

Navigation is part of our daily lives, whether it is for navigating a city, street or building. It is a complex task, mixing perception of our direct surroundings for safely avoiding obstacles and dangers, and a more global perception of our environment to plan an efficient route towards an objective. Nevertheless, according to the World Health Organisation (WHO), between 110 and 190 million people have mobility difficulties.

Technical aids such as wheelchairs, canes, audio guides and GPS can alleviate some difficulties, but do not compensate for all of them. For example, 90% of people with blindness or severe visual impairment still have difficulty moving around outdoors, even with technical aids. Accidents during journeys account for 60% of them, with head impacts and falls linked to collisions with the environment, lack of attention and changes in the environment [Sander 2005]. In addition, 57.7% of wheelchair users have already reported having had an accident. Whether it is a fall, accidental contact, skidding or a dangerous situation, the consequences of these accidents can be numerous and significant for users [Wy 2011]. Besides socio-environmental obstacles, all travel involves safety, location, orientation and information needs that are not always met for people with disabilities [Dejeammes 2008]. Thus, new mobility devices should provide additional information to users, with the aim of compensating for the difficulties associated with travelling.

Guidance during a navigation task provides the user with useful information to help them reach their destination. Nowadays, GPS-based navigation systems are the most common tool for guidance, either for pedestrians or vehicles. These systems typically provide visual and/or auditory feedback to guide users. However, such solutions can be in-adapted or inaccessible in some conditions, such as for people with visual, cognitive or mobility impairments. Indeed, these sensory channels can be overloaded: this could be avoided by using another feedback modality. For several years now, new mobility assistance systems using haptics have been emerging. In clinical research, haptic feedback technologies are also a promising field due to their non-intrusive and discreet nature. In fact, they can provide information and attract the user's attention when other sensory channels are already solicited. In this sense, guidance using haptic stimuli avoids adding information to be processed on the auditory or visual channels, which means they can be used for other tasks. Haptic interfaces for this kind of application take various forms: they can either be integrated into existing devices such as white canes or smartphones, wearable interfaces such as vests or wristbands, or standalone handheld devices. Each form factor has its advantages and disadvantages in terms of feedback accuracy and resolution, bulkiness, etc. Overall, these devices are a great solution but need to be adapted to users' specific needs, which is often hard to do.

Enhanced haptics for virtual interactions

Virtual Reality (VR) can be defined as the technologies that allow to simulate virtual environments in which users can be immersed and can interact [Fuchs 2006]. In the context of this thesis we focus on head-mounted displays (HMD), which are now the most common way to experience immersive VR experiences. Such displays provide both visual and audio feedback and have been combined with various haptic displays over the years. However, haptic feedback for VR is often focused on single specific interactions or sensations [Culbertson 2018], and the design of devices capable of rendering rich and realistic touch in a variety of interactions is a relatively recent development in the field [Wang 2020].

Developments in the latest generation of gaming peripherals also show an interest in enhanced and localized haptic feedback. For instance, the Nintendo Switch and Playstation 5 have moved away from the Eccentric Rotating Mass (ERM) actuators usually found in controllers and have opted to use Linear Resonant Actuators (LRA) or voice coils placed on either side of the controller. VR could also benefit from these enhanced haptic sensations, which requires the design of adapted haptic interfaces and rendering techniques.

The Dornell project

This thesis takes part in the Dornell project, funded by Inria. The project is a collaboration between Inria teams of Rennes, Paris, Bordeaux and Nancy, Institut des Systèmes Intelligents et de Robotique (ISIR), Institut des jeunes aveugles – Les Charmettes, and Pôle de Médecine Physique et de Réadaptation St Hélier. Dornell encompasses multiple objectives, with the overarching goal of creating a multisensory and customizable haptic handle to assist users of mobility assistance devices in navigation tasks. The handle could, for instance, provide guidance or help with obstacle avoidance. To do so, the project explores the use of multiple sensory modalities to provide information, designing handles that can be adapted on different mobility devices, including wheelchairs and walkers (see Figure 1). Innovative materials and 3D printing techniques are also explored, in order to create customizable handles with integrated sensors to detect users' intentions or status.

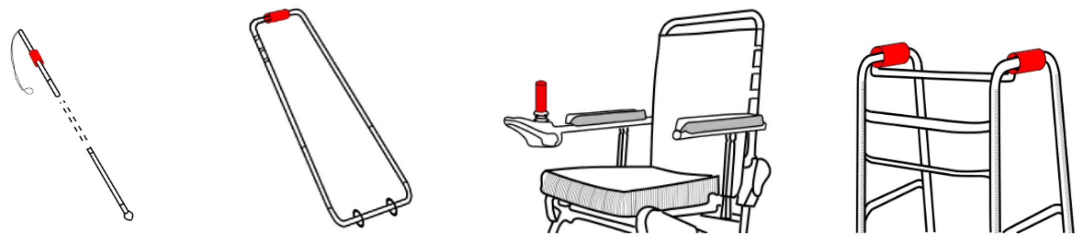

Figure 1: The envisioned application of the Dornell project: a haptic handle that would adapt to various existing mobility assitance devices (here a white cane, precane, power wheelchair and walker).

In this context, we are trying to address these challenges with a user-centred approach, involving users and clinicians in the design and evaluation processes. In early stages of the project, a needs assessment was also carried out with clinicians and potential users to better understand the motivations and interogations towards the envisioned device. Both populations expressed interest in the concept of the device, which could prove useful for navigating unfamiliar spaces or indicating obstacles. Some concerns were raised about getting used to the vibrations and understanding the vibrotactile signals while moving or driving, The rhythmic aspect of the vibrations was also considered relevant for users with Parkinson's disease. Overall, learning was considered necessary, but it was also accepted by all, as long as it offered an advantage in terms of autonomy or safety. This initial assessment suggests a number of important research questions for the Dornell project, some of which we attempt to answer in this thesis.

As part of this project, our research investigates the design of a handle that would display localized sensations, and the ways these sensations could be used to provide navigation information. Doing so, we use VR for our first exploration of multi-actuator feedback and as a platform to experiment with navigation using the device in virtual environments.

The objectives of this PhD are the following. First, it aims to design and develop handheld devices capable of delivering precise, localized sensations within the user's hand. Second, it seeks to create novel rendering techniques that effectively leverage these localized sensations, allowing for more immersive and intuitive feedback in various applications. Finally, the thesis explores the application of these devices in navigation contexts, investigating how they can improve spatial awareness and directional guidance.

Scientific challenges & contributions

Challenges

In the context of this PhD, we identified three underlying scientific challenges at the interface between haptics, VR and navigation. These challenges revolve around the design of handheld interfaces providing enhanced haptic sensations. These could benefit both VR interactions and navigation assistance, provided that rendering techniques capable of leveraging these sensations are developed.

I. Providing enhanced haptic feedback in handheld interfaces. Given the complexity and spread of the sense of touch, haptic interfaces focus on the stimulation of a limited area of the body, as well as a specific set of sensations to provide. In the case of handheld interfaces, they target a small yet highly sensitive area of the body. Combined with their limited volume in which to house haptic actuators, providing enhanced haptic sensations is thus especially challenging for this type of device. There are several ways to approach this challenge. On the hardware side, new devices can be created, exploring combination of actuators that provide complimentary sensations for multisensory feedback, or exploring the design of higher-resolution haptic displays, both in number and fidelity of actuators. Algorithms controlling these actuators can also rely on our tactile perception to create enhanced sensations, such as by leveraging sensory illusions to virtually create additional stimulus location or create sensations of movements.

II. Designing rich, multisensory interactions in virtual reality. With the development of higher fidelity haptic devices comes the need for designing rendering techniques that take full advantage of their capabilities. When manipulating an object in a virtual environment, for instance, algorithms have to be created to generate haptic sensations based on user interactions and object physical properties. Such sensations must be generated seamlessly and be realistic in order to enhance the user's experience. For multisensory interactions, this is especially challenging as each feedback modality has to be appropriately modelled. In this case, synchronicity of the different feedback modalities is also crucial. Beyond physical interactions, haptic devices can also be used to convey more abstract forms of information. For instance, haptic feedback could be employed to guide user's attention or to communicate complex data in innovative ways. As new rendering schemes are created, they must also be evaluated, whether in terms of realism, task performance or immersion. Assessing their impact on user's experience will ensure that they can provide benefits in practical applications.

III. Developing accessible, intuitive and personalized haptic navigation assistance solutions. Haptic navigation devices have been developed over the years, usually targeting specific groups of individuals. These interfaces often come with their own way of providing feedback, to which users have to adapt to and learn to use. In order to be easy to use by a large range of users, new haptic navigation devices should be customizable. First, the interface should adapt to users physically, by taking into account their morphology (for instance, the size or shape of the hand for handheld interfaces) and the context in which they are used, such as when used in combination with existing mobility devices. Secondly, the haptic sensations should also adapt to users by being customizable, allowing users to choose what information are displayed, as well as how and when. To do so, the design of different navigation techniques must be explored in order to find which ones are effective, whether they can be customized, and if so, to what extent they might be.

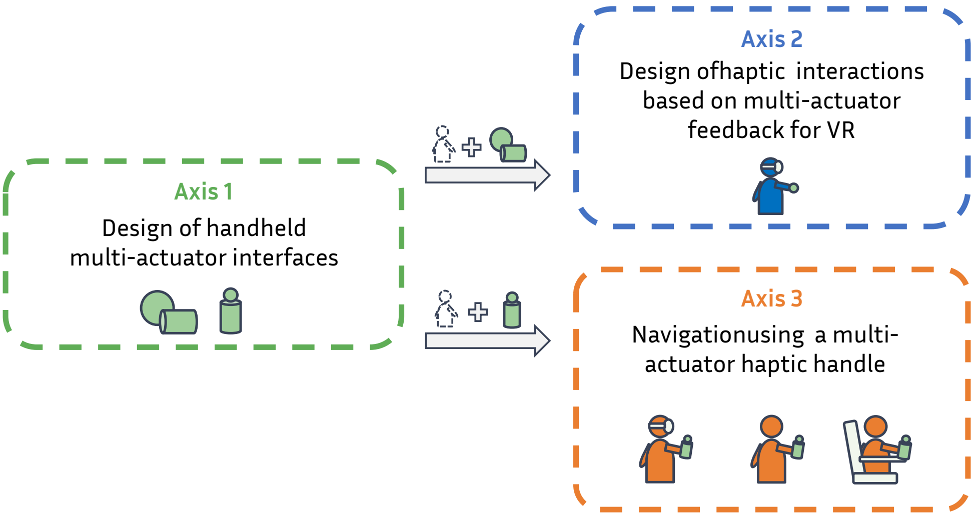

Figure 2: Our research articulates around three axes, addressing parts of the research challenges discussed in this section. In green, our first research axis focuses on the design of handheld multi actuator-interface. Our two other axes build upon the prototypes that were developped: in blue, our second axis investigated the design of haptic interactions based on multi-actuator feedback for VR. Finally, in orange, our third axis explores the use of a multi-actuator haptic handle for navigation.

Contributions and outline

Our research is thus structured around three axes, targeting more specific objectives under these three challenges. Our main contributions, denoted as Ci, are overviewed below, and represented in Figure 2 as part of our three axes.

Axis 1: Design of handheld multi actuator-interface. Within this axis we explore the use of multiple vibrotactile actuators within handheld interfaces. We first explore the combination of tangible props (i.e., passive, physical objects used to represent virtual objects) with a varying number of vibrotactile actuators. With these prototypes, we investigate the feasibility and limitations of the approach, assessing how many vibration location can be stimulated and how many actuators are needed to do so (C1). As vibration propagation limits the clarity of the feedback provided by vibrotactile interfaces, we then propose to use 3D printing of soft materials to create an isolating structure within a handheld devices (C4).

Axis 2: Design of haptic interactions based on multi-actuator feedback for VR. In this second axis, we explore the use of the multi-actuator vibrotactile prototypes we developed to provide enhanced haptic feedback in VR. We investigate the benefits of multi-actuator rendering schemes in combination with passive haptics on a set of VR manipulation tasks (C2). We also look further into impact rendering, using vibrations to provide more detailed information about impact direction and distance to users (C3).

Axis 3: Navigation using a multi-actuator haptic handle. As part of this third axis, we focus on using our isolated haptic handle in navigation applications. We first investigate its use to provide in-hand spatial awareness of obstacles in a virtual setting (C5). We then propose a set of navigation techniques based on localized vibrotactile cues to guide users while walking (C6). In an effort to investigate the use of the handle in combination with a power wheelchair, we investigate the impact of feedback location between the dominant driving hand and the non-dominant free hand (C7). Finally, we conduct a pilot user study with regular users of power wheelchair, evaluating the impact of our navigation system on driving as well as assessing its usability and acceptability (C8).

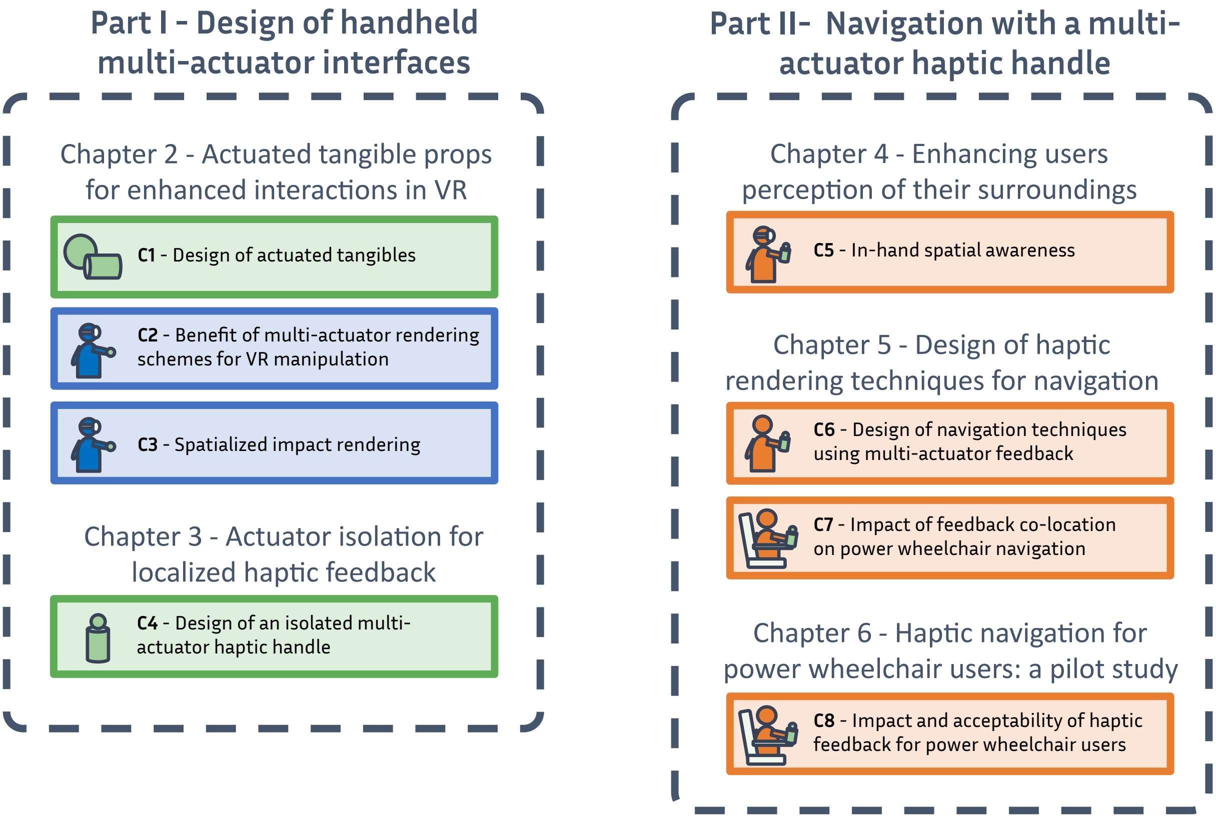

Figure 3: This manuscript is divided into two parts, each covering a selection of our contributions: Part I covers the design of multi-actuator handheld interfaces and their use in VR. Part II is focused on navigation application using our custom multi-actuator haptic handle. Contributions are represented using the colors of our three research axes, as illustrated in Figure 2.

The remainder of this manuscript is structured around these contributions, summarized in Figure 3.

Chapter 1 first presents the related work in the design and use of haptic devices for VR and navigation. After an overview of haptics in general, the use of haptics for providing navigation feedback is discussed, reviewing a selection of devices designed for this application for both pedestrians and users of mobility assistance devices. Then, we go over the use of haptic rendering for VR interactions, overviewing the different properties or information that haptic cues can provide in virtual environments. Continuing, we discuss multi-actuator haptic devices in more depth, focusing on the design of devices which display localized sensations in a handheld format.

The following chapters are divided into two parts. First, **Part I** focuses on the design of multi-actuator vibrotactile interfaces and associated rendering schemes.

In **Chapter 2**, we explore the combination of tangible props with a varying number of vibrotactile actuators for providing richer feedback in VR manipulation. We investigate the use of up to five actuators in a spherical object for VR manipulation, evaluating users' ability to discriminate localized sensations through user studies. We then propose a set of rendering schemes for various interactions in VR, and assess their benefit over traditional, monolithic feedback for object manipulation. Finally, we evaluate further the effectiveness of this approach with a two-actuator handle for rendering enhanced feedback of localized impacts.

Chapter 3 follows our investigation of multi-actuator feedback, this time with the objective of providing clearer, distinct in-hand localized vibrations. After discussing some design iterations, we introduce a deformable 3D printed structure for isolating the vibrations of four motors around a custom handle. We evaluate the benefits of this design in a vibrometry study, comparing the proposed version to a rigid structure. A set of perception studies is also conducted to evaluate the distinct perception of vibrations by users and the use of directional patterns.

Part II then addresses the use of our isolated haptic handle, focusing on its use for navigation.

In **Chapter 4**, we propose to augment the user's spatial awareness in VR using an in-hand haptic representation of their surroundings. Through human subjects studies, we evaluate the use of two directional haptic patterns, assessing their ability to help users avoid dynamic obstacles in VR, and evaluating the influence of this haptic representation of the personal space on static obstacle avoidance.

Chapter 5 discusses the design and experimental evaluation of haptic rendering techniques for navigating using localized vibrotactile stimuli provided by our haptic handle. We present two haptic rendering schemes combined with three navigation strategies which we evaluate in a user study, guiding walking participants along a set of paths. In an effort to combine our haptic interface with existing mobility assistance devices, we evaluate its use for navigation with a power wheelchair. Specifically, we investigate the effect of the co-localization of the haptic feedback with the joystick that controls the wheelchair, comparing navigation performance with the delocalization of the haptic handle in the non-dominant hand.

In **Chapter 6** we evaluate the use and acceptance of our haptic guidance system in a study with regular users of power wheelchairs, in collaboration with clinicians of the rehabilitation center of Pôle Saint Hélier in Rennes. We evaluate the use of two rendering schemes in a set of two experiments, evaluating the perception of feedback provided by the haptic handle in a static task and their use in a dynamic navigation task.

Finally, **Chapter 7** concludes this manuscript, summarizing our findings and discussing perspectives for future work.

LIST OF PUBLICATIONS

Journals

- P-A. Cabaret, T. Howard, G. Gicquel, C. Pacchierotti, M. Babel and M. Marchal. "Does Multi-Actuator Vibrotactile Feedback Within Tangible Objects Enrich VR Manipulation?". *IEEE Transactions on Visualization and Computer Graphics*, vol. 30, no. 8, pp. 4767-4779, Aug. 2024

International conferences

- P-A. Cabaret, T. Howard, C. Pacchierotti, M. Babel and M. Marchal. "Perception of spatialized vibrotactile impacts in a hand-held tangible for virtual reality". In *EuroHaptics 2022*

- P-A. Cabaret, C. Pacchierotti, M. Babel and M. Marchal. "Design of Haptic Rendering Techniques for Navigating with a Multi-Actuator Vibrotactile Handle". In *EuroHaptics 2024*

- P-A. Cabaret, A. Bout, M. Manzano, S. Guégan, C. Pacchierotti, M. Babel and M. Marchal. "Multi-actuator Haptic Handle Using Soft Material for Vibration Isolation". **Best Poster Honorable Mention.** In *EuroHaptics 2024*

- I. Lacôte, P-A. Cabaret, C. Pacchierotti, M. Babel, D. Gueorguiev and M. Marchal. "Do Vibrotactile Patterns on both Hands Improve Guided Navigation with a Walker?". In *EuroHaptics 2024*

National conferences

- P-A. Cabaret, C. Pacchierotti, M. Babel and M. Marchal. “Conception d’une poignée haptique multi-actionneurs pour l’aide à la navigation”. In *Handicap 2024 - 13e conférence de l’IFRATH sur les technologies d’assistance*

WIP/Demo

- P-A. Cabaret, C. Pacchierotti, M. Babel and M. Marchal. “Soft Material for Multi-Actuator Isolation in a Haptic Handle”. *WorldHaptics 2023*

CHAPTER 1 RELATED WORK

In this chapter, we present a review of the literature on haptics and their applications in the context of virtual reality (VR) and navigation. We first present a general introduction to the haptic sense and haptic technologies, before going over the design and use of haptic devices for navigation and VR interaction. Finally, we discuss multi-actuator interfaces in more details before concluding, highlighting current limitations that motivate the work conducted during the thesis.

1.1 Overview of haptics

In this section, we present a general overview of haptics, with the tactile system and the general classification of haptic devices.

1.1.1 The tactile system

Haptics, which refer to the sense of touch [Oakley 2000], enable humans to perform actions and interact with their environment. Indeed, without haptics, the simplest tasks such as grabbing a cup would become much harder. We rely on touch to perceive the shape, weight, friction and temperature of objects, among other relevant properties. Haptic sensations are typically divided into two categories, namely, kinesthetic and tactile sensations [Culbertson 2018; Oakley 2000]. Kinesthetic sensations refer to information of forces and torques, perceived by our muscles, tendons and joints, while tactile sensations encompass information perceived by nerve endings embedded in our skin, which are called *mechanoreceptors*. Such sensations include pressure, skin deformation or vibration.

There are four main types of these tactile receptors [Johansson 1978; Johansson 2008],

Receptor type	**Meisnerr**	**Pacinian**	**Merkel**	**Ruffini**
Adaptation rate	Fast	Fast	Slow	Slow
Location	Shallow	Deep	Shallow	Deep
Stimuli	Deformation, low-frequency vibration	High-frequency vibration	Sustained pressure, low-frequency vibration	Skin-stretch, pressure
Density (afferends per cm^2) 0 140				

Table 1.1: Mechanoreceptors characteristics in the hand. Adapted from Johansson 2009; Vizcay 2022.

each with different properties (see Table 1.1). Understanding the specific functions of these mechanoreceptors is essential for designing effective haptic devices, as each receptor type responds to different tactile inputs. Two types of fast-adapting mechanoreceptors, termed fast-adapting type I (FA-I) and type II (FA-II), are sensitive only to dynamic changes in skin stimulation, such as when making or breaking contact, or during vibration. The two other types, being slow-adapting type I (SA-I) and type II (SA-II), are sensitive to sustained skin deformation. Type I and type II differ by their location and size in the skin. Type II receptors have large receptive fields and located deeper into the skin than type I which have small, well-defined receptive fields. Across the human hand, the density of type I receptors is highest at the fingertips, while the density of type II is more uniform. On the rest of the body, some areas are more sensitive than others: the glabrous skin is indeed more densely populated with mechanoreceptors than the hairy skin. These different characteristics make the mechanoreceptors sensitive to different tactile sensations:

- Meissner corpuscules (FA-I) encode light touch sensations with a high resolution;
- Pacinian corpuscules (FA-II) are sensitive to high frequency vibrations;
- Merkel cells (SA-I) encode static deformation and deformation changes of lower frequencies;
- Ruffini endings (SA-II) are sensitive to skin-stretch and continuous pressure.

1.1.2 Haptic devices

Artificially generated haptic sensations have been researched for various applications: replacing a lost sense, providing additional information for teleoperation, or enhancing human-computer

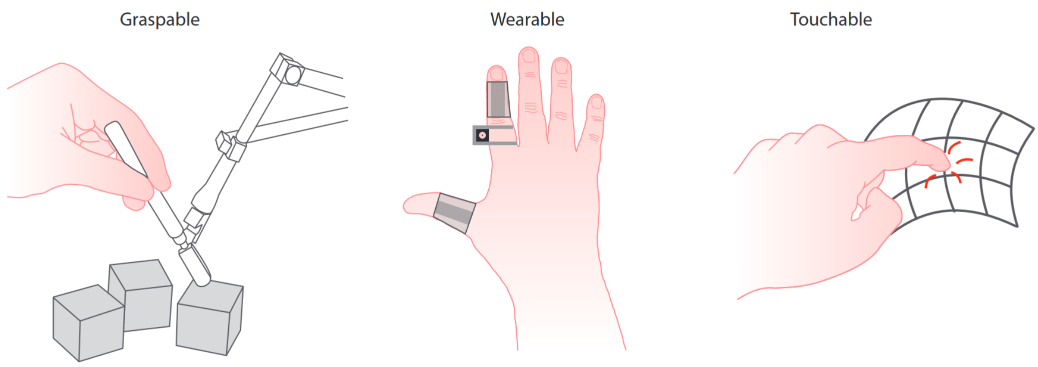

Figure 1.1: Haptic devices can be categorized between graspable, wearable and touchable devices. Graspable devices are handheld or grounded tools, wearable devices are attached directly to the user's body, and touchable systems are tactile surfaces. From Culbertson 2018.

interaction. All applications have one thing in common: a device is needed to generate haptic sensations to the user.

Haptic devices can be divided into kinesthetic and tactile devices depending on the type of feedback they can deliver. However, this distinction becomes blurry as new multisensory devices appear, sometimes providing both types of cues. We thus prefer to use the categories proposed by Culbertson et al., who classify haptic devices into three major categories: graspable, wearable and touchable systems (see Figure 1.1) [Culbertson 2018].

Graspable devices can either be handheld or grounded, with an end effector for users to interact with. Grounded devices accounted for a large part of the literature, with the most known examples being force feedback arms such as the Phantom haptic interface [Massie 1994]. Such grounded force feedback devices offer powerful force feedback, but are quite complex, large and have a limited operating space. On the other hand, handheld haptic devices are more focused on tactile feedback and can be more easily moved by users, at the cost of occupying the hand.

Wearable devices directly fit the user's body in order to provide haptic sensations, be it on their hands, arms, torso or any other part. Haptic gloves and exoskeletons are one of the main types of wearable haptic devices, usually providing force-feedback to the whole hand, sometimes in combination with tactile actuators. However, providing kinesthetic cues in this way often comes at the cost of a large and heavy form-factor. Readers can refer to the review from Wang et al. which focuses on wearable haptic gloves and their different actuation mechanisms [Wang 2019b]. Another approach is the use of smaller, lighter wearables devices focusing on providing tactile sensations such as vibrations or skin stretch using haptic actuators placed on the fingers, on a belt or bracelet. Such devices can be combined in different locations, and offer users more freedom than grounded devices. Pacchierotti et al. give an extended review of wearable devices focusing on the fingertips and the hand [Pacchierotti 2017].

Touchable devices are tactile displays that enable users to explore a surface using touch. They usually display different surface properties such as roughness, texture, shape, temperature, etc. Smartphones can be considered as the most common example of touchable devices, providing haptic feedback through vibrations when touching the screen.

In the context of this thesis, we are mostly interested in handheld and wearable devices, which are more fitted for navigation and VR applications where users must be able to move freely [Kappers 2022; Pacchierotti 2017]. We review and discuss devices designed for both of these applications in the following sections, respectively section 1.2 and section 1.3.

1.2 Haptics for navigation

Navigating complex or unfamiliar environments presents daily challenges, particularly for individuals with disabilities. Haptic devices offer a promising solution by providing sensory feedback for safe and efficient navigation. Nowadays, smartphone applications serve as the predominant mean for wayfinding, using GPS to display location data on screens, sometimes combined with audio guidance. However, for individuals with disabilities, impairments or those using mobility aids, auditory or visual information might not be a suitable choice. In such cases,haptic feedback offers an alternative method for guiding users. Indeed, as the haptic modality remains usually unengaged, providing haptic navigation information avoids interference with already overstimulated visual or auditory cues. Effective navigation requires instructions that users can quickly and easily interpret. Thus, one of the challenges of using haptic feedback for navigation is to find rendering schemes able to provide necessary information while staying easily understandable.

In this section, we first review a selection of haptic devices designed for such applications, which employ a range of different haptic modalities to convey information. Secondly, we discuss their use in the specific case of users with disabilities.

1.2.1 Haptic devices for navigation

Kappers et al. published two surveys on haptic navigation devices for “actual walking”, focused on handheld [Kappers 2022] and wearable devices [Kappers 2024]. The selection of haptic devices in these reviews focused on ones that targeted pedestrian navigation in the real world. Thus, devices that were evaluated in virtual environments or that provide other types of information such as collision avoidance feedback were not discussed. In this section, we overview a broader selection of haptic devices which we found relevant for providing navigation feedback, be it for guidance or obstacle avoidance. This includes some devices that were designed for or evaluated in virtual environments, or prototypes that were only evaluated in preliminary studies. We discuss these devices based on the types of haptic feedback they rely on to provide information to their users.

Vibrotactile feedback

Vibrotactile feedback is by far the most popular haptic modality, and its use for navigation is no exception. In this case, specific vibration patterns such as tactons (tactile icons) [Brewster 2004; Krauß 2020] can be used to encode different information, using location, rhythm or intensity.

Some devices rely on a single source of vibrations to provide information to the user. The "pocket navigator" [Pielot 2010], for example, is a handheld device that uses sequences of short and long vibrations to guide the user: the relative length of the two vibrations encodes the direction, and the duration of the longest pulse encodes how much the user should turn (see Figure 1.2A). Similarly, "NaviRadar" [Rümelin 2011] uses a radar metaphor: a regular pulse indicates the front direction, while a second one indicates the direction to follow. The timing between the two corresponds to the angle of the turn that the user must take. Additionally, the proximity of the turn is encoded on one of the parameters of this second vibration, between intensity, roughness or a number of pulses.

Other devices that also use a single actuator rely on the user actively moving the device around. This is the case of the "Stravigation" [Kawaguchi 2012], a hand-held device that lets the user scan the surrounding environment with it (see Figure 1.2B). The device vibrates when pointing towards the target, with the vibration frequency encoding the angular deviation (i.e., frequency is higher when in the correct direction). When not actively pointing around, the device informs the user about the distance to the target using the same encoding. A similar approach modulated the feedback depending on the number of possible routes when looking around (i.e., guidance was more precise when only one path was available), in the objective of giving more freedom to users [Robinson 2010].

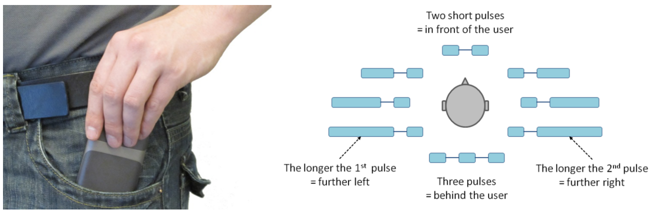

(A) Pielot 2010

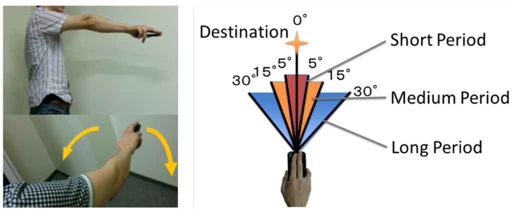

(B) Kawaguchi 2012

Figure 1.2: Examples of single-actuator handheld devices. Here, both the "Pocket Navigator" (A) and the "Stravigation" (B) use a smartphone as the base of the device.

Thanks to their small size, multiple vibrotactile actuators can be embedded into handheld interfaces. We discuss some examples of multi-actuator vibrotactile devices as part of this section, but we go more in depth into their design in section 1.4. Having multiple actuators can serve multiple purposes, such as providing more than one information or using more intuitive patterns for communicating to the user. With the “Haptic cricket”, Spiers et al. evaluated a handheld cube with three stimulation points (front, left and right of the cube, see Figure 1.3A) for providing two information simultaneously [Spiers 2016]. The front actuator encoded proximity to the target, while the actuators on the sides encoded the heading error, all using the intensity of the vibration to encode the information. When integrated in the handle of an existing mobility device such as a white cane (see Figure 1.3B), different vibration sources can be linked to different proximity sensors, each providing the distance to an obstacle in a direction [Pyun 2013; Wang 2012].

Multiple points of stimulation can also be used to create sensory illusions. “T-Mobile” used a 3 × 4 array of vibrating panels on the back of a smartphone (see Figure 1.3C) to display different vibration patterns using two sensory illusions, somatosensory saltation and phantom sensations [Yang 2010]. Apparent motion can be displayed on flat surfaces, but also on curved ones as shown by Lacôte et al., which explored the use of this principle to convey directional cues on one or two handles (see Figure 1.3D) [Lacôte 2023].

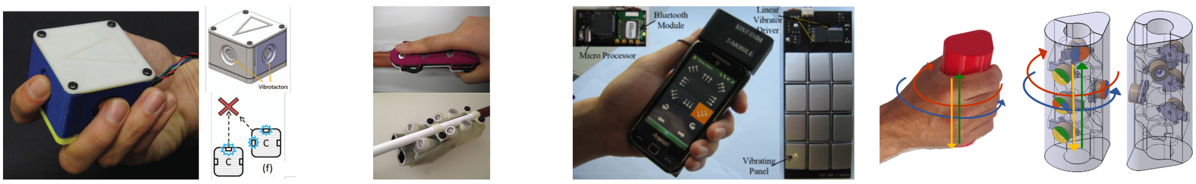

(A) Spiers 2016 (B) Pyun 2013 (C) Yang 2010 (D) Lacôte 2023

Figure 1.3: Examples of multi-actuator handheld devices. (A) The ‘Haptic cricket”, a handheld cube with three actuators on its sides; (B) A white cane detecting obstacles at different height levels, each linked to an actuator; (C) “T-Mobile”, a smartphone with an array of vibrating panels; (D) A haptic handle providing in-hand apparent motion using five actuators.

Wearables also benefit from the use of several actuators, in which case they rely on the location of haptic sensations in the user referential to convey directional feedback. Haptic gloves, for example, have been used to guide the hand of users in 3D space (see Figure 1.4A) [Günther 2018]. In this case, up to 10 actuators placed over the hand were used with push and pull metaphors to guide users, with the pull metaphor being preferred. For pedestrian navigation, haptic belts have been proposed to provide localized cues around the waist. Actuators can be used once at a time or simultaneously at fixed or interpolated intensities to display varying numbers of directions around users [Gay 2020; Heuten 2008]. Similar principles can be applied by placing actuators directly on the skin [Saint-Aubert 2020] or with various wearable form-factors such as bracelets [Devigne 2020; Dobbelstein 2016; Hugues 2015], vests [Bajpai 2020; Monica 2023] or even collars [Schaack 2019] (see Figure 1.4B and 1.4C).

(A) Günther 2018. (B) Dobbelstein 2016. (C) Bajpai 2020.

Figure 1.4: Examples of wearable multi-actuator devices. (A) A haptic glove with ten actuators used for hand guidance; (B) A haptic wristband; (C) A haptic belt with five actuators on the front of the user.

Skin stretch & pressure feedback

Skin deformation is another interesting modality for providing navigation feedback. Skin stretch, in particular, can be directly and easily linked to a direction. Aizawa et al. propose a handheld device with a sliding plate on which the thumb is placed, able to move in eight different directions (see Figure 1.5A) [Aizawa 2021]. Skin stretch can also be used on a non-planar surface: as an example, "HapticPole" is a handheld cylinder with a rotating ring, which can guide users by stretching the skin of the palm and ring finger (see Figure 1.5B) [Wiehr 2023]. A similar principle was also used on the handle of a walker, with a rotating wheel providing forward and backward directions [Pan 2018].Wearables also use this modality: skin stretch around the waist was used to keep a visually impaired runner in its lane (see Figure 1.5C) [Kayhan 2022], on the arms to provide guidance (see Figure 1.5D) [Barontini 2021; Chinello 2018; Yoon 2017], or even on the forehead [Kuang 2022].

Pin-displays can provide pressure sensation, usually under the fingertip. For instance, a pin display on the handle of a white was used to display the distance to an obstacle, increasing the frequency of pins movement as distance decreased [Obermoser 2018]. Using a denser pin-array, tactons (tactile icons) can be designed to provide more diverse feedback and be used to provide directions [Pietrzak 2009].

Thermal feedback

Thermal feedback is a less popular modality for navigation, as temperature is detected slower than other tactile sensations. Actuators also suffer from a certain latency, combined with the need for the skin to cool down or heat up after being stimulated. Still, some devices were proposed using hot or cold sensations. "Heat-Nav" is a wearable array of three thermal "cells" on the forearm (see Figure 1.6A) [Tewell 2017]. It was used to guide users in a virtual maze

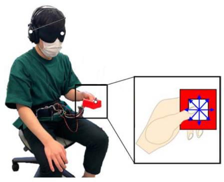

(A) Aizawa 2021

(B) Wiehr 2023

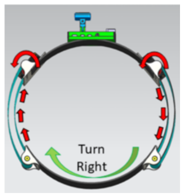

(C) Kayhan 2022

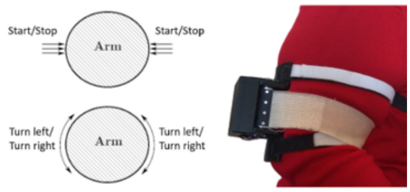

(D) Barontini 2021

Figure 1.5: Examples of skin-stretch devices. (A) A handheld with a sliding plate for diaplying directions; (B) A handle with a rotating ring, stretching the skin of the user's palm; (C) A haptic belt providing skin-stretch to the waist; (D) A skin-stretch armband.

on a screen, using a "hot and cold" guidance, where the device cools down when the user walks away from the path and warms up when getting back on track. While effective in this context, this approach is not really suited for real-life navigation as it requires trial and error to make progress along the path. "ThermalCane" is a white cane with four flexible peltier modules on its grip [Nasser 2020]. Different actuator configurations were tested with three to five modules (see Figure 1.6B). Cold sensations were easier to perceive and used to indicate the four cardinal directions, while a warm sensation was used to signal a danger. The device was compared to its vibrotactile equivalent, showing better discrimination results but similar performance in navigation.

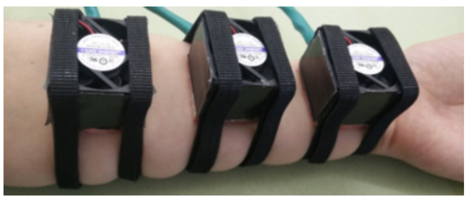

(A) Tewell 2017

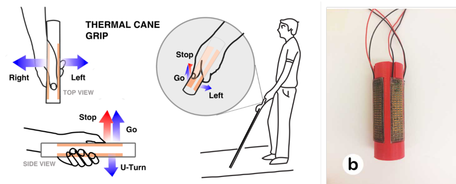

(B) Nasser 2020

Figure 1.6: Examples of thermal devices. (A) A wearable array of three thermal modules; (B) A white cane with four thermal modules.

Force/Torque feedback

Force-feedback is probably one of the most fitted haptic modalities for guidance, as it can effectively provide motion cues to the user. However, most force feedback devices are grounded, and thus inadapted for navigation without a vehicle of some sort to carry and power the device. For example, Devigne et al. used a force-feedback joystick in place of the regular joystick on a power wheelchair equipped with proximity sensors (see Figure 1.7A) [Devigne 2018]. The force feedback was used to correct the user input, guiding it to a joystick position that was safe from collisions. Hashimoto et al. proposed to use a force feedback joystick in a different way, mounting it on an walker (here, some sort of mobile platform) [Hashimoto 2006]. The joystick was not moving the walker, instead it allowed the user to explore their surroundings, feeling the walls and obstacles.

Handhelds can still provide force-feedback to some degree. As an example, Hemmert et al. proposed to use a shifting weight inside a handheld interface to provide guidance (see Figure 1.7B) [Hemmert 2010a]. Amemiya et al. explored the use of asymmetric acceleration to produce sensations of pulling forces in different handheld interfaces. Early version used a large, single degree of freedom mechanism which was then extended to two dimensions (see Figure 1.7C) and evaluated in a navigation task in a simple maze [Amemiya 2005; 2009]. A more compact version using vibration actuators was also developed [Amemiya 2014]. A similar principle was used with "Force-Blinker" with a rotating mass within a handle, with the goal of integrating the device in a white cane [Ando 2012]. Maeda et al. used the same principle of pseudo-force with two voice coil actuators placed between the thumb and index, which was shown more intuitive than simple vibrations in a simple navigation study (see Figure 1.7D) [Maeda 2024].

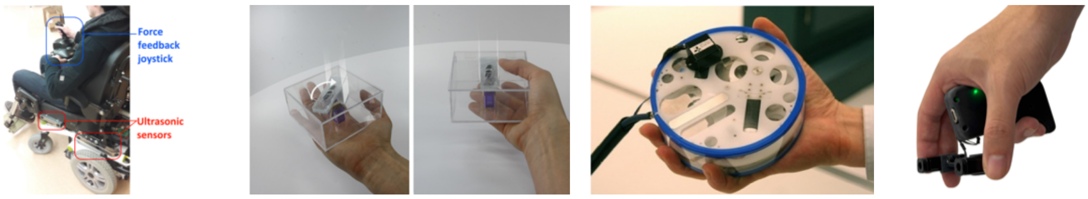

(A) Devigne 2018 (B) Hemmert 2010a (C) Amemiya 2009 (D) Maeda 2024

Figure 1.7: Examples of force-feedback devices. (A) A force-feedback joystick on a power wheelchair; (B) A weight shifting handheld interface; (C) A 2DoF device using asymetric acceleration of a moving mass; (D) A device using pseudo-force with two voice coil actuators.

Shape changing feedback

Our hands are naturally able to perceive the shape of objects with little effort. Shape changing devices aim at using this ability to convey information by changing their shape dynamically. In particular, Spiers et al. have designed and evaluated several navigation devices that focus on this haptic modality. The "Animotus" or "Haptic Sandwich" is a handheld cube (see Figure 1.8A), of which the upper half can translate and rotate in order to communicate direction and proximity to a target [Spiers 2015]. The device was evaluated in several navigation studies, and was also compared to a vibrotactile equivalent [Spiers 2016] and another shape-changing device called the "haptic Taco" which provided only proximity information by expanding or contracting (see Figure 1.8B) [Spiers 2017]. Extending this approach, the "S-Ban" is more ergonomic (see Figure 1.8C), with a 2DOF end effector positioned between the thumb and index [Spiers 2022].

Before these works, Hemmert et al. proposed to add shape-changing feedback to the back of a smartphone, with a moving plate that could indicate directions (see Figure 1.8D) [Hemmert 2010b]. However, only the perception of direction was evaluated, not the use in a real application. Similarly, "HAPMAP" shows another concept of a moving part within a handle that could provide left and right directional cues [Imamura 2011]. Moving parts are however not the only way of changing the shape of an interface: pin-displays such as the one used by Velázquez et al. can also be considered as such [Velázquez 2006]. In this case, the display is a portable tactile map that represents the user environment in real-time.

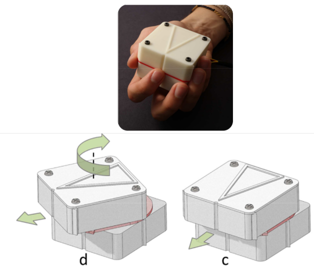

(A) Spiers 2015

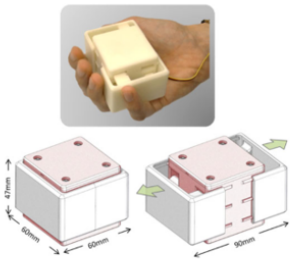

(B) Spiers 2017

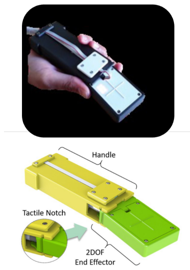

(C) Spiers 2022

(D) Hemmert 2010b

Figure 1.8: Examples of shape changing devices. (A) The "Haptic Sandwich", a handheld cube with a moving plate; (B) The "Haptic Taco", which can change its volume to provide proximity feedback; (C) The "S-Ban", with a 2 degrees-of-freedom moving plate; (D) Another example of a moving plate, here on the back of a smartphone.

1.2.2 Haptic navigation for people with disabilities

The navigation devices described so far are designed for a wide range of uses. As part of the Dornell project, we are particularly interested in the use of these devices in combination with existing mobility aids, such as white canes, wheelchairs, walkers and others. Numerous solutions have been proposed for the visually impaired, mainly focusing on the white cane. The vast majority use small vibrating actuators, positioned under one or more fingers, to provide proximity information to obstacles around users, generally relying on one or more ultrasonic sensors placed on the cane. Some approaches aim to extend the range of the traditional cane [Gallo 2010], or provide users with additional information, for example on types of obstacle undetectable via the cane such as low hanging obstacles [Wang 2012] or drop-offs [Pyun 2013]. Feedback can also provide broader guidance to complement the obstacle detection capabilities of the cane [Bhatlawande 2014; Nasser 2020]. Instead of complementing the existing assistive device, other approaches aim to replace existing devices altogether [Ando 2015].

Research has also been conducted on walkers: for example, Grzeskowiak et al. used vibration motors on the two handles to provide obstacle detection around the user [Grzeskowiak 2022]. Wachaja et al. used similar vibrating handles to guide users along a path [Wachaja 2017].

Multi-actuator handles on both sides of a walker were also evaluated for providing navigation instructions by using different apparent motion patterns on one or two hands [Lacôte 2024].

In the case of wheelchair users, proposed solutions focused on the joystick of power wheelchairs, using force feedback joysticks. In such cases, the joystick can help correct the user's trajectory [Devigne 2018]. Other approaches used wearables such as gloves [Uchiyama 2008] to provide guidance. For example, Devigne et al. used wearable armbands on both arms, each with four vibration motors, to either to indicate the closest obstacle or a direction to follow [Devigne 2020]. These solutions, while effective, are rather cumbersome for users which need to equip a wearable device when using the wheelchair or to heavily modify their device with a force-feedback joystick.

As users are used to their technical aids, it seems more appropriate to complement them with haptic navigation assistance, integrating devices as closely as possible to existing uses and adapting them to the specific needs of each user. Otherwise, there would be a high barrier for these devices, with users having to learn to use and trust a entirely new device. The advantage of integration with a device such as a wheelchair or walker is that it is easier to integrate sensors, or the power supply, without encumbering the user himself. This is advantageous for environments where localization is not yet feasible or precise enough.

1.2.3 Summary

Table 1.2 provides a summary of the devices previously referenced, with some additional information on the type of feedback and evaluation of the proposed devices. Out of all haptic modalities, vibrotactile feedback is the most popular one to be used in haptic navigation devices and has shown to be effective in various applications. Indeed, it has the benefits of being easy to integrate and control, at a little cost compared to other haptic sensations which require the design of more complex and adapted actuators.

Overall, different methods are used by these devices to guide users using haptics [Kappers 2024]. The simplest method is to provide left and right turn cues, which can be done relative to the whole body (e.g., by using wearables on both arms) or relative to a body part (e.g., a haptic bracelet with multiple actuators). Additional directions can be added, such as front/back or diagonals. Some devices can invert these directions, providing haptic feedback when the user deviates from the target direction or path. Other methods can inform about the distance/proximity to a target, sometimes using the direction in which the device is pointed, or use stimulation patterns to encode information. In every case, users have to learn how to use the haptic device. The duration of this learning phase will vary depending on the chosen strategy: mapping a stimulus location to an instruction might be easier to learn than a complex temporal pattern.

In their current state, haptic navigation applications for pedestrians could be used in real outdoor conditions, as geolocation is now widely available and precise enough for such application. Still, if targeting specific populations such as wheelchair users, data might be unavailable to plan an adapted route. Indoors, GPS systems cannot be used and specific localization and mapping systems are needed. They can be individual, such as with camera-based systems placed on the user and/or the device, or global, with BLE systems for instance. However, such systems would need to be installed in every building, making it only affordable in some specific cases (public buildings, hospitals, train station, etc.).

In general, haptic navigation devices are either targeted at pedestrian or at users of a specific device. Furthermore, feedback schemes are often heavily linked to the device's design, which leaves little room for the user to customize the way information is communicated. In the context of the Dornell project, we look into the design of interfaces that could be adapted to different use-cases and users. That is, haptic devices that could be used with different mobility assistance devices, while also exploring the personalization of the provided haptic feedback, as different users will have different needs and expectations for the device.

Table 1.2: Classification of haptic devices for navigation and related haptic displays. Arranged according to their order of appearance in in this section, depending on the type of haptic cue used.

	Device	Haptic cue(s)	Information	Evaluation
Pielot 2010	Mobile phone	Vibration	Direction	Navigation toward way-points in a city park
Rümelin 2011	Mobile phone	Vibration	Direction, Distance	Follow 400m routes
Kawaguchi 2012	Mobile phone	Vibration	Direction, Distance	Navigation toward way-point at 400m
Robinson 2010	Mobile phone	Vibration	Direction	Walk to an end point 700m away
Spiers 2016	Handheld	Shape-changing, Vibration	Direction, Distance	Navigation to sequence of targets (60m total)
Pyun 2013	White cane	Vibration	Obstacle	Reaction time, identification of obstacles
Wang 2012	White cane	Vibration	Obstacle	Detection evaluation, hallway with ten low hanging obstacles
Gallo 2010	White cane	Vibration, Force	Obstacle	Detection evaluation, hallway with obstacles

Continuation of Table 1.2				
	Device	Haptic cue(s)	Information	Evaluation
Ando 2015	White cane	Vibration	Obstacle	Detection evaluation, room with obstacles
Grzeskowiak 2022	Handle (walker)	Vibration	Obstacle	Collision avoidance in a room-scale maze
Wachaja 2017	Handle (walker), Belt	Vibration	Direction	Navigation along predefined path in a room
Lacôte 2024	Handle (walker)	Vibration	Direction	Navigation along predefined path in a 8x8m room
Heuten 2008	Belt	Vibration	Direction	Navigation to sequence of targets in an open field (375m)
Gay 2020	Vest	Vibration	Direction, Distance	Preliminary study, following a moving target
Hugues 2015	Handheld + Wristband	Skin-stretch, Vibration	Direction, Message	Navigation in a realistic VR scenario
Dobbelstein 2016	Wristband	Vibration	Direction	City navigation to a target 450m away
Devigne 2020	Armband	Vibration	Direction, Obstacle	Navigation in a circuit, guided along a path or informed of obstacles
Schaack 2019	Collar	Vibration	Direction	Navigation along a predefined route in a city
Aizawa 2021	Handheld	Skin stretch	Direction	Navigation to sequence of targets in a 4x2m area
Wiehr 2023	Handheld	Skin stretch	Direction	Not evaluated
Kayhan 2022	Belt	Skin stretch	Direction	Deviation correction when on a running track
Yoon 2017	Armband, Joystick	Skin stretch, Force	Direction	Guidance along trajectories in a virtual environment

Continuation of Table 1.2				
	Device	Haptic cue(s)	Information	Evaluation
Barontini 2021	Armband	Skin stretch	Direction, Message	Obstacle avoidance in a corridor
Kuang 2022	Wearable (forehead, arm, hand)	Skin stretch	Direction	Navigation along predefined path in a 4x4m room
Tewell 2017	Armband	Thermal	Deviation	Navigation in a virtual maze on a screen
Nasser 2020	White cane	Thermal, Vibration	Direction	Stimuli identification while walking in an open field
Devigne 2018	Joystick	Force	Direction	Collision avoidance in a corridor with obstacles
Hashimoto 2006	Joystick	Force	Map	Walk in a hallway
Amemiya 2009	Handheld	Force	Direction	Navigation in a maze
Amemiya 2014	Handheld	Force	Direction	Identification of directional cues
Ando 2012	White cane	Pseudo-force	Direction	Identification of directional cues
Maeda 2024	Handheld	Pseudo-force	Direction	Navigation in a VR maze (30x40m)
Spiers 2017	Handheld	Shape-changing	Distance	Navigation to sequence of 10 targets (5x5m room)
Spiers 2022	Handheld	Shape-changing	Direction	Navigation to sequence of 5 targets in VR
Imamura 2011	Handheld	Shape-changing	Direction	Not evaluated
Velázquez 2006	Surface	Shape-changing	Map	Recognition of the shape of virtual environments
Uchiyama 2008	Glove	Vibration	Direction	Identification of vibration patterns
Yang 2010	Mobile phone	Vibration	Direction	Identification of vibration patterns

Continuation of Table 1.2				
	Device	Haptic cue(s)	Information	Evaluation
Günther 2018	Glove	Vibration	Direction	Hand movement guidance
Saint-Aubert 2020	Ring	Vibration	Direction	Identification of vibration location and patterns
Monica 2023	Vest	Vibration	Obstacle	Obstacle avoidance in a VR task
Bajpai 2020	Vest	Vibration	Obstacle	Avoidance of fast moving obstacles in VR
Pan 2018	Handle (walker)	Skin stretch	Direction	Identification of directional cues
Chinello 2018	Armband	Skin stretch	Direction	Arm movement guidance and robotic manipulator control
Hemmert 2010a; b	Handheld	Shape-change	Direction	Identification of directional cues

1.3 Haptics for virtual reality

As virtual reality (VR) becomes more accessible and used in different domains, the sense of touch remains underexplored despite the fact that the whole body is covered with receptors that are usually highly stimulated when interacting with the environment. Haptic devices of all sorts have been proposed to provide sensations of touch in virtual interactionswith evidence that it may promote user engagement [Cooper 2018], performance [Brasen 2019], social presence [Cooper 2018; Kaul 2017] or embodiment toward a virtual avatar [Fröhner 2019; Richard 2020]. However, haptic feedback for VR is often focused on single specific interaction or sensation [Culbertson 2018], and the design of devices capable of rendering rich and realistic touch in a variety of interactions is a relatively recent development in the field [Wang 2020].

In the context of the Dornell project, VR is also a useful tool for experimenting with our haptic interfaces. We choose to first explore the use of multi-actuator vibrotactile feedback in VR, evaluating the perception of localized sensations and developing rendering schemes leveraging these sensations, which can then be transferred to other applications. We also use VR to experiment with navigation using virtual environments, which do not suffer from limitations of real life: technical challenges such as indoor localization can be set aside while also providing a safe and controlled environments for participants.

In this section, we propose an overview of haptic properties that can be rendered when manipulating or interacting with objects in a virtual environment. We focus on two approaches: vibrotactile feedback on the one hand, which is the most popular way of providing feedback, and, on the other hand, passive haptics (i.e., real, tangible objects), a less popular approach that we explore in our work. Indeed, passive haptics are ideal for providing realistic and natural contact feedback, but are limited by their inherent static physical properties. We believe that, in combination with the versatility of vibrotactile feedback, actuated tangible props could provide richer interactions when manipulating objects in VR.

1.3.1 Vibrotactile feedback for VR

Vibrotactile feedback is the most popular way of providing haptic feedback, thanks to the availability of actuators and the simplicity of their integration [Culbertson 2018]. Vibrations can be used in various ways, depending on the use of its different parameters and the properties of specific actuators. Here we overview how vibrations can be used to render different haptic properties of virtual objects and surfaces, which can be used for VR interactions. Namely, we discuss the use of vibrations to display *Forces* and *Impacts*, which are mainly perceived when moving an object or interacting with it, following with *Stiffness* and *Texture*, which are more predominant during object manipulation.

Forces: Vibrotactile feedback can render interaction forces by varying a vibration parameter (usually amplitude) proportionally to the reaction forces encountered [Cheng 1996; Herbst 2005]. With more control over the actuator, asymmetric vibrations can also render pseudo-forces: Niwa et al. used motors placed on the fingernail to produce an attraction force in any direction, by controlling the phase of four asymmetrically accelerating eccentric weights [Niwa 2010]. This principle was, for instance, used in the “Grabity” interface to render the weight of virtual objects [Choi 2017].

Impacts: In early work on impact rendering in interactions within virtual environments, Wellman et al. used a data-driven approach to play back recorded impact vibrations during virtual contacts on a voice-coil actuator embedded into the handle of a force-feedback devices [Wellman 1995]. Okamura et al. expanded this approach, compiling a library of vibration waveform which was generated by fitting a simplified vibration model based on an exponentially decaying sinusoid to recorded impact data [Okamura 1998]. Because this model provided an interesting compromise between perceived realism, impact property discrimination, and computing requirements, it has been widely adopted in virtual interactions [Kuchenbecker 2006; Sreng 2008]. In parallel, other data-driven approaches as well as simulation-based approaches have also been explored [Cirio 2013; Sreng 2008]. These usually have a comparatively high computational complexity and often still only achieve mixed results in terms of perceived realism and communication of impact properties.

Impact usually corresponds to contacts with other objects in the environment, but the content of some objects can also generate impacts inside them. For instance, Hummel et al. rendered the impacts of moving objects in a hollow container by using two voice coil actuators placed inside a 3D printed prop [Hummel 2022].

Stiffness: Stiffness perception is usually associated with sensations in the muscles and joints or with force and deformation of the skin. However, some studies found an effect of vibrotactile cues on stiffness perception [Visell 2014], in particular with low frequency vibrations. One experiment using a 5Hz stimulus showed that perceived softness decreased with the vibration amplitude [Porquis 2011].

In VR, Maereg et al. used vibrotactile actuators on the fingertips to display stiffness when interacting with virtual objects, allowing users to discriminate stiffness without the use of a kinesthetic device [Maereg 2017].

Texture: Vibrotactile feedback is a prime candidate for rendering textures. Textures can take various forms, with predominant directions and various levels of details. They can be categorized into macro texture (i.e. bumps, surface waviness) and micro texture (roughness) [Okamoto 2013] which are thought to be primarily mediated by spatial and vibrational cues respectively [Hollins 2000].

Roughness rendering interlinks with the concept of surface friction rendering because the phenomena are physically linked, although perceptually these properties are often considered independent due to the importance of lateral skin stretch in friction perception [Ito 2019; Okamoto 2013]. Regardless, vibrotactile cues are key components of haptic perception for both roughness [Hollins 2001; Lederman 1972] and to some extent friction [Okamoto 2013] and can thus effectively be applied for both.

Macro texture is usually rendered as a series of impacts depending on exploration velocity, texture geometry and applied force [Okamura 1998]. Micro texture rendering has been attempted with model-based approaches [Choi 2018; McDonald 2013; Okamura 1998] as well as data-driven approaches [Culbertson 2014; Guruswamy 2011]. Model-based approaches are often computationally intensive, and thus require simplifications that compromise realism or simply do not function in real-time VR [Culbertson 2017]. Among data-driven approaches, the *Penn Haptic Texture Toolkit* is an open-source model for procedurally generating vibrotactile feedback based on recordings of vibrations generated in exploration of real textures [Culbertson 2014].

Vibrotactile feedback can thus be used to render a large range of sensations when manipulating virtual objects. However, it suffers from two main drawbacks. First, vibrotactile actuators are often placed in direct contact with the user's skin, producing unwanted contact sensations that mismatch with the virtual contacts occurring in the virtual environment. Secondly, while vibrations can produce vibrations produced by virtual contacts, they are not able to provide any physical resistance to users motions which also induces a potential mismatch between the user's sensations and the virtual interaction. To provide realistic contact sensations, passive haptics are thus an interesting approach that we discuss in the following section.

1.3.2 Passive haptics for VR

The shape of an object is a more global property, which refers to its external boundaries. Sensations of making and breaking contact with the shape of an object are another key feature in enabling haptic exploration and direct manipulation of virtual objects. Arguably, the most effective way to achieve this is with a haptic interface actually making and breaking contact with the user's skin. This can be done by using passive haptics: instead of relying on actuators to generate haptic sensations, passive haptics provide realistic haptic sensations by using standalone, real, physical objects which are superimposed with virtual objects through a VR system [Azmandian 2016; Cheng 2018]. We usually refer to these physical props as tangibles. Without adding much complexity to the system, tangibles enable natural object manipulations in VR and provide shape and other physical sensations such as weight or stiffness. They only require adequate tracking of the props [Hoffman 1998] or prior calibration and virtual environment modelling [Brument 2019] combined with tracking of the user. This approach has been shown to significantly enhance interaction with virtual environments [Insko 2001].

Still, this approach has some limitations. First, passive haptics can become unwieldy for representing complex environments because each virtual object requires its own tangible counterpart. To counter this, tangibles have been combined with grounded force-feedback devices [Bae 2020] and encounter-type haptic displays [de Tinguy 2020; Kovacs 2020; Mercado 2021] to move the end effector in the user space, which can make the working area of a tangible prop virtually infinite. These hybrid solutions limit the number of distinct tangible objects required. Secondly, passive haptics cannot adapt to virtual objects which evolve within the environment. That is, one tangible object has a fixed mass, texture and shape that only corresponds to a limited number of objects in the virtual environment. To counter this limitation, internally actuated tangible props have been investigated for delivering ungrounded force feedback in VR manipulation [Sagheb 2019; Shigeyama 2019; Sinclair 2019]. As the user does not see the real object he manipulates when immersed in VR, the virtual object does not have to be exactly similar in shape [Tinguy 2019].

Devices such as the "Haptic PIVOT" [Kovacs 2020] aim to solve both of these limitations: experiments with the wrist-based encounter-type haptic display have shown that its moveable spherical end-effector could be used to represent objects other than spherical ones, such as the handle of larger objects. When shapes were too different, however, sensations were not judged realistic by the participants. For haptic properties other than the shape of the object itself, one way of enhancing tangible props can be the use of mixed haptics: combining the tangible object with other forms of haptic actuation to alter the perceived haptic properties of the object.

1.3.3 Current limitations

Vibrotactile feedback, as the most popular haptic modality, has been shown effective to render a wide range of virtual object properties. However, actuators are usually linked to a VR controller which has a specific shape, remarkably different from the one of the virtual objects the user interacts with. This might impact perceived realism and sensation of presence in the virtual environment. Furthermore, vibrotactile feedback in such controllers is, in the majority of cases, monolithic, making localized sensations impossible. We discuss the challenges of providing multi-actuator feedback in section 1.4. To provide more natural and realistic contact sensations, the approach of passive haptics has proposed to use tangible props for the user to interact with. Still, this approach has some limitations, including the fixed properties of the tangible props.

In our work, we sought to explore the combination of tangible objects with multiple vibrotactile actuators: this haptic modality is versatile, making it a great candidate for rendering multiple properties which could be combined with the benefits of passive haptics. Furthermore, vibrotactile actuators are small in size and easy to control, making them a great candidate for integration with tangible objects. This approach raises some interesting questions. First, about its feasibility: how can we design tangible that houses one or multiple actuators, so that users are able to perceive the vibrations from the different sources, and, if so, how many sources can we use in our designs ? Secondly, about the rendering schemes that we can design based on these new interfaces: which sensations can we render and which one can benefit from this approach?

Results and lessons learned from the use of multiple actuators in VR interactions also transfer to our following works on haptic navigation, where the precise localization of haptic cues is key and can be further exploited in combination with rich rendering schemes.

1.4 Multi-actuator vibrotactile devices

In order to provide more rich and intuitive information through haptic feedback, we are interested in multi-actuator haptic devices. Such devices can use multiple haptic effectors for different purposes, either to provide different haptic sensations (i.e., multimodal feedback) or, when using several of the same actuators, to provide localized haptic sensations. In the context of our works, we focus on multi-actuator device that aims to display localized haptic information to users. Indeed, this type of sensation can intuitively convey directional information to users, which is of particular interest for navigation application, our focus as part of the Dornell project.

More specifically, we are mainly interested in multi-actuator *vibrotactile* devices.

As part of our exploration of this type of haptic feedback, we first use VR to prototype and investigate localized feedback perception and rendering. This type of sensation is of interest for VR, as vibrotactile feedback in commercial controllers has focused on monolithic vibrations [Choi 2013] (i.e., the entire object vibrates), which remains inadequate for providing spatial information. Thus, haptic interactions in VR are, for now, limited to simple contacts or notifications. Multiple points of stimulation offered by multi-actuator interfaces could be used to provide richer sensations more easily and rapidly than with single-actuator devices. This can be applied for providing feedback when manipulating objects in VR, but also for providing new or more abstract information, such as ones about user's surroundings.

Building onto our findings in VR application, we then explore the design and use of multi-actuator haptic devices for navigation application. Navigation devices which usually rely more on temporal patterns, variations of intensity, duration or frequency can also benefit from such devices and provide more information to their users—or more effectively. Indeed, the location of the stimuli can already provide an information by itself, which can be enriched using the properties of the localized vibration such as frequency or intensity.

In this section, we overview a selection of multi-actuator devices focused on vibrotactile sensations, discussing the way multiple points of vibrotactile stimulation can be used, and how these interfaces take vibration isolation into account as part of their design.

1.4.1 Surface displays

If surface haptics are not our focus here, these interfaces are still able, for some, to create localized vibrotactile sensations using multiple actuators. Basdogan et al. provide a review of surface haptics in which they describe two approaches for generating localized sensations on such devices [Basdogan 2020].

First, some rely on sensory illusions to create stationary or moving phantom sensations. Examples include "T-Hive", a spherical device with 13 vibrating panels on its surface, each with a dedicated ERM actuator (see Figure 1.9A) [Ryu 2012; Yang 2009]. These panels are isolated using a layer of vibration absorber under each motor in order to provide stationary localized sensations. Locations displayed by a single panel are clearly distinct, with identification rates close to 100%. Directional patterns displayed by the sequential activation of actuators are also well identified. However, intermediate locations generated by simultaneous activation of motors are less effective, with scores between 45 and 75%. In cases where researchers focused on rendering directional information, vibration isolation is less critical. This is the case with devices such as the one in "Edge flow", on which actuators were placed on the sides of a mobile phone to display multiple patterns of vibration [Seo 2015] along the edges of the device's screen. We cover some other mobile devices in subsection 1.4.3, which are closer to handheld devices than surface displays.

The other way for surface haptics to provide localized vibration sensation is by generating vibrations only on a small area of the device. To do so, interferences of the vibrations produced by piezoelectric actuators can generate localized sensations on rigid, flat surfaces [Hudin 2013]. Another similar approach used interferences of voice coil actuator vibrations for a spherical surface [Coe 2021]. In this approach, however, it is unclear if authors considered the effect of the hand over the surface of the device, which could considerably influence vibration propagation on the surface of the device. Wave-guides [Jeannin 2023] can also be used to confine vibrations, as well as approaches using meta-materials (see Figure 1.9B and 1.9C) [Daunizeau 2021]. Still, these approaches often require complex materials or control methods in order to display these sensations. Simpler approach can use widely available and more affordable materials such as flexible ones: for instance, Ujitoko et al. propose to use a silicon rubber sheet in which eight vibration sources are placed around the hand, displaying spatio-temporal patterns rotating around the hand [Ujitoko 2022].

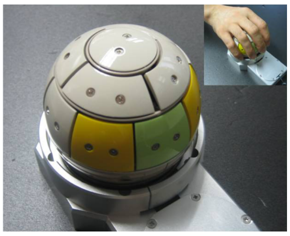

(A) Ryu 2012

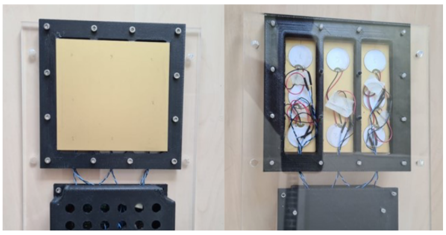

(B) Jeannin 2023

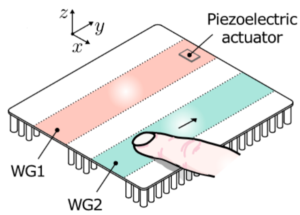

(C) Daunizeau 2021

Figure 1.9: Illustration of multi-actuator vibrotacile surface displays: (A) “T-Hive”, a spherical shape display with vibrating panels; (B) A plate with waveguides for 2D localized vibration; (C) Metamaterial waveguides for isolating vibrations.

1.4.2 Wearables

Multi-actuator vibrotactile devices are in majority wearable ones [Choi 2013; Pacchierotti 2017]. In most cases, the fabric that holds the actuators is flexible enough to prevent vibrations from transmitting through the device. Additionally, the stretch of the fabric on the skin ensures that motors are slightly pressed against the skin. Otherwise, multiple actuators can be distributed over a large area or distinct body parts so that stimuli are well separated from each other. Known examples of these types of devices include tactile belts (see Figure 1.10A), usually using six or eight actuators around the user’s waist [Bajpai 2020; Erp 2005]. The number of locations can also be increased using multiple actuators simultaneously [Heuten 2008]. Haptic vests can provide similar feedback on a larger area, for instance in [Monica 2023] with 40 actuators over the torso and back of the user.

Armbands and wristbands are also common (see Figure 1.10B). Stanke et al. compared the use of four electrotactile vs. vibrotactile actuators in a wristband, reporting that recognition is higher with electrotactile feedback, but that vibrations were judged more comfortable and less stressful [Stanke 2020]. Armbands can either use a limited number of actuators to communicate through spatio-temporal patterns [Lee 2010], or use the location of the vibration to communicate a direction [Devigne 2020]. Most approaches use fabric or flexible materials between actuators. Others propose designs close to existing smartwatches, such as Paneels et al. who proposed a watch-sized casing with six points of stimulation for the wrist (see Figure 1.10C) [Paneels 2013]. Within the device, the structure made of beams designed to prevent the propagation of vibration within the device, but can only provide stimulation at a single frequency of 100Hz.

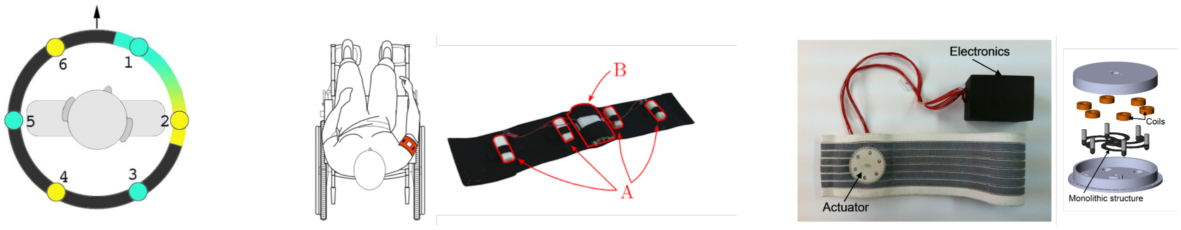

(A) Heuten 2008 (B) Devigne 2020 (C) Paneels 2013

Figure 1.10: Illustration of multi-actuator vibrotacile wearables. (A) "Tactile wayfinder", a multi-actuator haptic belt; (B) A vibrotactile armband providing directions to a wheelchair user; (C) A wrist-based device with six points of stimulation;

In VR, gloves with multiple points of stimulation are also popular [Wang 2019a]. For instance, Günther et al. proposed to guide the user's hand with a glove equipped with ten vibrotactile actuators [Günther 2018]. Similarly, Scalera et al. used a glove with four actuators (see Figure 1.11A) to guide the movements of the user when using a joystick [Scalera 2018].

At a smaller scale, some approaches look into delivering localized feedback directly on the finger: Hsieh et al. use 4 small erm actuators around the nail (see Figure 1.11B), achieving a 89% recognition rate of directional cues and numerical characters [Hsieh 2016]. Similarly, Saint-Aubert et al. placed 4 motors directly on the user proximal phalanx (see Figure 1.11C), where dynamic patterns were deemed less effective [Saint-Aubert 2020]. In these cases, vibrations are displayed directly in contact with the skin, with actuators separated from each other, thus not requiring an isolation mechanism.

1.4.3 Handhelds, graspable

While handheld devices could benefit from multi-actuator vibrotactile feedback, they are less common as they pose a greater challenge to prevent vibration propagation in their small form factor.

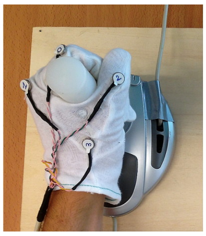

(A) Scalera 2018

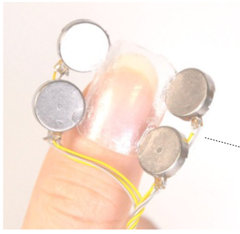

(B) Hsieh 2016

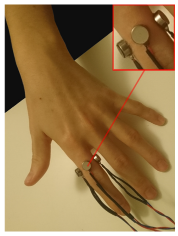

(C) Saint-Aubert 2020

Figure 1.11: Illustration of multi-actuator vibrotacile wearables. (A) A glove for joystick guidance; (B) Localized vibration on the nail; (C) Localized vibration on the finger.

In the case where actuators do not provide interfering sensations (e.g, two different types of sensations) they can simply be linked together, as in the work of Park et al., where an actuator provides impact forces and the other vibrotactile feedback [Park 2019]. Multiple devices for rendering the impact sensations of shaking a box have also been proposed. Actuators are usually placed on opposite sides of the object and can be solenoids [Sekiguchi 2003] or voice coils of varying sizes (see Figure 1.12A) [Hummel 2022; Tanaka 2012].

The most straightforward approach for a clear separation between vibration sources is to simply have actuators separated from each other. Gongora et al. used two handles linked by a thread to simulate the spatialization of impacts on a virtual bar connecting both hands, however this approach is closer to the use of two single actuator devices than a multi-actuator one [Gongora 2016]. Several devices have been proposed for both VR interactions and navigation based on asymmetric vibrations of two voice coil actuators to provide pseudo-force feedback. These sensations rely on the skin-stretch of the fingerpad generated by the vibrations [Culbertson 2016]. Thus, actuators are often simply attached to each finger, without a rigid connection to the rest of the device: this is the case wit “DualVib” (see Figure 1.12B), which combines the two actuators on the fingers with a third inside a handle [Tanaka 2020]. Actuators are therefore isolated from each other, but this makes the device separated into multiple separate parts. Other devices based on this same sensation rely on a lightweight structure connecting actuators together (see Figure 1.12C) [Choi 2017; Maeda 2023].

A number of approaches have sought to propose multiple points of vibration on the back of mobile devices. Hoggan et al., for instance, used four “C2 tactors” on the casing of a mobile device [Hoggan 2007]. These particular actuators are designed with a casing around the central moving part, providing stimulation at a single point (see Figure 1.13A). In this case, they were placed on the lower and upper thumb, and tip of the index and middle finger. Location was recognized in 100% of the cases, showing the effectiveness of the actuator design. A handheld interface for personal communication, used the same actuators to communicate through movements of localized vibrations [Heikkinen 2009]. While these actuators are effective in providing localized sensations, they are quite large with a diameter of 3 centimeters, which limits the

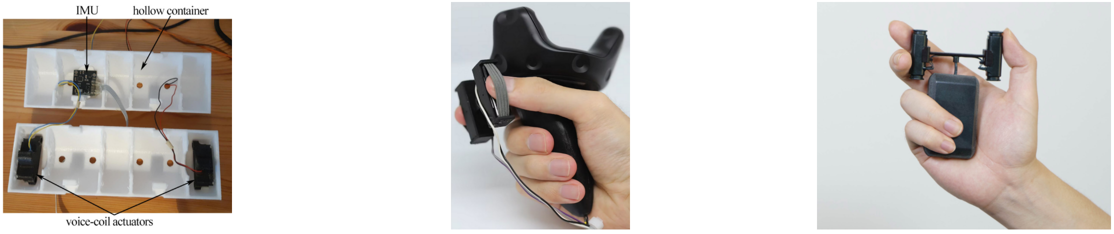

(A) Hummel 2022 (B) Tanaka 2020 (C) Maeda 2023

Figure 1.12: Illustration of multi-actuator vibrotactile handheld devices. (A) A hollow tangible cylinder equipped with two actuators for simulating impacts within the object; (B) Waylet, using a lightweight structure to hold two actuators; (C) DualVib, using two actuators placed directly on the fingers.

number of actuators that can fit a device and the distance between stimulation points.

Sahami et al. placed six smaller actuators within the case of a mobile phone, however, overall recognition of vibration location was only of 36%, due to propagation of vibration [Sahami 2008]. Yatani et al. proposed a sleeve for a mobile device (see Figure 1.13B) with five coin-type vibration motors to provide motion patterns on the palm [Yatani 2009]. It is unclear what material the sleeve was made of and whether it might have an effect on vibration propagation. Still, identification performance was better at around 90%. Following with this concept, Yatani et al. placed a 3x3 array of motors on the back of a mobile display to provide geographical information to visually impaired users (i.e., distance and direction to landmarks around the user) [Yatani 2012]. Motors seem to have been placed on foam pads to mitigate vibration propagation. In a more refined design, Yang et al. used arrays of twelve vibrating panels made of silicon rubber to display different vibration patterns on the back of a smartphone (see Figure 1.13C) [Yang 2010; Yang 2019].

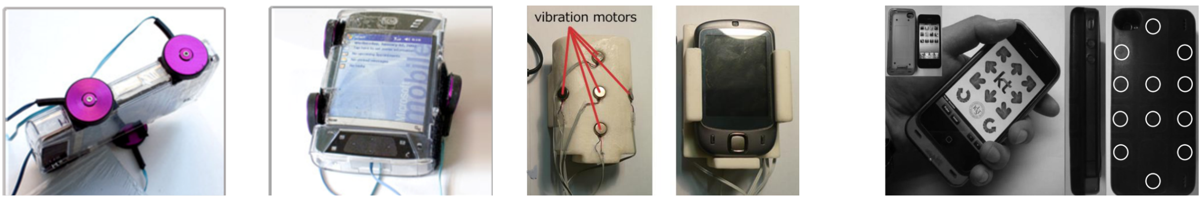

(A) Hoggan 2007 (B) Yatani 2009 (C) Yang 2019

Figure 1.13: Illustration of multi-actuator vibrotactile handheld devices based on mobile devices. (A) C2 tactors placed directly on the sides of a mobile device; (B) “SemFeel”, a sleeve with coin-type actuatorts; (C) A smartphone with vibrating silicon rubber pads on its back.

Coin-type actuators are also frequently used in handles, such as those of haptic white canes [Nasser 2020]. Isolation of such motors is not always discussed. Gallo et al. tested different damping materials (foam, elastic bands and hollow rubber joints) on the handle of a cane and found that hollow rubber joints were the most effective [Gallo 2010]. This approach was reused by Kim et al. for another white cane prototype [Kim 2015]. As C2 tactors mentioned earlier, some actuators come already equipped with an isolating structure, such as the ones used in the "Multivibes" handle (see Figure 1.14A) which prevents vibration from propagating in other directions [Richard 2023]. With actuators having a single axis of vibration, they can be placed normal to the skin in order to provide a single point of stimulation. Similarly, custom voice coils used in the handle proposed by Lacôte et al. are opened on one end (see Figure 1.14B), allowing the magnet to come in direct contact with the skin [Lacôte 2023]. However, these solutions only work as long as vibration intensity is limited. Stronger vibration will demand a dedicated, stronger mechanism to ensure isolation.

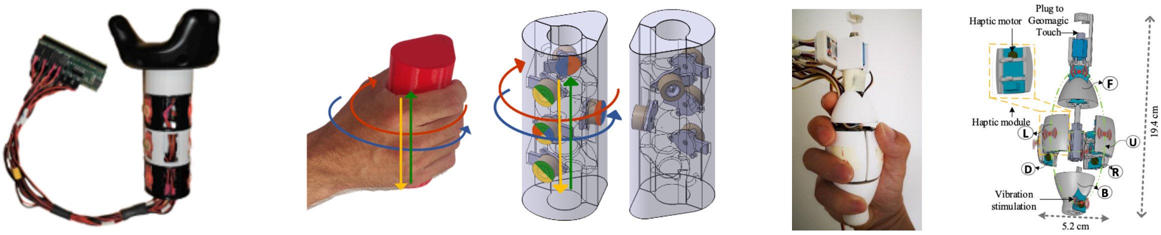

(A) Richard 2023 (B) Lacôte 2023 (C) Radhakrishnan 2024

Figure 1.14: Illustration of multi-actuator vibrotactile handheld devices. (A) "Multivibes", a haptic handle for VR interaction with ten actuators; (B) A haptic handle using five custom actuators to display apparent motion; (C) A 6-actuator handle with separated vibrating parts.

"RU-Netra" pushes the number of actuators in contact with the hand even further with 16 actuators in total, one per phalanx (see Figure 1.15A) [Shah 2006]. However, stimuli evaluated with this device do not use all actuators and recognition rates are rather low. Indeed, differentiating such a high number of stimuli locations on the hand is difficult and imposes a high cognitive load to the user. Such a large number of stimuli locations within the user's hand might not be practical for effectively conveying information. In a survey of the information transmission capability of haptic devices, Tan et al. focus on psychophysical studies of haptics which evaluate human performance in stimuli identification [Tan 2020]. Instead of reporting on the percentage of correct answers, they use information theory to quantify the amount of information a device can transmit to users. For multi-actuator devices that do not use movement illusions, authors highlight that the information transmission of tactor localization is limited in the upper extremities, and that the highest value is located on the palm, corresponding to about five distinct locations.

With a lower number of actuators, the "Haptic Sandwich" from Spiers et al. uses motors on three of the faces of a handheld cube [Spiers 2016]. Vibrations are isolated by keeping faces separated, with distances between actuators being still quite large for three points of stimulation. In a similar way, Radhakrishnan et al. designed a 6-actuator handle for motor skill training, providing localized contact feedback in a buzzwire task [Radhakrishnan 2024]. The handle was 3D printed and integrated six modules with actuators (see Figure 1.14C), with gaps between the parts weakening vibration transmission by around 70% between modules. However, participants could correctly identify the active motor 68% (55 to 90%) of the time, with confusion with adjacent panels of 13.6%. In a different form-factor, Scalera et al. proposed to use four actuators on the sides of a joystick for providing movement guidance (see Figure 1.15B) [Scalera 2018]. Motors were placed directly on the joystick handle, on a foam rubber ring in order to avoid vibration transmission. Similarly, Zikmund et al. used two vibration motors on a joystick to provide guidance to an aircraft-pilot [Zikmund 2019].

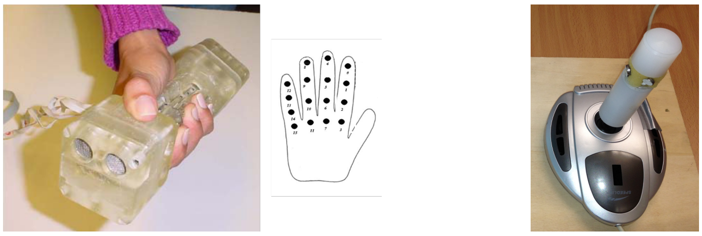

(A) Shah 2006 (B) Scalera 2018

Figure 1.15: Illustration of multi-actuator vibrotactile handheld devices. (A) “RU-Netra”, a 16-actuators handle for providing navigation feedback; (B) A joystick equipped with four actuators placed on a foam ring.

1.4.4 Design challenges for multi-actuator handheld devices

In Table 1.3 we propose a summary of multi-actuator devices we mentioned in this section, with details about their isolation mechanism, the type of information they rely on to communicate with the user and the application for which they were designed and/or evaluated.

Overall, wearable devices appear as the most straightforward way of providing multi-actuator feedback to users. However, these devices can be cumbersome, uncomfortable, or even inappropriate for some users, such as those with disabilities. Handheld multi actuator devices can solve these issues, but they are less common and pose a greater challenge as the small form factor of the interface makes it more difficult to effectively prevent vibrations from propagating through the whole structure. Indeed, out of twenty handheld devices reviewed by Adilkhanov et al., only one provided multi-actuator vibrotactile feedback [Adilkhanov 2022]. Wang et al. highlight that commercial VR controllers only provide global vibrotactile feedback and that an open challenge is to “achieve more abundant haptic feedback patterns within the compact volume of a handheld devices” [Wang 2019a]. One of the main challenges of multi-actuator feedback is thus to generate localized haptic stimuli that can easily and quickly be differentiated and located by users.

Isolation between the different tactile signals is closely related to the type of device: smaller, rigid interfaces will pose greater challenges than wearable devices. Out of all devices we mentioned in this section, several approaches can be observed in the design of multi-actuator vibrotactile interfaces. Some devices simply do not use any isolation mechanism, in which case vibrations can be somewhat localized but diffuse. This is mostly the case of interfaces that rely on spatio-temporal patterns around the device, or that do not need precise localization of sensations, such as ones targeting VR interactions. When vibration sources are isolated, it is usually through the use of a soft material (e.g., a layer of foam, silicon rubber or a deformable part), by using actuators with a moving part that contacts the skin or by partially separating vibrating parts of the device.

In addition to these mechanisms, compromise must be made between the number of actuators, their size and rendering capabilities such as the size, electrical consumption and computing power of handheld devices is limited. One way of mitigating these issues is to rely on haptic illusions to virtually increase the number of perceived stimulation points of the device [Lacôte 2023; Richard 2023].

To provide localized vibrotactile cues within the hand, propagations through the hand itself must also be considered. Dandu et al. measured the propagation of vibrations elicited at the fingertip through the hand using a multi-point vibrometer and showed that propagation decreases quickly with frequency [Dandu 2019]. Similar observations can be made from measurements taken with the accelerometer array designed by Shao et al. [Shao 2020]. In that respect, these properties of the hand must be taken into account in the design of a device and the haptic sensations it provides. Additionally, the pressure of the hand over the device will also have an effect on the propagation and perception of vibration [Choi 2013; Gallo 2010].

Despite those challenges, most of the devices discussed in this section were used for navigation or movement guidance, showing the relevance of multi-actuator feedback for this type of application. However, its combination with interfaces such as joysticks seems to have been only slightly investigated.

Table 1.3: Multi-actuator vibrotactile devices. Arranged according their order of appearance in this section, depending on their form-factor.

	Type	Number of actuators (type)	Isolation mechanism (if any)	Information	Application
Yang 2009	Spherical handle	13 (ERM)	unspecified absorbing material	Directional patterns, location	Joystick guidance
Seo 2015	Mobile phone	4 (LRA)		Directional patterns	
Hudin 2013	Surface	8 (piezoelectric)	Interference	Location	
Jeannin 2023	Surface	8 (piezoelectric)	Waveguides	Directional patterns	
Ujitoko 2022	Surface	8 (solenoids)	Silicon rubber sheet	Directional patterns	
Erp 2005	Belt	8		Location	Guidance
Bajpai 2020	Belt	8 (ERM)		Location	Obstacle avoidance
Heuten 2008	Belt	6		Location	Guidance
Monica 2023	Vest	40 (ERM)		Location	Obstacle avoidance
Lee 2010	Wristband	3 (ERM)	Fabric stretch	Patterns	Alert, notification
Devigne 2020	Armband	4 (ERM)	Fabric stretch	Location	Guidance, obstacle avoidance
Paneels 2013	Wristband	6 (custom)	Resonant structure	Patterns	Guidance
Stanke 2020	Ring + Wristband	4 (ERM)	Fabric stretch	Location, patterns	
Günther 2018	Glove	6 to 10	Fabric stretch	Location	Hand guidance
Scalera 2018	Glove / Joystick handle	4 (ERM)	Fabric / Foam	Location	Joystick guidance
Hsieh 2016	Nail-mounted	4 (ERM)		Location, patterns	Information transfer
Saint-Aubert 2020	Finger-mounted	4 (ERM)		Location, patterns	

Continuation of Table 1.3					
	Type	Number of actuators (type)	Isolation mechanism (if any)	Information	Application
Gongora 2016	Handheld	2 (LRA)	Separation	Location	Impact rendering
Tanaka 2020	Handheld	3 (2 VCA, 1 LRA)	Separation	Pseudo-force, texture	VR manipulation
Choi 2017	Handheld	2 (VCA)	Separation	Pseudo-force	VR manipulation
Maeda 2023	Handheld	2 (VCA)	Separation	Pseudo-force	Guidance, VR manipulation
Park 2019	Handheld	2 (1 VCA, 1 solenoid)		Impact, vibration	VR manipulation
Sekiguchi 2003	Handheld	2 (solenoid)		Impact	VR manipulation
Tanaka 2012	Handheld	2 (solenoid)		Impact	
Hummel 2022	Handheld	2 (VCA)		Impact	VR manipulation
Hoggan 2007	Mobile phone	4 (C2)	Actuator design	Location, patterns	Alert, notification
Heikkinen 2009	Handheld	4 (C2)	Actuator design	Patterns	Communication
Yatani 2009	Mobile phone	5 (ERM)		Location, patterns	Mobile applications
Sahami 2008	Mobile phone	6 (ERM)		Location	
Yatani 2012	Mobile phone	9 (ERM)		Location	Navigation
Yang 2010	Mobile phone	12 (LRA)	Silicon rubber panels	Directional patterns	
Yang 2019	Mobile phone	12 (LRA)	Silicon rubber panels	Directional patterns	
Nasser 2020	White cane handle	4 (ERM)	Foam	Location	Guidance
Kim 2015	White cane handle	4 (ERM)	Hollow rubber joints	Patterns	Obstacle distance
Richard 2023	Handheld controller	10 (VCA)	Actuator design	Location, patterns	VR interaction

Continuation of Table 1.3					
	Type	Number of actuators (type)	Isolation mechanism (if any)	Information	Application
Lacôte 2023	Handle (handheld, walker)	5 (custom VCA)	Actuator design	Directional patterns	Guidance
Radhakrishnan 2024	Handle	6 (LRA)	Gaps	Location	VR contact
Shah 2006	Handle	16 (ERM)	Dampening structure	Location, patterns	Obstacle detection
Spiers 2016	Handheld	3 (ERM)	Gaps	Location	Guidance
Zikmund 2019	Joystick handle	2 (ERM)		Location	Joystick guidance

1.5 Conclusion

In this chapter, we provided an overview of the existing literature on haptic devices for navigation and virtual reality (VR), as well as a more in depth discussion of multi-actuator vibrotactile interfaces. Both VR and navigation can benefit from richer haptic feedback: VR for providing more realistic feedback and rendering the multisensory interaction we can have with the world, navigation for providing more intuitive and detailed information to users about their environment. Indeed, in VR, current interfaces are still limited to monolithic feedback which prevents the display of localized sensations to users. In the context of navigation, wearable devices can provide intuitive, localized feedback. However, they still are cumbersome and inadapted for some users. While applications in these fields appear to be quite distinct, multi-actuator haptic feedback can in fact benefit both worlds. The design challenges are common to both fields, and learnings from one can transfer to the other.

In this thesis, we thus investigate the design of multi-actuator interfaces, which have the potential to benefit both of these areas. We focus on vibrotactile feedback, which was demonstrated as an effective way of providing diverse information in both domains. As this type of interface is being developed, we explore how they can provide a wider range of sensations and interactions, and how this might benefit users.

Part I

DESIGN OF HANDHELD MULTI-ACTUATORS INTERFACES

CHAPTER 2

ACTUATED TANGIBLE PROPS FOR ENHANCED INTERACTIONS IN VIRTUAL REALITY

As we investigate the use of multi-actuator vibrotactile devices, we first prototype interfaces in VR in order to explore their capabilities and the rendering possibilities they can offer. Consequently, we evaluate their use to enhance VR manipulation, which can greatly benefit from rich, informative and realistic haptic feedback.

This chapter covers our work on actuated tangible interfaces, in which we investigate the use of multiple vibrotactile actuators to provide spatialized feedback within handheld objects. These focuses mainly on VR manipulation, an area in which tangible props are an effective way of providing realistic contact at little cost. We first propose to evaluate the use of different number of actuators within a spherical object to display localized haptic sensations to users. We then propose a collection of VR interactions associated with multi-actuator rendering schemes, aimed at simulating multiple haptic interactions within a virtual environment, of which we evaluate the benefits compared to traditional monolithic feedback. Finally, we look further into impact rendering, this time with a handle-shaped interface with two actuators.

The contents of section 2.1 and 2.2 have been published in [Cabaret 2023], which we chose to separate here as they address two of our research axes. Contents of section 2.3 were published in [Cabaret 2022].

2.1 Localized multi-actuator vibrotactile rendering in a tangible sphere

In this section, we investigate the combination of vibrotactile feedback (VF) and tangible objects. Using a series of actuated tangible prototypes, we conduct three perception studies exploring the feasibility and benefit of localized vibrotactile feedback within a tangible object.

2.1.1 Design

System design

For our prototype and investigations, we used spherical tangible objects into which we embedded multiple voice-coil actuators (see Figure 2.1), as the symmetrical nature of the objects allows for easy repositioning of the actuators relative to the user's hand. We empirically determined that a 70mm sphere diameter allowed consistent grasping across many different hand morphologies, and thus chose this diameter for our tangible spheres. Our analyses looked into the effects of hand sizes in each of the presented experiments, but no significant effects were found.

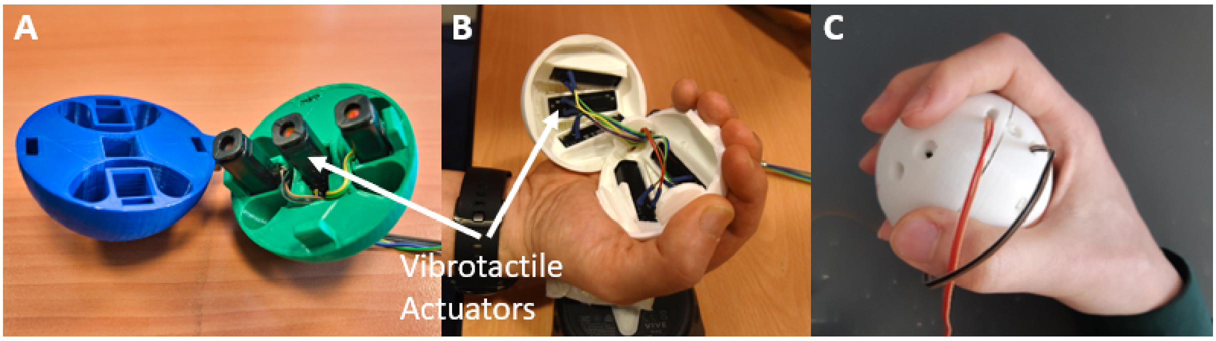

Figure 2.1: (A) Prototype tangible sphere containing 3 actuators: the lateral actuators enable localized VF while the central actuator enables monolithic VF for comparison. (B) Prototype tangible sphere containing 5 actuators arranged so that each is located directly beneath a fingertip during grasping. (C) Close-up of a user holding a vibrotactile tangible.

The most straightforward way to localize VF within an object is to use multiple actuators. We opted for this approach because of its technical simplicity, given our objective was first and foremost to validate the usefulness of localized VF in VR manipulation.

The actuators integrated into the device were Actronika's HapCoil-One voice coil actuators[1]. We chose these actuators despite their rather large form factor and mass because they are able to generate high-bandwidth and arbitrary waveforms with significant intensities, making them ideal for rendering a wide range of sensations [Choi 2013].

The actuators were driven using audio signals from a USB 7.1 surround sound card (see Figure 2.2-B), allowing up to 8 actuators to be driven simultaneously. The voltage from the sound card's audio output was insufficient to drive the vibrotactors, so we used TPA3116D2 dual-channel amplifiers (see Figure 2.2-B) powered by external 5V power supply units to drive the actuators in pairs. A calibration step was performed to adjust the amplifier gains in order to ensure they produced equal voltage output amplitude for a given input signal from the sound

[1] `https://tactilelabs.com/wp-content/uploads/2023/11/HapCoil_One_datasheet.pdf`

card. To do this, we connected each amplifier output to an oscilloscope and played back an identical signal on loop, adjusting the gain until the target output acceleration of 2.5g was reached. We assumed that since all actuators used are identical, they also should have a similar response. These values were empirically found to be perceptible, differentiable and comfortable.

All VF stimuli for the experiments were generated with Syntacts [Pezent 2020], an open-source software created specifically for audio-based haptics. This software offers a library of waveforms and modifiers to design haptic cues and provides precise control over latency. A Unity package is available for Syntacts, simplifying its integration within our system. Since this approach is not capable of generating procedural signals from scripts, we used the Unity audio engine for interactions requiring procedural signal generation, i.e., rendering texture roughness (see section 2.2.1).

Experimental setup design

Our first two experiments were dedicated to the use of a pair of localized vibrotactors, as this constitutes the basic building block for multi-actuator spatialization (see Figure 2.1-A). The

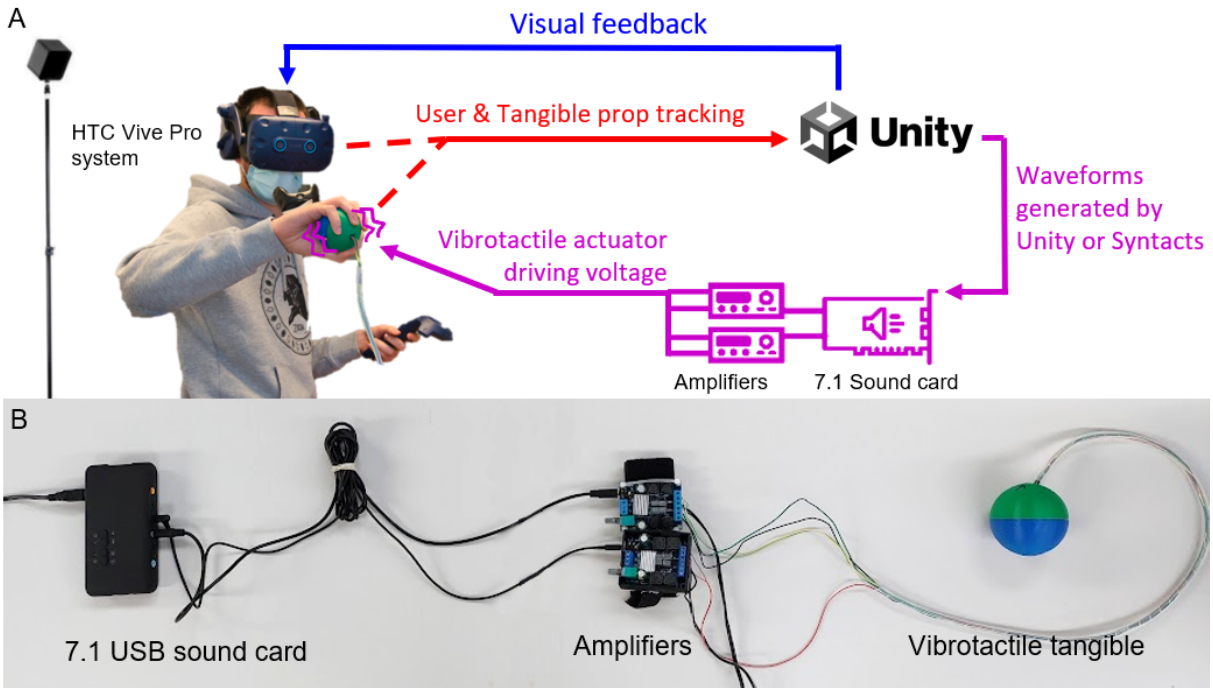

Figure 2.2: (A) The users hand and physical prop are simultaneously tracked using an HTC Vive Tracker. The virtual environment is simulated in Unity3D and rendered to the user's HTC Vive Pro HMD. The simulation outputs vibration patterns for the vibrotactors as audio signals which run through a custom-built amplification stage to drive the actuators. (B) Close-up of the sound card, amplification stage and an actuated tangible sphere.

third experiment used a sphere fitted with one actuator under each finger, for 5 actuators in total (see Figure 2.1-B).

All experiments were conducted in VR. The user viewed the virtual environment simulated in Unity3D through an HTC Vive VR headset (see Figure 2.2-A). A tracker was placed either on the back of the hand or on the forearm, thus leaving the volar face of the hand free of any obstruction or unwanted haptic stimuli. Information from the tracker served to reproduce movements of the user's hand onto the virtual hand while simultaneously providing information about the physical location of the tangible object. During all three experiments, participants used a Vive controller held in their non-dominant hand to answer experimental questions (see Figure 2.3). White noise was played throughout all experiments to mask any sound from the actuators that could bias participant responses. The study has been approved by Inria's ethics committee. Written informed consent was provided by all participants prior to each experiment.

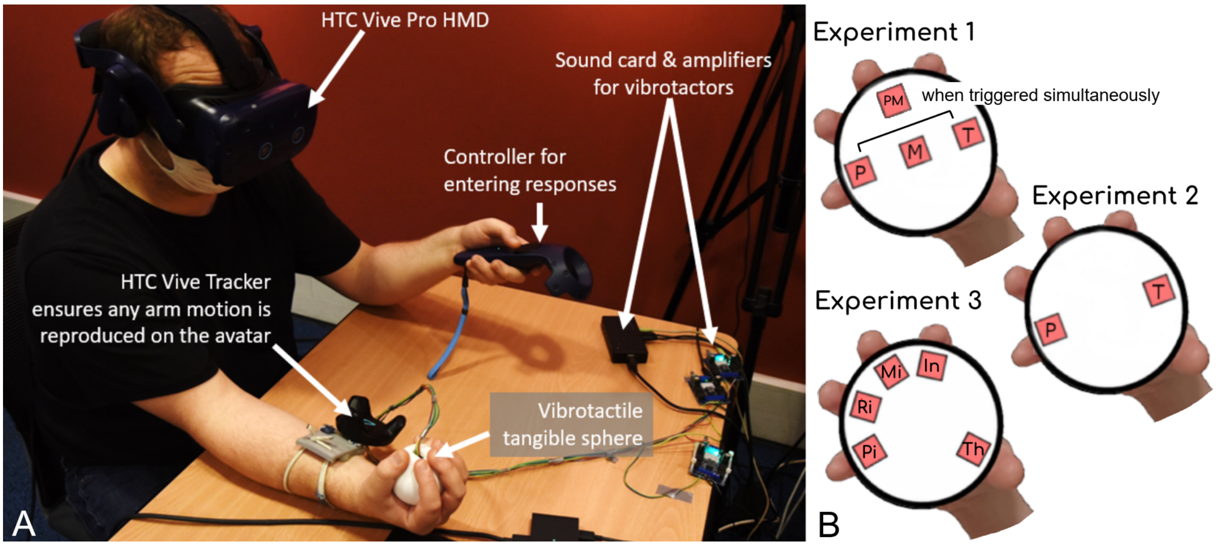

Figure 2.3: (A) Experiment setup: participants held a tangible sphere in their dominant hand tracked using a forearm-mounted tracker. They viewed the experimental environment through a HMD and responded to experimental questions with a controller held in their non-dominant hand. (B) Different actuators configurations are used throughout the experiments.

2.1.2 Effectiveness of multi-actuator vibrotactile feedback

Research question and hypotheses

To determine whether spatializing VF within a tangible object using multiple actuators is possible, we performed an initial experiment using the sphere fitted with 3 vibrotactors (see Figure 2.1-A). Specifically, we sought to determine whether in this simplest implementation, localized cues are discriminable from one another, as well as from monolithic vibrations of the tangible.

A well-documented phenomenon in vibrotactile feedback using multiple actuators is the phantom sensation [Alles 1970] or "funneling illusion" [v. Békésy 1958] wherein two distinct points of vibrotactile stimulation can be perceived as a single vibrotactile stimulus presented at an intermediary location. Because of this, we also aimed to assess whether monolithic single-actuator vibrations of the tangible object could be replaced by multiple localized vibrotactors symmetrically placed around the object and providing simultaneous stimuli at equal amplitudes. Finally, we sought to assess to what extent results are dependent on the stimulus waveform.

Our hypotheses were the following:

H1: Localized cues (played on P or T actuators) are distinguishable from one another, regardless of the cue waveform;

H2: Localized cues are distinguishable from perceptually amplitude-matched monolithic cues (played on the M actuator), regardless of the cue waveform;

H3: Monolithic cues can be simulated by simultaneously triggering symmetrically arranged localized actuators with equal-amplitude cues, regardless of the cue waveform.

Materials and methods

To investigate these questions, we performed a user study involving 16 participants (8F, 8M, all right-handed, ages 21–52 (M=26.9, SD=8.8)), following an oddball procedure. Participants were recruited in the lab, 12 of them having some experience with haptics. Using the apparatus described in subsection 2.1.1 above, participants held the spherical tangible in their dominant hand such that the lateral actuators were located respectively between the thumb and index (actuator location T) and below the pinkie (actuator location P). Visible markings on the sphere allowed the experimenter to ensure that the participant's hand was correctly positioned.

Stimuli were one of the three representative waveforms (see also Figure 2.4):

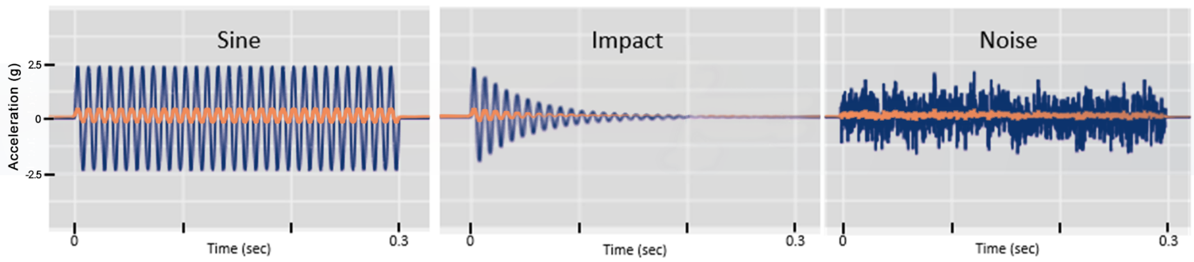

Figure 2.4: Waveforms used in the experiment. Weak (0.25g) and Strong (2.5g) levels used in subsection 2.1.4 are shown in orange and blue respectively.

- **Impact (I)**: a 150ms-long 100Hz exponentially decaying sinusoid (see e.g., Figure 2.2.2 on impact rendering for an example of use),
- **Noise (N)**: 300ms of white noise (see e.g., section 2.2.1 on texture rendering),
- **Sine (S)**: 300ms of a pure sine wave (see e.g., Figure 2.2.2 on rendering liquid contents).

We considered four stimulus locations (see Figure 2.3):

- **Thumb (T)**: Only the vibrotactor on the thumb side of the hand (localized)
- **Pinkie (P)**: Only the vibrotactor on the pinkie side of the hand (localized)
- **Monolithic (M)**: Only the vibrotactor at the center of the object (monolithic)
- **"Pseudo-monolithic" (PM)**: Both thumb- and pinkie-side actuators simultaneously (i.e. monolithic simulated with localized actuators).

Each trial consisted of a sequence of three stimuli of the same waveform, two of which had identical locations and one which had a different location from the others (the oddball, randomly positioned in the sequence). Stimuli were presented in sequence with a 1s pause between them, after which the participant was asked which stimulus felt most different. Using the controller held in their non-dominant hand, participants responded by choosing one of three options (first, second, last) presented as a menu in the VE. In a prior pilot study, stimulus intensities for each type and location were perceptually matched between one another to avoid bias due to unequal perceived stimulus amplitudes.

The experiment was divided into three blocks according to the cue waveform. Within each block, participants were provided with all possible stimulus location combinations (12 possibilities) for all possible oddball positions in the sequence (3 possibilities) in a fully randomized order (i.e. 36 trials per block).

Results

We calculated the oddball correct identification rates for the 6 possible location pairs, for each of the 3 stimulus waveforms (see Table 2.1).

Oddball identification rates were not normally distributed (Shapiro-Wilk normality tests). In all cases, they were found to be significantly above chance levels (one-sample Wilcoxon signed-rank tests). Stimuli on the lateral actuators (T/P) were correctly differentiated more than 83% of the time for all waveforms. Except for the N waveform, the same was the case for differentiation between the localized (T or P) and monolithic (M) actuator locations. The lateral actuator locations were more often confused with the pseudo-monolithic (PM) rendering, but performances were still above chance. Finally, the monolithic (M) and pseudo-monolithic (PM) rendering was often confused, but discrimination rates were still above chance.

	H3			vs		
	H1	H2		H3		
	T/P	**T/M**	**P/M**	**M/PM**	**T/PM**	**P/PM**
Impact I	**0,833***	**1***	**0,833***	**0,5***	**0,5***	**0,5***
	p =6,104e-5 effsize = 0,88 CI = [0,67 ; 0,92]	p = 6,104e-05 effsize = 0,88 CI = [0,75 ; 1]	p = 3,05e-5 effsize = 0,88 CI = [0,83 ; 0,92]	p = 0.002 effsize = 0,72 CI = [0,41 ; 0,67]	p = 0.0007 effsize = 0,77 CI = [0,42 ; 0,74]	p = 0.001 effsize = 0,76 CI = [0,34 ; 0,58]
Noise N	**0,833***	**0,667***	**0,917***	**0,667***	**0,833***	**0,667***
	p = 6,104e-5 effsize = 0,87 CI = [0,68 ; 0,92]	p = 0.0003 effsize = 0,85 CI = [0,5 ; 0,75]	p = 6,104e-5 effsize = 0,85 CI = [0,75 ; 1]	p = 0.0001 effsize = 0,84 CI = [0,5 ; 0,75]	p = 3,052e-5 effsize = 0,88 CI = [0,74 ; 0,91]	p = 0.0002 effsize = 0,78 CI = [0,5 ; 0,76]
Sine S	**1***	**0,833***	**0,833***	**0,5***	**0,833***	**0,917***
	p = 3.052e-05 effsize = 0,88 CI = [0,75 ; 1]	p = 6.104e-05 effsize = 0,87 CI = [0,67 ; 0,75]	p = 3.052e-05 effsize = 0,88 CI = [0,74 ; 0,91]	p = 0.0004 effsize = 0,79 CI = [0,42 ; 0,75]	p = 3.052e-05 effsize = 0,88 CI = [0,75 ; 0,92]	p = 3.052e-05 effsize = 0,88 CI = [0,74 ; 1]

0 1

Table 2.1: Median correct oddball identification rates for each location pair within each waveform condition (redder values indicate better performance). (*) indicates the median rate significantly differs from chance level (0.33) (Wilcoxon signed-rank tests: 95%-confidence intervals (CI) for the median, p-value and effect size are shown below).

Given the non-normal distribution of the data, we used a generalized linear mixed model to study participants responses with respect to the waveform, the pair of stimulus locations used and the position of the Oddball. Participants were considered as a random effect in the model. Analysis of deviance of the answers showed significant effects of the waveform, location and the oddball position ($p < 0.001$). We did not find any significant interaction effects between the waveform and the stimulus locations. We performed a post-hoc analysis on the different conditions using a Tukey test adapted to the logistic generalized regression model. Trials where the oddball was presented first had higher correct answer rates compared to when the oddball was in second ($Z = 4.02, p < 0.001$) or third position ($Z = 3.14, p = 0.005$). This would indicate that the task was likely cognitively easier when the oddball came first which might be caused by the primacy bias. However, given that the proportion of trials where the oddball came first was identical for all Waveform and Location pair conditions, it is unlikely to affect our conclusions.

Correct answer rates were significantly higher when the Sine waveform was used compared to Impact ($Z = -3.38, p = 0.002$) and Noise ($Z = -2.56, p = 0.028$). Participants had a significantly lower rate of correct answers for M/PM compared to all other pairs of stimuli except P/PM ($p < 0.001$), as well as for P/PM compared to T/P and M/P ($p < 0.001$).

Discussion

H1 is clearly supported, as trials combining `T` and `P` as the standard and oddball (and vice versa) yield a very high rate of correct answers, regardless of the cue type. H2 is also strongly supported, with trials respectively combining `T` or `P` and `M` as the standard and oddball (and vice versa) also yield correct identification rates significantly above chance levels, for all three cue types.

H3, however, is not supported. Despite discrimination rates between `M` and `PM` being among the lowest for all stimuli, these discrimination rates are still significantly above chance, indicating that `PM` yields a different sensation to `M`. While this does not conclusively prove that `PM` is unusable to provide the sensation of a central monolithic vibration of the object, caution should be exercised when considering substituting `M` with `PM`. Furthermore, for impact cues, confusion rates for `T` and `PM` as well as between `P` and `PM` are significantly higher than those between `T` and `M` and `P` and `M` respectively. This is likely due to an effect of stimulus duration on discrimination ability.

It is therefore sensible to conclude that spatializing stimuli within a hand-held object is possible using a multi-actuator approach, as cues from localized actuators are readily distinguishable from one another and localized cues are markedly different from monolithic cues. This effect also seems robust to large variations in the stimulus waveforms.

However, it appears that for situations where both monolithic feedback and localized feedback are required, "simulating" monolithic feedback by simultaneously triggering multiple localized actuators may not be a functional alternative. Thus, it is likely that additional actuators may be required in such cases.

2.1.3 Discrimination between localized vibrotactile cues

Research question and hypotheses

We hypothesize that when using localized VF, varying the amplitude distribution across the actuators at the `T` and `P` locations (see section 2.1.2) could yield an impression of the stimulus location moving from side to side. This idea is based on the "funneling illusion" [Alles 1970; v. Békésy 1958] previously discussed in section 2.1.2. To assess the potential effectiveness of this approach, we conduct an experiment aiming to calculate the just-noticeable-difference (JND) in stimulus location based on the balance of actuator amplitudes when a stimulus is simultaneously played on two opposing lateral actuators. Given the difficulty in discriminating between impact stimuli played on a single localized actuator and those played simultaneously on two actuators in the previous experiments (See T/PM and P/PM columns in Table 2.1), we expect any potentially occurring funneling illusion to be waveform-dependent.

Our hypotheses are the following:

H4: Varying the amplitude balance will lead to the impression of the resulting stimulus being located more towards one side or the other, regardless of the stimulus type.

H5: JNDs for the waveforms `N` and `S` will be lower than for `I` (i.e., more "location levels" will be discernible).

Materials and methods

To investigate this, we varied the amplitude distribution $R = A_P - A_T, R \in [-1; 1]$ between both lateral actuators (`T` and `P` locations) whose amplitude is respectively noted A_T and A_P.

We used a two-alternative forced choice (2AFC) procedure based on the method of constant stimuli. In each trial, participants were presented a reference stimulus with R=0 (equal amplitude on both actuators) and a test stimulus with R chosen from one of 21 possible levels (0.1 increments in $R \in [-1; 1]$). They were asked whether the test felt positioned more towards the thumb or towards the pinkie, compared to the reference. The order of test and reference stimuli was randomized within trials. We considered the same set of representative stimulus waveforms and controlled grasp position as in section 2.1.2.

The same group of 16 participants (8F, 8M, all right-handed, ages 21–52 (M=26.9, SD=8.8)) took part in the experiment, following the first one. They performed three blocks of 84 trials (4 repeats per value of R), with each block corresponding to one of the three stimulus types `I`, `N` or `S` (see section 2.1.2). The order of blocks was counterbalanced across participants. Trial order within blocks was fully random.

After the experiment, participants filled out a short questionnaire assessing their fatigue, perceived task difficulty and performance, and asking them to estimate the number of actuators inside the tangible sphere.

Results

We plotted the proportion of *"Test stimulus more towards the pinkie"* responses against the amplitude balance R ($R = 1$ indicated a stimulus played entirely on the pinkie-side actuator `P`) in Figure 2.5. We fit cumulative Gaussian distributions to each participant's data to obtain psychometric functions, from which we derive the 75%-JND.

Poor performance for the impact (`I`) stimulus prevented us from computing 75%-JNDs for all participants. For the `N` and `S` stimuli, mean JNDs were found at 0.27 (Med: 0.26, IQR: 0.12–0.41) and 0.42 (Med: 0.27, IQR: 0.22–0.53) respectively. Individual JNDs were not normally distributed (Shapiro-Wilk tests), and a non-parametric Friedman test showed no significant difference between the JND distributions for `N` and `S` ($W = 0.14, p = 0.13$).

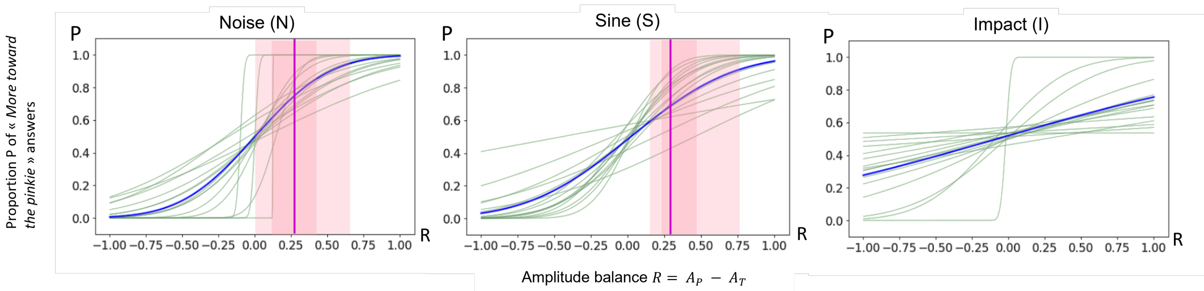

Figure 2.5: Psychometric functions for each cue type. Individual functions are shown in green and the mean psychometric function in blue. Dark red bars show the median JND, surrounded by areas respectively marking the interquartile range and full range of individuals' JNDs in increasingly lighter shades of red.

Discussion

When looking at participants' performances for $R = 1$ or $R = -1$, we note that the results appear coherent with data for the `P/PM` and `T/PM` location pairs from subsection 2.1.2.

H4 is not supported, as for `I` the effect is minimal and insufficient to calculate a 75%-JND value. It appears that the stimuli with longer durations (`N` and `S`) are better suited to achieving the desired effect, since they both allow approx. 7 virtual stimulus locations to be rendered by varying the amplitude balance, while `I` allows 2 to 3 locations to be rendered. H5 is therefore also supported. On average, questionnaires showed that participants estimated that the tangible sphere contained between 4 and 5 actuators (min: 1; max: 9). This confirms that varying R often yielded the illusion of a change of stimulus location within the object which is coherent with the calculated discriminable locations.

This means that for applications relying on longer stimuli, it seems reasonable to count on the funneling effect to use a minimal number of actuators to provide a localized sensation. In our case, this translates to 2 actuators possibly providing up to 7 discriminable virtual vibration locations within the sphere. For applications relying on shorter stimuli (e.g., impacts) where more than 3 distinct perceived vibration locations are desired, it seems that more actuators would be required.

2.1.4 Vibrotactor location identification

Research question and hypotheses

The goal of the present experiment was to assess the ability of participants to determine the location of one among many vibrotactors used alone inside a spherical tangible object, as well as possible effects of stimulus intensity on location discrimination performance. Prior experiments showed that approaches with many actuators may be particularly relevant to use-cases involving short stimuli (see subsection 2.1.3). With the design of vibrotactile tangibles discussed in section 2.1.1, the actuators are not mechanically isolated from one another in any particular way. Therefore, vibrations from one actuator may propagate throughout the object, stimulating the whole hand. This may prove problematic in the context of using many localized actuators to render short stimuli.

Because of the similar results observed for `S` and `N` stimuli in both previous experiments, we omitted the sine stimuli and chose to focus on impact stimuli at two different frequencies as well as noise stimuli for the present experiment. Our first hypothesis is **(H6)**: Stimulus waveform may affect location discrimination accuracy.

Tactile sensitivity varies across the hand. For example, the best vibrotactile acuity (in the millimeter range) is observed on the volar face of the fingers [Perez 2000; 1998], against ranges going up to a few centimeters on the palm [Sherrick 1990]. Thus, it seems reasonable to assume that actuator location with respect to the hand may affect location discrimination, leading us to hypothesize **(H7)**: Stimulus locations relative to the hand will affect location discrimination accuracy.

We suppose that intensity is a major factor in discriminating the location of a vibrotactor, and thus hypothesize **(H8)**: Stimulus intensity will affect location discrimination accuracy.

Materials and methods

This experiment used the spherical tangible capable of holding 5 vibrotactors (see Figure 2.1-B). The vibrotactors are located beneath each finger, in what we hypothesize is the best-case scenario for vibration source location discrimination as stimuli are generated close to the fingertips, i.e. the most sensitive part of the hand [Perez 2000; 1998]. Markings on the surface of the sphere allowed the experimenter to ensure participants' fingers were properly placed above the actuators.
We considered three experimental variables:

- **Wav** - The impact stimulus waveform (White noise, 50Hz exponentially decaying sine or 100Hz exponentially decaying sine).
- **Pos** - The pair of reference and comparison stimulus locations on the fingers.
- **Lvl** - The stimulus intensity level (weak or strong).

The weak intensities were chosen as the lowest mean intensity at which 100% of participants could detect a stimulus, as determined in a prior pilot study. The strong intensity was chosen as 10 times the weak intensity level.

The experiment involved 18 right-handed participants (13 M, 5 F, ages 21-33 (M=24.3, SD=3.8)).

Procedure

Participants performed a series of trials during which vibrations were played on a random actuator, after which they were asked to indicate where they felt the vibration using a continuous circular slider representing the tangible sphere (see Figure 2.6).

The experiment was divided into three blocks. Each block used a different type of stimulus played for 0.3 seconds: an exponentially decaying sinusoid at 50Hz, another at 100Hz or white noise. Each one of the 25 ordered pairs of stimulus locations inside the sphere was repeated three times, but at each of the two possible intensity levels for `Lvl`, for a total of 150 trials in each block. All conditions were balanced between participants to avoid any order effects. Participants' responses (i.e., slider position values) were collected for each trial.

The sphere having a circumference of 22cm, we measure mean localization errors ranging from -11cm to 11cm. Negative error values indicate a bias in the pinkie toward thumb direction, while positive values indicate a bias in the opposite direction (see Figure 2.6). The mean distance between finger pairs on the circular response slider was 3cm. In the following, we label the actuator positions as `Th` (Thumb), `In` (Index), `Mi` (Middle finger), `Ri` (Ring finger) and `Pi` (Pinkie) (see Figure 2.6).

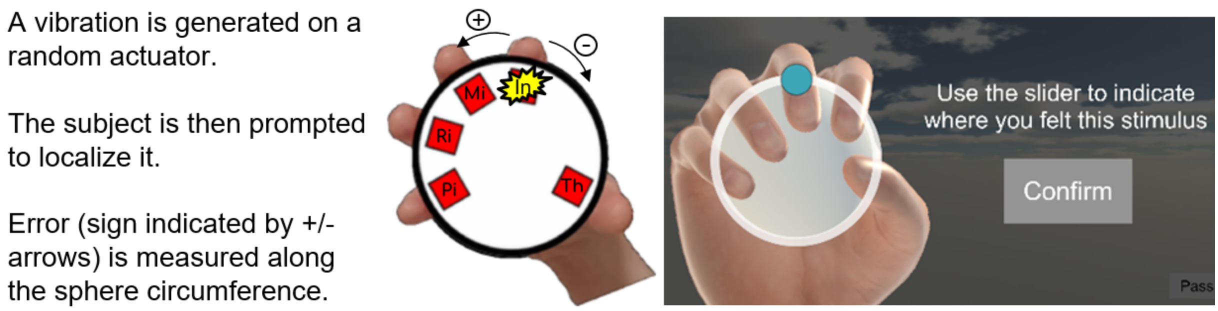

Figure 2.6: Location discrimination experiment: After a vibration, the participant must locate it within their hand using an on-screen circular slider.

Results

We used a linear mixed model on the collected data with respect to the three conditions (`Wav`, `Pos` and `Lvl`) to study participant responses with respect to the stimuli. Participants were considered as a random effect in the model.

Measures of mean location discrimination errors are reported in Table 2.2. An analysis of deviance for the slider position answer showed a significant effect on the `Pos` condition ($p < 0.001$). We did not find any significant effect for `Lvl` ($p = 0.29$) and `Wav` ($p = 0.45$). However, we observed an interaction effect between `Lvl` and `Pos` ($p < 0.001$). We performed a post-hoc analysis on the different conditions using a Tukey test adapted to the logistic generalized

	Th	*In*	*Mi*	*Ri*	*Pi*
Mean error ± SD (*cm along the circumference*)	-1,3 ± 2,6	-1,5 ± 3,7	0,4 ± 2,4	0,2 ± 2,9	1,9 ± 1,6

Table 2.2: Mean error in localization of the vibration source.

regression model. Regarding `Pos`, we found a significant effect between all the locations ($p < 0.001$), except between the `Th` and the `In` locations ($p = 0.56$) as well as between the `Th` and `Ri` location ($p = 0.13$) on the other side.

Discussion

Participants were generally accurate in estimating the position of the vibration source, placing it within a single between-finger distance from its actual position. The spread of errors is similar across fingers except for the index and pinkie which show higher spreads indicative of a higher uncertainty in participant responses.

H6 was not verified as `Wav` did not affect localization errors. Our results tend to support H7, as localization error significantly varies with respect to stimulus position. Furthermore, we observe a bias towards localizing stimuli at `Th` and `In` more in the direction of the thumb whereas stimuli at `Mi`, `Ri` and `Pi` are localized more towards the pinkie. Localization error for `Th` and to a lesser extent `In` could partly be explained by vibrations propagating to the nearby thenar eminence, which could skew the perception of location towards the side of the thumb. H8 was not verified, as localization errors were unaffected by `Lvl`.

With respect to the design of vibrotactile tangibles, these results indicate that applications requiring fine vibration location rendering on the object surface could likely use upwards of 5 vibrotactors. However, space and adequate mechanical isolation rapidly become challenging with an increased number of vibrotactors.

2.2 Multi-actuator vibrotactile rendering for VR manipulation

2.2.1 Multi-Actuator Vibrotactile Rendering

Based on the literature on vibrotactile rendering presented in subsection 1.3.1, we implemented feedback for sensations arising from manipulating vibrating or pulsating objects, impacts between a hand-held object and the environment, textures of the environment and forces or impacts resulting from the contents of a manipulated container. The present section details the algorithms for each of these haptic effects and how they can leverage the potential offered by stimulus spatialization. An evaluation of the added benefit of spatialization is discussed in subsection 2.2.2. In the proposed VR interactions, we use the same system setup as previously described in subsection 2.1.1, with a spherical tangible object containing three built-in vibrotactors (at locations `T`, `P` and `M`). This allows each of the proposed rendering schemes to generate either localized (using actuators at locations `T` and `P`) or monolithic (using actuator location `M`) vibrotactile feedback.

Vibrating and pulsating objects

Vibrotactile feedback can serve to render properties of manipulated objects themselves, in particular vibrations coming from an object held in hand (e.g., a motorized tool). In this case, there is no generally applicable rendering model as the vibrations depend on the object to be rendered.

Given that rendering object vibrations relies on prolonged sinusoidal stimuli (either pure sines or a superposition of sines), results from our prior experiments indicate that spatialization of these cues along an axis crossing the handheld object could be effective by continuously varying the balance of amplitudes between off-center vibrotactors (see subsection 2.1.3). In this manner, a virtual vibration source could be displayed more or less off center with respect to the position at which virtual object is grasped.

In addition to vibration, another phenomenon termed *haptic beats* [Yang 2014] can be used to render pulsing virtual objects held in hand. This phenomenon occurs when two sine waves with a small difference in frequency are delivered to two separate but close locations on the skin, introducing a “beating” sensation. It is especially perceivable under the fingertips and the palm [Yang 2014]. We reproduced this effect within the spherical end-effector by playing different frequency vibrations on two distinct vibrotactors. A similar but less marked effect arises when superimposing sinusoidal waveforms on a single actuator, allowing for a monolithic alternative.

Rendering impacts

When exploring a VE with their hand or interacting with the VE with a grasped object or tool, the user can impact virtual objects or surfaces, generating vibrations depending on impact location, speed and material of the objects involved. As discussed in subsection 1.3.1, vibrotactile impact rendering commonly uses an exponentially decaying sinusoid model [Okamura 1998; Wellman 1995]. The impact waveform used to generate the signal itself is defined by $x(t) = A(v)e^{-\beta t}\sin(\omega t)$, with A the amplitude, a function of the impact velocity, and β, ω depending on the simulated material. Here, we used material parameters identified by Choi et al. and Okamura et al. [Choi 2013; Okamura 1998]. We consider two impact scenarios.

A. A small object held in the hand (e.g., a baseball) impacts another (e.g., a table). In this situation a uniform vibration is generated within the object, and the impact can be rendered either using a single monolithic actuator or multiple localized actuators delivering simultaneous equal-amplitude stimuli ("pseudo-monolithic" case described in subsection 2.1.2). Alternatively, the impact location may be precisely rendered by varying the balance of amplitudes between simultaneously activated localized actuators, as described in subsection 2.1.3.

B. A large object held in hand (e.g., a bat) impacts another one (e.g., a ball) away from the hand. In this case, the impact should produce more intense vibrations on the side towards which the impacts occurs. Thus, a straightforward approach consists in displaying the impact on the closest localized actuator. However, since impact waveform location discrimination is not as good as for other waveforms (see subsection 2.1.2 and subsection 2.1.3), it may also be sufficient to use a monolithic or pseudo-monolithic approach. This question is further addressed in subsection 2.2.2.

Macroscopic texture

As discussed in subsection 1.3.1, macroscopic texture features are mediated predominantly by spatial cues, and often rendered as a series of impacts as users scan the virtual surface. Since setting up a collider to trigger impacts for every bump of a textured surface is rather cumbersome, we opt for a simplified approach where textured surfaces were modeled by two parameters: distance between bumps and bump orientation. As the user dragged a sphere over the virtual surface, we compute the estimated frequency of impacts from the velocity at the contact and adjust the rate at which impact stimuli are triggered based on the result.

Just like impacts at the level of the hand (case A in section 2.2.1), macro texture can be rendered using a monolithic vibrotactor or a pseudo-monolithic substitute. However, we hypothesized that triggering the impact waveforms on the actuator located in the direction towards which the user is moving the handheld object across the surface may reinforce the illusion, in which case localized rendering would be beneficial.

Texture roughness

We chose to adapt the open-source Penn Haptic Texture Toolkit [Culbertson 2014] to our needs in the present system. This toolkit follows a data-driven rendering approach based on real-world contact force and acceleration data during free exploration of textures. Each recorded texture is modeled as a collection of autoregressive processes stored in a Delaunay triangulation according to the scanning speed and normal force associated with them. At runtime, the speed of the user over the virtual texture is used to determine which models to interpolate.The resulting coefficients are used to generate the signals sampled at 10 kHz for the actuators.

Since procedural generation of audio signals is not possible using Syntacts, we used the Unity audio engine, through which custom filters can be applied over an audio source. This however offers little control over the haptic rendering latency.

Texture roughness could be rendered using a monolithic actuator, however we hypothesize that similarly to macro texture, vibrations on the actuator located towards the direction of motion may also reinforce the illusion. We further investigated this idea in subsection 2.2.2.

Rendering contents of a grasped object

Previous interactions focused on rendering information about contacts and haptic exploration interactions. Vibrotactile feedback provided inside a tangible object can, however, also serve to enrich manipulation interactions by providing physical information on the manipulated object itself.

In this context, we explored rendering virtual contents of a grasped object, such as the movement of a liquid in a glass or the movement of dices shaken inside a cup. Rendering small objects such as dice or marbles inside a cup is done using the physics simulation of the Unity engine. For every impact between the object in hand (the "container") and an object within it (the "contents"), the distance between the impact location and the position of all actuators is calculated. The closest to the virtual impact is then selected to play the impact effect. A higher number of actuators would thus theoretically enable a higher resolution, within the limits of users' ability to discriminate vibration locations (see section 2.1.4). We compare this spatialized approach to a simple monolithic rendering of solid content impacts, wherein the monolithic actuator is triggered every time the contents impact the container, in subsection 2.2.2.

To give the illusion of a fluid inside the object, we attach a virtual mass to the center of the virtual object with an underdamped spring, leading the mass to lag behind the object during movement and to oscillate when the movement stops. The amplitude of vibration displayed on each actuator is inversely proportional to the distance of the mass from said actuator, generating a sensation of motion between actuator locations.This approach can be seen as the vibrotactile equivalent to the purely mechanical rendering of fluids inside a tangible proposed by Sagheb et al. [Sagheb 2019]. We compare this approach to monolithic rendering of fluids, wherein a central actuator's stimulus amplitude is proportional to the lateral displacement of the mass away from the equilibrium point in subsection 2.2.2.

2.2.2 Does localized VF provide a benefit over monolithic VF in certain interactions?

Research questions and hypotheses

In this section, we investigate whether using multiple actuators for the rendering schemes discussed in subsection 2.2.1 provides added benefits over single-actuator monolithic feedback. We asked the same research question for each of the feedback schemes, i.e. whether users perceived the localized or monolithic stimuli provided as more coherent with the associated visual feedback.

Our hypotheses are the following:

H9: For pulsating objects (haptic beats), the stronger effect that is achievable by using two actuators rather than a superposition of waveforms on a single actuator will lead to the multi-actuator rendering being perceived as more coherent;

H10: For vibrating objects and impacts, the additional spatial information provided by localizing the VF towards the location of the virtual source of the vibration will lead to the combined visual and haptic feedback as being perceived as more coherent than monolithic VF;

H11: For cues generated in response to user motion (micro and macro texture, object contents), localizing the VF towards the direction of motion (of the handheld object or its contents) will reinforce the illusion of motion, leading to the feedback to be perceived as more coherent than monolithic VF.

Materials and methods

We determined the level at which `T`, `P` and `PM` vibrations were perceived at the same level as `M` through a pilot experiment using a method of adjustment. For each stimulus type and location, participants adjusted the intensity until it perceptually matched that of a monolithic reference stimulus. We used the same sphere and controlled grasp position as in section 2.1.2.

To answer our main experimental question, we evaluated the subjective perception of 7 different types of haptic sensations. The experiment is a collection of 6 independent component experiments, each following a within-subject design. This makes up 6 blocks, each dealing with a specific type of haptic sensation (i.e. vibrating object, pulsating object, impacts, macro and micro texture, solid content, liquid content). The order of blocks was counterbalanced across participants using a Latin square design. Within each block, trials consisted of participants being presented with pairs of sensations (one monolithic and one localized). The collected data were participants' subjective assessment of perceived coherence between visual and tactile stimuli in each condition, when asked in VR *which one felt more coherent between what they saw (visual) and what they felt (tactile).* 21 participants performed the experiment (8F, 13M, 20 right-handed, ages 22-33 (M=24.6, SD=3.2), 15 having some experience with haptics). Blocks contained 6 repetitions of each stimulus pair, and the pair presentation order was counterbalanced across participants.

Vibrating objects: In the vibrating object block (Figure 2.7-A), participants held a virtual sphere with a visible eccentric rotating mass on either side. In each trial, one mass would spin while either the central monolithic actuator or the closest localized actuator played an associated vibration.

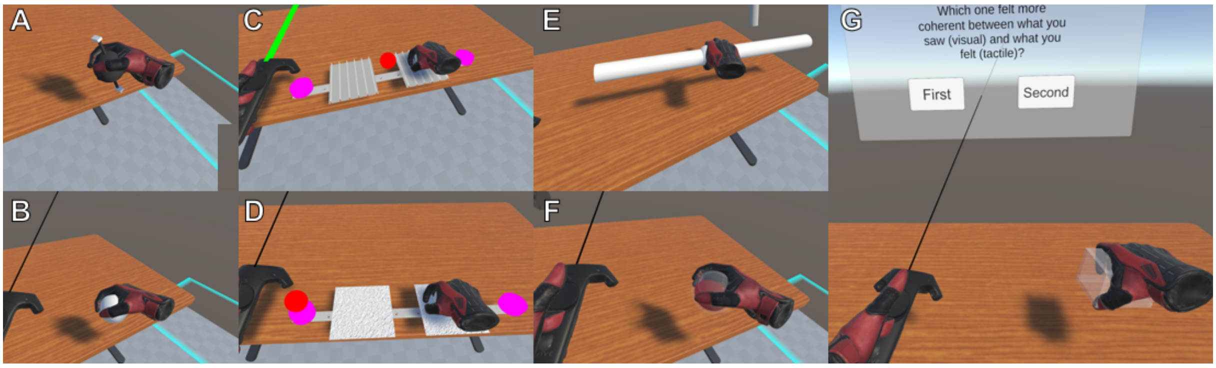

Figure 2.7: The experiment assessing perceived coherence of localized vs. monolithic VF focused on 7 different properties: (A) Vibration of objects, (B) pulsating objects, (C) macro texture (bumps), (D) texture roughness, (E) impacts between a handheld object and the environment, (F) liquids contained in a handheld container and (G) solids contained in a handheld container. Participants responses were recorded for each stimulus pair (G).

Pulsating objects: In the pulsating object block (Figure 2.7-B), participants held a sphere whose visual diameter periodically grew and shrunk at the specified pulse rate while a haptic beats effect was generated at the same rate. This beating effect was either generated by superimposing two different frequency sines on the monolithic actuator or by distributing each sine on one of the localized actuators.

Textures: In the textures block (Figure 2.7-C,D), the tangible sphere was fixed to a linear guide rail constraining its motion along one axis. Pairs of textured surfaces were displayed in front of the user, who was instructed to drag a virtual sphere across them. A visual guide was used to ensure consistency in hand motion speeds across all trials. The actuator location was switched between virtual surfaces, with playback occurring either on the monolithic central actuator or on the localized actuator to the side towards which motion occurred.

Impacts: In the impacts block (Figure 2.7-E), participants held a virtual stick extending symmetrically around the hand. An object would then fall and randomly impact the stick on one side. A corresponding vibration was either played on the monolithic actuator or on the localized actuator to the side of the virtual impact.

Contents: In the solid and liquid contents blocks (Figure 2.7-G,F), participants held a virtual transparent container with a visible marble inside. Participants were instructed to shake the container from side to side for 5 seconds. A ghost hand performing the desired motion was displayed to ensure consistency between trials. Corresponding VF was either played back from the monolithic actuator or using the pair of localized actuators as described in section 2.2.1.

Results

For each condition, we calculated the proportion of trials in which participants respectively expressed a higher perceived coherence for the monolithic or localized versions of the vibrotactile feedback (see Table 2.3). We compared each proportion of perceived coherence to the case where localized and monolithic feedback were perceived as equally coherent using exact binomial tests.

Vibrating and pulsating objects: Regardless of the side of the hand on which the virtual vibration occurs, participants perceive the localized VF of object vibration as more coherent than the monolithic alternative. We therefore conclude that H10 is verified for this rendering scenario. However, H9 does not appear to be verified since we fail to show any significant difference in perceived coherence for localized or monolithic feedback of object pulsation. It is worth noting that in this rendering case, localized feedback is not detrimental to perceived coherence despite it not showing any significant benefit.

Impacts: When rendering impacts on a virtual handheld object, participants seem to show no difference in perceived coherence towards localized or monolithic feedback of impact vibrations. This appears coherent with prior results showing poorer impact localization performance (see subsection 2.1.2 and subsection 2.1.3). A finer analysis of VF coherence as a function of the side to which the impact occurs reveals no significant difference from the overall trend. For rendering impacts, it thus appears that localized vibrotactile feedback provides neither a benefit nor a disadvantage. H10 is thus not verified in this case.

Macro Texture (bumps): Overall, we found no difference in perceived coherence towards localized or monolithic VF for macroscopic texture rendering, contradicting hypothesis H11. Since macroscopic texture is very similar to impacts, this appears coherent with our other results. An analysis of coherence as a function of the motion direction revealed that participants preferred localized feedback when the motion occurred towards the thumb (H11 supported), but preferred monolithic feedback when the motion occurred in the opposite direction (H11 contradicted).

Micro Texture (roughness): Overall, we see no difference in perceived coherence towards localized or monolithic VF for texture roughness. H11 is therefore not supported for rendering of texture roughness.

Contents: When rendering solid contents of a handheld container, participants again did not perceive localized or monolithic VF as more coherent with the VE. This is coherent with prior results on impact rendering for which H10 was not verified. For liquid contents, however, participants rate localized feedback as significantly more coherent than monolithic VF. H11 is therefore partially supported.

	Vibrating	T/M	P/M	**Pulsating**	**Impact**	T/M	P/M
Localized	63% *	60% *	66% *	53%	47%	45%	49%
Monolithic	37%	40%	34%	47%	53%	55%	51%
Statistics	p = 2.18e-5 $CI: \begin{pmatrix}0.69\\0.57\end{pmatrix}$	p = 0.025 $CI: \begin{pmatrix}0.69\\0.51\end{pmatrix}$	p = 2.29e-4 $CI: \begin{pmatrix}0.75\\0.58\end{pmatrix}$	p = 0.533 $CI: \begin{pmatrix}0.61\\0.44\end{pmatrix}$	p = 0.413 $CI: \begin{pmatrix}0.54\\0.41\end{pmatrix}$	p = 0.327 $CI: \begin{pmatrix}0.54\\0.36\end{pmatrix}$	p = 0.929 $CI: \begin{pmatrix}0.58\\0.40\end{pmatrix}$

	Bumps	T/M	P/M	**Texture**	T/M	P/M	**Liquid**	**Solid**
Localized	51%	40% *	63% *	46%	42%	51%	75% *	46%
Monolithic	49%	60%	37%	54%	58%	49%	25%	54%
Statistics	p = 0.753 $CI: \begin{pmatrix}0.57\\0.45\end{pmatrix}$	p = 0.025 $CI: \begin{pmatrix}0.49\\0.31\end{pmatrix}$	p = 0.005 $CI: \begin{pmatrix}0.71\\0.54\end{pmatrix}$	p = 0.396 $CI: \begin{pmatrix}0.54\\0.39\end{pmatrix}$	p = 0.155 $CI: \begin{pmatrix}0.53\\0.31\end{pmatrix}$	p = 0.913 $CI: \begin{pmatrix}0.62\\0.40\end{pmatrix}$	p = 9.61e-9 $CI: \begin{pmatrix}0.83\\0.67\end{pmatrix}$	p = 0.42 $CI: \begin{pmatrix}0.55\\0.37\end{pmatrix}$

Table 2.3: Percentage of perceived coherence between localized and monolithic stimuli for each interaction. For vibrating objects, impacts, macro and micro texture, T/M and P/M respectively show the detailed proportion of perceived coherence for localized stimuli presented on the thumb and pinkie side of the hand respectively. (*) indicates the distribution is different from a binomial distribution of parameter p = 0.5 (Exact binomial test: 95%-confidence intervals (CI) for the true proportion of perceived coherence towards localized VF are shown in brackets, p-value is shown above). Green indicates significant preferences.

Discussion

Both H10 and H11 are partly supported by our results.

Our preliminary investigation highlighted that using the rendering approaches proposed in subsection 2.2.1, users expressed a clear preference for localized VF for both the vibrating objects scenario (involving a prolonged sinusoidal stimulus without leveraging a "funneling" effect) and the liquid contents scenario (also involving a prolonged sinusoidal stimulus, this time leveraging a "funneling" effect). For such effects, using a localized VF setup within the tangible object will provide a benefit in terms of the experience being perceived as more coherent.

In most other scenarios, be they scenarios involving short stimuli (impacts and solid contents) or prolonged stimuli (pulsating objects, texture roughness), the proposed localized rendering approaches did not show any significant benefit in terms of perceived coherence. We can conclude that, for these effects, a localized setup is not necessary, but also not detrimental. Basically, if these effects are to be used alone in a VR scenario, using monolithic feedback would make sense given the lower system complexity. However, if used in a scenario where other effects which can benefit from localized VF are being used, a localized VF setup is a viable option for the entire set of considered stimuli.

It is also possible that using different waveforms could unlock untapped potential for localization in these scenarios, although this would require further investigation. Our perceptual studies have shown that funneling likely cannot be used in conjunction with shorter stimuli (impacts), which somewhat limits the scope of possibilities. There may however be potential benefits to be gained from modifying the proposed rendering approaches for e.g., pulsating objects or texture roughness in order to leverage “funneling” effects, to e.g., provides sensations of a moving origin of the pulsation within the object or a changing contact point between object and textured surface.

The results obtained in the macro texture are ambiguous. There seems to be a preference towards monolithic feedback when motion is done towards the thumb side of the hand, but for localized feedback when motion is done towards the pinkie side.The thumb side of the hand is more sensitive to VF due to the thenar eminence. This may cause the localized sensation on that sideto be perceived as stronger, or may lead to the bumps being felt too much on the side of the object, rather than towards the tip of the lower hemisphere of the object, where the virtual physical contact is expected to occur. This could have caused a higher perceived incoherence in the localized condition, for motions going towards the thumb side of the hand. Further investigation at different intensity levels and using the non-dominant hand could be interesting to verify this.

For this result, it is not possible to give clear guidelines for designers. If monolithic feedback is indeed preferred in a specific situation, this would mean that applications combining multiple effects would require a combination of localized and monolithic central actuators, which would be selected based on how appropriate they are to a given stimulus to be rendered.

Use-Cases

Since our experiment showed that multi-actuator localized rendering schemes were either beneficial over or equivalent to monolithic VF, we developed an VR use-case using only two lateral actuators and demonstrating the inclusion of all rendering schemes discussed in subsection 2.2.1 into a single coherent VE.

In the VE, users can explore an outdoor scene , manipulating various objects such as e.g., a ball (see Figure 2.8-A,B), a bat (see Figure 2.8-C), a hand-held mixer (see Figure 2.8-D) a wine bottle (see Figure 2.8-E) while receiving tangible haptic feedback. We render impacts (Figure 2.8-B,C,D), surface texture (Figure 2.8-A,B,C), vibrating handheld objects (Figure 2.8-D) as well as liquid contents (Figure 2.8-E) of manipulated objects as per the approaches described in subsection 2.2.1.

Figure 2.8: VR use-case showcasing the different possible interactions. Immersed users can grasp and manipulate objects (F), feel impacts (B,C,D) and textured surfaces through an object held in hand (e.g., sand and wood in A and B), manipulate vibrating tools (the mixer in D) and feel the dynamics of object contents (e.g., wine in the bottle in E).

2.3 Two-actuator tangible for spatialized impact rendering

In this section, we explore the rendering of spatialized impacts happening on a virtual hand-held object larger than the tangible held by the user (case B in section 2.2.1). We consider a tangible cylindrical handle that allows interaction with virtual objects, which can represent objects larger than its real size in the virtual environment. This handle is fitted with a pair of vibrotactile actuators with the objective of providing in-hand spatialized cues indicating direction and distance of impacts. We hypothesize that by using two actuators, we can provide localized vibrotactile feedback which can inform the user about the distance and direction where the impact occurred on the larger virtual object they are manipulating.

2.3.1 Design

We investigate the extent to which spatializing impact cues by distributing them between two actuators embedded in a cylindrical tangible handle (see Figure 2.9-A) is effective in providing users with information on impact direction. We also seek to understand how this approach affects perceived realism and impact properties, and whether it is compatible with existing approaches to rendering impact distance in a setup using a single actuator (e.g. [Gongora 2016; Sreng 2008]).

To investigate this, we compare distance and direction discrimination performances, as well as perceived realism and virtual object material properties in VR, using different impact vibration models (see Table 2.4).

We formulate the following hypotheses:

H1: Spatialization of impacts in hand by assigning impact waveforms to distinct vibrotactors will allow discrimination of impact direction, regardless of the chosen impact vibration model.

H2: Impact models coding distance with more redundant parameters (see Sec. 2.3.1 for the details of the models) will yield better distance discrimination performance.

Handle design

The haptic handle is a cylinder (see Figure 2.9–A) made of two interlocking parts each housing a vibrotactile actuator. Parts are 3D printed using PLA, measuring 5cm in diameter and 10cm on length once assembled. We use two voice-coil actuators (HapCoil One, Actronika) to render vibrotactile signals, both wired to an external amplifier. Vibration signals were generated using Unity and the Syntacts plugin [Pezent 2020], with the audio output of the computer linked to the amplifier and actuators.

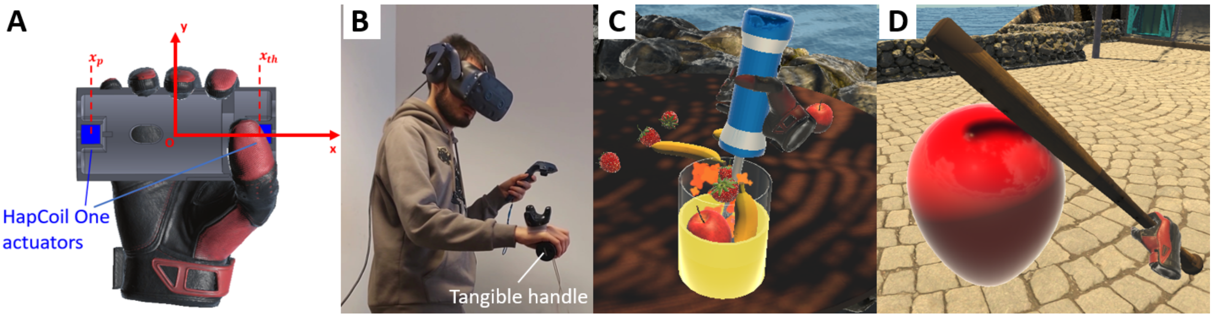

Figure 2.9: (A) Close up CAD of the tangible handle being held by the user's avatar; (B) User manipulating the handle in VR; (C,D) VR interactions causing impacts at different distances and in different directions from the hand.

Impact rendering models

For rendering impact vibrations, we based our approach on the simplified impact vibration model introduced by Okamura et al. [Okamura 1998], where $\alpha(x,t)$ denotes the waveform amplitude at the instant t for an impact at a distance x from the hand (see Figure 2.10): $\alpha(x,t) = A(x)e^{-\beta(x)t}sin(\omega(x)t)$.

In realistic impacts, the peak amplitude A, decay β and angular frequency ω would all be functions of impact distance as well as impact dynamics and properties of the materials involved. However, such impact models can sometimes be less effective at communicating usable information on impact distance [Sreng 2008].

An alternative is to select a subset of model parameters (A, β, ω) to encode impact distance, possibly leaving the remainder free for encoding other impact properties. Given these three parameters, there are seven different possibilities (see Table 2.4) for encoding impact distance (see Figure 2.10) depending on the combinations of vibration parameters used. In our models, A and ω exponentially decreased and β exponentially increased as a function of the distance between hand and impact (see Figure 2.10-B).

Model	No. of parameters encoding distance	Equation	Model	No. of parameters encoding distance	Equation
Amp	1	$\alpha(x,t) = A(x)\ e^{-25\,t}\ \sin(2\pi\,300\,t)$	Freq	1	$\alpha(x,t) = 0{,}6\ e^{-25\,t}\ \sin(\omega(x)\,t)$
Dec	1	$\alpha(x,t) = 0{,}6\ e^{-\beta(x)\,t}\ \sin(2\pi\,300\,t)$	AmpFreq	2	$\alpha(x,t) = A(x)\ e^{-25\,t}\ \sin(\omega(x)\,t)$
AmpDec	2	$\alpha(x,t) = A(x)\ e^{-\beta(x)\,t}\ \sin(2\pi\,300\,t)$	DecFreq	2	$\alpha(x,t) = 0{,}6\ e^{-\beta(x)\,t}\ \sin(\omega(x)\,t)$
AmpDecFreq	3	$\alpha(x,t) = A(x)\ e^{-\beta(x)\,t}\ \sin(\omega(x)\,t)$			

Table 2.4: Impact vibration models for encoding impact distance x from the hand studied in our experiments. The model names indicate the vibration parameters that vary as a function of impact distance, with *Amp* referring to amplitude A, *Dec* referring to the decay β and *Freq* referring to the frequency ω. (Left) Models used in experiment 1; (Right) Models used in experiment 2; *AmpDecFreq* was common to both experiments.

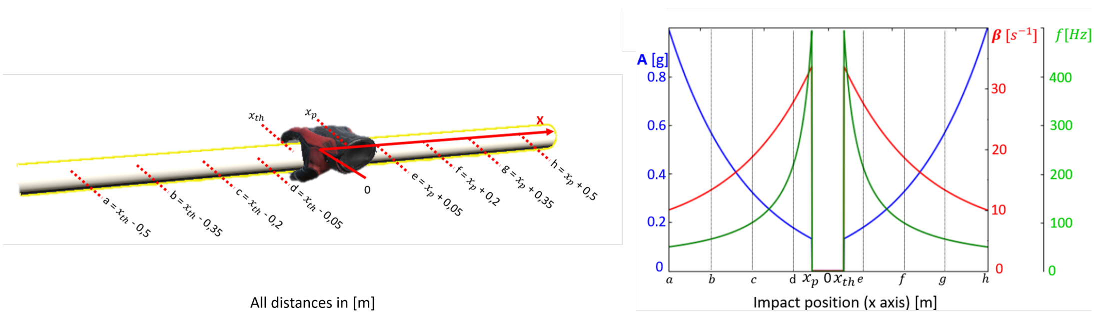

Figure 2.10: (A) Virtual rod manipulated in the experiment with 4 possible impact distances extending symmetrically around the virtual hand. x_{th} and x_p respectively denote the thumb and pinkie side actuator positions. (B) Evolution of vibration amplitude A, decay β and frequency $f = 2\pi\omega$ as a function of impact distance for both actuators. Values were determined based on literature and a pilot study. We do not consider any impact occurring within the hand, hence the null values between x_{th} and x_p.

2.3.2 Experiment

To investigate the formulated hypotheses, we designed a set of two experiments assessing impact direction and distance perception in VR.

Hardware.

Participants sat at a table, wearing an HTC Vive Pro head-mounted display (HMD). They held the vibrotactile handle in their dominant hand which was tracked using an HTC Vive Tracker, attached using an adhesive silicon fixture to keep the palm and inside of the fingers unobstructed.

They used an HTC Vive Controller held in their non-dominant hand to answer experimental questions directly within the virtual environment (see Figure 2.11-A).

Experimental Task.

The common experimental task for both experiments was inspired from Sreng et al. [Sreng 2008]. Participants were asked to hold the tangible handle in their dominant hand. Within the virtual environment, participants could observe their virtual hand holding a virtual rod with the same diameter as the tangible handle, but extending symmetrically outward 0.5m beyond the edges of the tangible handle. By moving this virtual rod up and down, it could impact a lightweight and unconstrained object at one of four distances $d_i = 0.05, 0.2, 0.35, 0.50m$ from either the thumb or the pinkie side of the hand (see Figure 2.10-B,C). These impacts were rendered according to one of the impact models summarized in Table 2.4. During the experiment, the impacted object was obstructed from view so as to provide no visual feedback of the impact location (see Figure 2.11-C). Participants placed the rod at the starting location, then were prompted to move it downward. On the way down, the stick impacted a first virtual object which appeared randomly on the left or right at one of the distances d_i. Upon reaching the target location, participants were prompted to return the stick to the start location and repeat the process. A second object appeared on the same side as the first, at one of the four possible distances, generating a second impact, after which participants answered a pair of experimental questions:

Q1 Which side did the impacts occur on? (Left/Right)

Q2 Was the second impact further away from the hand than the first? (Yes/No)

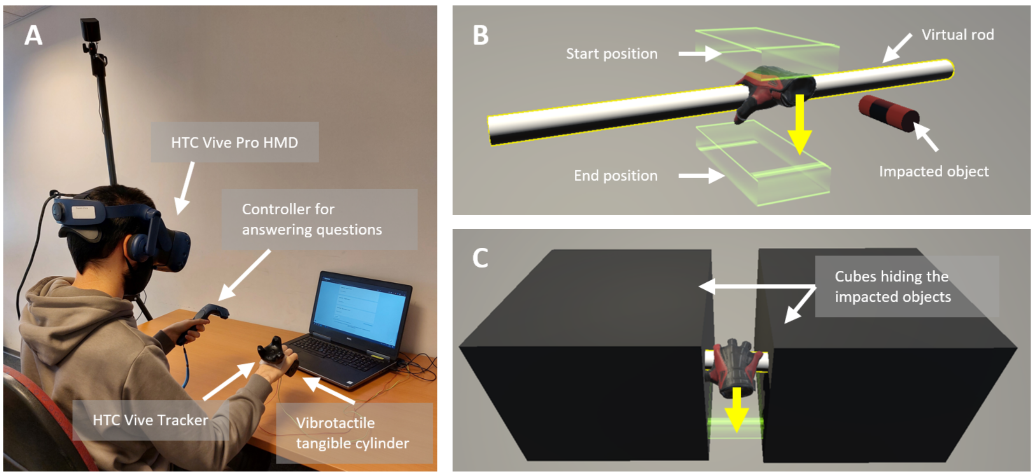

Figure 2.11: (A) A participant performing the experiment. (B) VR view of the familiarization task, where the impacted objects are visible. (C) VR view of the actual task, where the impacted objects are hidden and only haptic feedback of impacts is provided.

Experimental Design.

For achieving a shorter experiment, we split our investigation into two identical experiments containing 4 blocks each.

Impacts were rendered respectively using *Amp, Dec, AmpDec, AmpDecFreq* for experiment 1 and *Freq, AmpFreq, DecFreq, AmpDecFreq* for experiment 2 (see Table 2.4). 24 participants (19 m., 5 f., ages 21-30 (Mean:24.9y), 20 right-handed) took part in the study after providing written informed consent. Participants were randomly assigned to one of the two experiments.

In each experiment, participants first performed a familiarization task where the virtual environment was not obstructed, showing the hand-held virtual stick and the impacted virtual objects (see Figure 2.11-B). During this task we ensured that participants moved at a similar speed, though the vibration did not depend on it. They were informed that the rod and impacted object properties might vary during the course of the subsequent experiment. Participants filled out an initial questionnaire indicating personal data and prior experience with haptics, VR and perception studies.

The experiment was then divided into 4 blocks, one for each impact model, whose order was counterbalanced between participants. Within each block, participants performed 3 repetitions of the task for each of the 16 combinations of impact distances occurring on either side, totalling 96 trials presented in a fully random order. Post-block questionnaires assessed perception of the stick and impacted object's material and geometric properties, their variability, and perceived impact realism.

2.3.3 Results

We computed the rates of correct impact direction identification (correct responses to Q1) in order to test H1. Impact directions were consistently correctly identified between 94% and 97% of the time across all impact models. Most errors occurred for pairs of low amplitude and duration stimuli.

To test for H2, participants were separated into two groups for each impact model, based on whether they interpreted the impact model as intended (increased impact distance perceived as an increased impact distance) or in an inverted manner (increased impact distance perceived as a decreased impact distance). Inversion rates (percentage of participants interpreting an increase in impact distance as a decrease) were around 50% for all models not involving *Freq*, and varied between 92% and 100% for all models involving *Freq*.

We then computed the 75%-just-noticeable-difference (JND) for distance discrimination as a Weber fraction for each participant by fitting cumulative Gaussians to the data. Finally, we compared the distribution of JNDs across impact vibration models (see Figure 2.12). Data from the experiment 1 (Figure 2.12-B) were not normally distributed, and a Friedman test showed no significant differences between conditions. Data from the experiment 2 were normally distributed, and a 2-way ANOVA showed a significant effect of impact model ($F(3) = 4.132$, $p = 0.021$) but no significant differences between participants. A post-hoc Tukey HSD test revealed the only significant difference to lie between the JNDs for the *Freq* and *AmpDecFreq* conditions ($p = 0.016$).

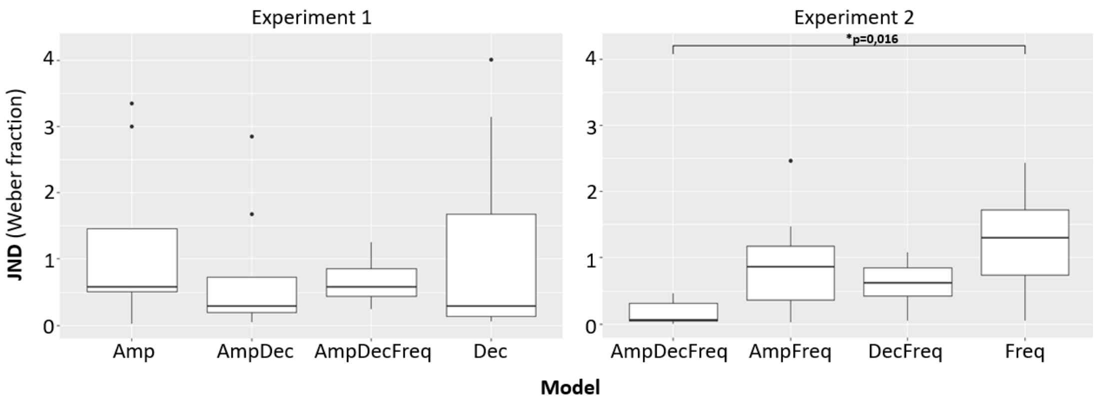

Figure 2.12: JNDs for impact distance, expressed as Weber fractions, for both experiments.

The properties of the virtual rod were rated most consistent (median 2 of 7) in all conditions but *Amp* (median 3 of 7) and *AmpDecFreq* (median 4 of 7), however none of these differences were significant. The properties reported as changing between trials were rod material (*Freq, AmpDec, AmpDecFreq*), stiffness (all models except *Dec*), length (*Dec, AmpDec, AmpFreq*), fill (*Dec, AmpDec*), weight (*Freq, AmpDecFreq*). Subjectively reported rod materials were dominated by “metal" and “plastic" for all models involving *Amp*, as well as the *Dec* model, with qualifiers such as “resonating" and “tube". Models involving *Freq* but not *Amp* yielded more “wood" and “plastic" responses, with qualifiers such as “soft", “damped" and “warm". *AmpDecFreq* yielded an almost even mix of all three material categories. Realism was consistently rated as average across all models (median 3 of 7) and was considered slightly variable across all models (median 3 of 7).

2.3.4 Discussion

The impact direction identification rates between 94% and 97% indicate that regardless of the chosen impact model, spatializing the impacts between two actuators allowed participants to correctly and intuitively identify the side on which the impact occurred with a high degree of accuracy. Hypothesis H1 is therefore verified. Looking at inversion rates, it is interesting to note that all models involving *Freq* tended to be systematically inverted (92% to 100% of participants perceived an increase in distance as a decrease) which would indicate the evolution of ω may be the cause for this.

Weber fractions for distance discrimination were consistently high across all impact models except *AmpDecFreq* (m=0.17), ranging from 0.6 (*DecFreq*, experiment 2) to 1.32 (*Amp*, experiment 1). This indicates that while distance discrimination was mostly possible, it was far from an easy task. The only statistically significant difference observed (*Freq-AmpDecFreq*, experiment 2) is in favor of hypothesis H2, and the mean JNDs seem to also support the hypothesis. However, given the poor performance of *AmpDecFreq* in experiment 1 and the fact that none but one of the differences are statistically significant, we cannot conclude that H2 is supported. This may be due to H2 being wrong, or to flaws in the stimulus or experimental task design. If H2 is not verified, there may be a lot of headroom to encode various impact properties by distributing them across different parameters without adversely impacting performance.

The high inversion rates due to using ω as a parameter led us to hypothesize that models combining ω with A, β or both may have been confusing to half the participants that did not invert their interpretation of *Amp* and *Dec*. This hypothesis cannot be easily tested because participants that performed *Amp* and *Dec* did not perform *AmpFreq* and *DecFreq*. Yet, analysing the results from experiment 1 revealed that 6 out of 12 participants had inverted both *Amp* and *Dec* while 5 of 12 had not (the remaining subject inverted only one of both models). By looking at the JNDs for each of these groups of participants in the *AmpDecFreq* condition, we note that the group that inverted both *Amp* and *Dec* performed better at *AmpDecFreq* (JNDs: 0.07 to 1.96, mean=0.83) than the group that did not invert *Amp* and *Dec* (JNDs: 2.15 to 9.33, mean=4.63). This would tend to support our interpretation and argue for the need to redesign the function $\omega(x)$ in our rendering approach. Furthermore, it may be necessary to consider the frequency dependence of vibration amplitude perception in such a redesign. However, given the very small sample size, this conclusion must be seen as tentative.

The spread in JNDs between participants indicates a large inter-subject variability in the ability to perform the task. During the experiment, several participants noted that the task was really difficult until they “chose” a way to understand the mapping of the stimuli to impact distance. Thus, we believe this variability shows that participants displayed different capacities for adapting to the difficulty of the experimental tasks and choosing an effective response strategy. This means that the haptic representation of impact distance is far from intuitive or natural with the chosen models, although *AmpDecFreq* shows some promise in experiment 2. This may indicate poor model design, or the fact distance discrimination is really hard without any context such as e.g. visual feedback of impacts.

All models were perceived as equally (un)realistic, indicating that either the impact model used is unrealistic, that spatialization impacted realism, or both.

2.4 Conclusion

In this chapter, we investigated the inclusion of vibrotactile feedback within tangible objects to enrich haptic manipulation in VR. Through a series of perception studies, we showed that multi-actuator localized vibrations can yield sensations which are perceivably localized within a handheld object, and can in some cases be used to create a haptic funneling effect within a handheld tangible object. We explored the use of these multiple vibrotactors to render spatial properties of virtual interactions. We showed that this allows a multitude of dynamic haptic properties to be rendered during interaction with the virtual environment. These include rendering vibrating and pulsating objects, impacts, texture components as well as rendering virtual contents of handheld containers. We then assessed the added benefit of these localized sensations in terms of perceived coherence between visual and haptic feedback through a user study. In certain circumstances, multi-actuator localized vibrotactile feedback was shown to yield more coherent haptic feedback than monolithic object vibration, and is almost never detrimental to perceived coherence.

The approach we investigate has the major advantage of not encumbering the user and avoids any potentially disruptive haptic stimuli caused by wearables not matching expected stimuli from the virtual environment. However, this approach is not without challenges that still need to be overcome. First of all, actuating tangible objects can require comparatively more actuators and thus a higher system complexity and cost. Second, for our approach to work, the tangible object requires an internal power source or has to be wired. Both challenges may limit freedom of manipulation. Because of this, the advantages of our approach are particularly prominent for interfaces and systems where interaction is constrained to a single tangible object (e.g., [Azmandian 2016]). They can, however, be extended to conventional passive haptics using multiple tangible objects (e.g., [Cheng 2018]), encounter-type haptic devices supporting multiple end-effector tangibles (e.g., [Mercado 2021]), or even grounded force feedback devices with tangibles as end-effectors (e.g., [Bae 2020]). Finally, our current rendering schemes ignored vibration propagation and mechanical effects which may impact the quality of the perceived stimuli.

Mixed haptics approaches open up vast possibilities for enriching interaction through the complementary nature of tangible and VF, which particularly fit the multi-sensory context of immersive VR. We focused on augmenting interaction realism by rendering richer haptics, but our system design also offers possibilities for providing abstract information to support interaction performance, convey affective information and support communication in VR.

CHAPTER 3

ACTUATOR ISOLATION FOR EASIER IN-HAND STIMULI DISCRIMINATION

Following our exploration of actuated tangible objects, we observed that localized feedback could be effective without vibration isolation. However, for certain applications such as navigation, these sensations are too diffuse to efficiently provide localized sensations to users. In order to pursue our investigation of multi-actuator feedback in the field of navigation, we first need a device able to provide these sensations in a more effective way as well as in a more appropriate form factor.

In this chapter, we present the design of a multi-actuator haptic handle, which provides localized vibrotactile feedback in a small form-factor. To isolate the vibrations generated from the different actuators, we design an original 3D printed deformable structure integrated into the handle. Compared to existing devices, both the handle and the isolation structure are fully 3D printed, aiming to an easily replicable design based on cheap and widely available actuators and materials. This design also has the benefit of not requiring a complex assembly process, and being easily adaptable to other actuators. We evaluate the benefits of our isolation structure in a vibrometry study, comparing the proposed version to a rigid structure. We then conduct a set of perception studies. In a first study, we evaluate the distinct perception of vibrations between the two versions of the handle, assessing the benefits of our isolation structure. In a second study, we assess the use of our haptic handle to provide additional directional cues, evaluating the discrimination between different haptic patterns displayed by the handle.

Part of this chapter has been published in [Cabaret 2024a], to which we added a discussion of the designs explored during the prototyping phase as well as an additional perception study.

3.1 3D-printed structures for vibration isolation in a haptic handle

3.1.1 Prototyping process

Our previous investigation of multi-actuator feedback was conducted with tangible props, especially with spherical prototypes which can be used to represent various virtual objects. As our focus moves towards navigation, we want to transfer these findings into a handle-shaped interface that could provide navigation instructions to users.

As a first approach, we designed a handle that integrated actuators in a similar way than our actuated tangibles. Given that a handle has less room to spare, the four voice coil actuators were placed around the handle, directly in contact with the skin (see Figure 3.1). We tested this prototype in some preliminary studies, where participants were guided in a maze using the handle by mapping each motor to a direction around the user. These experiments took place either in immersive VR, where users had the handle in hand and moved using an arm-swinging technique, or on a screen, where they had the handle mounted on a gaming joystick. From these preliminary studies, we make two main observations. First, vibrations were quite diffuse within the handle, which made it difficult for users to correctly identify directions. This was somewhat dependent on users, with some having no difficulty in navigating while following the vibrations, and others being completely lost as they could not discriminate directions. Secondly, when placed on the joystick, vibrations were dampened by the added mass to the device, making it harder to identify vibrations.

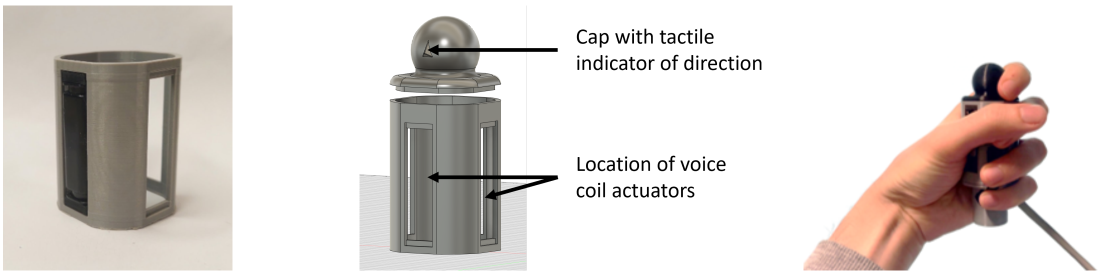

(A) (B) (C)

Figure 3.1: The first handle protoype using four voice coil actuators. (A) The handle equipped with a single acuator in one of the four actuators slots; (B) A render of the handle 3D model; (C) The handle held by a user.

This first prototype highlights the need for isolating vibrations around the handle in order to provide clear navigation instructions. As discussed in section 1.4, there are multiple ways of preventing vibration propagation. Here, we are interested in using 3D printing for the fabrication of the handle. This would allow for the handle to be customizable and easy to build by anyone, as long as the haptic components and materials used are widely available. This also motivates the use for more affordable and simpler actuators.

Isolation mechanisms usually rely on a deformable part to absorb vibrations (e.g., with foam, springs or silicone rubber). As a base for our handle, we designed a four-sided case that could house isolation modules on its sides (see Figure 3.2). This case was designed to be easily held in hand, with a diameter of 40mm that fits most hand sizes. Given the limited space available within the handle, we design the isolation modules to fit small ERM motors (7x20mm).

(A)

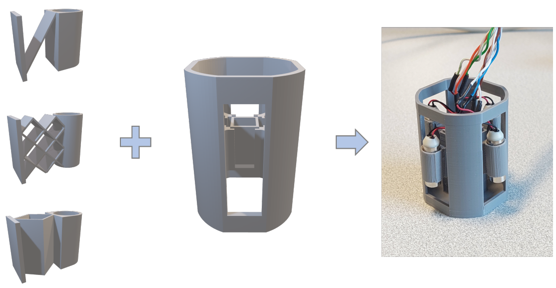

(B)

Figure 3.2: Illustration of our modular prototype used to test different 3D printed isolating modules. (A) A selection of various modules, using either PLA (in grey) or TPU (in black); (B) The modular handle prototype can house four isolating modules on its sides, which are equipped with ERM actuators for displaying vibrations.

To create such a mechanism with 3D printing, we first investigated the use of the properties of PLA, the most common plastic used in 3D printing. We took inspiration from compliant mechanism that use the slight flexibility of PLA to create actuated or adapting parts printed in a single piece: first prototypes were made of a thin blade of plastic which was able to deform and press the actuator against the user's skin (see Figure 3.2 and 3.3). Various modules were designed, changing the size, direction and number of blades to link the handle and the handle (see Figure 3.2). While this mechanism was effective in isolating vibrations, the brittle nature of PLA was not adapted to regular deformation at this scale.

We followed our prototyping phase by experimenting with another material, TPU, another 3D printable plastic that comes in different degrees of flexibility. One interesting way to use this material is to create oriented microstructures to control the direction of deformation of 3D printed parts [Tricard 2020]. We designed a series of deformable isolation modules based on this idea, using *Phasor* and *Polyfoam* infills from the IceSL slicer[1] (see Figure 3.2 and 3.3). These modules achieve higher deformability than previous PLA modules, while still preventing vibrations from propagating within the handle. While this approach is effective, it can be difficult to print these structures correctly given the orientation of layers and the material characteristics.

[1] `https://icesl.loria.fr/`

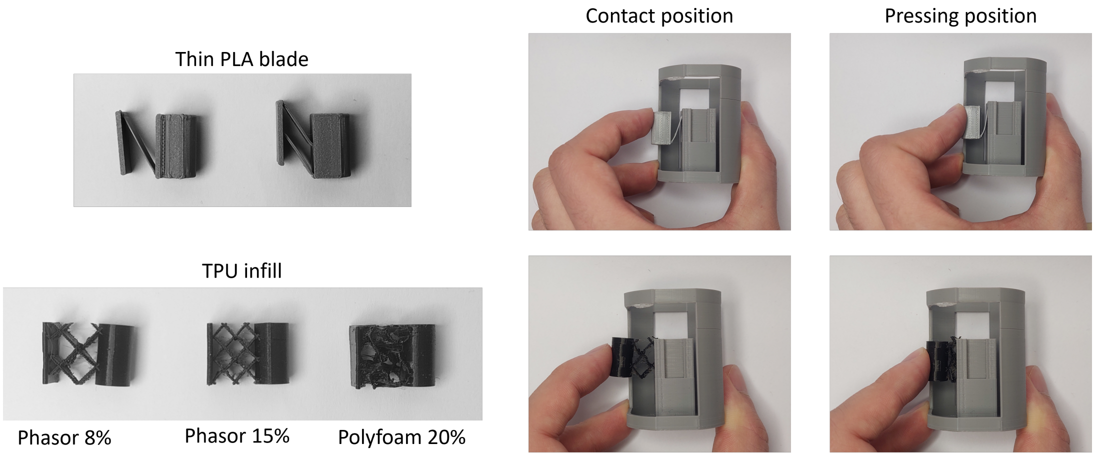

Figure 3.3: Close-up on some of the protoype modules printed in PLA (top-left) and flexible TPU (bottom-left). (right) When pressed with the finger, these modules compress, pushincg against the user's finger.

Developing these prototypes provided useful insights on the design of a 3D printed isolation structure. In the following section, we present our following iteration, using a more reliable structure that uses the deformation of TPU to provide localized vibrations to users. We move away from the modular structure of our handle prototype in order to create a more robust device. However, such an approach could be further investigated in the future to customize the devices based on users needs and preferences.

3.1.2 Final Multi-actuator Handle Design

The proposed multi-actuator handle is illustrated in Figure 3.4. Its structure is fully 3D printed. Four ERM actuators (Vybronics VZ6DL2B0055211) are located symmetrically around the cylindrical structure. We used widely available ERM actuators so that the handle could be easily replicated and customizable. These ERMs are able to produce sinusoidal vibrations between 50 and 200 Hz. Vibration frequency and intensity are linearly linked to the input voltage. The handle is designed to be simply held in the hand or plugged onto a gaming joystick (see Figure 3.6).

The outer shell of the handle is 40 mm in diameter (grey in Figure 3.4), topped with a removable spherical part resembling a head, with a tactile indent on one side, resembling a nose. Doing this, haptic cues from the handle can be easily mapped to a direction relative to the user in, e.g., navigation tasks. Both of these parts are printed out of PLA. Within this rigid shell, we designed a deformable structure made of four modules (yellow in Figure 3.4), inspired by the cells used in metamaterials mechanisms [Ion 2016]. These modules resemble 3D printed lattice cellular structures, which were shown to have vibration isolation properties [Al Rifaie

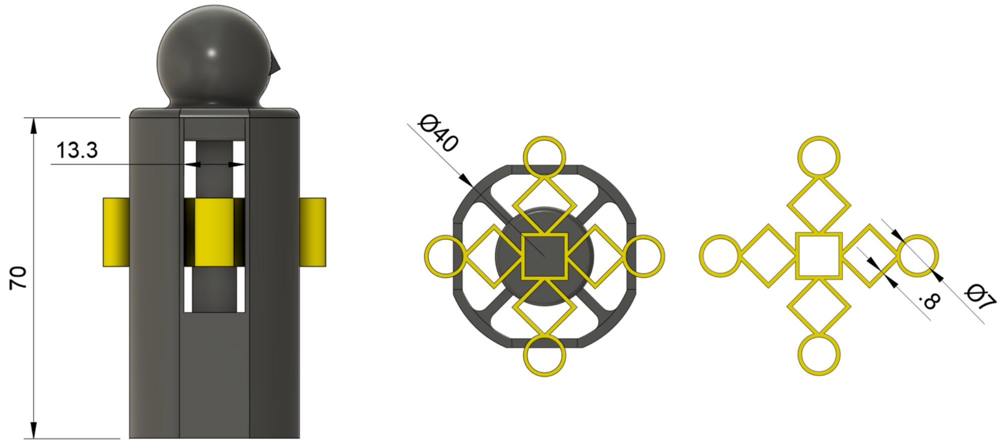

Figure 3.4: The proposed multi-actuator haptic handle is made of three 3D printed parts. The shell and cap are printed in rigid PLA (grey in the Figure) while the inner structure is printed using soft TPU (yellow). This latter soft structure houses four vibrating actuators in 7mm-diameter cylinders at its extremities. Dimensions are in millimeters.

2022; Yin 2023]. Each module houses one of the four ERM actuators of the handle. We printed this structure using TPU Filament Filaflex 82A, with a width of 0.8 mm for all elements (see Figure 3.4). Such a material has already been used in printing spring-like structure [Gunarathna 2022]. The soft modules can deform when compressed (see Figure 3.5), pushing the actuators against the user's fingers. They play two key roles: first, they ensure a permanent contact between the actuator and the user's skin. Secondly, they greatly reduce vibration propagation from the motors to the other parts of the handle, thus helping the user better identifying the stimuli source. When held in hand, the handle provides localized stimuli on the thumb, palm, index and middle finger (see Figure 3.5). The structure parameters were chosen iteratively, giving priority to vibration attenuation while ensuring good contact with the skin.

An ESP32 microcontroller controls the four motors using PWM signals between 0 V and 4 V. Commands can be sent using a serial connection or wirelessly via ROS2 when connected to a battery.

3.2 Evaluation of a soft-structure for vibration isolation

3.2.1 Vibrometry Study

We conducted a vibrometry study to evaluate the effectiveness of our design to isolate vibrations within the handle. An optical vibrometer was used to collect the velocity and frequency of skin vibrations at four locations of the hand while holding the handle. To assess the repeatability of measures, 6 participants (5M-1F, Ages 18-47, all right-handed) took part in the study. Hand sizes ranged from 190 to 170 mm, from the wrist to the tip of the index finger.

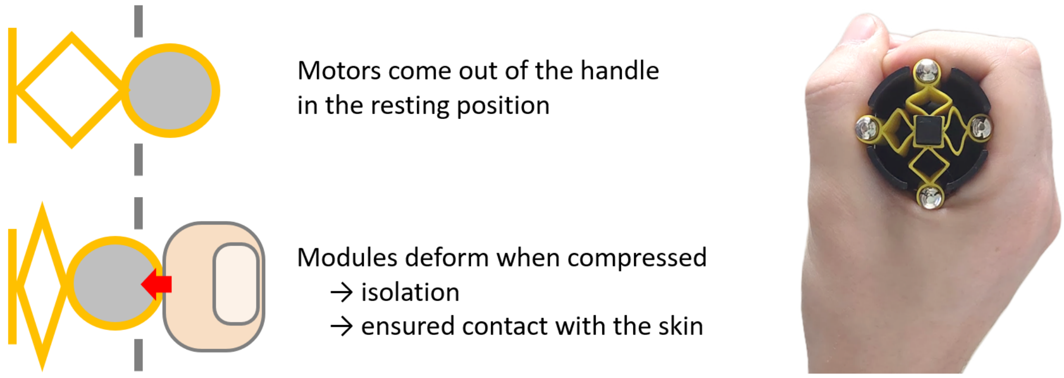

Figure 3.5: The soft structure within the handle is 3D printed with TPU. Each module holds one of the actuators and plays a dual role: ensuring the contact between the user's hand and the motor while also isolating vibrations from the rest of the handle.

Experimental Setup

Skin vibrations were measured using a laser doppler vibrometer (VibroFlex Neo, Polytech[2]). Participants held the handle with their right hand, placing the vibrating motor at the front of the handle, in-between the intermediate and distal phalanges of their index. The laser was then targeted at the desired measuring point, i.e., on the finger at the level of the actuator (see Figure 3.6-right). We selected four points of measurement (see Figure 3.6-left):

- (A) on the intermediate phalanx of the index;
- (B) on the proximal phalanx of the index;
- (C) on the back of the hand, between the thumb and index;
- (D) on the proximal phalanx of the thumb.

Measurements were taken at these points while always activating the same actuator placed under the intermediate phalanx of the index (point A). Measurements are repeated three times for each point at (i) ten levels of increasing input voltage (from 0.7 to 3.7V with 0.3V increases, spanning the full actuation space of the motors), (ii) two levels of grasping force (loose grip and tight grip), and (iii) with the proposed isolating structure vs. with a rigid version of the structure (i.e., non-isolating) made of rigid PLA. For the rest of this chapter, these two versions will be referred to as the "flexible handle" and the "rigid handle", respectively. The rigid handle was designed to have the actuators at a similar location than with the flexible handle when it was compressed.

[2] https://www.polytec.com/int/vibrometry/products/single-point-vibrometers/vibroflex

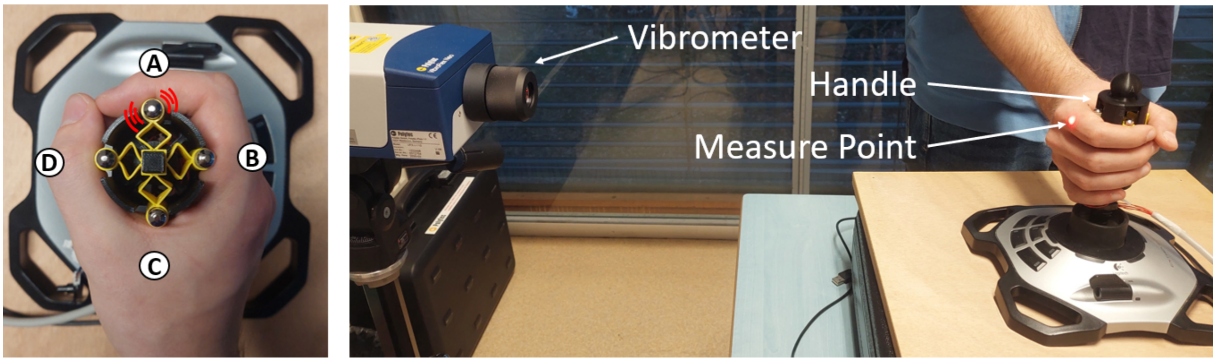

Figure 3.6: (Left) The velocity of skin vibration was measured at four different locations on the hand, while activating the motor at point `A`. (Right) We used a laser doppler vibrometer pointed at the hand to measure the skin vibration due to the motor actuation.

Subjects were asked to grasp the handle as in Figure 3.6 at the two considered levels of grasping force. Force levels were visually monitored based on the deformation of the structure (at the maximum level of force, the modules are fully pushed inside the handle). Each measure cycle was repeated three times to ensure consistency.

During the study, commands were sent to the handle via a Matlab script. Once in position, the motor is successively activated at the ten levels of vibration intensity for two seconds each. A dSPACE (DS1104) controller board was used to record velocity data from the vibrometer as well as the input voltage of the motor. Data is captured at 10 kHz, with a range of 100 mm/s. Preliminary tests were performed on the motors to ensure their performance and reproducibility of their signals over time.

Results

The data is composed of 480 recordings per participant: three repetitions of each combination of conditions (input voltage, measuring point, grasping force, handle), for a total of 2880 measures. We extracted, from each record, the Root Mean Square (RMS) velocity of the skin, a metric also used in [Dandu 2019]. Data for each participant across conditions can be seen in Figure 3.7.

Overall, RMS velocity of skin vibration ranges from 0.8 mm/s to 69 mm/s. As seen in Figure 3.7, mean velocity with the flexible handle at point `A` increases rapidly with the input voltage, from 5 mm/s to a maximum of 35 mm/s. A clear attenuation can also be seen between point `A` and the three other measuring points `B`, `C`, and `D`, as expected. For the highest vibration intensity, velocity at point `A` is up to 11 times higher than at the other points. In comparison, velocity is much lower when considering the rigid handle, with mean values ranging from 2 mm/s to 13 mm/s. The difference between points around the hand is much lower in this case: values at point `B`, `C`, and `D` range between 0.5 and 1 times the velocity at point `A`. This result show how the proposed isolating design significantly improve the localization of the vibrations with

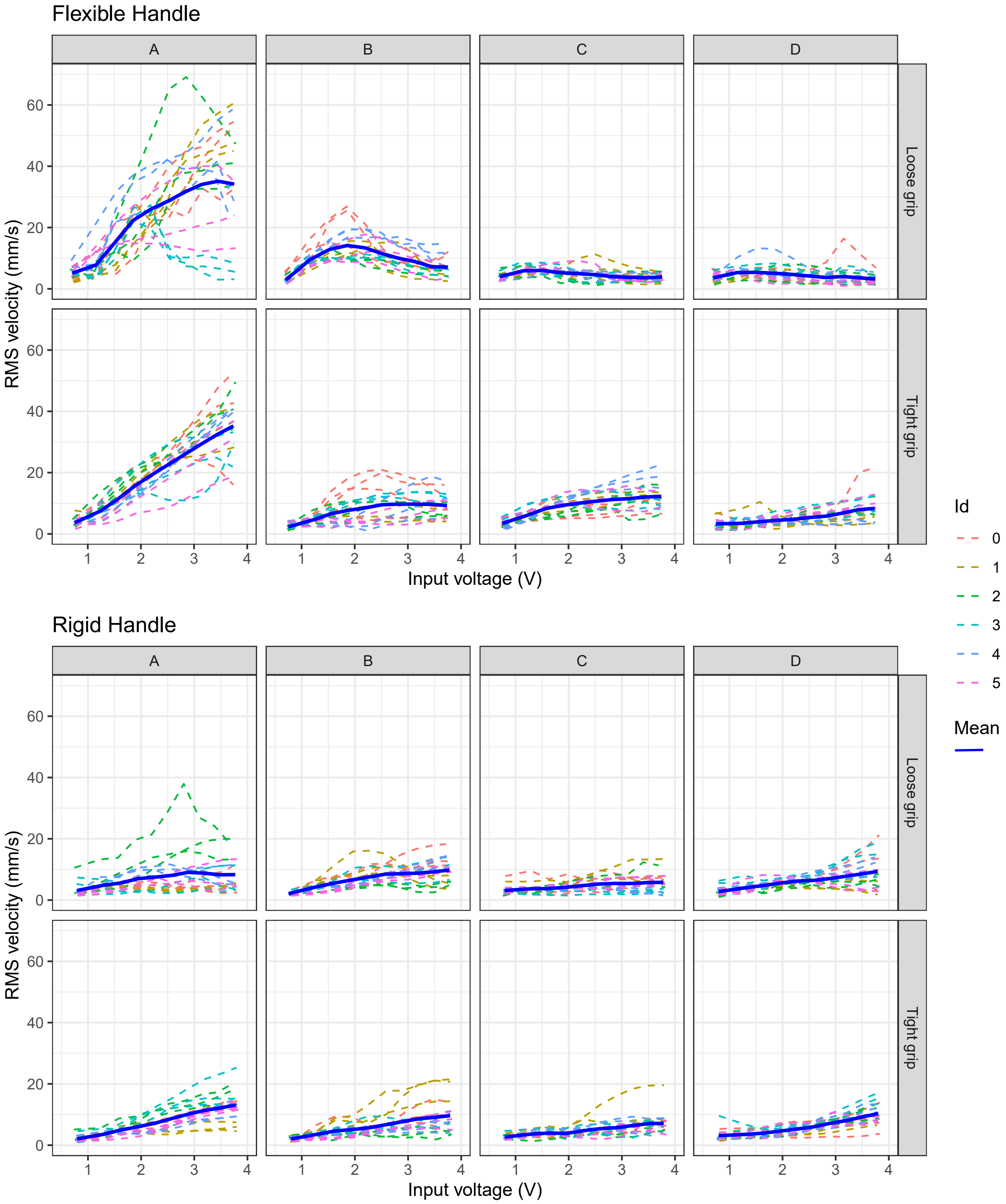

Figure 3.7: RMS velocity of skin vibration for each of the four measure points, for the flexible (top) and rigid (bottom) handles. Individual participant data are shown in dashed lines. Mean RMS velocity value is shown in a solid blue line.

the handle.

As the index finger is in contact with the vibration source, located at point `A`, we observe higher velocities at point `B` than with other fingers: this is due to the propagation of vibration through the finger. As shown by Dandu et al., this propagation through the finger decreases as frequency increases [Dandu 2019]. This can indeed be observed at point `B` with the flexible handle and loose grip force, where velocity rises at lower frequencies before dropping at higher frequencies.

Between the two levels of grasping force, we can observe that the velocity is higher in the non-stimulated fingers when the handle is held tightly with the flexible handle. This might be due to the isolating structure being less effective when fully compressed, or the hand conducting vibrations more effectively when closed firmly. Differences in RMS velocity is also clear between the two handles: at point `A`, where the vibration originates, the flexible handle shows 2 to 3.5 times higher vibration velocities than with the rigid handle.

Regarding the frequency response (see Figure 3.8), we can observe the expected increase in frequency with the input voltage. It appears that for higher levels of input voltage, we measure frequencies in a ± 25Hz range. As the same motor was used for all measurements, this would either indicate that vibration frequency is altered by the way the device is held by participants (potentially an effect of different deformation of the isolating structure, small hand movements or morphology) or that our experimental setup is not precise enough for this type of measurement.

3.2.2 Discussion

The results of the vibrometry study showcases a clear difference between the two versions of the handle. Indeed, vibrations are much more intense at the stimulated location with the flexible handle, while keeping vibrations on the other fingers at a much weaker level. While the grasping force on the handle appears to lower the intensity of vibrations at the stimulated point, it stays well above the intensity of other points on the hand. Some improvements in the shape of the handle, such as a more ergonomic form factor and a more complex soft lattice structure could add more control to the modules deformation, and also mitigate the propagation of vibrations through the hand.

Given the structure simplicity, the proposed handle design could be adapted to other actuators of different sizes or shapes. However, each module needs space to deform freely, which limits the applicability of this design in existing interfaces (e.g., VR controllers).

3.3 Discrimination of haptic patterns

In addition to the vibrometry study discussed in the previous section, we conducted two user studies, to further evaluate the benefits of our isolation structure and assess its use in displaying

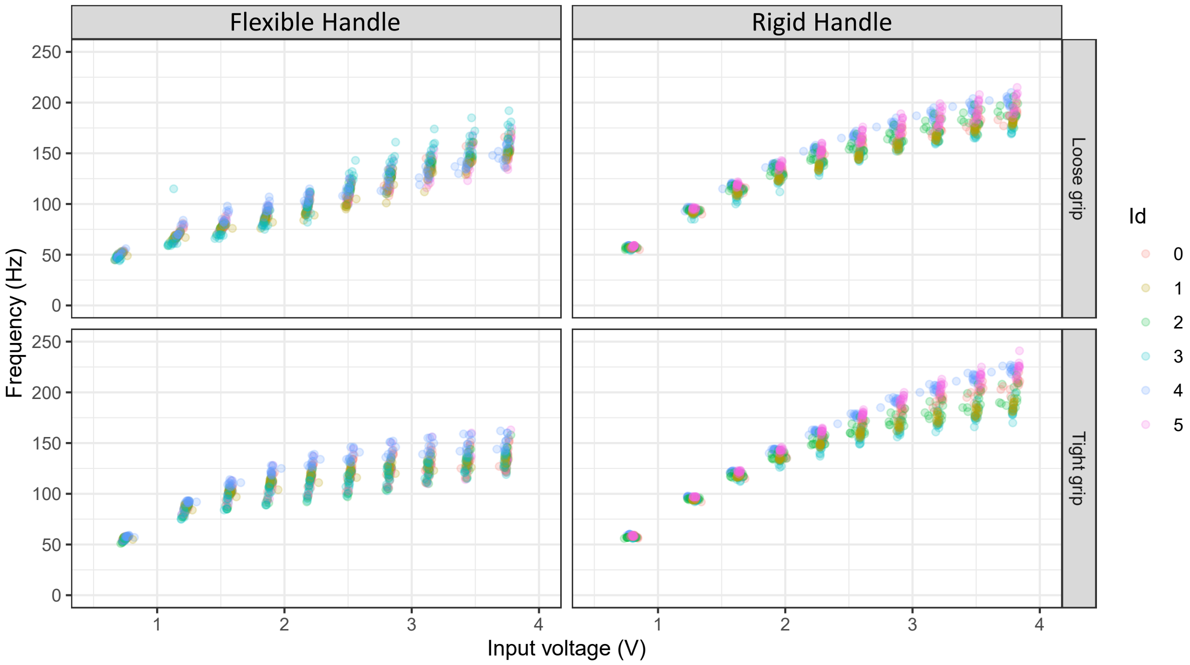

Figure 3.8: Principal frequency of skin vibration for the flexible (left) and rigid (right) handles at two levels of grip force.

directional cues.

3.3.1 User Study #1 - Discrimination of localized cues

In this first user study, we compare the discrimination of localized cues between our proposed isolated handle and its rigid counterpart. Twelve participants took part in this experiment (5M, 7F, 10 right-handed, aged 20-66, mean age 37.5). The study has been approved by Inria's ethics committee.

Experimental Setup

This study was performed with participants sitting at a desk and the haptic handle mounted on a joystick (as in Figure 3.9).A screen displayed relevant information during the experiment, and a keyboard was used to answer each trial. Participants were presented with the handle and were instructed on how to place their dominant hand on the handle before a familiarization phase with the vibrations. A headset displayed noise throughout the experiment to hide potential audio cues from the actuators.

Participants performed two series of 40 trials in which they had to identify the location of 0.2-s-long vibrations between the four possible ones (left, right, front, and back actuators).

Each of the four vibration locations was presented 10 times. Trials order was randomized across participants. Participants performed the first series of trials with one of the two handles (i.e., flexible and rigid), and the second series with the other one. The presentation order for the type of handle was counter-balanced across participants.

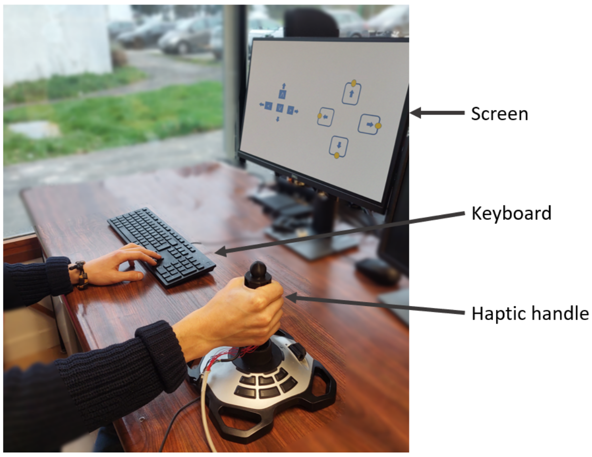

Figure 3.9: Experimental setup for the perception study. Participants sat at a desk in front of a screen, holding the handle in their dominant hand. The haptic handle is mounted on a joystick to keep it in position. A keyboard was used to select the location at which they felt the vibration while the screen displayed relevant information.

Results

Overall, participants were able to identify the vibration location most of the time, with success rates ranging from 81% to 98% for the flexible handle and 68% to 93% for the rigid one (see the confusion matrix in Figure 3.10). We used a generalized linear mixed model to study participants responses with respect to the vibration location and type of isolation of the handle. Participants were considered as a random effect in the model. Analysis of deviance of the answers showed significant effects of both the vibration location and the isolation type ($p < 0.001$). A post-hoc analysis on the different conditions was performed using a Tukey test. Trials with the flexible handle had significantly higher correct answer rates compared to when the rigid one was used ($Z = 4.81$, $p < 0.001$). Correct answer rates were lower for the back location compared to the front and left locations ($p<0.001$), as well as for the right location compared to the left and front location ($p<0.001$).

After each series of trials, participants were asked to rate whether vibrations were difficult to locate on a 7-item Likert scale (1=Totally disagree, 7=Totally agree). A Wilcoxon signed rank test showed a significant difference ($p< 0.001$) between the evaluated difficulty with the flexible (mean=2.83, SD=0.937) and rigid (mean=4.42, SD=1.44) handles (see Figure 3.10). Even though participants were highly successful with both handles, they found the task to be (much) easier with the flexible handle. This is also supported by comments from the participants, who found the vibrations from the flexible handle to be clearer.

Figure 3.10: (Left) Confusion matrix for the perception experiment: identification rates for each vibration location with the flexible and rigid handles. (Right) Participants evaluation (7-item Likert scale) of the difficulty to identify the vibration location on both handles.

3.3.2 User Study #2 - Discrimination of directional patterns

In this second study, we evaluate the discrimination of two types of stimuli designed to provide eight directions to users using the four motors of our haptic handle. We recruited 12 participants (11 males, 10 right-handed, aged 22–47, mean age 28), to perform in this part of the user study. Only four of them had significant experience with haptic feedback.

Stimuli design

The four vibrotactile actuators around the handle allow for spatialized haptic feedback in the users' hand around four main directions around the user (Front, Back, Left and Right). By using multiple actuators simultaneously or sequentially, the handle could provide richer information. We propose to use the handle to display eight different directions: the four cardinal directions as well as four diagonals. We designed two types of tactile patterns to communicate directional information to the user towards eight different directions (see Figure 3.11 for an illustration of the patterns):

- `Static` feedback cues (Figure 3.11-left): a single 0.2-s vibration burst is displayed on either one actuator (for Left/Right/Front/Back directions) or two adjacent actuators (for diagonal directions).

- `Dynamic` feedback cues (Figure 3.11-right): a sequence of 0.15-s vibration burst is displayed on two actuators (e.g., Left and then Right for a Left-to-Right cue).

Such patterns could be used to convey different kinds of information. Dynamic cues might be able to provide information about moving objects more easily as they rely on motion inside the hand. Both types of cues could also co-exist and provide complementary information, e.g., about two different types of obstacles.

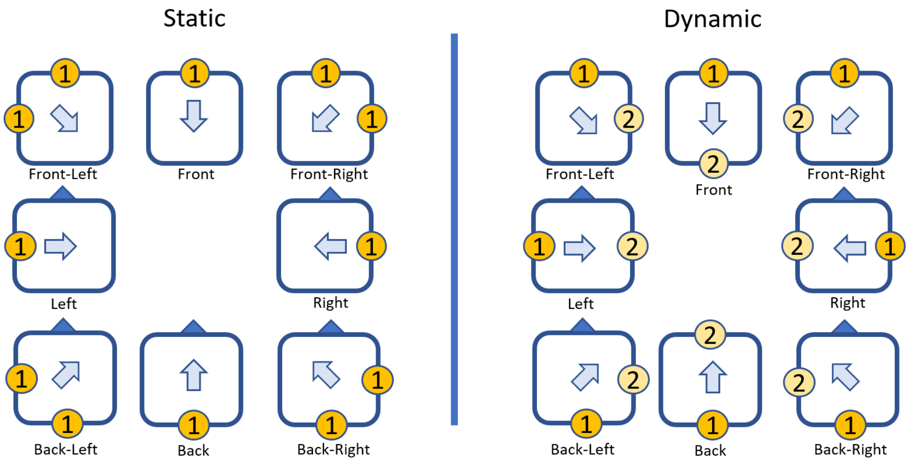

Figure 3.11: `Static` and `Dynamic` feedback cues used to provide directional information.The handle is shown from the top, represented by a blue solid shape; the arrows show the target direction cue; the yellow circles show which motor(s) are activated and in which sequence (“1” and then, in the dynamic case, “2”). (Left) `Static` cues activate one motor for `Left`, `Right`, `Front` and `Back`directions, or two motors simultaneously for `Front-left`, `Front-right`, `Back-left` and `Back-right` directions. (Right) `Dynamic` cues activate two motors, one after another, to indicate a direction.

The experiment is performed with participants sitting at a desk in front of a screen, with a keyboard, and the haptic handle mounted on a joystick (see Figure 3.9). Participants are presented with the handle and then instructed on how to place their dominant hand on the handle before a familiarization phase with the vibrations. A headset displays noise throughout the experiment to hide potential audio cues from the actuators.

Experimental task and design

We evaluate the ability of participants to discriminate the different types of haptic cues provided by the handle, as introduced in section 3.3.2 and shown in Figure 3.11, considering the following conditions:

- *Type of haptic pattern:* `Dynamic` or `Static` feedback.

- *Direction:* eight directions, i.e., `Front`, `Front-left`, `Left`, `Back-left`, `Back`, `Back-right`, `Right` or `Front-right`, as illustrated in Figure 3.11.

The experiment is made of two blocks, one for each type of haptic patterns. The order of the blocks is counter-balanced between participants. During a block, each direction is randomly displayed 10 times, for a total of 80 trials per block. Participants experience cues in a randomized order and must indicate, using the numerical pad of a keyboard, the direction that was communicated by the handle. After each answer, the next cue is displayed after a short delay.

For each trial, we collected the answer of the participants and the time they took to answer after the display of the stimulus. At the end of each block, we asked participants to evaluate the difficulty of the completed task using a 7-point Likert scale.

The hypotheses were the following:

(H1) Both `Static` and `Dynamic` feedback cues delivered by the haptic handle can be identified with a high accuracy;

(H2) `Dynamic` feedback cues take longer to be recognized than `Static` ones;

(H3) Diagonal directions are easier to recognize with `Dynamic` feedback cues than with `Static` ones.

Results

Figure 3.12 shows the confusion matrix reporting the displayed stimuli vs. the recognized stimuli rate for each type of haptic pattern and rendered direction. Overall, both types of cues appear to be well identified, with varying accuracy depending on the type of cues and the direction.

Results show static cues to provide better results for the `Front`, `Back`, `Right` and `Left` directions (i.e., the non-diagonal directions) with identification rates ranging from 81 to 97%. Diagonal cues, in the `Static` condition, are identified with lower accuracy, with identification rates ranging from 48 to 69%. On the other hand, identification rates for `Dynamic` cues are generally lower with respect to `Static` ones, with less contrast between diagonal and non-diagonal directions: identification rates range from 58 to 72%, except the `Back` direction which is identified with an 83% accuracy.

For `Static` cues, errors tend to be made with adjacent directions, while for `Dynamic` cues, errors seem to be spread similarly across all directions.

Individual identification rates (see Figure 3.13) show that the lower identification rates of `Dynamic` cues can be attributed to a few participants who performed worth than the others. Looking at individual results, we can confirm that some participants achieve similar scores in both `Static` and `Dynamic` conditions while some fail in the `Dynamic` condition while succeeding in the `Static` one. Notably, the median identification rate is higher for `Dynamic` cues than for `Static` ones.

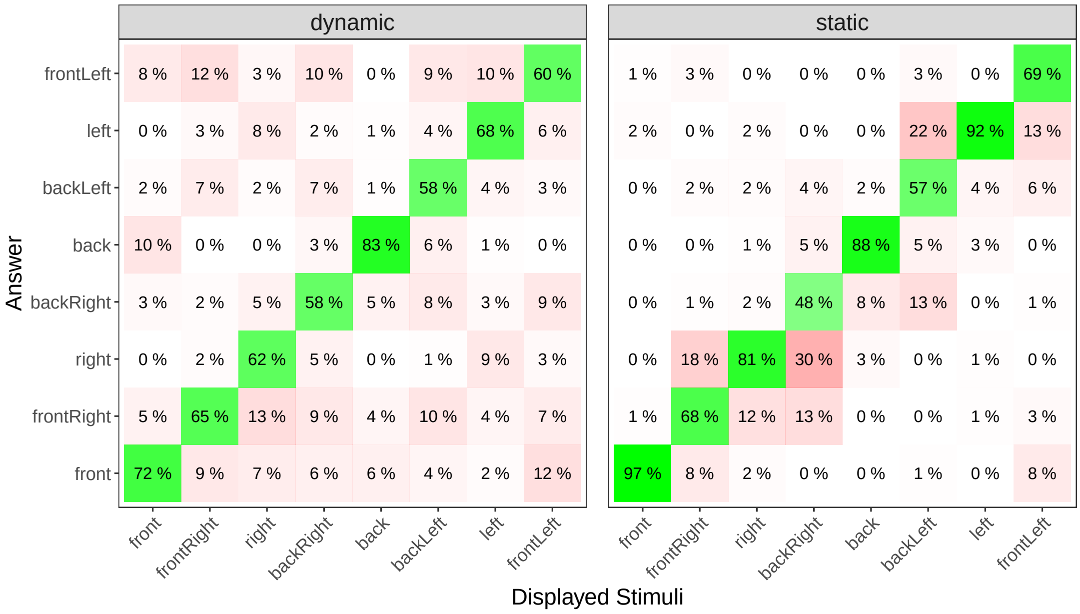

Figure 3.12: Experiment #1. Confusion matrix across conditions: recognition rates of `Dynamic` (left) and `Static` (right) feedback cues. Participants had to identify the direction communicated by the haptic handle through the motors placed around it.

We analyzed the identification rates with a Generalized Linear Mixed Model (GLMM), using a logistic model. Independent variables are the type of cue (`Static` or `Dynamic`) and the direction (`Front`, `Front-left`, `Left`, `Back-left`, `Back`, `Back-right`, `Right`, `Front-right`). Participants are considered as a random effect. We observed a significant effect of the type of cue (χ^2 (1, N=1920) = 34.75, p<0.001), the direction (χ^2 (7, N=1920) = 130.39, p<0.001) and a significant interaction between these two variables (χ^2 (7, N=1920) = 47.29, p<0.001). Post-hoc tests were performed with simultaneous pairwise comparisons using Tukey's test. Results show that `Front`, `Left` and `Right` directions are identified with higher accuracy with `Static` cues than with `Dynamic` cues (p<0.001).

In the `Dynamic` condition, the `Back` direction is identified with a higher accuracy than the `Back-left`, `Back-right` and `Front-left` directions (p<0.001), the `Front-right` and `Left` directions (p<0.05) and the `Right` direction (p<0.01).

In the `Static` conditions, `Back-left` and `Back-right` diagonals are identified with a lower accuracy than `Back`, `Front`, `Left` and `Right` directions (p<0.001). `Front`, `Back` and `Left` directions are identified better than `Front-left` and `Front-right` diagonals (p<0.01). `Front` direction identification is better than `Right` direction (p<0.01), and the `Front-left` and `Front-right` diagonals are identified better than the `Back-right` direction.

Regarding the time taken to answer (see Figure 3.13), the median with the `Dynamic` patterns

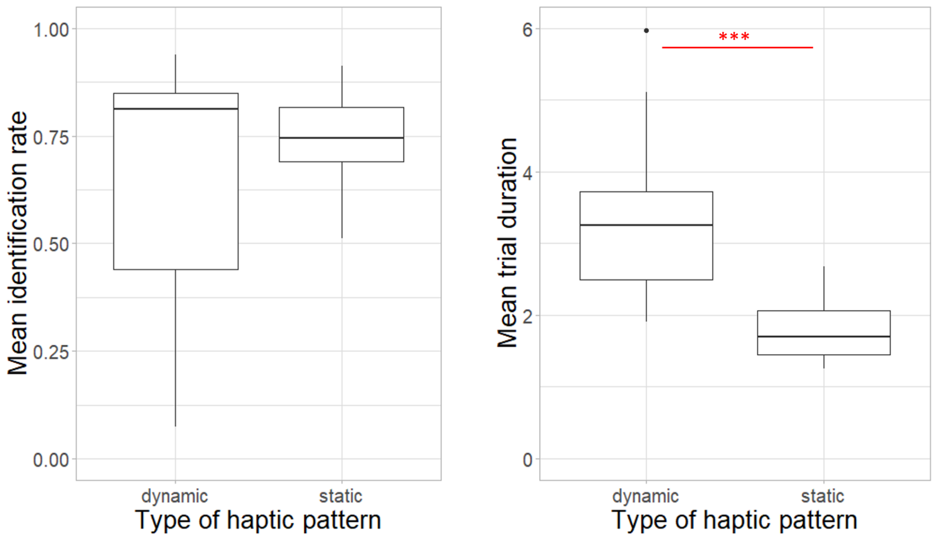

Figure 3.13: Experiment #1. Distribution of participants identification rates & trial duration.

was higher (3.254, IQR = 1.218) than the `Static` patterns (1.697, IQR = 0.605). This difference was statistically significant according to a Wilcoxon signed-rank test (Z = 2.93, $p<0.001$).

On the subjective difficulty of the task, participants evaluated the `Static` cues as easier to identify (Mean = 4.42, SD = 1.16) than the `Dynamic` cues (Mean = 3.17, SD = 1.53). However, only 7 participants out of 12 selected the `Static` cues as their preferred type of cue. Some participants reported that `Dynamic` cues felt easier to identify, but that the mapping to the direction was difficult to understand.

Overall, results show that both types of directional cues can be accurately identified by participants, with lower results for the `Dynamic` pattern. These lower results seem to be tied to individuals: most participants showed high accuracy for both types of stimuli, while some showed lower results for `Dynamic` cues. H1 is thus only partially supported. Trials with `Dynamic` cues showed longer answer time, supporting H2. Finally, H3 is not supported, as no significant difference was found for diagonal direction identification between the two haptic conditions.

3.3.3 Discussion

In the first study, we showed that even though both flexible and rigid versions of our haptic handle were effective in displaying localized cues, participants found the flexible version to provide more easily discriminable sensations. In that respect, our design of a flexible isolating structure within the handle was shown to be effective. In practice, this would allow us to design easily identifiable localized haptic cues with a larger range of vibration intensities in the users' hand. Even if location identification is possible without isolation, our design facilitates the perception of the haptic cues provided by the handle. In addition, during the perception study, participants were solely focused on identifying the vibration location. We can expect that results would be lower if this was only a secondary task. For instance, it would be the case if the handle is used in navigation scenarios where users would have to also focus on other tasks, e.g., interacting with the environment or other users. In such a case, having more easily-identifiable haptic cues is beneficial. Moreover, people with lower tactile sensitivities could also benefit from better-contrasted tactile cues with such a multi-actuator device.

In the second study, we introduced more complex cues in order to display eight directions with the handle. Identification rates were lower than with four directions only, but they were also tied to individuals, with some outperforming others. Given the results, `Static` cues would be the best option for communicating information to the user in the most efficient and intuitive way. `Dynamic` cues could also be a good fit, but some training and/or explanation would be needed before using the device. The timing of sequential activations, direction mapping and other parameters should also be investigated further, as more optimal patterns could probably improve discrimination accuracy. Individual differences support the need for personalization of haptic cues: depending on the application, users should be able to choose what type of pattern they prefer.

3.4 Conclusion

In this chapter, we presented the design of a multi-actuator haptic handle. It features a custom deformable structure at its center which holds four actuators, so as to better isolate their vibrations. We evaluated the benefits of this design in a vibrometry study, where we showed an increased vibration intensity at the point of stimulation. In two user studies, we then evaluated the benefits of our multi-actuator isolation design. We first assessed the ability of participants to identify the vibration location easily around the handle, showing a clear preference towards the isolated handle which displayed sensations that were judged easier to discriminate. We then evaluated the discrimination of more complex patterns using multiple actuators in order to display eight directions around the handle. Results for these cues were lower than using only four directions, but were highly variable depending on participants.

The current handle design, while effective, still has some limitations. The non-negligible size of the isolation structure for each motor might limit its use in other devices. Additionally, the current system can be subject to some issues when motors are moved in contact with the rigid body of the handle or, in some rare cases, when motors slip within the handle. These limitations could be mitigated by improving the design of the isolating structure to prevent deformation in unwanted directions but might have an effect on isolation. The shape of the handle might also not be adapted to all users. Indeed, the actuator placed in contact with the palm is not as close to the skin as the other actuators depending on hand size and grasping positions, which should be taken into account in future design iterations. Adaptation on mobility devices is also challenging with the current design, especially for walkers or white canes, on which the grasping position would be much different.

Regarding the haptic cues displayed by the handle, the choice of ERM actuators limits the possibilities: with little control over the vibration frequency, using multiple actuators simultaneously can have signals interfering with each others. While haptic cues can still be discriminated, higher-grade actuators might be able to provide clearer sensations to users.

In the next part of this manuscript, we explore the use of our haptic handle in various navigation-related application, making use of the different haptic cues we discussed and evaluated.

Part II

NAVIGATION USING A MULTI-ACTUATOR HAPTIC HANDLE

CHAPTER 4

ENHANCING USERS PERCEPTION OF THEIR SURROUNDINGS

In virtual environments, intrusions of this space by people or objects can be undetected if they occur outside the field of vision or center of attention, thus raising a series of interesting questions about how to convey this information to the user [Medeiros 2021; Slater 2016]. The use of sensory feedback to inform users of moving threats was particularly studied by Bajpai et al. in a task where participants had to avoid moving obstacles with the help of combinations of visual, audio, and haptic cues provided by a haptic belt [Bajpai 2020]. Tactile cues provided improved users' performance, as did visual feedback, which was, however, considered as more intrusive on the user's field of view. Hence, haptic sensations are often chosen as to avoid overloading the other sensory channels.

In this chapter, we propose to use our haptic handle to augment the user's spatial awareness in virtual reality, using the device as an in-hand haptic representation of their surroundings (see Figure 4.1). While users navigate through virtual environments, the handle provides intuitive

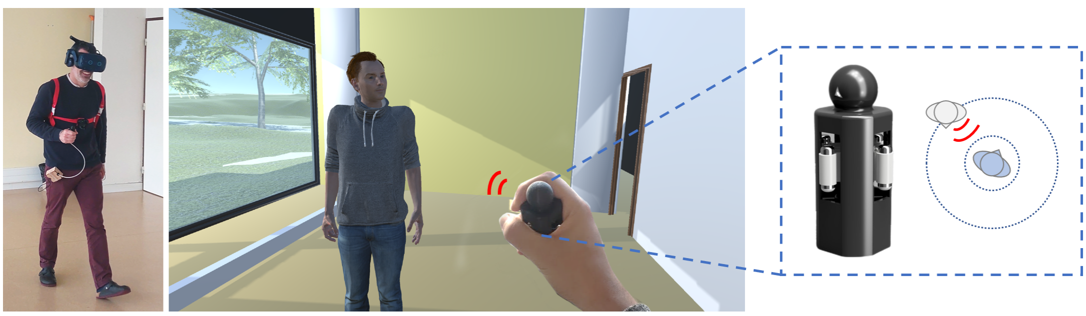

Figure 4.1: This chapter explores the use of our haptic handle as a handheld haptic representation of the user's surroundings in virtual environments, displaying information regarding obstacles entering the personal space of the user, such as virtual humans or obstacles.

feedback about the proximity of obstacles within their personal space. We conduct a pair of user studies, assessing the ability of the proposed device and concept to help user avoiding dynamic obstacles in VR, and evaluating the influence of this haptic representation of the personal space when walking around static obstacles, including virtual humans.

4.1 Haptic feedback for obstacle avoidance

4.1.1 Experimental task and design

In this experiment, we evaluated the ability of participants to use the directional cues of the haptic handle to avoid approaching obstacles moving towards them. This experiment is inspired by the work of Bajpai et al., where a haptic belt is used in a similar scenario [Bajpai 2020]. Twelve participants took part in this study (11M, 10 right-handed, aged 22–47, mean age 28). Before that, they took part in the discrimination study presented in subsection 3.3.2, which allowed them to familiarize with the haptic cues used in the experiment.

We considered the two types of haptic patterns presented in subsection 3.3.2 (`Dynamic`, `Static`) to display eight directions (`Front`, `Front-left`, `Left`, `Back-left`, `Back`, `Back-right`, `Right` and `Front-right`) from which the obstacles can enter the user's personal space.

This experiment is made of two blocks, one for each type of haptic pattern. The blocks are counter-balanced between participants. Each direction is repeated 10 times in each block, for a total of 80 trials each. Trials are completed in a randomized order.

The experimental setup and the virtual environment are shown in Figure 4.2. The virtual environment is composed of an octagonal room. At the beginning of each trial, the user is placed at the center of the room. A moving obstacle is spawned at one of the 8 possible directions around the participant and moves towards the center. As the obstacle approaches the user, the latter is alerted by the haptic handle, according to the considered rendering pattern. Detection occurs 5m from the user, with obstacles moving at 3m/s. The haptic handle is mounted on a joystick, enabling the user to move their avatar within the environment to avoid the moving obstacle. The movement of the joystick is tied to translations on the x and z axis with respect to the scene (i.e., the camera orientation is fixed and the virtual avatar can only translate, not rotate. Participants are instructed to avoid the moving obstacles relying on the feedback provided by the haptic handle. Participants are shown the point of view of their virtual avatars on the screen (see Figure 4.2), so that they can see obstacles coming from the `Front`, `Front-left` and `Front-right` directions. On the other hand, they cannot see obstacles coming from the other directions. This is done to replicate the setup used in [Bajpai 2020]. At the beginning of each new trial of the task, the participant is moved back to the center of the virtual room. It is not possible to move before the first feedback cue is provided.

We collected the trajectories of participants in the virtual environment and the number of

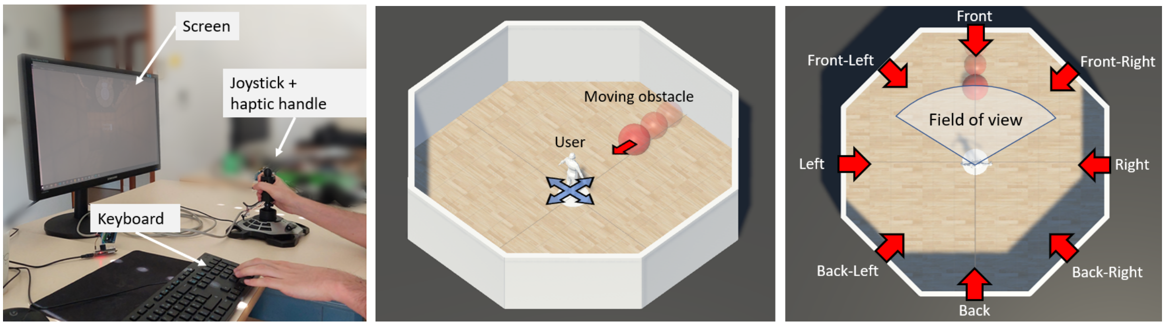

(A) (B)

Figure 4.2: (A) Setup for the experiment. Participants sat at a table and used the joystick to move in the virtual environment displayed on a screen. (B) Virtual environment used in the experiment. Participants are placed at the center of a virtual octagonal room. Obstacles (red spheres) are spawned randomly from one of eight walls of the room, representing the eight directional information provided by the haptic handle, and move towards the center. Participants can see in front of them and must avoid the obstacles using a joystick.

collisions with the obstacles. After each block, participants are asked to rate the difficulty of the task.

We hypothesized that:

(H1) Both `Static` and `Dynamic` feedback cues delivered by the haptic handle enable the users to effectively avoid obstacles;

(H2) `Dynamic` feedback cues will outperform `Static` ones.

4.1.2 Results

Some first observations can be made looking at the success rate, i.e., the number of trials in which the participant avoided the obstacle (see Figure 4.3A and Figure 4.3B). First, we see that when the obstacle is visible (i.e., in the `Front`, `Front-left` and `Front-right` directions), participants are able to avoid it in almost all cases. For the other directions, two cases can be observed: for obstacles coming from the sides (i.e., `Left`, `Right`, `Back-left` and `Back-right` directions), avoidance rates range from 63 to 88%, with slightly higher values in the `Static` condition. For obstacles coming from the `Back`, avoidance rates is much higher at 98% (see Figure 4.3B).

Trajectories of the participants can be seen in Figure 4.4, as well as an overview of the direction taken by participants across conditions in Figure 4.5. As we can expect, collisions occur on the path of the obstacle (i.e., for an object coming from `Back-left`, collisions occur on `Back-left` and `Front-right`). We can observe that for obstacles coming from the `Front-right` and `Front-left` diagonals, participants tend to move either on the side or forward. For obsta-

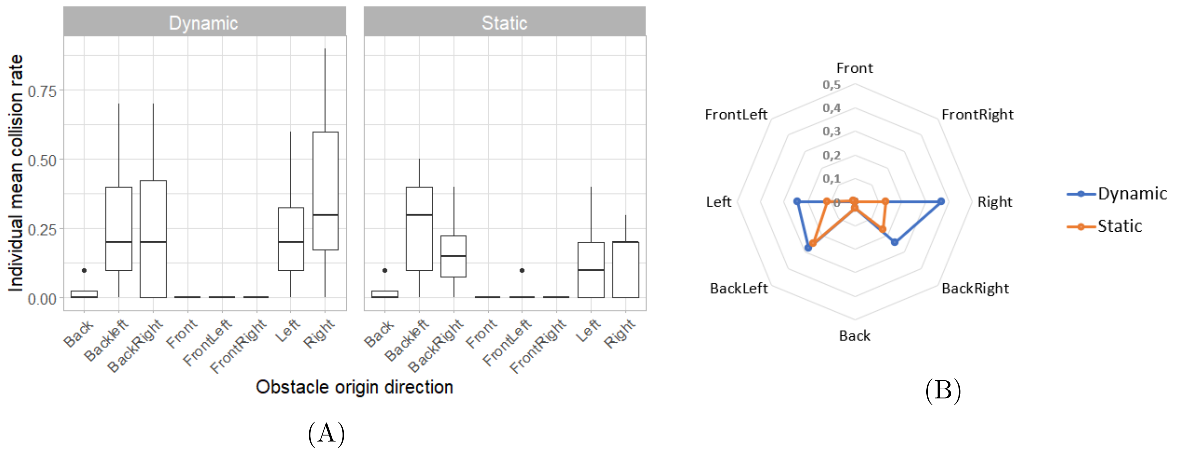

Figure 4.3: (A) Distribution of individual collision rates for both haptic patterns. The collision rate is provided for each obstacle direction. (B) Global collision rates for both haptic patterns. There is no collisions for the front directions (`Front`, `Front-right` and `Front-left`).

cles coming from the `Back-right` and `Back-left` diagonals, participants seem to prefer going towards the other rear-diagonal (e.g., moving toward `Back-left` when an obstacle comes from `Back-right`).

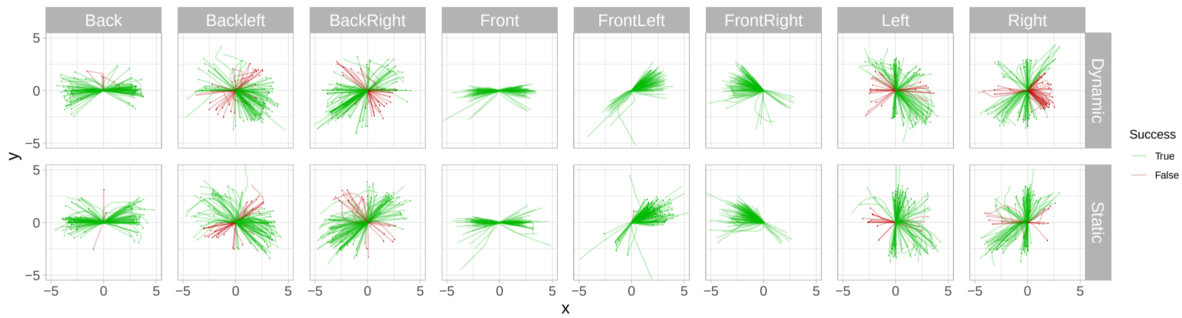

Figure 4.4: Participants trajectories across conditions. Trajectories are shown in green when the obstacle is avoided successfully, and in red if a collision occurred.

We analyzed the success rates with a Generalized Linear Mixed Model (GLMM), using a logistic model. Independent variables are the type of cue (`Static` or `Dynamic`) and the direction of the incoming obstacle (`Front`, `Front-left`, `Left`, `Back-left`, `Back`, `Back-right`, `Right`, `Front-right`). Participants are considered as a random effect. Given that the results of the frontal directions, which presented visual feedback in addition to haptic feedback, have no variance, we do not include them in the analysis.

We observed a significant effect of both the type of cue (χ^2 (1, N=1200) = 18.71, p<0.001) and the obstacle direction (χ^2 (4, N=1200) = 43.11, p<0.001). Post-hoc tests were performed with simultaneous pairwise comparisons using Tukey's test. Results show that avoidance rates

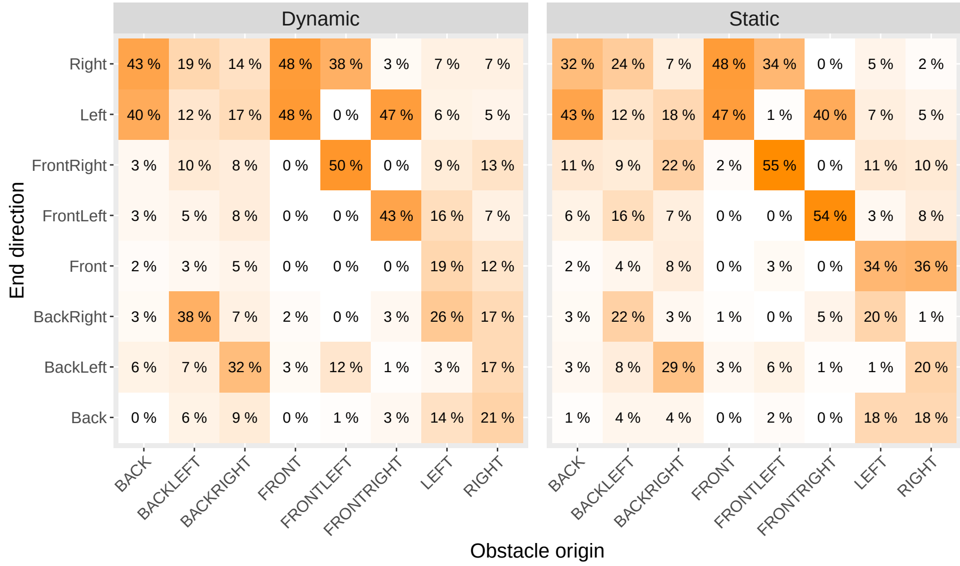

Figure 4.5: Confusion matrix of the directions taken by participants. Ideally, the correct directions should be orthogonal to the obstacle origin.

are significantly lower in the `Dynamic` condition compared to the `Static` condition ($Z = -4.33$, $p<0.001$), and that obstacle coming from the `Back` are avoided better than other those in other directions ($p<0.001$).

Regarding the subjective difficulty of the task, participants rated the ease to avoid obstacles similarly in both conditions (`Static`: Mean = 5.25, SD = 0.45, `Dynamic`: Mean = 5.0, SD = 1.20).

4.1.3 Discussion

In this first experiment, results show that participants were mostly able to avoid obstacles, therefore supporting H1. Participants were however more successful in avoiding obstacles using `Static` cues, thus invalidating H2.

One interesting result for this second experiment is the noticeably high avoidance rate for the `Back` direction compared to other non-visible directions. While this could be attributed in part to the higher discrimination rate of this direction compared to the diagonals, it is still noticeably higher than the avoidance rates for `Left` and `Right` directions, which were also well recognized by participants. Bajpai et al. highlighted a similar pattern in their experiment, and argued that it might be due to the dynamics of the human body, with a step to the side being faster than a step forward or backward [Bajpai 2020]. In our case, movement speed is the same in any direction as we move with a joystick. The similarity with real human motion might indicate that users transfer this behavior from the real to the virtual world, showing the intuitiveness of the proposed haptic representation in VR.

4.2 In-hand haptic proxemics

In a second experiment, we evaluate the effects of the haptic representation of the user's personal space in VR on participants trajectories around static obstacles using the previously introduced static cues. Participants walked across a room in VR with one or two static obstacles, which were signaled by the haptic handle using directional vibrotactile cues.

4.2.1 Personal space representation

The study of the "Personal space", called Proxemics, was introduced by Edward T. Hall in 1966 [Hall 1969]. We use our personal space in social interactions, but also to process events and to detect the presence of obstacles when navigating [Gérin-Lajoie 2008]. Personal space perception is thus essential for comfortable and safe navigation.

This space can be modeled in different ways [Rios-Martinez 2015], one of the simplest approaches being a series of concentric circles around the user. More complex representations include a larger area in front of the user and/or a smaller space on the user's dominant side, taking into account the way users perceive their surroundings. It has also been proven that the personal space does not depend on the walking speed and that it plays an important role in navigating cluttered environments [Gérin-Lajoie 2008]. Thus, the user's personal space can change depending of the scenarios, including in VR [Medeiros 2021; Slater 2016]. In fact, it was shown that in a VR setting, distance from obstacles was higher than in real life. In addition, people also did not show the same behavior with anthropomorphic obstacles than with inanimate objects [Sanz 2015].

Haptics have the potential to add another degree of perception of user's personal space. For example, floor based vibrations rendering the steps of virtual humans were shown to improve social presence in VR, as well as increasing avoidance behavior when virtual humans intruded users personal space [Lee 2017]. Another study with floor vibrations in augmented reality also highlighted slower walking speeds with haptic feedback than without [Lee 2018]. Multimodal cues can also be used to provide warnings when passersby enter the tracking space of the user [Medeiros 2021; Von Willich 2019]. In the real world, devices such as the encounter-type haptic interface proposed by Yabe et al. can inform users of the presence of obstacles around an autonomous vehicle [Yabe 2021]. This envelope, represented by the interface, could be seen as a sort of extended personal space. Augmented white canes that use haptic cues to extend the range of detection can be considered as an extension of the user personal space.

However, to the best of our knowledge, no studies have explored how to map the user's personal space to a handheld tangible object providing haptic sensations.

4.2.2 Experimental task and design

We recruited 12 participants (ages 18-58, 11 males, all right-handed) to perform this study.

The experiment was conducted in a 8m×5m room with a wireless HTC Vive VR headset. The room was recreated at scale in the virtual environment so that participants could walk confidently without worrying about collisions. Participants wore a harness to which was fixed a tracker, used to measure their position and orientation. The handle was linked to a portable battery, attached to the belt of participants (see Figure 4.6) and was controlled wirelessly. The VR headset headphones were used to display white noise during the experiment.

Based on results from the previous studies, we chose to focus on Static cues. We designed two haptic rendering schemes, each with two levels of vibration depending on the proximity with the closest obstacle. The two levels of proximity used for the mapping of vibrations correspond to the limits of the personal space (1.2m) and intimate space (0.45m) as determined by Hall [Hall 1969]. The two haptic rendering schemes used series of 0.15-s vibration burst, displayed on one or two actuators (see Static in 3.11). The first haptic rendering scheme, H_Freq, displayed haptic cues at two levels of frequencies (3.3Hz and 1.6Hz) depending on proximity. The second scheme, H_Int, displayed haptic cues at 3.3Hz with two levels of increasing intensity depending on proximity.

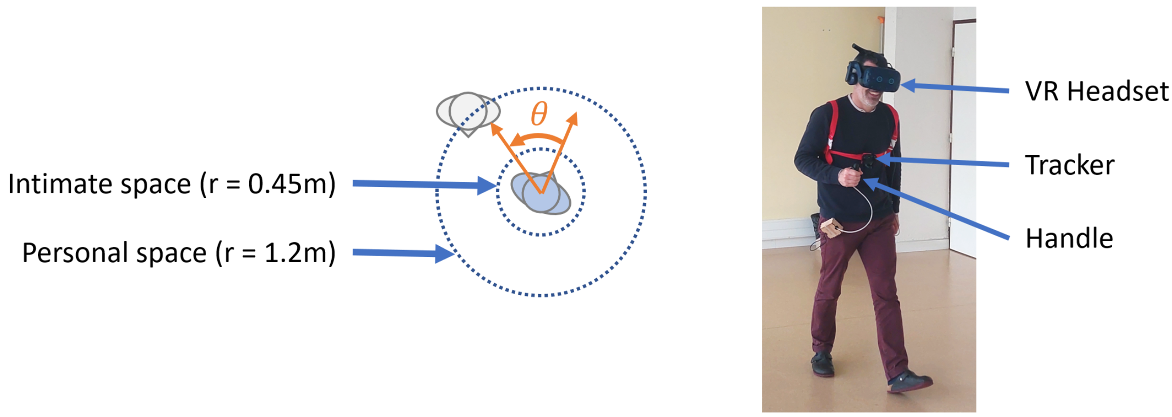

Figure 4.6: (left) We model users' space as two circles corresponding to the personal and intimate space. When an obstacle enters the users personal space, the handle is activated in the direction of the obstacle (i.e., θ is mapped to the corresponding directional stimulus on the handle as seen in Figure 3.11). (right) Participant are equipped with a wireless VR headset, a tracker and the handle. They can walk freely in the virtual space, which is a realistic representation of the actual space.

For this study, we consider the following conditions:

- *Feedback scheme:* H_Freq, H_Int or Visual (i.e., no haptic feedback).
- *Number of obstacles:* one or two, positioned as seen in Figure 4.7.

- *Type of obstacles:* human or box obstacle.

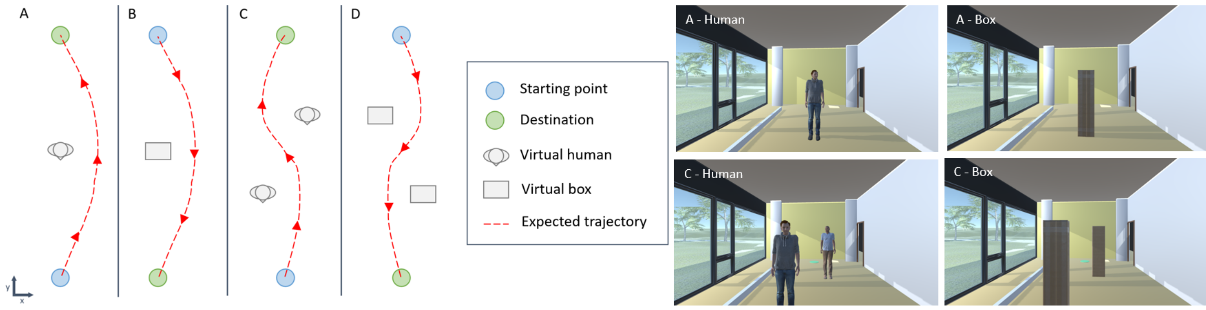

Figure 4.7: (left) During the experiment, participant walk from one side of the room to the other while avoiding one (A,B) or two (C,D) static obstacles. These obstacles are either animated virtual humans or virtual boxes. (right) The experiment takes place in a virtual environment, which represents the real-life room. Here are shown screenshots from the point of view of the participants at the starting point for the different types of obstacles.

The experiment was made of three blocks, one for each feedback condition. Condition order was counter-balanced across participants. In each block, all combinations of type and number of obstacles were repeated six times in a random order. Across the six repetitions, we ensured that participants avoided obstacles three times from each side. Obstacles are always visible from participants (i.e., they are still visible even within haptic conditions), and are all of the same dimensions.

During a block, participants were asked to walk from one side of the room to the other while avoiding the obstacles on their way. Trial ended once they got to the opposite side of the room. The next trial started in the other direction after they turned around. Before each block, they were informed of the active feedback scheme, which they were able to familiarize with before the start of the experiment.

We collected the trajectories of participants in the virtual environment, along with distances from the virtual obstacles during trials. After each block, participants were asked to judge how careful they were in avoiding both types of obstacles, and how much they relied on haptic and visual feedback.

We hypothesized that:

- (H1) Distances from obstacles will be greater with haptic feedback;
- (H2) Distance from humans will be greater than from objects.

4.2.3 Results

Individual and mean trajectories across conditions are shown in Figure 4.8. From the collected data, we extract the maximal lateral deviation from each obstacle, mean walking speed, minimal distance from obstacles (i.e., clearance distance) and area of the user deviation (see Figure 4.8). Some trials in which participants did not follow the instructions were removed before analysis. We analyzed the effect of experimental conditions on those metrics using separate linear mixed model analysis of variance, followed by post-hoc tests with simultaneous pairwise comparisons using Tukey's test.

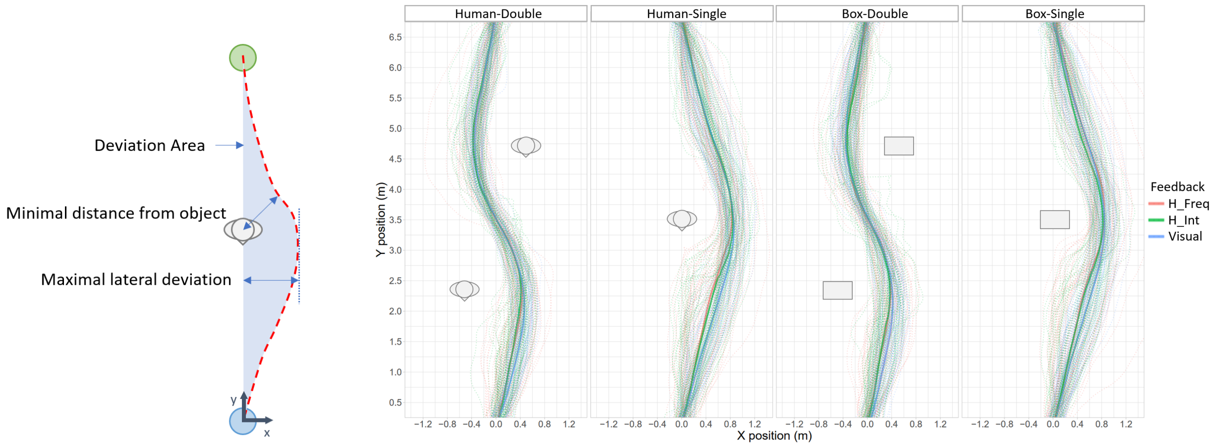

Figure 4.8: (left) We compare maximal deviation, minimal clearance distance and deviation area from users trajectories. (right) Individual trajectories and mean trajectories for each conditions. In trials with haptic feedback, participants tend to get closer to the front of the obstacle, waiting for feedback to be displayed.

Maximal lateral deviation: Results indicated a statistically significant effect on the maximal deviation of the number of obstacles ($F(1, 1290) = 49.44, p < .001$) and their type ($F(1, 1290) = 16.22, p < .001$), but not of the feedback scheme. No significant interactions were observed. Post-hoc tests indicated that deviation was greater in trials with two obstacles ($t(1272) = 7.03, p < 0.001$), and that it was also greater in trials with humans ($t(1272) = 4.03, p < 0.001$).

Deviation area: For this metric, we separated trials with one and two obstacles, as the trajectory is shaped differently. For trials with a single obstacle, results showed a significant effect of the feedback scheme ($F(2, 415) = 7.46, p < 0.001$) but not the type of obstacle. Post-hoc tests indicated a smaller deviation area for trials with haptic feedback compared to those with only visual feedback (`H_Freq` vs. `Visual`: $t(415) = -3.05, p < 0.01$; `H_Int` vs. `Visual`: $t(415) = -3.58, p < 0.01$). For trials with two obstacle, results showed a significant effect of both the feedback scheme ($F(2, 414) = 4.74, p < 0.01$) and the type of obstacle ($F(1, 414) = 13.13, p < 0.01$) . Post-hoc tests indicated a larger deviation area for trials with human obstacles compared to those with boxes ($t(414) = 3.624, p < 0.001$), and a smaller deviation area between trials with `H_Int` and `Visual` feedback ($t(414) = -3.06, p < 0.01$).

Mean walking speed: Results indicated a statistically significant effect on mean walking speed of the number of obstacles ($F(1, 843) = 14.07, p < 0.001$) and feedback scheme ($F(2, 843) = 104.26, p < 0.001$). Post-hoc tests indicated lower mean walking speed in trials with two obstacles than those with one ($t(843) = -3.64, p < 0.001$), as well as in trials with haptic feedback compared to visual feedback only (`H_Freq` vs. `Visual`: $t(843) = -11.08, p < 0.001$; `H_Int` vs. `Visual`: $t(843) = -13.55, p < 0.001$).

Clearance distance: Results indicated a statistically significant effect on minimal clearance distance of the feedback scheme only ($F(2, 843) = 5.31, p < 0.01$). Post-hoc tests indicated a slightly lower clearance distance in trials with haptic feedback compared to visual feedback only (`H_Freq` vs. `Visual`: $t(843) = -2.71, p < 0.05$; `H_Int` vs. `Visual`: $t(843) = -2.92, p < 0.01$).

Questionnaire: Participants rated their carefulness around both types of objects similarly (`Human`: Mean = 5.08, SD = 1.59, `Object`: Mean = 4.33, SD = 1.75). Overall, participants indicated that they relied more heavily on visual feedback than on haptic feedback to avoid obstacles (`Haptic`: Mean = 2.33, SD = 1.85, `Visual`: Mean = 6.55, SD = 0.77).

4.2.4 Discussion

For this experiment, results showed that the use of the haptic handle made participants walk somewhat closer to the obstacles. This goes against our initial hypothesis (H1): we expected that the haptic feedback would increase distances from obstacles, as it would have provided a sense of intrusion in the user's personal space. Actually, participants rated their reliance on the haptic feedback quite low compared to the visual feedback. Similar conclusions were drawn in other works [Berton 2020; Monica 2023], where users relied mainly on visuals. Still, some tended to walk closer to the obstacles at the start of the trials, waiting for the haptic feedback to activate before starting to walk on the side. Walking speed was also lower with the haptic feedback, which could indicate a more careful behavior from participants, even if they did not report as such. As observed in other virtual proxemics studies [Sanz 2015], distances from human obstacles was higher than those from inanimate objects, thus validating our hypothesis (H2). Despite the potential difficulty to map the in-hand cues to directions in the environment, the concept of an in-hand haptic representation of the personal space was easily understood by participants, which is promising for future works on the subject.

Since the range of deviation distances from the obstacles was mostly contained within the personal space limits, haptic feedback was active during most of the users' trajectory. More advanced models of the shape of the user's space could be explored. For example an elliptical shape, as discussed by Sanz et al., might change the way users rely on the haptic feedback [Sanz 2015]. Feedback could also be modulated depending on the distance to obstacles to provide a finer level of information.

4.3 Conclusion

In this chapter we introduced an in-hand haptic representation of user's surroundings: using our multi-actuator haptic handle and associated feedback schemes, we proposed to represent the user and their personal space. The handle can communicate the presence of objects around the user using distributed haptic feedback, providing intuitive spatialized information.We first investigated the use of these cues to alert the user of an imminent collision with a moving obstacle in a virtual environment. Both types of cues showed similar results in avoiding the obstacles. Interestingly, participants avoided obstacles approaching from behind them more effectively than those in other directions. This behavior had also been observed in real-life scenarios. Secondly, we evaluated the impact of this haptic representation of personal space in a VR proxemics study. The results showed that while participants mostly relied on visual feedback, distance from obstacles and walking speeds were lower when the haptic handle was used.

Our approach only considered specific conditions in which the handle informed users of near obstacles or virtual humans. It would be beneficial to investigate other conditions that better reflect the potential use of this concept in real application. For instance, we could envisage to use such feedback to inform users of the presence of others in their surroundings, whether they are in the virtual or real world. Additionally, for its use in obstacle detection, different levels of difficulty should be tested with the handle as well as more realistic conditions in which users approach obstacles while navigating.

CHAPTER 5

DESIGN OF HAPTIC RENDERING TECHNIQUES FOR NAVIGATION

One of the challenges of using haptic feedback for navigation is finding a rendering scheme able to provide necessary information while staying easily interpretable. Localized sensations appear to be a good fit for providing rich directional information, but they need to be coupled with an intuitive and informative navigation paradigm.

In this chapter, we first design and evaluate a set of haptic rendering techniques for navigation, combining three navigation strategies and two rendering schemes using our custom multi-actuator haptic handle. The three navigation strategies offer guidance by indicating a direction to follow, the deviation from the path, or the direction to return, while the two rendering schemes offer different level of granularity of the navigation information, utilizing the localized feedback as a distinctive directional cue relative to the user orientation. Our haptic handle is not strictly limited to pedestrian navigation. We start to investigate its use in combination with a power wheelchair. In this context, we explore how the colocation of the haptic navigation feedback with the joystick used for moving the wheelchair might impact navigation, and if providing navigation feedback in the other hand might be better for users.

The design and evaluation of navigation techniques which we cover in section 5.1 were published in [Cabaret 2024b].

5.1 Multi-actuator navigation techniques for pedestrian navigation

5.1.1 Guidance feedback

We designed three navigation strategies and two haptic rendering schemes for our haptic handle to guide users along reference paths. Each strategy starts by computing an angle θ, defined as the angle between the user and a navigation target on the path to follow, dependant on both the user orientation and position, as detailed in Figure 5.1. θ is then mapped to a directional stimuli to be displayed by the haptic handle depending on the active rendering scheme, as described in Figure 5.2.

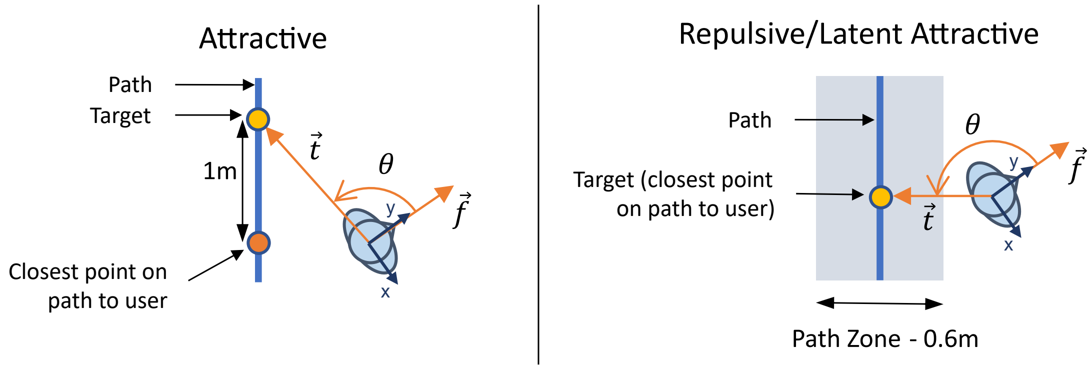

Figure 5.1: Each navigation strategy (Attractive `A`, Repulsive `R`, Latent Attractive `LA`) computes a signed angle θ between the user heading direction $\overrightarrow{f}$ and a vector pointing towards a target on path $\overrightarrow{t}$. The Attractive strategy sets the target as the point on the path one meter ahead from the closest point on path to the user. The Repulsive and Latent strategies set the target to the closest point on path to the user.

The three navigation strategies provide information regarding the position of the user with respect to the target path. The Attractive strategy (`A`) provides navigation information through 0.2-s-long vibratory cues conveyed regularly every second. The Repulsive strategy (`R`) provides navigation information only when the user is more than 30 cm away from the path (i.e., out of the 60-cm-wide path zone or neighbourhood seen in Figure 5.1, corresponding to the width of a side step on each side of the path), continuously conveying vibratory cues opposite to the desired motion direction. The Latent Attractive strategy (`LA`) also provides navigation information only when the user is more than 30 cm away from the path, but it continuously convey vibratory cues *towards* the desired motion direction.

The two rendering schemes provide the directional information with different levels of granularity: `4Dir` provides four directional cues while `8Dir` provides eight, as described in Figure 5.2.

Representative examples of the considered combination of strategies and rendering schemes

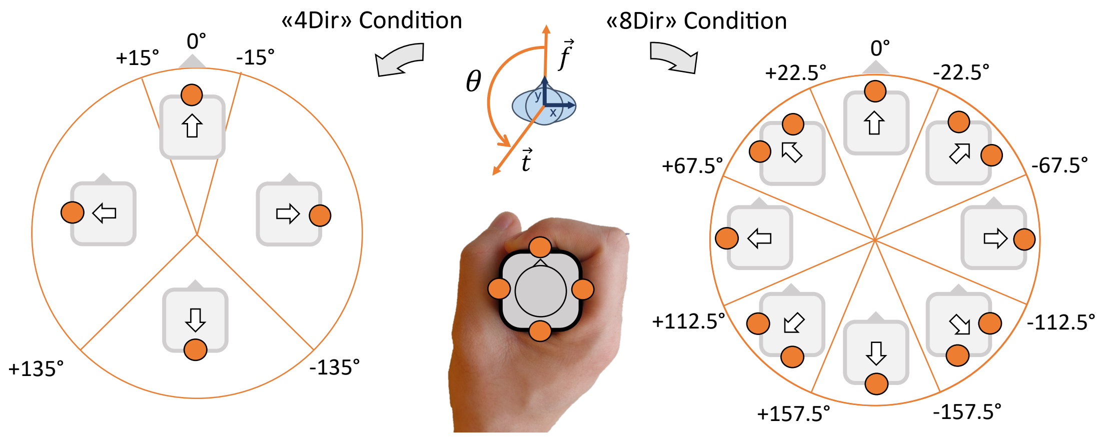

Figure 5.2: Each navigation strategy can map θ into vibratory stimuli with two rendering schemes, using four (4Dir) or eight (8Dir) directions. In 4Dir, θ is mapped into the four directions left, right, front, back, using one motor at a time; 8Dir considers four additional directions, front-left, front-right, back-left, back-right, which simultaneously use two actuators. The location and interpretation of each stimulus are linked, e.g., the "left" stimulus is provided on the left side of the handle. Depending on the strategy used to guide the user, these stimuli are played as 0.2-s-burst every second (A) or continuously (R, LA).

are shown in Fig. 5.3.

5.1.2 User Study

We recruited 18 participants (14M, 4F, aged 20-47: mean = 27.28, SD = 6.25) to take part in the study, all of whom gave their written informed consent. The study has been approved by Inria's ethics committee (COERLE, No. 2023-49). Before the start of the experiment, participants were introduced to the haptic handle and familiarized with the different haptic cues.

Experimental Setup

We conducted the experiment in a 8×8 m room. A Vive tracking system tracked the user pose. Participants wore a harness on which the Vive tracker was positioned and held the handle in their dominant hand, with the control box attached to their belt (see Figure 5.4-b). A noise-cancelling headset was used to hide potential audio cues from the vibrations in the handle. We considered three target paths, shown in Figure 5.4-a, which were not visible to the participants. These paths were designed to have similar lengths ($13.5 \pm 1m$), each with a different combination of angles between path segments (90° for P1, 45° for P1 and both 90° and 45° for P1), which could highlight differences between 4Dir and 8Dir rendering schemes. Two possible starting points on opposite sides of the room were used during the experiment to minimize learning effects (i.e., the target path could be rotated 180 degrees around the center of the room, with

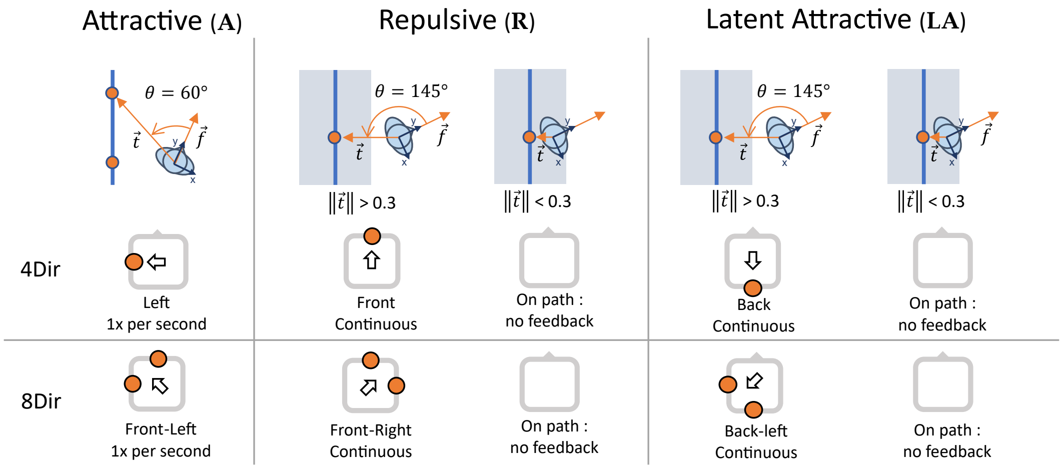

Figure 5.3: Navigation strategies (Attractive A, Repulsive R, Latent Attractive LA) are combined with the two rendering schemes (4Dir, 8Dir). The orange circles (bottom) represent the actuators which are activated on the handle, depending on the position and orientation of the user relative to the path (top).

no changes in the overall trajectory participants would follow).

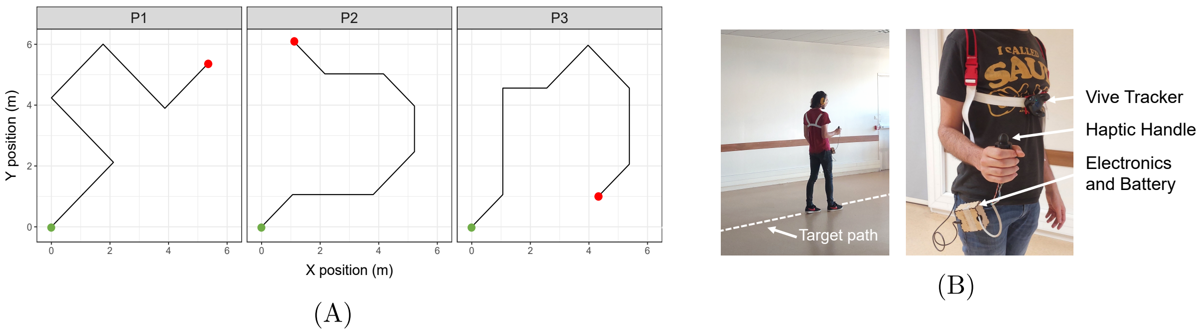

Figure 5.4: (A) Three paths P1, P2, and P3 were used throughout the experiment. The starting point of each path is displayed in green and the end point in red. The paths were regularly rotated by 180 degrees, so as to minimize learning effects without changing their shape. (B) During trials, participants were guided along one of these paths without seeing it. Participants held the device in-hand while wearing a tracker for measuring their position in the room.

Experimental Design

We evaluated the ability of the proposed haptic navigation strategies and rendering schemes to guide participants along target paths. We considered the following experimental variables:

- Navigation strategy: A, R, and LA, as presented in subsection 5.1.1 and Figure 5.1;

- Rendering scheme (information granularity): `4Dir` and `8Dir`, as shown in Figure 5.2;
- Target paths: `P1`, `P2`, `P3`, as shown in Figure 5.4.

The experiment was made of three blocks, one for each navigation strategy. Within each block, the considered navigation strategy was used with both rendering schemes on the three paths, one after the other (i.e., 6 trials per block). Strategies and rendering schemes presentation order was counter-balanced across participants, while path order was randomized. The starting point changed every three trials, i.e., when the rendering scheme changed.

At the beginning of each block, participants received explanations on the navigation strategy that would be used in the block. They were asked, for each trial, to follow the handle instructions to the best of their ability. Trials started with participants standing at the starting point and facing towards the opposite corner of the room. Trial stopped when reaching the end of the path (0.5 m or less from the end point) or after four minutes, whichever came first.

Collected Data

We collected the position and orientation of the participant, duration of the trial, and information displayed by the handle. After each trial, participants were asked to evaluate their perceived success on a scale from 1 to 7. Participants also judged each rendering scheme, rating three statements on a 7-item Likert scale (1=Totally disagree, 7=Totally agree): Vibrations were tiring (*Tiring*); Vibrations were easy to locate (*Locate*); Vibrations were difficult to interpret (*VibInterpret*). Participants also rated each navigation strategy through ten statements: I navigated confidently (*NavConfidence*); The navigation strategy was easy to use (*Use*); The guidance instructions were hard to interpret (*NavInterpret*); I could use it without preliminary instructions (*Instructions*); I learned to use it quickly (*LearnSpeed*); It is easy to learn to use it (*Learn*); It is fun to use (*Fun*); It is pleasant to use (*Pleasant*); The task is mentally demanding (*MentalDemand*); The task is physically demanding (*PhysicalDemand*). We also collected open comments throughout the experiment. At the end, participants were asked for their preferred strategy.

Results

We considered successful trials as trials where (i) participants reached the end of the path (i.e., 0.5 m or less from the end point) in less than four minutes and (ii) they did not walk from one section of the path to another, i.e., did not "cut" the path. A plot of all trajectories can be seen in Figure 5.6, with individuals' trajectories available in Appendix II. Participants were successful in 90% of trials (see Table 5.1 for results per strategy and rendering scheme; see Figure 5.5 for trajectories representative examples). We used a Generalised Linear Mixed Model to analyze the participants success. Navigation strategy, rendering scheme, and path were considered as the independent variables, while participants as a random effect. We observed a significant effect of the navigation strategy only (χ^2(2, N=324) = 15.01, p<0.001). Post-hoc analysis using Tukey's test highlighted a greater success for `A` vs. `R` (Z=2.74, p<0.05) and `A` vs. `LA` (Z=3.61, p<0.01).

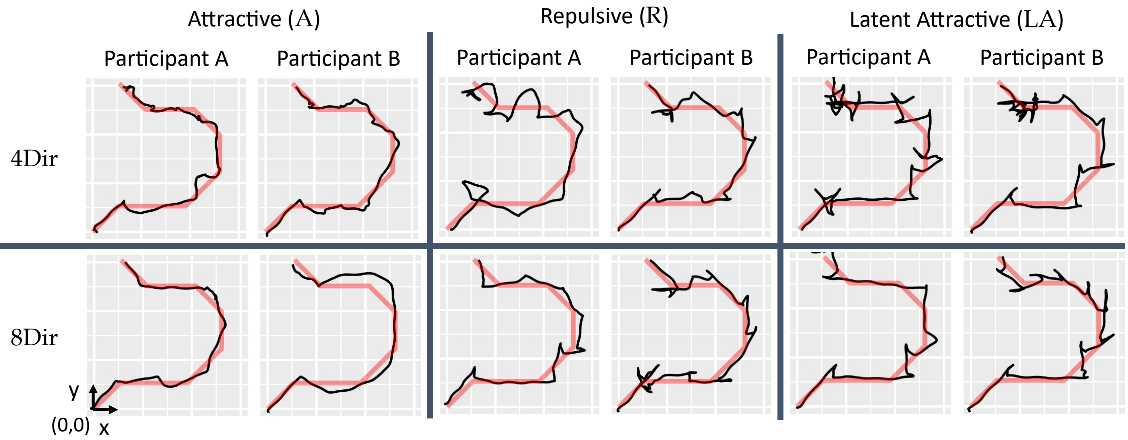

Figure 5.5: Examples of trajectories of two participants on P2 (red: target path, black: participant trajectory). Trajectories tend to be smoother with the `A` strategy.

Table 5.1: Mean success rates for each combination of strategy and rendering scheme.

	`Attractive`	`Repulsive`	`Latent Attractive`
`4Dir`	100%	93%	83%
`8Dir`	98%	87%	80%

For the rest of this section, we only take into account successful trials.

Path efficiency ratio. Path efficiency ratio, measured as the ratio between the distance walked by participants and the length of the path, is minimal for `A` (Mean=1.35, SD=0.33), and greater for `LA` (Mean=2.87, SD=1.77) than for `R` (Mean=2.32, SD=1.09). Wilcoxon signed-rank test show a significant difference between all pairs of navigation strategies (p<0.01). While this difference is significant, it must be taken into account that the `R` and `LA` strategies provided feedback only when deviating more than 0.3 m from the path, so a higher error is expected. This effect can be observed when looking at the user's distance the path, which is lower for `A` than for the other strategies (`A`: mean=0.27, median=0.19; `R`: mean=0.35, median=0.31; `LA`: mean=0.36, median=0.31).

Self evaluated success. We also analyze the self-evaluated success from participants using a Cumulative link mixed-effects model. Results show a significant effect of the navigation strategy (χ^2(2, N=291) = 10.06, p<0.01) and path (χ^2(2, N=291) = 7.15, p<0.05). As expected, post-

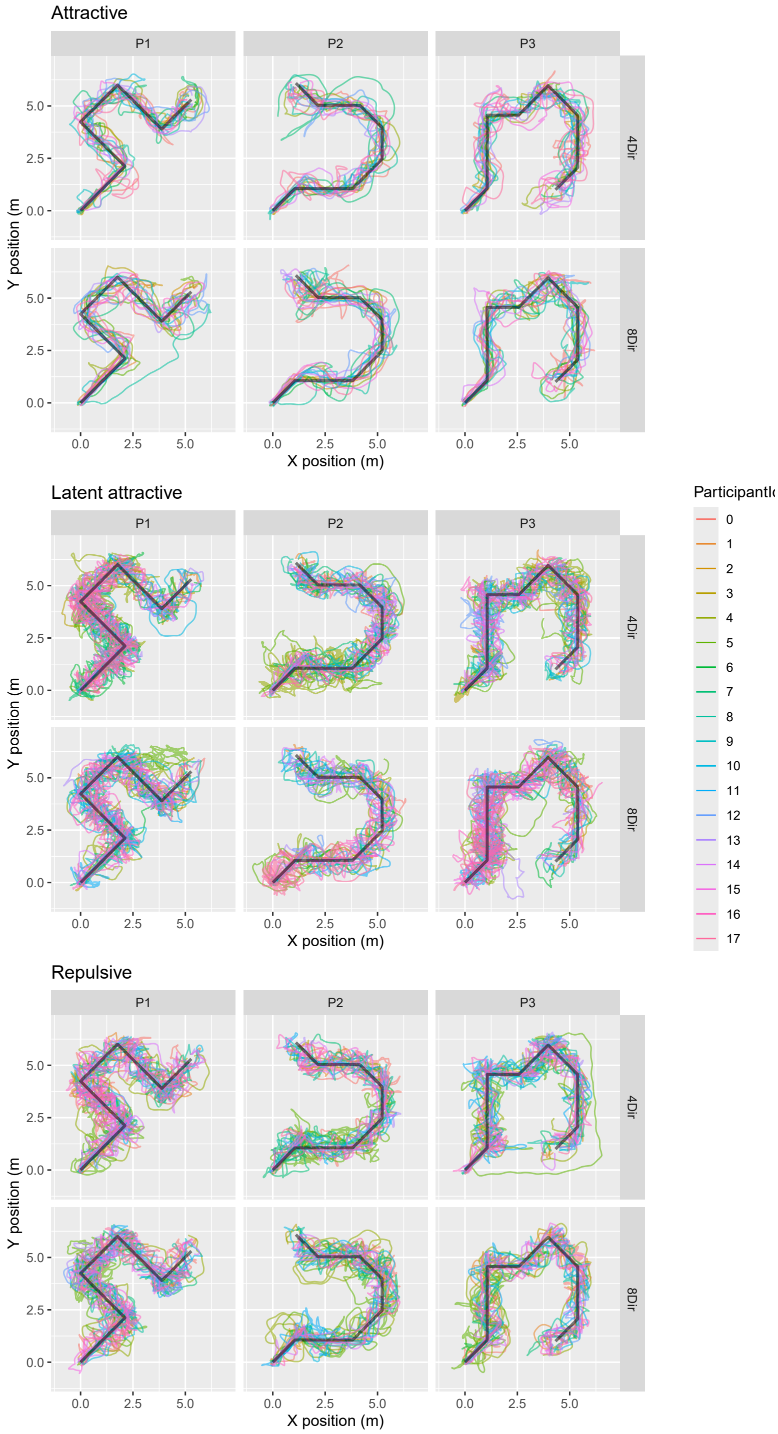

Figure 5.6: Participants trajectories across conditions. Reference paths are shown in black and participants trajectories in color. Individuals trajectories are available in Appendix II.

hoc Tukey's test showed higher evaluated success for A vs. R (Z=2.38, p<0.05) and A vs. LA (Z=2.95, p<0.01). P1 also showed significantly better results than P2 (p<0.05) for this metrics.

Subjective evaluation. Regarding the subjective questionnaire (see Sec. 5.1.2), Wilcoxon signed-rank tests showed significant differences for *Use* between A and LA (mean: 5.5 vs. 4.0 , p<0.05), *Instructions* between A and LA (mean: 5.1 vs. 2.8 , p<0.01) and A and R (mean: 5.1 vs. 3.0 , p<0.01), *Learn* between A and R (mean: 5.9 vs. 4.6 , p<0.05), and for *Fun* between A and LA (mean: 6.0 vs. 4.6 , p<0.05). Significant differences were also observed for *VibInterpret* between A and LA (mean: 2.7 vs. 3.7 , p<0.01) and A and R (mean: 2.7 vs. 3.8 , p<0.01), as well as for *VibLocate* between 4Dir and 8Dir (mean: 5.8 vs. 5.1 , p<0.01). Other questions did not show significant differences. Corresponding boxplots are shown in Figure 5.7.

At the end of the experiment, 11 out of 18 participants chose A as their preferred strategy, 3 chose R, and 4 chose LA.

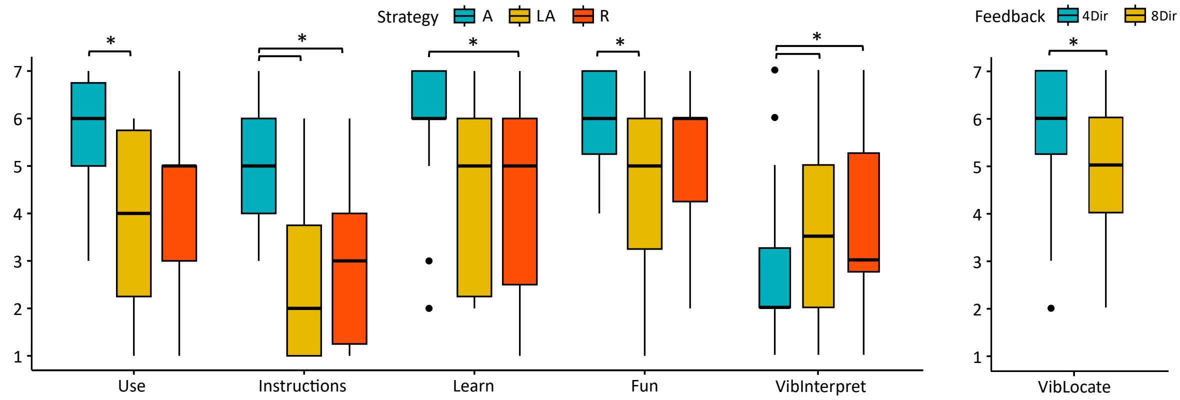

Figure 5.7: Participants answers to items of the questionnaire over 7-item Likert scales.

5.1.3 Discussion

Our experiment evaluated the effectiveness of the proposed haptic navigation strategies and rendering schemes in guiding participants along target paths. Results showed that users were able to follow the proposed guidance successfully most of the time. Participants were able to use all three strategies successfully and quickly adapted to their use, confirming the intuitive nature of multi-actuator feedback in such a scenario. Overall, results show an advantage of A: trajectories carried out when being provided with this navigation strategy are smoother than the others (see, e.g., Figure 5.5) and participants walked lower distances overall. This result is probably linked to the fact that the A strategy (i) is always active, continuously providing information, and that (ii) it conveys an intuitive information, i.e., the direction to go, similarly to turn-by-turn GPS systems.

However, the other navigation strategies still showed promising results. Indeed, several participants reported that evaluating their success in the attractive strategy `A` was harder, as they did not know how far they were from the target path (this strategy continuously provide feedback). These comments suggest that a promising approach could be to devise an adaptive navigation strategy, providing either information about the direction to follow or the deviation from the path, according to the user's performance or position: the `A` strategy could be used when users are close to the path, while `LA` or `R` could be used when deviation is too large.

After `A`, the `R` strategy seems to perform (slightly) better than `LA`. Comments from participants suggest that the information `R` provides is intuitive: vibrations can be interpreted as obstacles on which the user "bounces" and changes direction towards the correct path. Indeed, many participants described their experience with `R` and `LA` as "bumping into virtual walls", and compared the use of `A` to that of "a compass", which we found interesting. These two interpretations of the navigation strategies can be observed on the recorded trajectories. We highlight examples of these behaviors in Figure 5.8. In failed trials, participants sometimes walked in the reverse direction of the path, which could be prevented by modifying the navigation strategy. In cases where users 'bounced' around the path (e.g., with `R`), some tended to turn around too much, thus walking from one side of the path to the other without making progress.

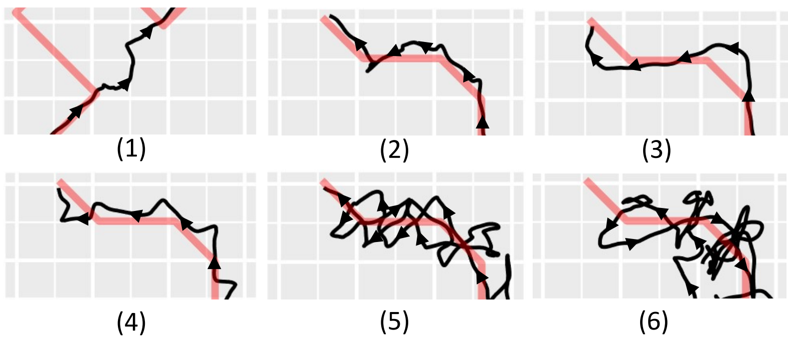

Figure 5.8: Representative examples of participants behavior during navigation (red: target path, black: participant trajectory, arrows indicate the direction of motion). (1) Cut (unsuccessful trial): the participant goes too far from the path, directly reaching the other end and failing the trial; (2) Compass: a behavior often observed in the `A` strategy, the participant reorients at regular intervals using the handle as a compass; (3) Overshoot: the participant goes too far at turns, a result of either a fast walking speed or a long response time to navigation instructions; (4-5) Bouncing: a behavior often observed in the `R` and `LA` strategies, were participants tend to bounce from one side of the path to the other; (6) Never reaching the end (unsuccessful trial): the participant turned around before reaching the end of the path.

There does not seem to be a clear preference between `4Dir` and `8Dir`, with some participants finding the perception of `8Dir` difficult and other finding it intuitive and richer. If interpreted correctly, `8Dir` provides richer feedback, which allows users to change their trajectory more smoothly, as can be observed in Figure 5.5. This result validates the use of both stimuli granularity for navigation, according to user's preference and expertise. Indeed, the personalization of the rendering stimuli is a challenging area of research that is promising in haptics.

Having vibrations displayed once every second for `A` was considered too much for some participants, while others found this frequency appropriate. Continuous vibration used in `R` and `LA` also received mixed feelings, showing again the importance of customization of the stimulation. The same applies for the intensity of the vibration, that some participants found appropriate and others too strong. Given the task and path chosen for the experiment, the frequency at which successive indications are provided seems appropriate: a longer delay between stimulation would have taken participants farther from the target path before the next instruction. A promising strategy in this respect is to consider a predictive guidance strategy, in which the instruction frequency depends on the (local) path complexity and speed of the user.

Finally, most participants reported that they enjoyed using the handle during the navigation task, with some of them finding `R` or `LA` strategies more "game-like", as if they were exploring a maze.

5.2 Investigating the effect of feedback location during joystick navigation

Our haptic handle is not solely designed to be used by pedestrians. In this context, we start to investigate its use in combination with a power wheelchair. With the handle placed directly on the joystick, the hand that is controlling the joystick has to manage both the driving of the wheelchair and the haptic information delivered by the device. This colocation of information in the driving hand might impact navigation. Similar questions were previously investigated in different contexts. For instance, haptic feedback provided on the opposite wrist showed better results for stiffness discrimination in a VR experiment [Adeyemi 2024]. Ivanova et al., on the other hand, did not find an effect in motor performance when providing physical assistance on the opposite hand in a tracking task [Ivanova 2023].

It is thus unclear whether the location of the haptic handle will have an effect in the context of navigation using a joystick. Here, we thus explored how the colocation of the haptic navigation feedback with the joystick used for moving the wheelchair impacts navigation, and if providing navigation feedback in the other hand benefits users in terms of navigation accuracy and cognitive load.

5.2.1 User study

We recruited 16 participants (14M, 2F, 13 aged between 18 and 35, 3 between 36 and 50, all right-handed) to take part in this experiment. Participants were not regular wheelchair users and did not express any disabilities. Half of participants reported being familiar with haptics. Before the start of the experiment, they were able to familiarize with the power wheelchair by driving in the experimental area. The study has been approved by Inria's ethics committee (COERLE - 332).

Experimental Setup

This experiment was conducted with a Salsa M2 power wheelchair from SUNRISE medical. In order to adapt the handle on the wheelchair, we designed an improved version that directly fits onto the shaft of the power wheelchair joystick (see Figure 5.9). This new version was equipped with a RJ45 port, which allows an easy connection to a M5Stack placed on the back of the wheelchair. The M5Stack was equipped accordingly with a custom board which contains two RJ45 ports, allowing for two handles to be connected at the same time: one placed on the joystick, and another placed in the non-driving hand. The handles and wheelchair communicated with the experimenter computer wirelessly using the MQTT protocol. A Unity program managed the experiment and communication of the navigation instructions based on the position data provided by a Qualisys tracking system.

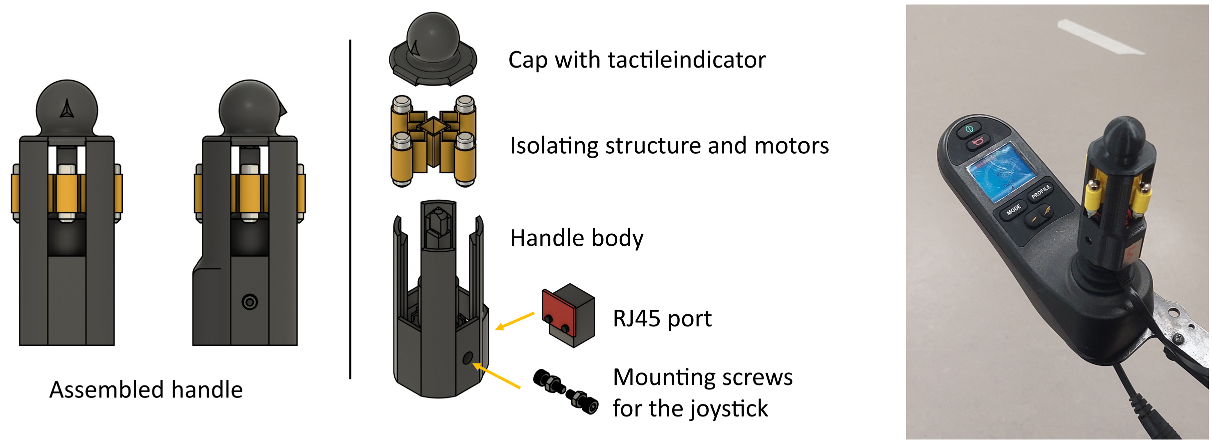

(A) (B)

Figure 5.9: (A) We adapted the design of our haptic handle to fit the shaft of the existing power wheelchair joystick. Two screws hold the handle onto the joystick. A RJ45 port allows the handle to be easily plugged into a M5Stack used for controlling the handle. (B) The handle placed on the joystick.

The experiment was conducted in a 8×12m area set up in a sports hall. To track the power wheelchair, we used the Qualisys tracking system, with eight cameras placed around the area (see Figure 5.10A). A custom tracking constellation was placed on top of the wheelchair in order to track its position and orientation. Due to the limited space, the maximum linear velocity of the wheelchair was reduced to 0.45m/s.

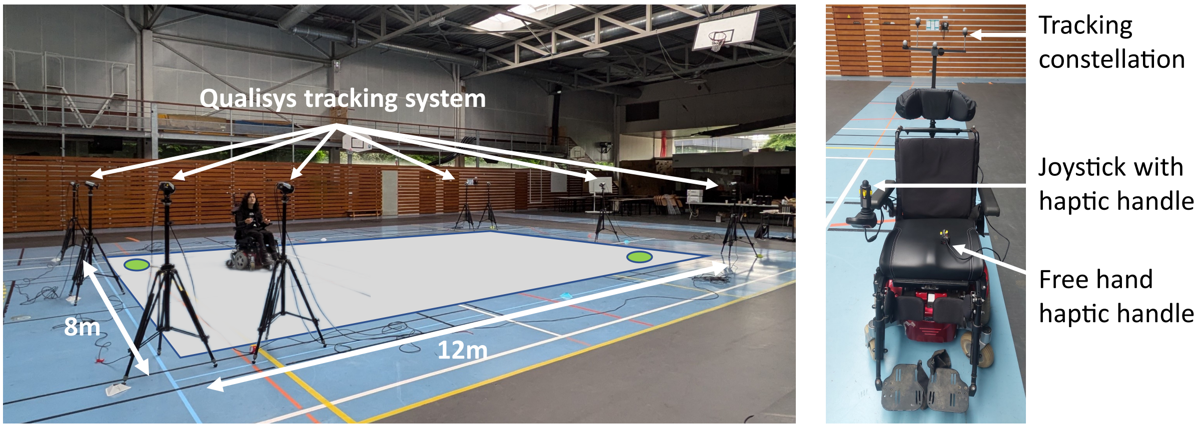

(A) (B)

Figure 5.10: (A) The experiment took place in a 8x12m zone, inside which the wheelchair was tracked using a Qualisys tracking system. The two starting points used in the experiment are shown in green. (B) The power wheelchair was equipped with a custom tracking constellation and two haptic handles: one placed on the joystick, and a second that can be held in the free, non-dominant hand.

Experimental Design

Based on the results of the previous navigation experiment, we chose to focus on the use of the "Attractive" strategy introduced in subsection 5.1.1. The strategy and rendering schemes were slightly modified. The angle of the front direction in `4Dir` was made larger to take into account the lower rotation speed compared to pedestrian navigation (see Figure 5.11B). The guidance strategy was made to prevent guidance to points on the path that were already reached. This ensured that participants will not be guided to previous sections of the path when missing turns or getting lost. Additionally, the distance ahead of the closest point on the path (d_{ahead}) used to set the navigation target was made dependent on the distance of the user from the path ($d_{fromPath}$), with

$$d_{ahead} = \begin{cases} 1, & \text{if } \; d_{fromPath} \leq 0.6 \\ 1 - \dfrac{d_{fromPath} - 0.6}{1.4}, & \text{if } \; 0.6 < d_{fromPath} \leq 2 \\ 0 & \text{otherwise.} \end{cases}$$

We once again considered three target paths, shown in Figure 5.11A, which participants did not see during the experiment. Paths were of variable lengths (P1: 18m, P2: 22m, P3:16m), using different combinations of turns (P1, P3: 45°, P2: 90°) to modulate difficulty. As in the previous experiment, the starting point was changed regularly to minimize learning effects.

We evaluate the ability of participants to drive the power wheelchair along the target paths following the handle navigation instructions. The following experimental variables were considered:

- `Feedback location`: colocated with the joystick (`CoLoc`) or delocated in the non-driving hand (`DeLoc`);
- `Rendering scheme`: `4Dir` or `8Dir`;
- `Target path`: `P1, P2, P3` as shown in Figure 5.11A.

The experiment is made of two blocks, each using one of the handle locations. Within each block, participants drove along the three target paths using both rendering schemes, one after the other for a total of 6 trials per block. Feedback location and rendering schemes presentation orders were counter-balanced across participants, and path order was randomized. Starting point changed every three trials.

At the beginning of each condition, participants were able to familiarize with the feedback provided by the handle. Participants were asked to drive the wheelchair to the best of their ability, following the instructions provided by the haptic handle. Trials started once participants were positioned on the starting point and ended when reaching the end of the path (0.7m or less from the end point).

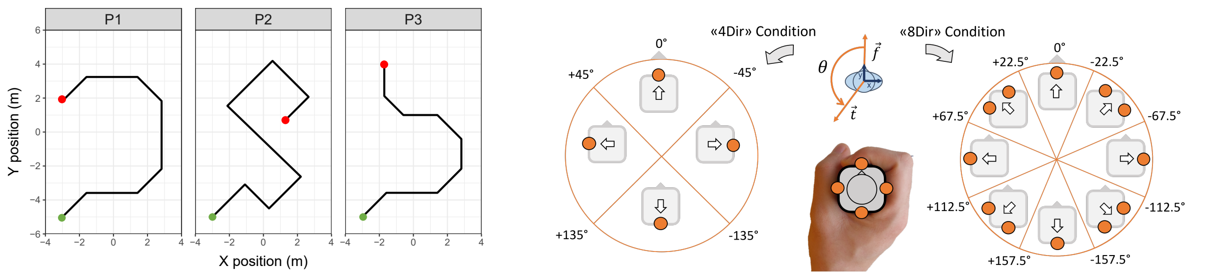

(A) (B)

Figure 5.11: (A) The three target paths used in this experiment. Green dots represents the starting points, and red dots the end point of each path. (B) The two rendering schemes used in the experiment. `4Dir` was slightly changed compared to the previous experiment.

Collected Data

During the experiment, we collected the position and orientation of the wheelchair, the joystick inputs, and the trial duration. Participants were asked to evaluate their success on a 7-item Likert scale at the end of each trial. In addition, they also judged each handle and rendering scheme combination, rating the following affirmations on a 7-item Likert scale:

- *Loc*: Vibrations from the handle were easy to locate in the hand;

- *Int*: Vibrations from the handle were difficult to interpret;
- *Ment*: The task was mentally demanding.

Comments from participants were collected throughout the experiment. At the end of the experiment, participants were asked to select which rendering scheme and handle location they preferred.

Results

Trajectories from the 16 participants are shown in Figure 5.13, separated between rendering schemes and feedback location conditions and the three target paths. Individual trajectories can be seen in Appendix II. Overall, all participants were successful in the task: they all reached the end of the target paths, following their global shapes.

Path efficiency ratio & distance to path. We compute the path efficiency ratio and mean distance to the path for all trajectories performed by participants.

Overall, distances travelled by participants are close to the target distance, with path efficiency values being close to 1 ($M = 1.11$, $SD = 0.11$), as can be seen in Figure 5.12. We use a Linear Mixed Model (LMM) to analyze these measures, considering `Feedback location`, `Rendering scheme` and `Target path` as independent variables and by-participants random slopes for `Feedback location`. A log transformation was used as measures were gamma distributed. An analysis of variance indicated a statistically significant effect on the path efficiency ratio of `Target path` ($F(2, 150) = 16.8, p < 0.005$), `Rendering scheme` ($F(1, 15) = 12.6$, $p < 0.005$) and a slight effect of `Feedback location` ($F(1, 150) = 3.78$, $p = 0.05$). There was also a slight interaction between `Feedback location` and `Rendering scheme` ($F(1, 150) = 4.37$, $p < 0.05$).

We conducted post-hoc pairwise comparisons using Tukey's HSD test. Estimates are reported with their 95% confidence interval (i.e., $[lowerlimit, upperlimit]$). Path efficiency values on `P1` were lower (1.06, $[1.03, 1.10]$) than for `P2` (1.14, $[1.11, 1.18]$) and `P3` (1.10, $[1.07, 1.13]$), which was statistically significant, as well as the difference between `P2` and `P3` (`P1-P2`: $t(150 = -5.8$, $p < 0.001$; `P1-P3`: $t(150 = -2.77$, $p < 0.05)$; `P2-P3`: $t(150 = 3$, $p < 0.01)$). For the `Rendering scheme`, values were lower for `4Dir` (1.08, $[1.05, 1.11]$) than `8Dir` (1.12, $[1.09, 1.16]$), which was also statistically significant (`4Dir-8Dir`: $t(15) = -3.5$, $p < 0.005$). Ratios for `Feedback location` with `CoLoc` (1.09, $[1.06, 1.12]$) were slightly lower than with `DeLoc` (1.11, $[1.08, 1.14]$), which was close to significance (`CoLoc-Deloc`: $t(150) = -1.945$, $p = 0.054$).

Regarding the mean distance from path (see also Figure 5.14), we used another LMM considering the same parameters. An analysis of variance indicated a statistically significant effect on the path efficiency ratio of `Target path` ($F(2, 150) = 23.3$, $p < 0.001$) and `Rendering scheme`

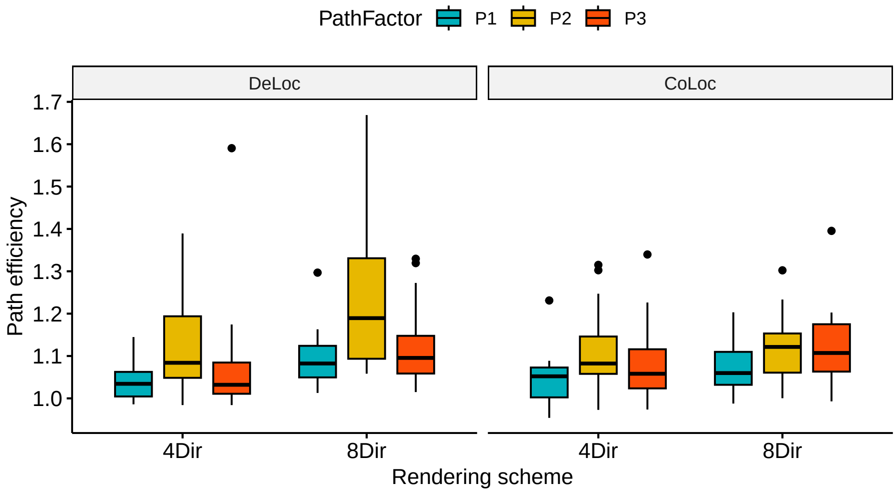

Figure 5.12: Distribution of path efficiency ratio across conditions. `P2` shows significantly higher values than `P1` and `P3`. Values for `P1` are also lower than those of `P3`. `4Dir` also shows lower travelled distances than `8Dir`.

($F(1, 15) = 24.1$, $p < 0.001$). Mean distance from path for `P2` (0.32, $[0.27, 0.37]$) was higher compared to both `P1` (0.24, $[0.21, 0.28]$) and `P3` (0.25, $[0.22, 0.29]$), which was statistically significant (`P2-P1`: $t(150 = -6.23$, $p < 0.001$; `P2-P3`: $t(150 = -5.51$, $p < 0.001$). Distances using `4Dir` (0.23, $[0.20, 0.27]$) were also lower than with `8Dir` (0.31, $[0.26, 0.37]$), `4Dir-8Dir`: $t(15 = -4.91$, $p < 0.001$).

Self evaluated success. The self-evaluated success of participants was analyzed using a Cumulative link mixed-effects model (CLMM). We considered `Feedback location`, `Target path` and `Rendering scheme` as independent variables, and used by-participants random slopes for `Feedback location`.

An analysis of variance indicated a statistically significant effect on the self evaluated success of `Target path` ($\chi^2(2, N = 192) = 34.34$, $p < 0.001$) and `Rendering scheme` ($\chi^2(1, N = 192) = 5.71$, $p < 0.05$). There were no significant interactions. Evaluated success for `P2` (4.7, $[4.23, 5.17]$) was lower than for `P1` (5.56, $[5.19, 5.92]$) and `P3` (5.34, $[4.94, 5.74]$), which was statistically significant (`P2-P1`: $Z = -5.49$, $p < 0.001$; `P2-P3`: $Z = -4.14$, $p < 0.001$). Using `4Dir`, success was also evaluated higher (5.55, $[5.20, 5.90]$) than with `8Dir` (4.85, $[4.29, 5.41]$), which was statistically significant (`4Dir-8Dir`: $Z = 2.54$, $p < 0.05$).

Subjective evaluation. Participants answers to the questionnaire are shown in Figure 5.16. As answers did not follow a normal distribution and were multifactorial, a non-parametric analysis of variance based on the Aligned Rank Transform (ART) was used to evaluate the effect of

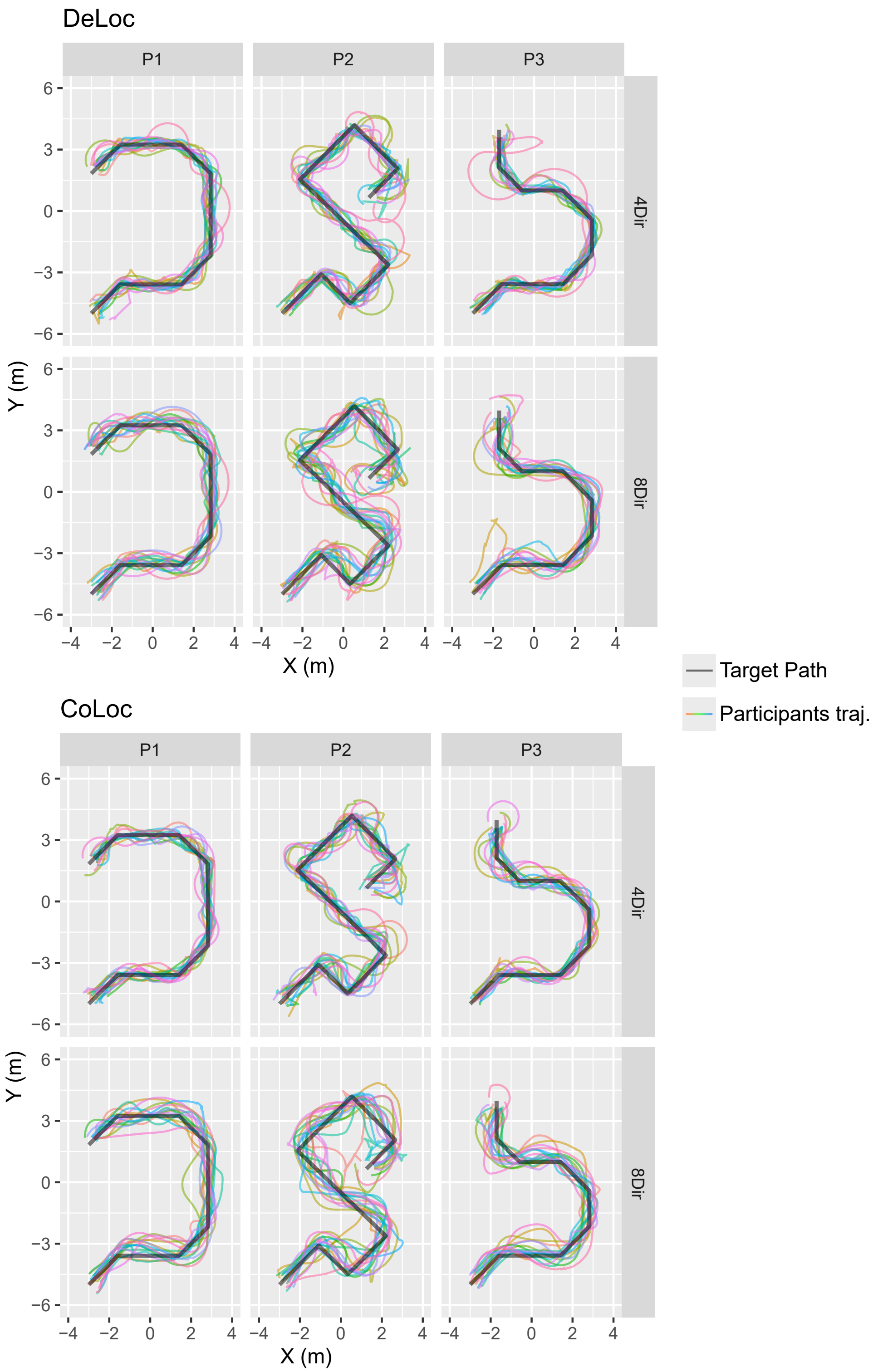

Figure 5.13: Participants trajectories across conditions. Target path shown in black, individuals trajectories shown in colors. Individual trajectories can be seen in Appendix II.

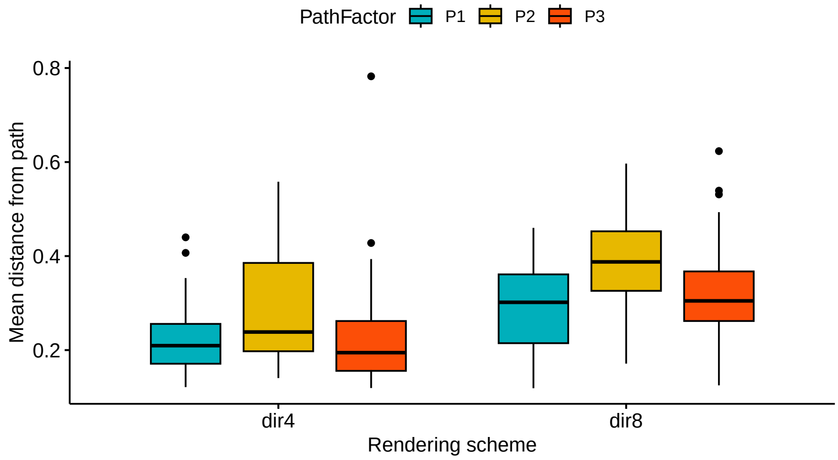

Figure 5.14: Distribution of mean distance from path values. P2 shows greater values than both P1 and P3. Distance from path with 4Dir are also lower than with 8Dir.

Rendering scheme and Feedback location on the answers.

For Int, only Rendering scheme had a significant effect ($F(1, 45) = 17.2$, $p < 0.001$), with vibrations being more difficult to interpret with 8Dir ($M = 3.69$, $SD = 1.42$) than with 4Dir ($M = 2.31$, $SD = 1.35$). The same goes for Loc ($F(1, 45) = 28.02$, $p < 0.001$), with vibrations being easier to locate with 4Dir ($M = 5.15$, $SD = 0.81$) than with 8Dir ($M = 3.88$, $SD = 1.34$). There was also a significant effect only of Rendering scheme ($F(1, 45) = 12.4$, $p < 0.01$) on Ment, with mental demand evaluated higher for 8Dir ($M = 3.69$, $SD = 1.62$) than for 4Dir ($M = 2.94$, $SD = 1.41$).

When asked to choose their preferred feedback location, 5 chose Deloc and 11 chose CoLoc. For their preferred rendering scheme, 5 chose 8Dir and 11 chose 4Dir. Overall, two participants preferred both Deloc and 8Dir, and eight preferred both CoLoc and 4Dir

5.2.2 Discussion

In this experiment, we investigated the effect of providing haptic feedback for navigation either colocated with a haptic handle mounted on the joystick of a power wheelchair or de-located, with the handle held in the free, non-dominant hand. Results showed that participants were successful in the navigation task across all conditions, as they were able in all cases to follow target paths until the end without significant deviations from it, thus confirming the intuitive use of our navigation strategy and its compatibility with power wheelchair navigation.

Overall, our statistical analysis did not show any significant effect of the location of the haptic handle on navigation. If any, a small effect on path efficiency would indicate a slight advantage for co-locating the handle with the joystick. Most participants preferred having the

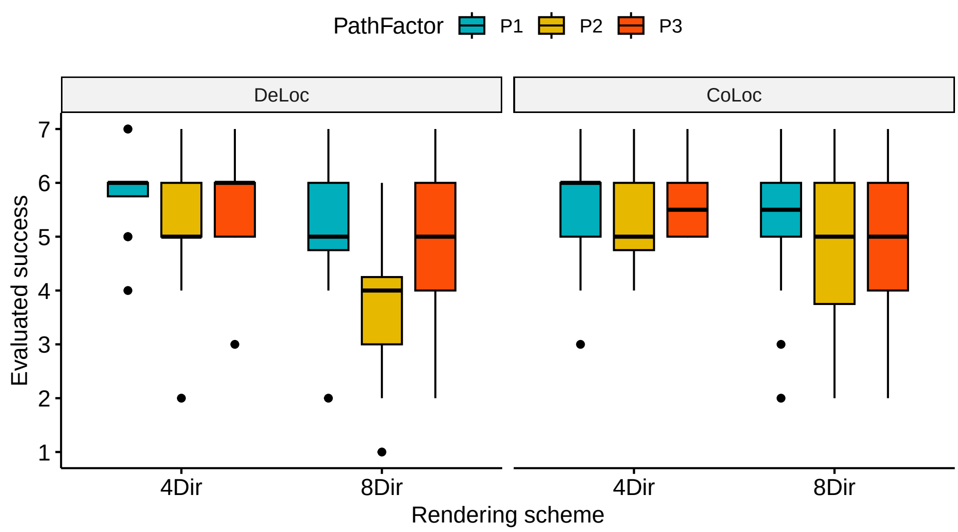

Figure 5.15: Participants evaluation of their success in the navigation task.

handle placed on the joystick, where the location of stimuli is directly linked to the movement to perform. In cases where stimuli are more complex, such as with `8Dir`, some reported that identifying vibrations was easier in their free hand. However, mapping the vibration direction from one hand to the other was often found more difficult in this case, as the free hand might be in a different and/or changing orientation. Having the handle fixed on the joystick in `CoLoc` had thus the advantage of keeping the cues referential fixed and aligned with the wheelchair.

Out of the two directional rendering schemes that we tested, `4Dir` appeared as the most intuitive and effective of the two, with `8Dir` having a more negative effect on performance. Participants comments on `8Dir` were mixed, some having a hard time identifying diagonal directions and finding the mental effort to be higher, while others appreciated the additional directions provided by this scheme, allowing them to anticipate turns and taking them more smoothly.

Target paths used in the experiment also had a significant impact on navigation. Most importantly, `P2` showed lower performance of users, which can probably be attributed to its more complex shape, having sharper and closer turns than the two other paths. Indeed, participants tended to overshoot in these sharp turns, which increased the perceived difficulty of these specific trials. The guidance strategy could be adapted to take into account these difficulties, for instance by providing turn indications earlier in case of sharp turns. Additionally, the dynamics of the wheelchair could also be taken into account to predict its position.

Additionally, some participants reported that the task required attention, in which case they were more focused on the handle and vibrations than on their environment. This point could be investigated in the future, in order to determine if adequate training would allow users to

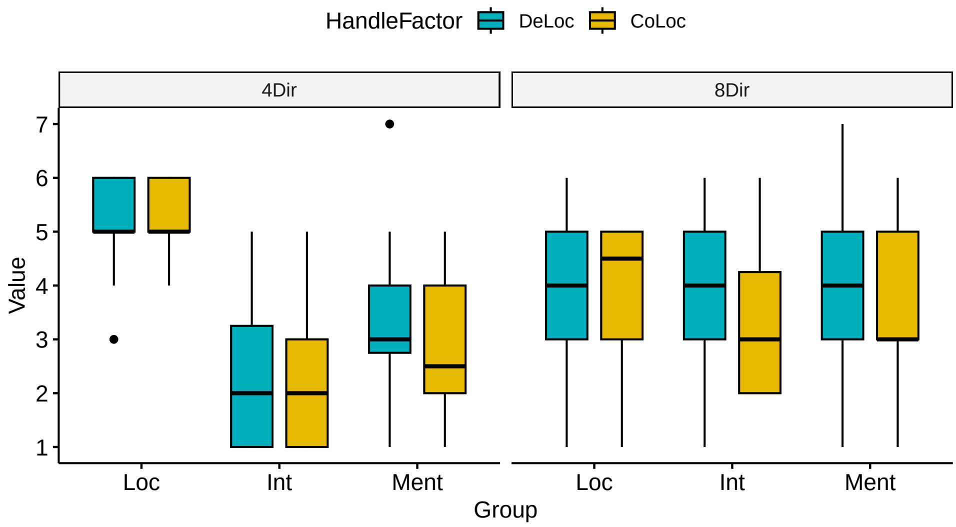

Figure 5.16: Boxplots of the 7-item likert scale questions results (1=Not at all, 7=Extremely), rating the following affirmations: Vibrations from the handle were easy to locate in the hand (*Loc*); Vibrations from the handle were difficult to interpret (*Int*); The task was mentally demanding (*Ment*).

use the device while still being attentive to their direct environment. The lack of experience in power-wheelchair navigation might also have impacted participants in the task.

Overall, our haptic handle and navigation technique were shown to be effective for providing haptic guidance during navigation of a power wheelchair. Feedback location, our main interest in this experiment, was not shown to have any effect. This is an informative result, as it would suggest that the handle can be used in different ways while still being effective. For most users, having the handle colocated with the joystick will probably be the most effective solution as it does not hinder the freedom of the other hand. Still, some might prefer having the handle in the other hand, such as users with lower tactile sensitivity. Since our participants were mostly young and male, and did not present disabilities, future investigations should look into more diverse population which might have other preferences.

5.3 Conclusion

In this chapter, we introduced three navigation strategies for a multi-actuator haptic handle, considering two rendering schemes. We conducted a user study evaluating the use of these strategies in a walking navigation task. Results showed the ability of the proposed techniques to provide effective navigation instructions within our haptic handle. All navigation strategies were able to effectively guide participants along the target path. However, the "Attractive" strategy performed the best in terms of self-evaluated success, path efficiency ratio, and ease of learning. We then evaluated the use of our haptic handle and the “Attractive” strategy for power wheelchair navigation, investigating the effect of the location of the haptic feedback relative to the joystick controlling the movement of the wheelchair. Participants were all able to accurately follow the paths along which they were guided, with little effect of the handle location between the two hands.

Overall these results highlight the diversity of possible uses of our haptic handle in conjunction with multiple feedback schemes, which could allow users to personalize their experience with the device. The strategies we proposed could be explored even further, evaluating the effect of the various parameters they rely on. Power wheelchair navigation was investigated with participants that were not users of mobility assistance devices. Next steps should look into the use of the device and navigation techniques with real users of power wheelchair, investigating effects on navigation that more diverse profiles and potential disabilities could have.

CHAPTER 6
HAPTIC NAVIGATION FOR POWER WHEELCHAIR USERS: A PILOT STUDY

As seen in the previous chapter, the use of haptic guidance appears to be a promising method for efficiently providing navigation indications in the context of power-wheelchair navigation. In this chapter, we present the preliminary results of a pilot study conducted with regular users of power wheelchair. This is an important step towards the use of haptic navigation solutions by end users. Conducting such a study was made possible thanks to the involvement of the different partners working together as part of the Dornell project.

In this pilot study, we evaluate the use of our haptic handle by regular users of power wheelchairs. We divided this study in two separate tasks. First, we evaluated the discrimination of the two rendering schemes evaluated previously (`4Dir` and `8Dir`), providing directional information without moving the wheelchair. We then evaluated the use of the handle to guide users in a navigation task, following the investigations conducted in the previous chapter. Acceptability of the device was also evaluated with the participants, assessing their projection into the use of such a device.

6.1 Pilot study

6.1.1 Study design and participants

The study is a joint effort with clinicians from Pôle Saint-Hélier, a rehabilitation center located in Rennes, France. This is an observational pilot study: its main objective is to evaluate the perception of haptic feedback displayed by the handle and its impact on navigation with regular users of power wheelchair. The study was approved by the local ethics committee of Pontchaillou Rennes University hospital.

(A)

(B)

Figure 6.1: (A) One of the two power wheelchairs used in the experiment. A tracking constellation is placed on top of the wheechair in addition to the haptic handle on the joystick, similarly as in section 5.2. (B) The room in which the navigation task took place, with a 14x10m tracking area covered by a Qualisys tracking system. Starting point was indicated on the ground for participants to easily reposition themselves after each trial.

Participants were recruited by their occupational therapists, according to the following inclusion criteria: (1) being over 18 years old; (2) having freely consented to participate in the study; (3) using a power wheelchair, either with a prescription or learning to drive with the center's professionals. Exclusion criteria were the following: (1) having difficulties to understand and follow instructions; (2) presenting motor disorders preventing from correctly using the haptic handle; (3) being unable to express consent; (4) being pregnant. The study took place in the facilities of Pôle Saint-Hélier. Upon arriving, participants were welcomed by one of the clinicians which presented them the participation modalities and objective of the experiment, before signing a consent form. Before taking part in the experiment, demographic data were collected. We also collected the participants driving experience and assessed their driving ability using the WST-QF questionnaire (v5.4 [1]). Finally, we assessed participants tactile sensitivity using the two point discrimination test [Jones 2006].

The study was then separated into two experimental tasks: first, a discrimination study of the haptic cues provided by the handle without the power wheelchair, and secondly, a navigation study using the haptic cues while driving. For the duration of the study, participants were installed in one of the two available power wheelchairs (Salsa M2, Sunrise Medical), each equipped with our haptic handle and tracking apparatus (see Figure 6.1A). The two wheelchairs allowed for two participants to perform separate parts of the experiment in parallel, each accompanied by an experimenter and clinician.

[1] `https://wheelchairskillsprogram.ca/en/skills-manual-forms/`

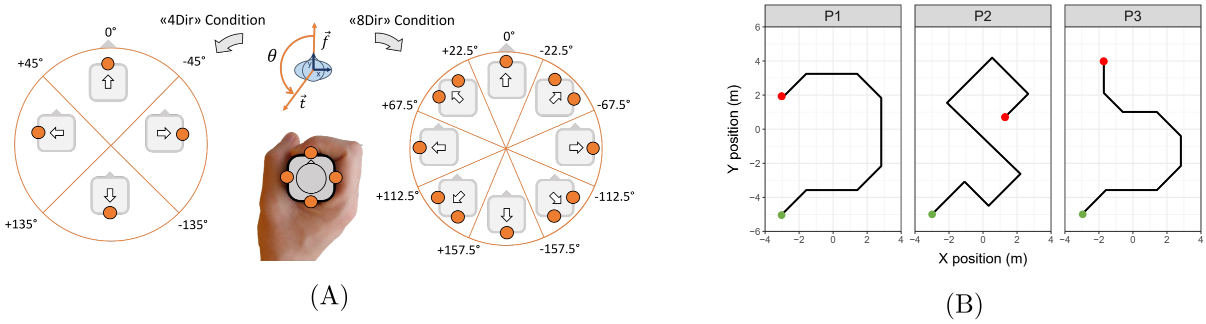

Figure 6.2: (A) The two rendering schemes used in this study to provide directional information to participants. `4Dir` uses each of the four motors around the handle to display the four cardinal directions. `8Dir` adds four intermediate directions by using motors simulaneously. (B) During the navigation task, participants are guided along three target paths. Starting points are shown in green and end points in red.

6.1.2 Task #1: Experimental setup & design

The objective of this first task was to evaluate the discrimination of haptic cues displayed by the haptic handle. In this part of the study, participants were seated in the power wheelchair, with the handle and joystick positioned on the side they are used to drive with. The control of the wheelchair via the joystick was disabled for the duration of the task, thus making the wheelchair stationary. This way, the discrimination task was performed in conditions close to those of the real use of the wheelchair with the device.

This part of the experiment was made of two blocks, each using one of the two rendering schemes we previously evaluated (`4Dir` and `8Dir`, see Figure 6.2A and refer to chapter 5 for more details). For both conditions, each direction was presented five times (i.e., there are 40 trials in the `8Dir` condition and 20 in the `4Dir` condition). Before the start of each block, participants were able to try the different haptic cues to familiarize with them. Trial order was randomized within each block, and conditions order was counter-balanced across participants. Each time a haptic cue was presented, participants were asked to move the joystick in the direction indicated by the stimulus. Once the joystick was moved back to the center, the next trial starts automatically after a 3-second delay.

After each block, participants answered a NASA-TLX questionnaire to evaluate their perceived workload. During the experiment, we collect joystick inputs during all trials.

6.1.3 Task #2: Experimental setup & design

The objective of this second task was to evaluate the use of the haptic handle for navigation guidance with the power wheelchair. We considered the use of the two rendering schemes used in the previous part of the experiment (`4Dir` and `8Dir`) in combination with the "Attractive" navigation strategy we previously evaluated with power wheelchairs in section 5.2. This task took place in a 14x10m area free of obstacles (see Figure 6.1B). Two starting points were indicated on the ground for participants to position easily. We used 10 Qualisys tracking cameras placed around the room to track participants position and orientation. Each wheelchair was equipped with a custom tracking constellation, and their linear velocity was capped at 0.45m/s.

This part of the experiment was made of two blocks, one for each rendering scheme. Each block was made of three trials, each corresponding to one of the three target paths we considered (see Figure 6.2B). Trial order was randomized, with the starting point changing at the start of each block to prevent learning effects. Blocks order was counter-balanced across participants. Participants were asked to drive the wheelchair by following the instructions displayed by the haptic handle.

After each block, participants also answered a NASA-TLX questionnaire to evaluate their perceived workload. During the experiment, we collected trajectory data of participants during each trial as well as joystick inputs.

6.2 Results

Given the influence of the diverse profiles of the participants and the pathologies to which they are subject, the results are diverse and make the analysis process complex. The results we discuss in this section are preliminary and subject to an ongoing analysis with the clinicians involved in the study.

6.2.1 Participants profiles

14 power wheelchair users took part in the study (4M, 10F) with an average age of 56 years (SD=14.28). Of these, 13 were right-handed and 1 was ambidextrous. The pathologies leading to the use of the electric wheelchair were varied (6 strokes, 3 Multiple Sclerosis, 1 Parkinsonian Syndrome, 1 Spinal Cord Injury, 1 Neuromuscular Disease, 1 Cerebral Palsy, 1 Ehlers-Danlos syndrome).

In terms of their experience with power wheelchairs, 11 had already received a prescription and 3 were still apprentices in the rehabilitation department. Their average driving experience was 82.43 months (SD=99.10)

Driving skills were evaluated through the WST-QF questionnaire, according to three items: performance, confidence and frequency. The average score for performance was 76.80% (SD 16.93), 70.54% (SD 18.87) for confidence and 59.60% (SD 19.83) for frequency.

Sensitivity of the hand that would use the haptic handle was evaluated using the two-point discrimination test. The test was performed using a calliper, with increments of 5mm. Participant's hand was hidden from view for the duration of the test. Results are visible in

Figure 6.3. Of all participants, 11 had normal sensitivity in all 5 fingers (5mm), and of these 2 had weaker sensitivity in the thumb (10mm), 2 others had poor sensitivity (10mm) in more than 3 long fingers and one person had total insensitivity in the last 3 fingers. The results for the palm of the hand were more variable, with sensitivity ranging from 5mm to 20mm depending on the area of the hand.

6.2.2 Task #1

Discrimination accuracy

For each trial, we consider the main direction participants identified as the angle of the furthest point in which the joystick was moved. Individual results can be observed in Figure 6.5. For each rendering scheme and direction, we also computed discrimination rates. Answers were considered correct if the identified direction was within the range of the expected direction (i.e., $\pm 45°$ for `4Dir` and $\pm 22.5°$ for `8Dir`). Global discrimination rates are visible in Figure 6.4.

We can observe a clear difference between the two rendering schemes. For `4Dir`, overall discrimination rate is 86%, with values ranging from 81% to 90% (see Figure 6.4A). Most participants were able to identify directions, and responses are visibly orthogonal (see Figure 6.5), with the notable exception of participants 6 and 10. Participant 6 results might be affected by their poor tactile sensitivity. Participant 10 responses are mostly correct but rotated by about

	Hand Area									
Participant number	1	2	3	4	5	6	7	8	9	10
1	5	5	5	5	5	10	15	10	10	10
2	5	5	5	5	5	10	10	5	10	5
3	5	5	5	5	5	15	10	10	15	10
4	10	10	10	10	10	10	15	10	20	10
5	10	5	5	5	5	5	5	10	10	5
6	5	5				15	15	15		15
7	5	5	10	10	10	10	10	10	10	15
8	5	5	5	5	5	10	10	5	5	10
9	5	5	5	5	5	10	15	5	5	10
10	5	5	5	5	5	10	10	5	15	15
11	5	5	5	5	5	15	15	10	10	10
12	10	5	5	5	5	10	5	10	15	15
13	5	5	5	5	5	10	10	10	5	10
14	5	5	5	5	5	15	20	15	15	20

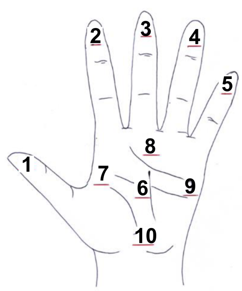

Figure 6.3: Results for the two-point discrimination test, with distances in millimeters. Normal thresholds values tend to be ≤ 5mm for the fingertips and around 10mm on the palm [Jones 2006]. Cells are colored according to sensitivity level: normal (green), low (yellow), poor (red), none (black).

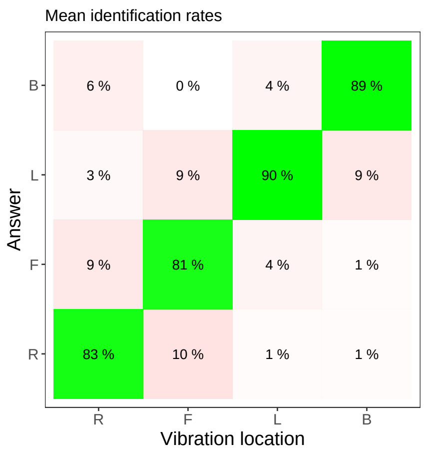

(A)

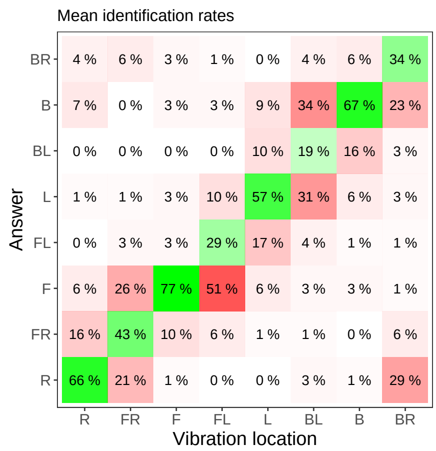

(B)

Figure 6.4: Confusion matrix for the static experiment, with global identification rates for the `4Dir` and `8Dir` conditions.

30° clockwise.

For `8Dir`, overall discrimination rate is much lower at 49%. Cardinal directions show better results (see Figure 6.4B), with values ranging from 57% to 77%. Discrimination rates of diagonals ranges from 19% to 43%, with worst results for left diagonals. Confusion occurs mainly with the adjacent directions, which is also observed on the individual joystick trajectories.

Perceived workload

Distribution of the answers to the TLX questionnaire can be seen in Figure 6.7. As data were not normally distributed, we performed paired samples Wilcoxon tests to compare conditions. Significant differences were only observed for Performance ($p<0.05$) and RawTLI ($p<0.01$). Participants thus reported higher success in the `4Dir` condition, which reflects in the RawTLI score. Looking at other items of the questionnaire, while the difference is not statistically significant, we can observe a similar trend in mental and physical demand as well as for the effort. Indeed, mental demand was really high for some participants.

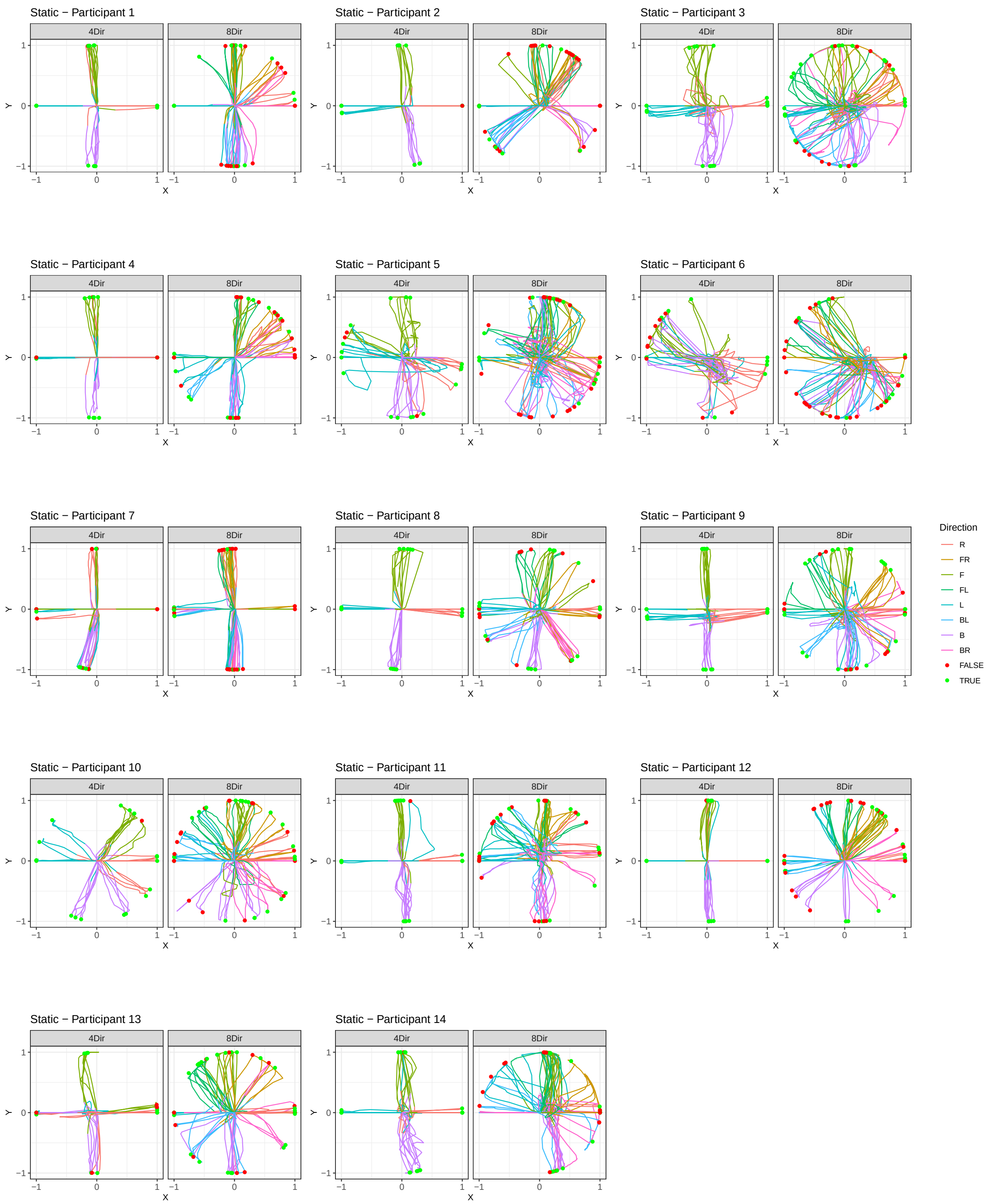

Figure 6.5: Joystick trajectories of participants in the discrimination experiment. Trajectories colors indicate which direction was displayed by the haptic handle. Green and red dots on the end of each trajectory indicate whether the direction was correctly identified.

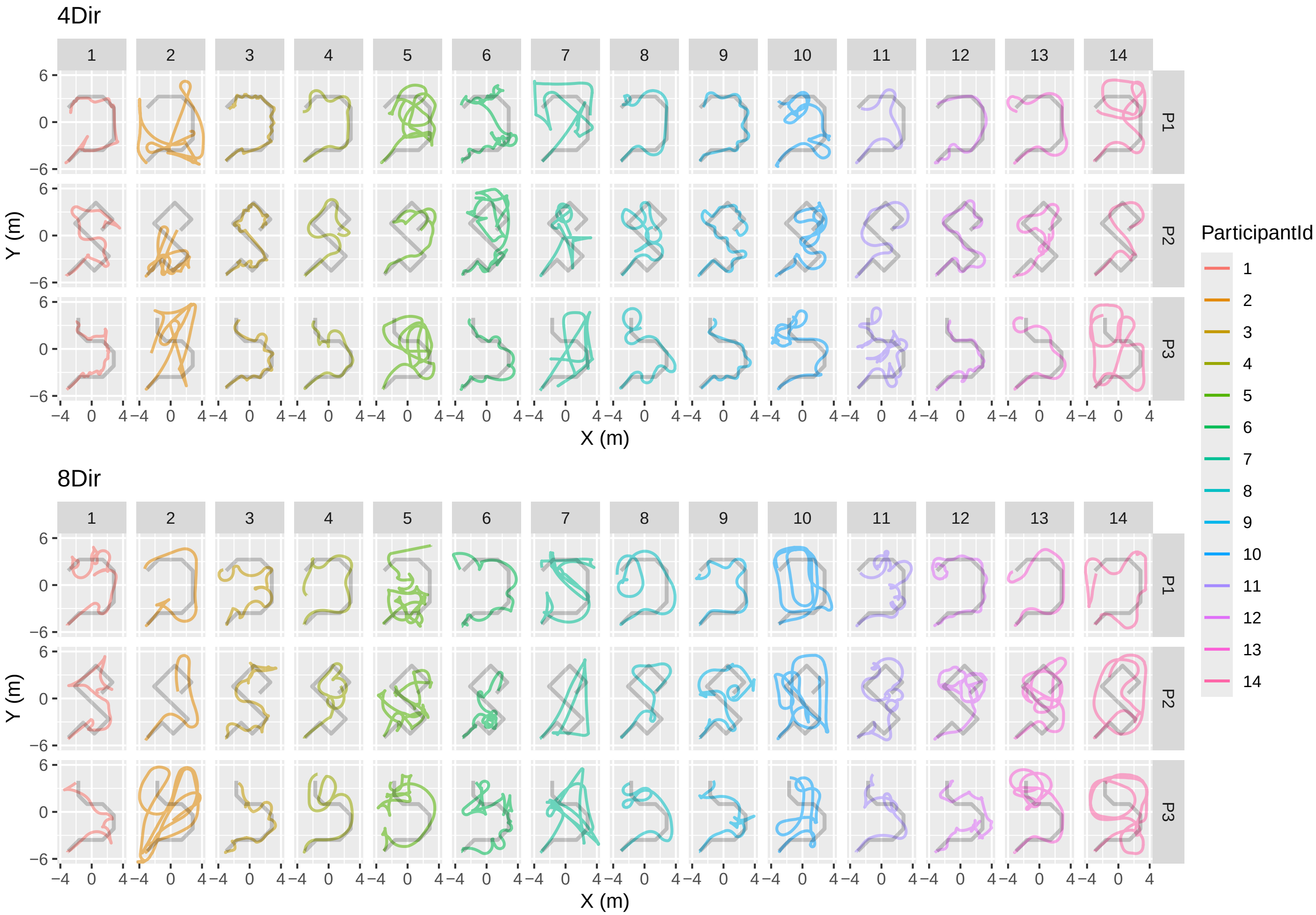

Figure 6.6: Participants trajectories accross condition in the navigation task. Reference paths are shown in black and participants trajectories in color. Individual trajectories can be seen in more details in Appendix II.

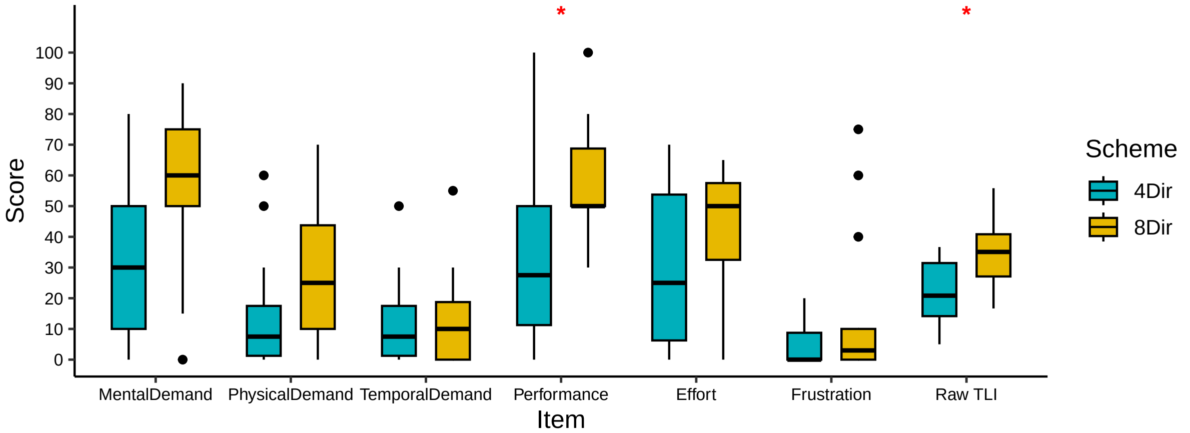

Figure 6.7: Distribution of answers to the TLX questionnaires filled at the end of each block. Red stars indicate significant differences according to a paired samples Wilcoxon test. Answers range from 0 (low) to 100 (high), except for Performance for which low values indicate success. Raw TLI is the average of all items.

6.2.3 Task #2

Trajectories

Compared to our previous experiment with participants without disabilities, trajectories are more diverse and, for some, more chaotic (see Figure 6.6). Individual trajectories can also be seen in Appendix II. We can observe a subset of participants that are mostly successful in following the target path. Namely, in the `4Dir` condition, trajectories of participants 1, 3, 4, 9, 12 and 13 follow the overall shape of the path, with participants 8, 10, and 11 showing more overshoot and errors. Participants 2, 5, 6, 7 and 14 show much less success: they tend to miss the first turn and/or overshoot significantly, sometimes ending up turning around the whole room. In the `8Dir` condition, trajectories are more erratic even for participants who were successful with `4Dir`. Participants 1, 3, 4, 8, 9, 11, 12 and 13 tend to still follow the shape of the path but with much more turns and overshoots. As in the previous experiment, we can observe that `P2` is more challenging: for instance, participants 4 and 13 miss the first sharp turn in the `4Dir` condition.

Perceived workload

Distribution of the answers to the TLX questionnaire can be seen in Figure 6.8. There were no significant differences between conditions according to paired samples Wilcoxon tests. The contrast between the two conditions is less visible than in the first task. We can still observe slightly higher values for `8Dir`, following the trend observed previously.

Compared to the previous task, we can observe a global increase of the perceived workload (mean RawTLI in task 1 vs. 2 for `4Dir`: 21.4 vs. 40.2 ; `8Dir`: 35.4 vs. 46.2). In particular, frustration is higher, reflecting participant's sentiment after unsuccessful trials (mean Frustration in task 1 vs. 2 for `4Dir`: 4.29 vs. 27.5 ; `8Dir`: 15.1 vs. 37.9).

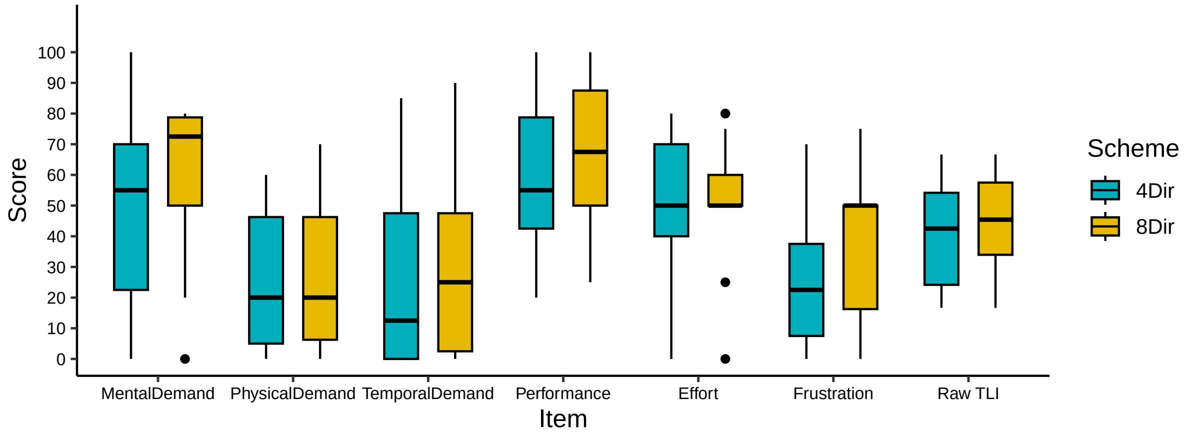

Figure 6.8: Distribution of answer to the TLX questionnaires filled at the end of each block. Answers range from 0 (low) to 100 (high), except for Performance for which low values indicate greater perceived success. Raw TLI is the average of all items.

6.2.4 Acceptability

The acceptability of the haptic handle was evaluated using a questionnaire based on the UTAUT model (Unified Theory of Use and Acceptance of Technology [Venkatesh 2003]). This model, derived from social psychology, is preferred for use surveys because of the diversity of factors to be explored. It combines variables that question the ergonomic characteristics of a device (expected performance, perceived effort, etc.) as well as user perceptions (social influence, social function, etc.). The questionnaire makes it possible to gather the participants' intention to use the device, and to question the determinants of this intention, based on a series of items rated on a 7-point Likert scale. According to these answers, usage intention is considered negative for scores between 1 and 3.49, neutral for scores between 3.5 and 4.49, and positive for those between 4.5 and 7. The different items used in the questionnaire are detailed in Table 6.1.

Cronbach's alpha is a measure of the relationship between a group of questions. It assesses the internal consistency of a questionnaire and therefore its reliability. In this case, Cronbach's alpha coefficient is 0.94, demonstrating the overall internal reliability of the questionnaire. A more in-depth analysis of consistency for each construct gives the following results:

- Performance expectancy: $\alpha = 0.93$ (Excellent)
- Effort expectancy: $\alpha = 0.82$ (Good)

UTAUT questionnaire items	
Performance expectancy	
UP1	The usefulness of the device for guidance
UP2	The usefulness of the 4 vibrations to indicate directions
UP3	The usefulness of the 8 vibrations to indicate directions
UP4	The usefulness of the device in providing reassurance during a journey
AR1	The usefulness of the device as a route guide compared with other existing solutions (GPS, vibrating watch...)
AR2	The usefulness of the device to assist you when driving compared with other existing solutions (GPS, vibrating watch...)
AA1	The integration of this system into your daily travel routine
AA2	Your confidence in this device to assist you when driving
RA1	The safety provided by this system
RA2	The reassurance this system brings to your daily travels
RA3	The autonomy this system provides for indoor travel
RA4	The autonomy this system provides for outdoor travel
Effort expectancy	
EF1	The ease of use of the device when first using it
EF2	The ease with which the system can be used every day
EF3	The perception of different directions through vibrations in the handle
EF4	The understanding of the information conveyed by the handle
EF5	The effort of concentration required to use the device
Facilitating conditions	
CF1	The comfort of the device
CF2	The robustness of the devices
CF3	The aesthetics of the device
Social influence	
FSP1	The interest other power wheelchair users would show for this device
FSP2	The interest your relatives would show for this device
FSP3	The interest your therapists would show for this device
IM1	The image reflected by the use of this device
Behavioral intention	
PU1	Your projection in the use of this device
PU2	Your desire to propose it to other users
PU3	Your desire to use the device if it was available

Table 6.1: Contructs and their corresponding items for the UTAUT-based questionnaire. Each item is rated on a 7-item Likert scale (1: negative; 7: positive).

	Performance expectancy	Effort expectancy	Social influence	Facilitating conditions	Behavioral intention (self - PU1/3)	Behavioral intention (others - PU2)
Mean	4.26	4	4.73	4.84	3.27	4.61
SD	1.42	1.46	1.76	1.04	2.15	2.21

Table 6.2: Scores for each contruct in the UTAUT questionnaire.

- Social influence: $\alpha = 0.82$ (Good)
- Facilitating conditions: $\alpha = 0.48$ (Questionable)
- Behavioral intention: $\alpha = 0.89$ (Good)

The coefficient related to the “Facilitating conditions” construct shows a low value, which would indicate that answers are not correlated or that the items of this construct deal with different elements. The three items of this construct evaluated the comfort (CF1), robustness (CF2) and aesthetics (CF3) or the device. A more in-depth analysis was carried out on the construct, showing that the removal of items CF2 increased internal consistency to 0.66. This item will thus be discussed separately. For behavioral intention, item PU2 lowers the internal consistency of behavioral intention and will be discussed separately.

Distribution of answers for the different items can be seen in Figure 6.9. Results for each construct are reported in Table 6.2.

The results show that in terms of expected performance, all the items are neutral except for UP1 (usefulness of the device for guidance; mean=4.64), UP2 (usefulness of 4 vibrations; mean=4.93) and RA1 (safety provided by the device; mean=4.93) which are positive. Regarding effort expectancy, EF1 and EF2 (ease of first and daily use) are positive (EF1: mean=4.86; EF2: mean=5.21). Item EF4 (understanding of the information) is neutral (mean=3.71), while other items related to the perception of vibrations and concentration effort are negative (EF3: mean=3.42; EF5: mean=2.85). Social influence is positive for all items (FSP1: mean=5.25; FSP3: mean=4.69; IM1: mean=4.84) except for FSP2 (the interest of relatives for the device; mean=4.38). Projection in the use of the devices is negative when asked for the participants' profiles (PU1: mean=3.15; PU3: mean=3.38). When asked about other users (PU2: mean=4.61), the projection of use is neutral. Finally, for facilitating conditions, comfort (CF1) and robustness (CF2) are positive while aesthetics (CF3) is evaluated as neutral (CF1: mean=5.46; CF2: mean=5.23; CF3: mean=4.23).

6.3 Discussion

The results of this pilot study show major differences from the previous study on participants without disabilities. The `4Dir` condition performed better than the `8Dir` condition, as was pre-

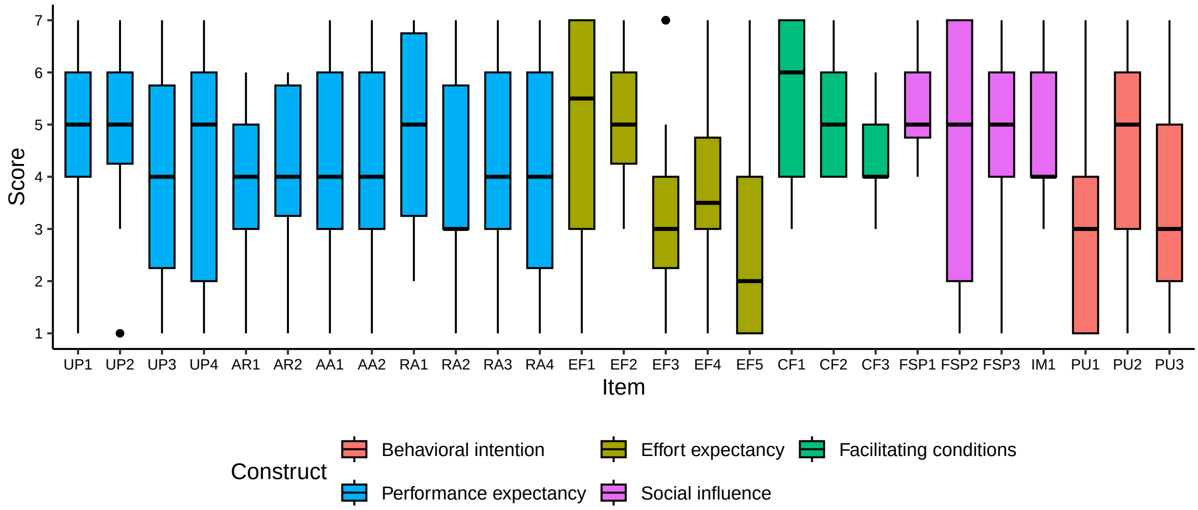

Figure 6.9: Distribution of answers to the UTAUT questionnaire. Colors correspond to contructs in which the items are grouped. Questions associated to items are detailled in Table 6.1.

viously observed, but this time with a greater contrast. Indeed, results for the discrimination of `8Dir` were very poor for diagonal directions. These cues were shown to be harder to discriminate in a previous experiment (see section 3.3), but results are lower here with diagonal cues on the left side showing high confusion with adjacent directions. One factor that might explain these lower results is the handling of the joystick. Indeed, participants had to adapt to a new way of moving the joystick. While they were used to move the joystick with their fingers, here, the position of the handle imposes to use the wrist. Diagonal movements are also more challenging to perform with the wrist, especially moving backward: the radial deviation is typically limited to 10°, and ulnar deviation to 15° [Eschweiler 2022]. This could explain higher variability in rear directions. As these directions are less used during driving, removing them from the rendering scheme could be beneficial for users without affecting navigation.

Higher confusion in `8Dir` also had an impact on navigation, with some participants getting lost quickly using this rendering scheme. Results in navigation with `4Dir` were somewhat better, but a subset of participants were unable to follow navigation instructions at all. There might be an effect of fatigue, as participants already performed the first part of the experiment before the navigation task. These differences might also be related to the pathologies and profiles of participants, which will be the subject of further investigation with clinicians involved in the study.

Mixed results in the navigation task could also be affected by user's expectations as to what type of path they were guided along. Indeed, the chosen paths differed from those the participants might follow in their everyday travels. It would be interesting to follow up this study by evaluating the use of haptic navigation in a realistic environment where expectations of guidance are more clearly defined.

Regarding acceptability, the use of the device itself was evaluated positively, but transmission of information by the handle was found complex and required considerable effort. The `4Dir` condition was found to be more useful than `8Dir`, which showed worse results in both experimental tasks. Participants did not project themselves into the use of the device. This is coherent with their profiles: they were expert drivers which did not need additional guidance. However, they thought that other users and therapists could see benefits from the device.

6.4 Conclusion

In this chapter, we presented the preliminary results of a pilot user study conducted with regular users of power wheelchair. This study, conducted with clinicians, evaluated the perception of feedback provided by our haptic handle and its use in a navigation task. Fourteen participants of diverse profiles took part in the study. We conducted a first analysis of participants performance in the two experimental tasks. Results show great discrimination results for the four cardinal directions displayed by the handle. When adding diagonal directions, however, performance is much weaker. These discrimination transfer to the navigation task, in which participants had more trouble with the more complex rendering scheme. Navigation results vary greatly between participants. Still, a number of them were able to follow target paths using the haptic device.

Acceptability of the device was also evaluated. The use of the device was evaluated positively, but participants did not project themselves into using the device as they did not need such guidance in their current situation. However, they did find the device to have potentials benefits for other users.

Further analysis of the results with clinicians will investigate the impact of participants pathologies and profiles. These initial results with real users of mobility device provide valuable insights which may impact future developments in the Dornell project.

CHAPTER 7

CONCLUSION

In this thesis we were primarily interested the design of in multi-actuator vibrotactile interfaces, with the objective of using them for navigation assistance. Our work revolved around three research axes (as introduced in Figure 2). First, we investigated the **design of handheld multi-actuator interfaces** which could then be employed at the service of our two other axes: **designing rich interactions in virtual reality**, and secondly, **navigating using a multi-actuator haptic handle**.

In our work, we first explored the sensations that multi-actuator devices could provide through the development of prototypes in virtual reality. Consequently, we also investigated the use and relevance of localized haptic sensations for VR interactions. We then looked into the design of a multi-actuator haptic handle, using 3D printing of flexible materials to provide distinct sensations to users. This handle was the foundation for our work on haptic navigation, in which we proposed to use in-hand localized sensations to provide diverse information to users regarding their environment and destination. Finally, we explored the use of our handle in combination with a power wheelchair, setting up the premises for the use of the system by real users.

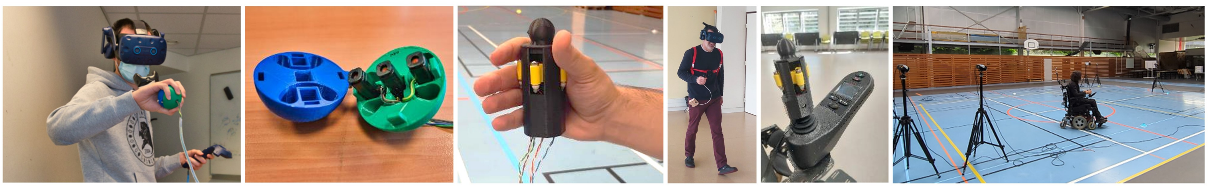

Figure 7.1: A selection of illustrations of devices and experiments presented in this thesis.

7.1 Summary of contributions

In chapter 2, we began our investigation of multi actuator feedback with prototypes of actuated tangible props: handheld objects fitted with multiple vibrotactile actuators to provide localized sensations to users. Through user studies, we evaluated the extent to which this approach was able to display localized sensations, and the ability of participants to discriminate them. Even with this simple approach, a limited number of actuators are able to create discernible spatialized vibrations within the object held by users. Building on these capabilities, we designed rendering schemes for various interactions with virtual objects in a VR environment using these actuated tangibles. For some of these interactions, we showed that this approach was beneficial to the experience in terms of perceived coherence. We then looked further at impact rendering using spatialized vibrations, with the objective of providing users with both direction and distance information when an impact occurred in the virtual environment. The different vibration models we evaluated showed mixed results, emphasizing the difficulty of the distance discrimination task.

In chapter 3 we continued with the design of multi-actuator devices, looking into new ways to isolate vibrations within the interface in order to provide clear sensations to users. We presented the design of a haptic handle equipped with four vibrotactile actuators, based on a soft 3D printed structure created to prevent vibration propagation and ensure contact between the user's hand and the motors. A vibrometry study was conducted to assess the effect of the structure, which resulted in a notable reduction in vibration intensity at non-stimulated points. Those results were corroborated by a user study, in which participants, while still able to discriminate vibration location without the deformable structure, expressed a large preference for the isolated handle. We then evaluated its use to provide directional cues with multiple actuators, successfully displaying eight directions around the handle. The handle and haptic cues it displays represent the foundation on which our following investigations are based.

In chapter 4, we focused on using our haptic handle as a representation of the user's surroundings. In VR, we evaluated the use of the handle and localized cues to avoid both static and dynamic obstacles through two user studies. We observed similar behavior in moving obstacle avoidance as was observed in existing studies with wearables. As a haptic representation of users' personal space, haptic feedback also showed limited effect on participants' behavior.

In chapter 5, we followed with the use of our haptic handle for navigation, this time to provide navigation guidance. We proposed three guidance strategies, providing users with different information related to their position along a path. We conducted a user study, evaluating the use of these strategies in combination with two sets of directional haptic cues. Overall, participants were able to navigate successfully with the haptic handle, with a preference for the more direct, turn by turn strategy. Studies were thus far only focused on pedestrian navigation. In the context of the Dornell project, we also investigate the use of our haptic navigation system with power wheelchair. We evaluated the use of one of our navigation strategies, testing the effect of the handle placement, either onto the power wheelchair joystick or in the non-driving hand of participants. Participants were again able to successfully follow target paths with the haptic guidance, and were mostly not affected by the two different feedback locations. The results of both studies highlight the diverse possible uses of the handle, which could provide different options for users to choose from.

Finally, in chapter 6 we conducted a user study with regular users of power wheelchairs, evaluating the use of our system and its acceptance. Preliminary results are contrasted between participants. Overall, the discrimination of intermediate directions displayed by the handle was difficult for some participants, which transferred to the use of the handle while driving. While participants did not project themselves into using such a device, they saw an interest in this system for users with less expertise. These initial results with real users of mobility devices provide valuable insights that will shape future works in this direction.

7.2 Future work

7.2.1 Short term perspectives

We first discuss short-term perspectives, representing future work which directly follow some of our contributions presented in this manuscript.

Actuated tangible props for VR

The studies we conducted showed the potential of multi-actuator vibrotactile feedback within tangible objects in VR, but currently only yield a limited range of scenarios where this approach is beneficial. Other interactions might benefit from this approach, which should be investigated by studying additional rendering schemes.

Our investigations were done with the tangible object grasped in hand, so it may be interesting to investigate cases where grasp and release occur, or where the hand only touches the tangible, as these could further extend the applicability of the proposed approach. However, the current interface would have to be combined with a system such as the WeATaViX [de Tinguy 2020] to allow users to grasp and release the tangible freely.

In our VR study, we only investigated subjective preference of rendering schemes. It may be useful to look at impacts on task performance in the future to get a more nuanced view of what spatialization of vibrotactile cues can achieve. Additionally, our current rendering schemes ignored vibration propagation and mechanical effects which may impact the quality of the perceived stimuli. Future work could look at integrating the isolation mechanism we designed for our haptic handle, and evaluate potential effects on manipulation.

Haptic handle design

Following the various comments we collected during our diverse experimentation with the handle, its design could be refined to take into account different hand sizes and morphologies. Indeed, a better placement of the actuators within user's hand could improve the discrimination and isolation of stimuli. More radical adaptations could also be beneficial for disabled users, adapting the shape of the handle to their specific needs.

While the isolating structure was shown to be effective, it would be interesting to further characterize the parameters of the structure: other materials, shapes and printing parameters should be considered. Several goals could be pursued this way: the size of the modules might be reduced, or the direction of deformation could be better controlled.

Actuators were chosen for their small size and affordability. While effective, the limited control over the vibration frequency can cause interference effects that would impact discrimination results. The use of more precise actuators should be investigated, as it could improve accuracy and/or allow for a wider range of sensations.

In hand spatial awareness

The concept of a haptic representation of the personal space felt somewhat limited in its current form. It would be interesting to further investigate this use of the handle, possibly in VR scenarios that are closer to real applications. For instance, proximity to real users intruding the tracking space or presence of others in a collaborative space could be useful information for VR users.

A more exploratory concept could be to use the handle as a haptic representation of the user itself: additional cues representing physiological information of the user or his avatar as well as its interactions with the environment could be displayed by the handle.

Navigation using a multi-actuator haptic handle

The navigation strategies we evaluated are only a subset of the possibilities offered by our system to guide users. Following comments of participants, one interesting direction would be to combine the proposed strategies to provide adaptive feedback depending on the user position. More diverse rendering schemes could also be designed and evaluated, taking other parameters into account. For instance, the frequency of instructions could be changed dynamically, adapting it depending on the local path shape and user movements. The effect of the different parameters should be investigated, both in terms of users' preference and performance. Results would provide insights on how the system could be customized based on users' profiles and expectations.

The performance of power wheelchair users with the system showed room for improvements. Participants were not familiar with the device, and the navigation task in an empty space was quite different from what they were used to. It would be interesting to evaluate the use of the device after a more extensive training phase in which users could familiarize with the inner workings of the system.

7.2.2 Middle-term perspectives

Mixed haptics

Our initial approach of actuated tangible only considered the combination of tangibles with vibrations. Exploring the use of other haptic modalities would be interesting to provide more diverse sensations to users. Among others, adding pressure and skin stretch sensations to the fingers could be an interesting way to change the surface properties of the grasped object. Rendering of stiffness was limited with the current device. Exploring the use of other, more deformable materials for the sphere could also lead to new interesting ways of altering our perception

Real world navigation

Our navigation experiments focused on small-scale target paths in a free area. The logical continuation for this application would be to evaluate the use of the system for navigating in realistic environments. Doing so, guidance will have to be adapted to their specificities: indoor and outdoor navigation will not impose the same constraints. This raises some technical challenges for real world navigation: while outdoor localization systems are accessible, navigating indoor will ask for dedicated systems to track users, equipping either users or buildings with sensors. VR could be an interesting platform to conduct preliminary evaluation of the use of the haptic handle within virtual buildings, setting aside limitations of the real world.

Bidirectional interface

The haptic handle we designed for navigation is limited in its interactivity: users are unable to interact with the device as it does not provide an input mechanism. Adding input support would provide more control for users, allowing them for instance to request feedback instead of receiving it continuously. There are different ways the handle could be interacted with. In its current form, the top of the device could simply be equipped with a joystick or button. Input from users could also be done passively with sensors that could detect the user's state or intentions, for instance, by detecting the grip force of the hand on the device. One interesting way of doing so could be to integrate soft 3D printed sensors [Aguilar-Segovia 2024] within the handle, ideally combining them with the existing soft isolating structure.

7.2.3 Towards a personalized haptic handle for mobility assistance

The work carried out during this thesis and, more broadly, those carried out as part of the Dornell project, have explored different ways of using haptic sensations for navigation. In this context, we had the opportunity to conduct a first exploratory study with regular users of mobility assistance devices and clinicians. This collaboration is a great step towards the design of a more adapted and customizable device which can only be achieved with the input from users and therapists. There are still a lot of leads to explore, as was already discussed here, and I personally hope that future work with lead to the design of a device that real users will be able to benefit from.

BIBLIOGRAPHY

[**Adeyemi 2024**] Adeyemi, A., Sen, U., Ercan, S. M., and Sarac, M. (2024), “Hand Dominance and Congruence for Wrist-Worn Haptics Using Custom Voice-Coil Actuation”, *in*: *IEEE Robotics and Automation Letters* 9.*4*, pp. 3053–3059, DOI: 10.1109/LRA.2024.3360815.

[**Adilkhanov 2022**] Adilkhanov, A., Rubagotti, M., and Kappassov, Z. (2022), “Haptic Devices: Wearability-Based Taxonomy and Literature Review”, *in*: *IEEE Access* 10, pp. 91923–91947, DOI: 10.1109/ACCESS.2022.3202986.

[**Aguilar-Segovia 2024**] Aguilar-Segovia, J. E., Manzano, M., Guégan, S., Le Breton, R., Farhi-Rivasseau, A., Lefebvre, S., and Babel, M. (2024), “Multi-Material Torque Sensor Embedding One-Shot 3D-Printed Deformable Capacitive Structures”, *in*: *IEEE Sensors Letters* 8.*9*, pp. 1–4, DOI: 10.1109/LSENS.2024.3440195.

[**Aizawa 2021**] Aizawa, T., Iizima, H., Abe, K., Tadakuma, K., and Tadakuma, R. (2021), “Study on Portable Haptic Guide Device with Omnidirectional Driving Gear”, *in*: *Advanced Robotics* 35.*5*, pp. 320–336, DOI: 10.1080/01691864.2021.1888796.

[**Al Rifaie 2022**] Al Rifaie, M., Abdulhadi, H., and Mian, A. (2022), “Advances in Mechanical Metamaterials for Vibration Isolation: A Review”, *in*: *Advances in Mechanical Engineering* 14.*3*, p. 168781322210828, DOI: 10.1177/16878132221082872.

[**Alles 1970**] Alles, D. S. (1970), “Information Transmission by Phantom Sensations”, *in*: *IEEE Transactions on Man-Machine Systems* 11.*1*, pp. 85–91, DOI: 10.1109/TMMS.1970.299967.

[**Amemiya 2005**] Amemiya, T., Ando, H., and Maeda, T. (2005), “Virtual Force Display : Direction Guidance Using Asymmetric Acceleration via Periodic Translational Motion”, *in*: *World Haptics Conference*, pp. 619–622, DOI: 10.1109/WHC.2005.146.

[**Amemiya 2014**] Amemiya, T. and Gomi, H. (2014), “Buru-Navi3: Movement Instruction Using Illusory Pulled Sensation Created by Thumb-Sized Vibrator”, *in*: *ACM SIGGRAPH 2014 Posters*, pp. 1–1, DOI: 10.1145/2614217.2614254.

[**Amemiya 2009**] Amemiya, T. and Sugiyama, H. (2009), “Haptic Handheld Wayfinder with Pseudo-Attraction Force for Pedestrians with Visual Impairments”, *in*: *Proceeding of the eleventh international ACM SIGACCESS conference on Computers and accessibility - ASSETS ’09*, DOI: 10.1145/1639642.

[**Ando 2015**] Ando, B., Baglio, S., Marletta, V., and Valastro, A. (2015), “A Haptic Solution to Assist Visually Impaired in Mobility Tasks”, *in*: *IEEE Transactions on Human-Machine Systems* 45.*5*, pp. 641–646, DOI: 10.1109/thms.2015.2419256.

[**Ando 2012**] Ando, T., Tsukahara, R., Seki, M., and Fujie, M. G. (2012), “A Haptic Interface "Force Blinker 2" for Navigation of the Visually Impaired”, *in*: *IEEE Transactions on Industrial Electronics* 59.*11*, pp. 4112–4119, DOI: 10.1109/tie.2011.2173894.

[**Azmandian 2016**] Azmandian, M., Hancock, M., Benko, H., Ofek, E., and Wilson, A. D. (2016), “Haptic Retargeting: Dynamic Repurposing of Passive Haptics for Enhanced Virtual Reality Experiences”, *in*: *Conference on Human Factors in Computing Systems - Proceedings*, pp. 1968–1979, DOI: 10.1145/2858036.2858226.

[**Bae 2020**] Bae, Y., Cha, B., and Ryu, J. (2020), “Calibration and Evaluation for Visuohaptic Collocation in Haptic Augmented Virtuality Systems”, *in*: *International Journal of Control, Automation and Systems* 18.*5*, pp. 1335–1342, DOI: 10.1007/s12555-018-0882-3.

[**Bajpai 2020**] Bajpai, A., Powell, J. C., Young, A. J., and Mazumdar, A. (2020), “Enhancing Physical Human Evasion of Moving Threats Using Tactile Cues”, *in*: *IEEE Transactions on Haptics* 13.*1*, pp. 32–37, DOI: 10.1109/toh.2019.2962664.

[**Barontini 2021**] Barontini, F., Catalano, M. G., Pallottino, L., Leporini, B., and Bianchi, M. (2021), “Integrating Wearable Haptics and Obstacle Avoidance for the Visually Impaired in Indoor Navigation: A User-Centered Approach”, *in*: *IEEE Transactions on Haptics* 14.*1*, pp. 109–122, DOI: 10.1109/toh.2020.2996748.

[**Basdogan 2020**] Basdogan, C., Giraud, F., Levesque, V., and Choi, S. (2020), “A Review of Surface Haptics: Enabling Tactile Effects on Touch Surfaces”, *in*: *IEEE*

Transactions on Haptics 13.*3*, pp. 450–470, DOI: 10.1109/toh.2020.2990712.

[**Berton 2020**] Berton, F., Grzeskowiak, F., Bonneau, A., Jovane, A., Aggravi, M., Hoyet, L., Olivier, A. H., Pacchierotti, C., and Pettre, J. (2020), "Crowd Navigation in VR: Exploring Haptic Rendering of Collisions", *in*: *IEEE Transactions on Visualization and Computer Graphics*, DOI: 10.1109/tvcg.2020.3041341.

[**Bhatlawande 2014**] Bhatlawande, S., Mahadevappa, M., Mukherjee, J., Biswas, M., Das, D., and Gupta, S. (2014), "Design, Development, and Clinical Evaluation of the Electronic Mobility Cane for Vision Rehabilitation", *in*: *IEEE Transactions on Neural Systems and Rehabilitation Engineering* 22.*6*, pp. 1148–1159, DOI: 10.1109/tnsre.2014.2324974.

[**Brasen 2019**] Brasen, P. W., Christoffersen, M., and Kraus, M. (2019), "Effects of Vibrotactile Feedback in Commercial Virtual Reality Systems", *in*: *Interactivity, Game Creation, Design, Learning, and Innovation*, ed. by A. L. Brooks, E. Brooks, and C. Sylla, pp. 219–224, DOI: 10.1007/978-3-030-06134-0_25.

[**Brewster 2004**] Brewster, S. and Brown, L. M. (2004), "Tactons: Structured Tactile Messages for Non-Visual Information Display", *in*: *Proceedings of the Fifth Conference on Australasian User Interface - Volume 28*, pp. 15–23, DOI: 10.5555/976310.976313.

[**Brument 2019**] Brument, H., Fribourg, R., Gallagher, G., Howard, T., Lécuyer, F., Luong, T., Mercado, V., Peillard, E., de Tinguy, X., and Marchal, M. (2019), "Pyramid Escape: Design of Novel Passive Haptics Interactions for an Immersive and Modular Scenario", *in*: *2019 IEEE Conference on Virtual Reality and 3D User Interfaces (VR)*, pp. 1409–1410, DOI: 10.1109/VR.2019.8797848.

[**Cabaret 2024a**] Cabaret, P.-A., Bout, A., Manzano, M., Guégan, S., Pacchierotti, C., Babel, M., and Marchal, M. (2024a), "Multi-Actuator Haptic Handle Using Soft Material for Vibration Isolation", *in*: *2024 Eurohaptics Conference*.

[**Cabaret 2023**] Cabaret, P.-A., Howard, T., Gicquel, G., Pacchierotti, C., Babel, M., and Marchal, M. (2023), "Does Multi-Actuator Vibrotactile Feedback Within Tangible Objects Enrich VR Manipulation?", *in*: *IEEE Transactions on Visualization and Computer Graphics*, pp. 1–13, DOI: 10/gstgjf.

[**Cabaret 2022**] Cabaret, P.-A., Howard, T., Pacchierotti, C., Babel, M., and Marchal, M. (2022), "Perception of Spatialized Vibrotactile Impacts in a Hand-Held Tangible for Virtual Reality", *in*: *Haptics: Science, Technology, Applications*, pp. 264–273, DOI: 10.1007/978-3-031-06249-0_30.

[**Cabaret 2024b**] Cabaret, P.-A., Pacchierotti, C., Babel, M., and Marchal, M. (2024b), "Design of Haptic Rendering Techniques for Navigating with a Multi-Actuator Vibrotactile Handle", *in*: *2024 Eurohaptics Conference*.

[**Cheng 2018**] Cheng, L.-P., Chang, L., Marwecki, S., and Baudisch, P. (2018), "iTurk: Turning Passive Haptics into Active Haptics by Making Users Reconfigure Props in Virtual Reality", *in*: *Proceedings of the 2018 CHI Conference on Human Factors in Computing Systems*, pp. 1–10, DOI: `10.1145/3173574.3173663`.

[**Cheng 1996**] Cheng, L.-T., Kazman, R., and Robinson, J. (1996), "Vibrotactile Feedback in Delicate Virtual Reality Operations", *in*: *Proceedings of the Fourth ACM International Conference on Multimedia - MULTIMEDIA '96*, pp. 243–251, DOI: `10.1145/244130.244220`.

[**Chinello 2018**] Chinello, F., Pacchierotti, C., Bimbo, J., Tsagarakis, N. G., and Prattichizzo, D. (2018), "Design and Evaluation of a Wearable Skin Stretch Device for Haptic Guidance", *in*: *IEEE Robotics and Automation Letters* 3.*1*, pp. 524–531, DOI: `10.1109/lra.2017.2766244`.

[**Choi 2017**] Choi, I., Culbertson, H., Miller, M. R., Olwal, A., and Follmer, S. (2017), "Grabity: A Wearable Haptic Interface for Simulating Weight and Grasping in Virtual Reality", *in*: *Proceedings of the 30th Annual ACM Symposium on User Interface Software and Technology*, pp. 119–130, DOI: `10.1145/3126594.3126599`.

[**Choi 2018**] Choi, I., Ofek, E., Benko, H., Sinclair, M., and Holz, C. (2018), "CLAW: A Multifunctional Handheld Haptic Controller for Grasping, Touching, and Triggering in Virtual Reality", *in*: *Proceedings of the 2018 CHI Conference on Human Factors in Computing Systems*, pp. 1–13, DOI: `10.1145/3173574.3174228`.

[**Choi 2013**] Choi, S. and Kuchenbecker, K. J. (2013), "Vibrotactile Display: Perception, Technology, and Applications", *in*: *Proceedings of the IEEE* 101.*9*, pp. 2093–2104, DOI: `10.1109/jproc.2012.2221071`.

[**Cirio 2013**] Cirio, G., Marchal, M., Lécuyer, A., and Cooperstock, J. R. (2013), "Vibrotactile Rendering of Splashing Fluids", *in*: *IEEE Transactions on Haptics* 6.*1*, pp. 117–122, DOI: `10.1109/TOH.2012.34`.

[**Coe 2021**] Coe, P., Evreinov, G., Ziat, M., and Raisamo, R. (2021), "Generating Localized Haptic Feedback over a Spherical Surface:" *in*: *Proceedings of the 16th International Joint Conference on Computer Vision, Imaging and Computer Graphics Theory and Applications*, pp. 15–24, DOI: `10.5220/0010189800150024`.

[**Cooper 2018**] Cooper, N., Milella, F., Pinto, C., Cant, I., White, M., and Meyer, G. (2018), "The Effects of Substitute Multisensory Feedback on Task Performance and the Sense of Presence in a Virtual Reality Environment", *in*: *PLOS ONE* 13.*2*, e0191846, DOI: `10.1371/journal.pone.0191846`.

[**Culbertson 2014**] Culbertson, H., Jose Lopez Delgado, J., Kuchenbecker, K. J., Delgado, L., and Jose, J. (2014), *The Penn Haptic Texture Toolkit for Modeling, Rendering, and Evaluating Haptic Virtual Textures*, tech. rep., p. 299.

[**Culbertson 2017**] Culbertson, H. and Kuchenbecker, K. J. (2017), "Importance of Matching Physical Friction, Hardness, and Texture in Creating Realistic Haptic Virtual Surfaces", *in*: *IEEE Transactions on Haptics* 10.*1*, pp. 63–74, DOI: `10.1109/TOH.2016.2598751`.

[**Culbertson 2018**] Culbertson, H., Schorr, S. B., and Okamura, A. M. (2018), "Haptics: The Present and Future of Artificial Touch Sensation", *in*: *Annual Review of Control, Robotics, and Autonomous Systems* 1.*1*, pp. 385–409, DOI: `10.1146/annurev-control-060117-105043`.

[**Culbertson 2016**] Culbertson, H., Walker, J. M., and Okamura, A. M. (2016), "Modeling and Design of Asymmetric Vibrations to Induce Ungrounded Pulling Sensation through Asymmetric Skin Displacement", *in*: *IEEE Haptics Symposium, HAPTICS* 2016-April, pp. 27–33, DOI: `10.1109/haptics.2016.7463151`.

[**Dandu 2019**] Dandu, B., Shao, Y., Stanley, A., and Visell, Y. (2019), "Spatiotemporal Haptic Effects from a Single Actuator via Spectral Control of Cutaneous Wave Propagation", *in*: *2019 IEEE World Haptics Conference, WHC 2019*, pp. 425–430, DOI: `10.1109/whc.2019.8816149`.

[**Daunizeau 2021**] Daunizeau, T., Gueorguiev, D., Haliyo, S., and Hayward, V. (2021), "Phononic Crystals Applied to Localised Surface Haptics", *in*: *IEEE Transactions on Haptics* 14.*3*, pp. 668–674, DOI: `10.1109/TOH.2021.3072566`.

[**de Tinguy 2020**] de Tinguy, X., Howard, T., Pacchierotti, C., Marchal, M., and Lécuyer, A. (2020), "Weatavix: Wearable Actuated Tangibles for Virtual Reality Experiences", *in*: *Lecture Notes in Computer Science (including subseries Lecture Notes in Artificial Intelligence and Lecture Notes in Bioinformatics)* 12272 LNCS, pp. 262–270, DOI: `10.1007/978-3-030-58147-3_29`.

[**Dejeammes 2008**] Dejeammes, M., Uzan, G., Seck, M., and Sidot, C. (2008), *Déplacements des déficients visuels en milieu urbain: analyse des besoins en sécurité, localisation et orientation et pistes d'évolution*, tech. rep., Centre d'études sur les réseaux, les transports, l'urbanisme et les constructions publiques (CERTU).

[**Devigne 2020**] Devigne, L., Aggravi, M., Bivaud, M., Balix, N., Teodorescu, C. S., Carlson, T., Spreters, T., Pacchierotti, C., and Babel, M. (2020), “Power Wheelchair Navigation Assistance Using Wearable Vibrotactile Haptics”, *in*: *IEEE Transactions on Haptics* 13.*1*, pp. 52–58, DOI: 10.1109/toh.2019.2963831.

[**Devigne 2018**] Devigne, L., Pasteau, F., Babel, M., Narayanan, V. K., Guegan, S., and Gallien, P. (2018), “Design of a Haptic Guidance Solution for Assisted Power Wheelchair Navigation”, *in*: *2018 IEEE International Conference on Systems, Man, and Cybernetics (SMC)*, pp. 3231–3236, DOI: 10.1109/smc.2018.00547.

[**Dobbelstein 2016**] Dobbelstein, D., Henzler, P., and Rukzio, E. (2016), “Unconstrained Pedestrian Navigation Based on Vibro-tactile Feedback around the Wristband of a Smartwatch”, *in*: *Proceedings of the 2016 CHI Conference Extended Abstracts on Human Factors in Computing Systems*, pp. 2439–2445, DOI: 10.1145/2851581.2892292.

[**Erp 2005**] Erp, J. B. F. V., Veen, H. A. H. C. V., Jansen, C., and Dobbins, T. (2005), “Waypoint Navigation with a Vibrotactile Waist Belt”, *in*: *ACM Transactions on Applied Perception* 2.*2*, pp. 106–117, DOI: 10.1145/1060581.1060585.

[**Eschweiler 2022**] Eschweiler, J., Li, J., Quack, V., Rath, B., Baroncini, A., Hildebrand, F., and Migliorini, F. (2022), “Anatomy, Biomechanics, and Loads of the Wrist Joint”, *in*: *Life* 12.*2*, p. 188, DOI: 10.3390/life12020188.

[**Fröhner 2019**] Fröhner, J., Salvietti, G., Beckerle, P., and Prattichizzo, D. (2019), “Can Wearable Haptic Devices Foster the Embodiment of Virtual Limbs?”, *in*: *IEEE Transactions on Haptics* 12.*3*, pp. 339–349, DOI: 10.1109/TOH.2018.2889497.

[**Fuchs 2006**] Fuchs, P., Moreau, G., and Berthoz, A. (2006), *Le traité de la réalité virtuelle volume 1 : L'Homme et l'environnement virtuel.*

[**Gallo 2010**] Gallo, S., Chapuis, D., Santos-Carreras, L., Kim, Y., Retornaz, P., Bleuler, H., and Gassert, R. (2010), “Augmented White Cane with Multimodal Haptic Feedback”, *in*: *2010 3rd IEEE RAS and EMBS International Conference on Biomedical Robotics and Biomechatronics, BioRob 2010*, pp. 149–155, DOI: 10.1109/biorob.2010.5628066.

[**Gay 2020**] Gay, J., Umfahrer, M., Theil, A., Persson, N.-K., Korn, O., Buchweitz, L., Lindell, E., and Guo, L. (2020), “Keep Your Distance: A Playful Haptic Navigation Wearable for Individuals with Deafblindness”, *in*: *Proceedings of the 22nd International ACM SIGACCESS Conference on Computers and Accessibility*, DOI: 10.1145/3373625.3418048.

[**Gérin-Lajoie 2008**] Gérin-Lajoie, M., Richards, C. L., Fung, J., and McFadyen, B. J. (2008), "Characteristics of Personal Space during Obstacle Circumvention in Physical and Virtual Environments", *in*: *Gait & Posture* 27.*2*, pp. 239–247, DOI: `10/cg6s7f`.

[**Gongora 2016**] Gongora, D., Nagano, H., Konyo, M., and Tadokoro, S. (2016), "Experiments on Two-Handed Localization of Impact Vibrations", *in*: *Lecture Notes in Electrical Engineering* 432, pp. 33–39, DOI: `10.1007/978-981-10-4157-0_6`.

[**Grzeskowiak 2022**] Grzeskowiak, F., Devigne, L., Pasteau, F., Dutra, G. S. V., Babel, M., and Guegan, S. (2022), "SWALKIT: A Generic Augmented Walker Kit to Provide Haptic Feedback Navigation Assistance to People with Both Visual and Motor Impairments", *in*: *2022 International Conference on Rehabilitation Robotics (ICORR)*, pp. 1–6, DOI: `10/grx8jv`.

[**Gunarathna 2022**] Gunarathna, C. H., Ranasinghe, A. D., Piyumal, N. A., Kulasekera, A. L., and Jayaweera, N. D. (2022), "Design and Characterization of a 3D Printed Wave Spring for Use in a Flexible Robotic Arm", *in*: *2022 Moratuwa Engineering Research Conference (MERCon)*, pp. 1–6, DOI: `10.1109/MERCon55799.2022.9906257`.

[**Günther 2018**] Günther, S., Kirchner, J., Müller, F., Dezfuli, N., Funk, M., and Mühlhäuser, M. (2018), "TactileGlove: Assistive Spatial Guidance in 3D Space through Vibrotactile Navigation", *in*: *ACM International Conference Proceeding Series*, pp. 273–280, DOI: `10.1145/3197768.3197785`.

[**Guruswamy 2011**] Guruswamy, V. L., Lang, J., and Lee, W.-S. (2011), "IIR Filter Models of Haptic Vibration Textures", *in*: *IEEE Transactions on Instrumentation and Measurement* 60.*1*, pp. 93–103, DOI: `10.1109/TIM.2010.2065751`.

[**Hall 1969**] Hall, E. T. (1969), *The Hidden Dimension.*

[**Hashimoto 2006**] Hashimoto, H., Sasaki, A., Ohyama, Y., and Ishii, C. (2006), "Walker with Hand Haptic Interface for Spatial Recognition", *in*: *International Workshop on Advanced Motion Control, AMC* 2006, pp. 311–316, DOI: `10.1109/amc.2006.1631677`.

[**Heikkinen 2009**] Heikkinen, J., Rantala, J., Olsson, T., Raisamo, R., Lylykangas, J., Raisamo, J., Surakka, V., and Ahmaniemi, T. (2009), "Enhancing Personal Communication with Spatial Haptics: Two Scenario-Based Experiments on Gestural Interaction", *in*: *Journal of Visual Languages & Computing* 20.*5*, pp. 287–304, DOI: `10.1016/j.jvlc.2009.07.007`.

[**Hemmert 2010a**] Hemmert, F., Hamann, S., Löwe, M., Wohlauf, A., Zeipelt, J., and Joost, G. (2010a), "Take Me by the Hand: Haptic Compasses in Mobile Devices through Shape Change and Weight Shift”, *in*: DOI: 10.1145/1868914.1869001.

[**Hemmert 2010b**] Hemmert, F., Hamann, S., Löwe, M., Zeipelt, J., and Joost, G. (2010b), “Shape-Changing Mobiles: Tapering in Two-Dimensional Deformational Displays in Mobile Phones”, *in*: *CHI ’10 Extended Abstracts on Human Factors in Computing Systems*, pp. 3075–3080, DOI: 10.1145/1753846.1753920.

[**Herbst 2005**] Herbst, I. and Stark, J. (2005), “Comparing Force Magnitudes by Means of Vibro-Tactile, Auditory, and Visual Feedback”, *in*: *IEEE International Workshop on Haptic Audio Visual Environments and Their Applications*, DOI: 10.1109/HAVE.2005.1545654.

[**Heuten 2008**] Heuten, W., Henze, N., Boll, S., and Pielot, M. (2008), “Tactile Wayfinder: A Non-Visual Support System for Wayfinding”, *in*: *ACM International Conference Proceeding Series* 358, pp. 172–181, DOI: 10.1145/1463160.1463179.

[**Hoffman 1998**] Hoffman, H. G. (1998), “Physically Touching Virtual Objects Using Tactile Augmentation Enhances the Realism of Virtual Environments”, *in*: *Virtual Reality Annual International Symposium*, pp. 59–59, DOI: 10.1109/VRAIS.1998.658423.

[**Hoggan 2007**] Hoggan, E., Anwar, S., and Brewster, S. A. (2007), “Mobile Multi-actuator Tactile Displays”, *in*: *Haptic and Audio Interaction Design*, ed. by I. Oakley and S. Brewster, pp. 22–33, DOI: 10.1007/978-3-540-76702-2_4.

[**Hollins 2001**] Hollins, M., Bensmaïa, S. J., and Washburn, S. (2001), “Vibrotactile Adaptation Impairs Discrimination of Fine, but Not Coarse, Textures”, *in*: *Somatosensory & Motor Research* 18.4, pp. 253–262, DOI: 10.1080/01421590120089640.

[**Hollins 2000**] Hollins, M. and Risner, S. R. (2000), “Evidence for the Duplex Theory of Tactile Texture Perception”, *in*: *Perception & Psychophysics* 62.4, pp. 695–705, DOI: 10.3758/BF03206916.

[**Hsieh 2016**] Hsieh, M.-J., Liang, R.-H., and Chen, B.-Y. (2016), “NailTactors: Eyes-Free Spatial Output Using a Nail-Mounted Tactor Array”, *in*: *Proceedings of the 18th International Conference on Human-Computer Interaction with Mobile Devices and Services*, pp. 29–34, DOI: 10.1145/2935334.2935358.

[**Hudin 2013**] Hudin, C., Lozada, J., and Hayward, V. (2013), “Localized Tactile Stimulation by Time-Reversal of Flexural Waves: Case Study with a Thin Sheet of Glass”, *in*: *2013 World Haptics Conference (WHC)*, pp. 67–72, DOI: 10.1109/WHC.2013.6548386.

[**Hugues 2015**] Hugues, O., Fuchs, P., Brunet, L., and Megard, C. (2015), “Evaluation of a Vibrotactile Device For Outdoor and Public Transport Pedestrian Navigation Using Virtual Reality", *in*: *International Conference on Advances in Computer-Human Interactions (ACHI 2015).*

[**Hummel 2022**] Hummel, E., Pacchierotti, C., Gouranton, V., Gaugne, R., Nicolas, T., and Lécuyer, A. (2022), "Haptic Rattle: Multi-modal Rendering of Virtual Objects Inside a Hollow Container", *in*: *Haptics: Science, Technology, Applications*, pp. 189–197, DOI: `10.1007/978-3-031-06249-0_22`.

[**Imamura 2011**] Imamura, Y., Arakawa, H., Kamuro, S., Minamizawa, K., and Tachi, S. (2011), "HAPMAP: Haptic Walking Navigation System with Support by the Sense of Handrail", *in*: *ACM SIGGRAPH 2011 Posters, SIGGRAPH'11*, DOI: `10.1145/2037715.2037766`.

[**Insko 2001**] Insko, B. E. (2001), "Passive Haptics Significantly Enhances Virtual Environments", PhD thesis.

[**Ion 2016**] Ion, A., Frohnhofen, J., Wall, L., Kovacs, R., Alistar, M., Lindsay, J., Lopes, P., Chen, H.-T., and Baudisch, P. (2016), "Metamaterial Mechanisms", *in*: *Proceedings of the 29th Annual Symposium on User Interface Software and Technology*, pp. 529–539, DOI: `10/ggcpmh`.

[**Ito 2019**] Ito, K., Okamoto, S., Yamada, Y., and Kajimoto, H. (2019), "Tactile Texture Display with Vibrotactile and Electrostatic Friction Stimuli Mixed at Appropriate Ratio Presents Better Roughness Textures", *in*: *ACM Trans. Appl. Percept.* 16.*4*, 20:1–20:15, DOI: `10.1145/3340961`.

[**Ivanova 2023**] Ivanova, E., Peña-Perez, N., Eden, J., Yip, Y., and Burdet, E. (2023), "Dissociating Haptic Feedback from Physical Assistance Does Not Improve Motor Performance", *in*: *2023 45th Annual International Conference of the IEEE Engineering in Medicine & Biology Society (EMBC)*, pp. 1–5, DOI: `10.1109/EMBC40787.2023.10340983`.

[**Jeannin 2023**] Jeannin, M., Dhiab, A. B., Hudin, C., and Panëels, S. (2023), "Dynamic Pattern Recognition with Localised Surface Haptics and Apparent Motion", *in*: *2023 IEEE World Haptics Conference (WHC)*, pp. 474–480, DOI: `10.1109/WHC56415.2023.10224427`.

[**Johansson 1978**] Johansson, R. S. (1978), "Tactile Sensibility in the Human Hand: Receptive Field Characteristics of Mechanoreceptive Units in the Glabrous Skin Area.", *in*: *The Journal of Physiology* 281, pp. 101–125.

[**Johansson 2008**] Johansson, R. S. and Flanagan, J. R. (2008), "Tactile Sensory Control of Object Manipulation in Humans", *in*: *The Senses: A Comprehensive Reference* 6.

[**Johansson 2009**] Johansson, R. and Flanagan, J. R. (2009), “Coding and Use of Tactile Signals from the Fingertips in Object Manipulation Tasks”, *in*: *Nature Reviews Neuroscience* 10.*5*, pp. 345–359, DOI: 10.1038/nrn2621.

[**Jones 2006**] Jones, L. A. and Lederman, S. J. (2006), “Tactile Sensing”, *in*: *Human Hand Function*, ed. by L. A. Jones and S. J. Lederman, p. 0, DOI: 10.1093/acprof:oso/9780195173154.003.0004.

[**Kappers 2022**] Kappers, A. M., Fa Si Oen, M., Junggeburth, T. J., and Plaisier, M. A. (2022), “Hand-Held Haptic Navigation Devices for Actual Walking”, *in*: *IEEE Transactions on Haptics*, pp. 1–12, DOI: 10.1109/toh.2022.3209350.

[**Kappers 2024**] Kappers, A. M., Holt, R. J., Junggeburth, T. J., Oen, M. F. S., van de Wetering, B. J., and Plaisier, M. A. (2024), “Hands-Free Haptic Navigation Devices for Actual Walking”, *in*: *IEEE Transactions on Haptics*, pp. 1–18, DOI: 10.1109/TOH.2024.3405551.

[**Kaul 2017**] Kaul, O. B., Meier, K., and Rohs, M. (2017), “Increasing Presence in Virtual Reality with a Vibrotactile Grid Around the Head”, *in*: *Human-Computer Interaction – INTERACT 2017*, pp. 289–298, DOI: 10.1007/978-3-319-68059-0_19.

[**Kawaguchi 2012**] Kawaguchi, H. and Nojima, T. (2012), “STRAVIGATION: A Vibrotactile Mobile Navigation for Exploration-Like Sightseeing”, *in*: *Lecture Notes in Computer Science (including subseries Lecture Notes in Artificial Intelligence and Lecture Notes in Bioinformatics)* 7624 LNCS, pp. 517–520, DOI: 10.1007/978-3-642-34292-9_48.

[**Kayhan 2022**] Kayhan, O. and Samur, E. (2022), “A Wearable Haptic Guidance System Based on Skin Stretch around the Waist for Visually-Impaired Runners”, *in*: *2022 IEEE Haptics Symposium (HAPTICS)*, pp. 1–6, DOI: 10.1109/haptics52432.2022.9765618.

[**Kim 2015**] Kim, Y., Harders, M., and Gassert, R. (2015), “Identification of Vibrotactile Patterns Encoding Obstacle Distance Information”, *in*: *IEEE Transactions on Haptics* 8.*3*, pp. 298–305, DOI: 10.1109/toh.2015.2415213.

[**Kovacs 2020**] Kovacs, R., Ofek, E., Franco, M. G., Siu, A. F., Marwecki, S., Holz, C., Sinclair, M., and States, U. (2020), “Haptic PIVOT : On-Demand Handhelds in VR”, *in*: *UIST 2020*, DOI: 10.1145/3379337.3415854.

[**Krauß 2020**] Krauß, A.-M., Ballin, P., Ramian, A., Wittchen, D., and Freitag, G. (2020), “NAVIGONS — Analyzing Tactons for Navigation”, *in*: *Mensch und Computer 2020 - Workshopband*, DOI: 10.18420/muc2020-ws121-360.

[**Kuang 2022**] Kuang, L., Aggravi, M., Giordano, P., Pacchierotti, C., and Robuffo Giordano, P. (2022), “Wearable Cutaneous Device for Applying Position/Location

Haptic Feedback in Navigation Applications”, *in*: *2022 IEEE Haptics Symposium (HAPTICS)*, pp. 1–6.

[**Kuchenbecker 2006**] Kuchenbecker, K., Fiene, J., and Niemeyer, G. (2006), “Improving Contact Realism through Event-Based Haptic Feedback”, *in*: *IEEE Transactions on Visualization and Computer Graphics* 12.*2*, pp. 219–230, DOI: 10.1109/tvcg.2006.32.

[**Lacôte 2024**] Lacôte, I., Cabaret, P.-A., Pacchierotti, C., Babel, M., Gueorguiev, D., and Marchal, M. (2024), “Do Vibrotactile Patterns on Both Hands Improve Guided Navigation with a Walker?”, *in*: *2024 Eurohaptics Conference*.

[**Lacôte 2023**] Lacôte, I., Pacchierotti, C., Babel, M., Gueorguiev, D., and Marchal, M. (2023), “Investigating the Haptic Perception of Directional Information Within a Handle”, *in*: *IEEE Transactions on Haptics*.

[**Lederman 1972**] Lederman, S. J. and Taylor, M. M. (1972), “Fingertip Force, Surface Geometry, and the Perception of Roughness by Active Touch”, *in*: *Perception & Psychophysics* 12.*5*, pp. 401–408, DOI: 10.3758/BF03205850.

[**Lee 2018**] Lee, M., Bruder, G., Höllerer, T., and Welch, G. (2018), “Effects of Unaugmented Periphery and Vibrotactile Feedback on Proxemics with Virtual Humans in AR”, *in*: *IEEE Transactions on Visualization and Computer Graphics* 24.*4*, pp. 1525–1534, DOI: 10.1109/TVCG.2018.2794074.

[**Lee 2017**] Lee, M., Bruder, G., and Welch, G. F. (2017), “Exploring the Effect of Vibrotactile Feedback through the Floor on Social Presence in an Immersive Virtual Environment”, *in*: *2017 IEEE Virtual Reality (VR)*, pp. 105–111, DOI: 10.1109/VR.2017.7892237.

[**Lee 2010**] Lee, S. and Starner, T. (2010), “BuzzWear: Alert Perception in Wearable Tactile Displays on the Wrist”, *in*: *Proceedings of the SIGCHI Conference on Human Factors in Computing Systems*, pp. 433–442, DOI: 10.1145/1753326.1753392.

[**Maeda 2023**] Maeda, T., Yamamoto, J., Yoshimura, T., Sakai, H., and Minamizawa, K. (2023), “Waylet: Self-Contained Haptic Device for Park-Scale Interactions”, *in*: *SIGGRAPH Asia 2023 Emerging Technologies*, pp. 1–2, DOI: 10.1145/3610541.3614567.

[**Maeda 2024**] Maeda, T., Yoshimura, T., Yamamoto, J., Sakai, H., and Minamizawa, K. (2024), “Design and Validation of Pseudo-Force Haptic Device for Actual Walking”, *in*: *2024 IEEE Haptics Symposium (HAPTICS)*, pp. 104–110, DOI: 10.1109/HAPTICS59260.2024.10520860.

[**Maereg 2017**] Maereg, A. T., Nagar, A., Reid, D., and Secco, E. L. (2017), “Wearable Vibrotactile Haptic Device for Stiffness Discrimination during Virtual Interactions", *in*: *Frontiers in Robotics and AI* 4, DOI: 10.3389/frobt.2017.00042.

[**Massie 1994**] Massie, T. H. and Salisbury, J. K. (1994), "The PHANTOM Haptic Interface: A Device for Probing Virtual Objects", *in*: *Proceedings of the ASME winter annual meeting, symposium on haptic interfaces for virtual environment and teleoperator systems.*

[**McDonald 2013**] McDonald, C. G. and Kuchenbecker, K. J. (2013), "Dynamic Simulation of Tool-Mediated Texture Interaction", *in*: *2013 World Haptics Conference (WHC)*, pp. 307–312, DOI: 10.1109/WHC.2013.6548426.

[**Medeiros 2021**] Medeiros, D., Anjos, R. dos, Pantidi, N., Huang, K., Sousa, M., Anslow, C., and Jorge, J. (2021), "Promoting Reality Awareness in Virtual Reality through Proxemics", *in*: *2021 IEEE Virtual Reality and 3D User Interfaces (VR)*, pp. 21–30, DOI: 10.1109/VR50410.2021.00022.

[**Mercado 2021**] Mercado, V. R., Howard, T., Si-Mohammed, H., Argelaguet, F., and Lécuyer, A. (2021), "Alfred: The Haptic Butler On-Demand Tangibles for Object Manipulation in Virtual Reality Using an ETHD", *in*: *2021 IEEE World Haptics Conference (WHC)*, pp. 373–378, DOI: 10.1109/WHC49131.2021.9517250.

[**Monica 2023**] Monica, R. and Aleotti, J. (2023), "Improving Virtual Reality Navigation Tasks Using a Haptic Vest and Upper Body Tracking", *in*: *Displays* 78, p. 102417, DOI: 10.1016/j.displa.2023.102417.

[**Nasser 2020**] Nasser, A., Keng, K. N., and Zhu, K. (2020), "ThermalCane: Exploring Thermotactile Directional Cues on Cane-Grip for Non-Visual Navigation", *in*: *ASSETS 2020 - 22nd International ACM SIGACCESS Conference on Computers and Accessibility*, DOI: 10.1145/3373625.3417004.

[**Niwa 2010**] Niwa, M., Nozaki, T., Maeda, T., and Ando, H. (2010), "Fingernail-Mounted Display of Attraction Force and Texture", *in*: *Lecture Notes in Computer Science (Including Subseries Lecture Notes in Artificial Intelligence and Lecture Notes in Bioinformatics)*, vol. 6192 LNCS, pp. 3–8, DOI: 10.1007/978-3-642-14075-4_1.

[**Oakley 2000**] Oakley, I., Mcgee, M., Brewster, S., and Gray, P. (2000), "Putting the Feel in 'Look and Feel'", *in*: *Conference on Human Factors in Computing Systems - Proceedings*, DOI: 10.1145/332040.332467.

[**Obermoser 2018**] Obermoser, S., Klammer, D., Sigmund, G., Sianov, A., and Kim, Y. (2018), "A Pin Display Delivering Distance Information in Electronic Travel Aids", *in*: *Proceedings of the IEEE RAS and EMBS International Confer-*

ence on Biomedical Robotics and Biomechatronics 2018-August, pp. 236–241, DOI: 10.1109/biorob.2018.8487659.

[**Okamoto 2013**] Okamoto, S., Nagano, H., and Yamada, Y. (2013), “Psychophysical Dimensions of Tactile Perception of Textures”, *in*: *IEEE Transactions on Haptics* 6.*1*, pp. 81–93, DOI: 10.1109/TOH.2012.32.

[**Okamura 1998**] Okamura, A. M., Dennerlein, J. T., and Howe, R. D. (1998), “Vibration Feedback Models for Virtual Environments”, *in*: *Proceedings - IEEE International Conference on Robotics and Automation*, vol. 1, pp. 674–679, DOI: 10.1109/robot.1998.677050.

[**Pacchierotti 2017**] Pacchierotti, C., Sinclair, S., Solazzi, M., Frisoli, A., Hayward, V., and Prattichizzo, D. (2017), “Wearable Haptic Systems for the Fingertip and the Hand: Taxonomy, Review, and Perspectives.”, *in*: *IEEE transactions on haptics* 10.*4*, pp. 580–600, DOI: 10.1109/toh.2017.2689006, PMID: 28500008.

[**Pan 2018**] Pan, Y. T., Shih, C. C., Debuys, C., and Hurl, P. (2018), “Design of a Sensory Augmentation Walker with a Skin Stretch Feedback Handle”, *in*: *RO-MAN 2018 - 27th IEEE International Symposium on Robot and Human Interactive Communication*, pp. 832–837, DOI: 10.1109/roman.2018.8525695.

[**Paneels 2013**] Paneels, S., Anastassova, M., Strachan, S., Van, S. P., Sivacoumarane, S., and Bolzmacher, C. (2013), “What’s around Me Multi-actuator Haptic Feedback on the Wrist”, *in*: *2013 World Haptics Conference, WHC 2013*, pp. 407–412, DOI: 10.1109/whc.2013.6548443.

[**Park 2019**] Park, C., Park, J., Oh, S., and Choi, S. (2019), “Realistic Haptic Rendering of Collision Effects Using Multimodal Vibrotactile and Impact Feedback”, *in*: *2019 IEEE World Haptics Conference (WHC)*, pp. 449–454, DOI: 10.1109/WHC.2019.8816116.

[**Perez 2000**] Perez, C. A., Holzmann, C. A., and Jaeschke, H. E. (2000), “Two-Point Vibrotactile Discrimination Related to Parameters of Pulse Burst Stimulus”, *in*: *Medical and Biological Engineering and Computing* 38.*1*, pp. 74–79, DOI: 10.1007/BF02344692.

[**Perez 1998**] Perez, C., Holzmann, C., and Sandoval, E. (1998), “Two Point Vibrotactile Spatial Resolution as a Function of Pulse Frequency and Pulse Width”, *in*: *Proceedings of the 20th Annual International Conference of the IEEE Engineering in Medicine and Biology Society. Vol.20 Biomedical Engineering Towards the Year 2000 and Beyond (Cat. No.98CH36286)*, vol. 5, 2542–2545 vol.5, DOI: 10.1109/IEMBS.1998.744968.

[**Pezent 2020**] Pezent, E., Cambio, B., and O'Malley, M. K. (2020), "Syntacts: Open-Source Software and Hardware for Audio-Controlled Haptics", *in*: *IEEE Transactions on Haptics* PP, pp. 1939–1412, DOI: 10.1109/toh.2020.3002696.

[**Pielot 2010**] Pielot, M., Poppinga, B., and Boll, S. (2010), "PocketNavigator: Vibro-Tactile Waypoint Navigation for Everyday Mobile Devices", *in*: *Proceedings of the 12th International Conference on Human Computer Interaction with Mobile Devices and Services*, pp. 423–426, DOI: 10/djq57w.

[**Pietrzak 2009**] Pietrzak, T., Crossan, A., Brewster, S. A., Martin, B., and Pecci, I. (2009), "Creating Usable Pin Array Tactons for Nonvisual Information", *in*: *IEEE Transactions on Haptics* 2.*2*, pp. 61–72, DOI: 10.1109/TOH.2009.6.

[**Porquis 2011**] Porquis, L. B., Konyo, M., and Tadokoro, S. (2011), "Representation of Softness Sensation Using Vibrotactile Stimuli under Amplitude Control", *in*: *Proceedings - IEEE International Conference on Robotics and Automation*, pp. 1380–1385, DOI: 10.1109/icra.2011.5980378.

[**Pyun 2013**] Pyun, R., Kim, Y., Wespe, P., Gassert, R., and Schneller, S. (2013), "Advanced Augmented White Cane with Obstacle Height and Distance Feedback", *in*: *IEEE International Conference on Rehabilitation Robotics*, DOI: 10.1109/icorr.2013.6650358.

[**Radhakrishnan 2024**] Radhakrishnan, U., Kuang, L., Koumaditis, K., Chinello, F., and Pacchierotti, C. (2024), "Haptic Feedback, Performance and Arousal: A Comparison Study in an Immersive VR Motor Skill Training Task", *in*: *IEEE Transactions on Haptics* 17.*2*, pp. 249–262, DOI: 10.1109/TOH.2023.3319034.

[**Richard 2023**] Richard, G., Pietrzak, T., Argelaguet, F., Lécuyer, A., and Casiez, G. (2023), "MultiVibes: What If Your VR Controller Had 10 Times More Vibrotactile Actuators?", *in*: *ISMAR 2023 - 22nd IEEE International Symposium on Mixed and Augmented Reality*, p. 1.

[**Richard 2020**] Richard, G., Pietrzak, T., Argelaguet, F., Lécuyer, A., and Casiez, G. (2020), "Studying the Role of Haptic Feedback on Virtual Embodiment in a Drawing Task", *in*: *Frontiers in Virtual Reality* 1, DOI: 10.3389/frvir.2020.573167.

[**Rios-Martinez 2015**] Rios-Martinez, J., Spalanzani, A., and Laugier, C. (2015), "From Proxemics Theory to Socially-Aware Navigation: A Survey", *in*: *International Journal of Social Robotics* 7.*2*, pp. 137–153, DOI: 10/ghjv5n.

[**Robinson 2010**] Robinson, S., Jones, M., Eslambolchilar, P., Murray-Smith, R., and Lindborg, M. (2010), ""I Did It My Way": Moving Away from the Tyranny of

Turn-by-Turn Pedestrian Navigation", *in*: *ACM International Conference Proceeding Series*, pp. 341–344, DOI: 10.1145/1851600.1851660.

[**Rümelin 2011**] Rümelin, S., Rukzio, E., and Hardy, R. (2011), "NaviRadar: A Tactile Information Display for Pedestrian Navigation", *in*: *UIST'11 - Proceedings of the 24th Annual ACM Symposium on User Interface Software and Technology*, pp. 293–302, DOI: 10.1145/2047196.2047234.

[**Ryu 2012**] Ryu, D., Yang, G. H., and Kang, S. (2012), "T-Hive: Bilateral Haptic Interface Using Vibrotactile Cues for Presenting Spatial Information", *in*: *IEEE Transactions on Systems, Man and Cybernetics Part C: Applications and Reviews* 42.*6*, pp. 1318–1325, DOI: 10.1109/tsmcc.2011.2182647.

[**Sagheb 2019**] Sagheb, S., Liu, F. W., Bahremand, A., Kidane, A., and LiKamWa, R. (2019), "SWISH: A Shifting-Weight Interface of Simulated Hydrodynamics for Haptic Perception of Virtual Fluid Vessels", *in*: *UIST 2019 - Proceedings of the 32nd Annual ACM Symposium on User Interface Software and Technology*, pp. 751–761, DOI: 10.1145/3332165.3347870.

[**Sahami 2008**] Sahami, A., Holleis, P., Schmidt, A., and Häkkilä, J. (2008), "Rich Tactile Output on Mobile Devices", *in*: *Ambient Intelligence*, ed. by E. Aarts, J. L. Crowley, B. de Ruyter, H. Gerhäuser, A. Pflaum, J. Schmidt, and R. Wichert, pp. 210–221, DOI: 10.1007/978-3-540-89617-3_14.

[**Saint-Aubert 2020**] Saint-Aubert, J. (2020), "Identifying Tactors Locations on the Proximal Phalanx of the Finger for Navigation", *in*: *Lecture Notes in Computer Science (Including Subseries Lecture Notes in Artificial Intelligence and Lecture Notes in Bioinformatics)*, vol. 12272 LNCS, pp. 42–50, DOI: 10.1007/978-3-030-58147-3_5.

[**Sander 2005**] Sander, M.-S., Bournot, M.-C., Lelièvre, F., and Tallec, A. (2005), *La Population En Situation de Handicap Visuel En France: Importance, Caractéristiques, Incapacités Fonctionnelles et Difficultés Sociales*, Exploitation d'enquêtes HID 1998/99. Observatoire Régional de La Santé Des Pays de La Loire.

[**Sanz 2015**] Sanz, F. A., Olivier, A.-H., Bruder, G., Pettré, J., and Lécuyer, A. (2015), "Virtual Proxemics: Locomotion in the Presence of Obstacles in Large Immersive Projection Environments", *in*: *2015 IEEE Virtual Reality (VR)*, pp. 75–80, DOI: 10/grzmb7.

[**Scalera 2018**] Scalera, L., Seriani, S., Gallina, P., Di Luca, M., and Gasparetto, A. (2018), "An Experimental Setup to Test Dual-Joystick Directional Responses to Vibrotactile Stimuli", *in*: *IEEE Transactions on Haptics* 11.*3*, pp. 378–387, DOI: 10.1109/TOH.2018.2804391.

[**Schaack 2019**] Schaack, S., Chernyshov, G., Ragozin, K., Tag, B., Peiris, R., and Kunze, K. (2019), "Haptic Collar: Vibrotactile Feedback around the Neck for Guidance Applications", *in*: *Proceedings of the 10th Augmented Human International Conference 2019*, pp. 1–4, DOI: 10.1145/3311823.3311840.

[**Sekiguchi 2003**] Sekiguchi, Y., Hirota, K., and Hirose, M. (2003), "Haptic Interface Using "Estimation of Box Contents" Metaphor", *in*: *Proceedings of ICAT* 203, pp. 197–202.

[**Seo 2015**] Seo, J. and Choi, S. (2015), "Edge Flows: Improving Information Transmission in Mobile Devices Using Two-Dimensional Vibrotactile Flows", *in*: *2015 IEEE World Haptics Conference (WHC)*, pp. 25–30, DOI: 10.1109/WHC.2015.7177686.

[**Shah 2006**] Shah, C., Bouzit, M., Youssef, M., and Vasquez, L. (2006), "Evaluation of RU-Netra - Tactile Feedback Navigation System For The Visually Impaired", *in*: *2006 International Workshop on Virtual Rehabilitation*, pp. 72–77, DOI: 10.1109/iwvr.2006.1707530.

[**Shao 2020**] Shao, Y., Hu, H., and Visell, Y. (2020), "A Wearable Tactile Sensor Array for Large Area Remote Vibration Sensing in the Hand", *in*: *IEEE Sensors Journal* 20.*12*, pp. 6612–6623, DOI: 10.1109/jsen.2020.2972521, arXiv: 1908.08199.

[**Sherrick 1990**] Sherrick, C. E., Cholewiak, R. W., and Collins, A. A. (1990), "The Localization of Low- and High-frequency Vibrotactile Stimuli", *in*: *The Journal of the Acoustical Society of America* 88.*1*, pp. 169–179, DOI: 10.1121/1.399937.

[**Shigeyama 2019**] Shigeyama, J., Hashimoto, T., Yoshida, S., Narumi, T., Tanikawa, T., and Hirose, M. (2019), "Transcalibur: A Weight Shifting Virtual Reality Controller for 2D Shape Rendering Based on Computational Perception Model", *in*: *Proceedings of the 2019 CHI Conference on Human Factors in Computing Systems*, pp. 1–11, DOI: 10.1145/3290605.3300241.

[**Sinclair 2019**] Sinclair, M., Ofek, E., Gonzalez-Franco, M., and Holz, C. (2019), "CapstanCrunch: A Haptic VR Controller with User-Supplied Force Feedback", *in*: *UIST 2019 - Proceedings of the 32nd Annual ACM Symposium on User Interface Software and Technology*, pp. 815–829, DOI: 10.1145/3332165.3347891.

[**Slater 2016**] Slater, M. and Sanchez-Vives, M. V. (2016), "Enhancing Our Lives with Immersive Virtual Reality", *in*: *Frontiers in Robotics and AI* 3, DOI: 10.3389/frobt.2016.00074.

[**Spiers 2017**] Spiers, A. and Dollar, A. M. (2017), "Design and Evaluation of Shape-Changing Haptic Interfaces for Pedestrian Navigation Assistance", *in*: *IEEE Transactions on Haptics* 10.*1*, pp. 17–28, DOI: 10.1109/toh.2016.2582481.

[**Spiers 2016**] Spiers, A. and Dollar, A. M. (2016), "Outdoor Pedestrian Navigation Assistance with a Shape-Changing Haptic Interface and Comparison with a Vibrotactile Device", *in*: *IEEE Haptics Symposium, HAPTICS* 2016-April, pp. 34–40, DOI: 10.1109/haptics.2016.7463152.

[**Spiers 2015**] Spiers, A., van der Linden, J., and Oshodi, M. (2015), "First Validation of the Haptic Sandwich: A Shape Changing Handheld Haptic Navigation Aid", *in*: DOI: 10.1109/ICAR.2015.7251447.

[**Spiers 2022**] Spiers, A., Young, E., and Kuchenbecker, K. J. (2022), "The S-BAN: Insights into the Perception of Shape-Changing Haptic Interfaces via Virtual Pedestrian Navigation", *in*: *ACM Transactions on Computer-Human Interaction*, DOI: 10.1145/3555046.

[**Sreng 2008**] Sreng, J., Lécuyer, A., and Andriot, C. (2008), "Using Vibration Patterns to Provide Impact Position Information in Haptic Manipulation of Virtual Objects", *in*: *Lecture Notes in Computer Science (Including Subseries Lecture Notes in Artificial Intelligence and Lecture Notes in Bioinformatics)*, vol. 5024 LNCS, pp. 589–598, DOI: 10.1007/978-3-540-69057-3_76.

[**Stanke 2020**] Stanke, D., Duente, T., and Rohs, M. (2020), "TactileWear: A Comparison of Electrotactile and Vibrotactile Feedback on the Wrist and Ring Finger", *in*: *Proceedings of the 11th Nordic Conference on Human-Computer Interaction: Shaping Experiences, Shaping Society*, pp. 1–13, DOI: 10.1145/3419249.3420107.

[**Tan 2020**] Tan, H. Z., Choi, S., Lau, F. W. Y., and Abnousi, F. (2020), "Methodology for Maximizing Information Transmission of Haptic Devices: A Survey", *in*: *Proceedings of the IEEE* 108.*6*, pp. 945–965, DOI: 10.1109/JPROC.2020.2992561.

[**Tanaka 2012**] Tanaka, Y. and Hirota, K. (2012), "Shaking a Box to Estimate the Property of Content", *in*: *Haptics: Perception, Devices, Mobility, and Communication*, ed. by P. Isokoski and J. Springare, pp. 564–576, DOI: 10.1007/978-3-642-31401-8_50.

[**Tanaka 2020**] Tanaka, Y., Horie, A., and Chen, X. '. (2020), "DualVib: Simulating Haptic Sensation of Dynamic Mass by Combining Pseudo-Force and Texture Feedback", *in*: *Proceedings of the 26th ACM Symposium on Virtual Reality Software and Technology*, pp. 1–10, DOI: 10.1145/3385956.3418964.

[**Tewell 2017**] Tewell, J., Bird, J., and Buchanan, G. R. (2017), "Heat-Nav: Using Temperature Changes as Navigational Cues", *in*: *Conference on Human Factors in Computing Systems - Proceedings* 2017-May, pp. 1131–1135, DOI: 10.1145/3025453.3025965.

[**Tinguy 2019**] Tinguy, X. D., Pacchierotti, C., Emily, M., Chevalier, M., Guignardat, A., Guillaudeux, M., Six, C., Lecuyer, A., and Marchal, M. (2019), "How Different Tangible and Virtual Objects Can Be While Still Feeling the Same?", *in*: *2019 IEEE World Haptics Conference (WHC)*, pp. 580–585, DOI: 10.1109/WHC.2019.8816164.

[**Tricard 2020**] Tricard, T., Tavernier, V., Zanni, C., Martínez, J., Hugron, P.-A., Neyret, F., and Lefebvre, S. (2020), "Freely Orientable Microstructures for Designing Deformable 3D Prints", *in*: *ACM Transactions on Graphics* 39.*6*, pp. 1–16, DOI: 10.1145/3414685.3417790.

[**Uchiyama 2008**] Uchiyama, H., Covington, M. A., and Potter, W. D. (2008), "Vibrotactile Glove Guidance for Semi-Autonomous Wheelchair Operations", *in*: *Proceedings of the 46th Annual Southeast Regional Conference on XX, ACM-SE 46*, pp. 336–339, DOI: 10.1145/1593105.1593195.

[**Ujitoko 2022**] Ujitoko, Y., Tokuhisa, R., and Hirota, K. (2022), "Vibrotactile Spatiotemporal Pattern Recognition in Two-Dimensional Space Around Hand", *in*: *IEEE Transactions on Haptics* 15.*4*, pp. 718–728, DOI: 10.1109/TOH.2022.3213313.

[**v. Békésy 1958**] v. Békésy, G. (1958), "Funneling in the Nervous System and Its Role in Loudness and Sensation Intensity on the Skin", *in*: *The Journal of the Acoustical Society of America* 30.*5*, pp. 399–412, DOI: 10.1121/1.1909626.

[**Velázquez 2006**] Velázquez, R., Fontaine, E., and Pissaloux, E. (2006), "Coding the Environment in Tactile Maps for Real-Time Guidance of the Visually Impaired", *in*: *2006 IEEE International Symposium on Micro-Nano Mechanical and Human Science, MHS*, DOI: 10.1109/mhs.2006.320235.

[**Venkatesh 2003**] Venkatesh, V., Morris, M. G., Davis, G. B., and Davis, F. D. (2003), "User Acceptance of Information Technology: Toward a Unified View", *in*: *MIS Quarterly* 27.*3*, pp. 425–478, DOI: 10.2307/30036540, JSTOR: 30036540.

[**Visell 2014**] Visell, Y. and Okamoto, S. (2014), "Vibrotactile Sensation and Softness Perception", *in*: pp. 31–47, DOI: 10.1007/978-1-4471-6533-0_3.

[**Vizcay 2022**] Vizcay, S. (2022), "Contributions to the Use of Electrotactile Feedback in Hand-based Interactions in Virtual Reality", PhD thesis.

[**Von Willich 2019**] Von Willich, J., Funk, M., Müller, F., Marky, K., Riemann, J., and Mühlhäuser, M. (2019), "You Invaded My Tracking Space! Using Augmented Virtuality for Spotting Passersby in Room-Scale Virtual Reality", *in*: *Proceedings of the 2019 on Designing Interactive Systems Conference*, pp. 487–496, DOI: `10.1145/3322276.3322334`.

[**Wachaja 2017**] Wachaja, A., Agarwal, P., Zink, M., Adame, M. R., Möller, K., and Burgard, W. (2017), "Navigating Blind People with Walking Impairments Using a Smart Walker", *in*: *Autonomous Robots* 41.*3*, pp. 555–573, DOI: `10/f9xm33`.

[**Wang 2019a**] Wang, D., Guo, Y., Liu, S., Zhang, Y., Xu, W., and Xiao, J. (2019a), "Haptic Display for Virtual Reality: Progress and Challenges", *in*: *Virtual Reality & Intelligent Hardware* 1.*2*, pp. 136–162, DOI: `10.3724/SP.J.2096-5796.2019.0008`.

[**Wang 2020**] Wang, D., Ohnishi, K., and Xu, W. (2020), "Multimodal Haptic Display for Virtual Reality: A Survey", *in*: *IEEE Transactions on Industrial Electronics* 67, pp. 610–623, DOI: `10.1109/TIE.2019.2920602`.

[**Wang 2019b**] Wang, D., Song, M., Naqash, A., Zheng, Y., Xu, W., and Zhang, Y. (2019b), "Toward Whole-Hand Kinesthetic Feedback: A Survey of Force Feedback Gloves", *in*: *IEEE Transactions on Haptics* 12.*2*, pp. 189–204, DOI: `10.1109/toh.2018.2879812`.

[**Wang 2012**] Wang, Y. and Kuchenbecker, K. J. (2012), "HALO: Haptic Alerts for Low-hanging Obstacles in White Cane Navigation", *in*: *2012 IEEE Haptics Symposium (HAPTICS)*, pp. 527–532, DOI: `10.1109/haptic.2012.6183842`.

[**Wellman 1995**] Wellman, P. and Howe, R. D. (1995), "Towards Realistic Vibrotactile Display in Virtual Environments", *in*: *Proceedings of the ASME Dynamic Systems and Control Division*, vol. 57, pp. 713–718.

[**Wiehr 2023**] Wiehr, F., Unger, A., and Krueger, A. (2023), "HapticPole: Running Navigation Through Skin Drag and Shape Change", *in*: *Augmented Humans Conference*, pp. 354–356, DOI: `10.1145/3582700.3583694`.

[**Wy 2011**] Wy, C., Y, J., Jd, W., Wn, H., Cc, C., Hf, M., and Yh, W. (2011), "Wheelchair-Related Accidents: Relationship with Wheelchair-Using Behavior in Active Community Wheelchair Users", *in*: *Archives of physical medicine and rehabilitation* 92.*6*, DOI: `10.1016/j.apmr.2011.01.008`.

[**Yabe 2021**] Yabe, T. and Yano, H. (2021), "Haptic Interface for Presenting Enveloping Force from Remote Obstacles in a Personal Vehicle", *in*: *2021 IEEE 2nd International Conference on Human-Machine Systems (ICHMS)*, pp. 1–4, DOI: `10/grzhg3`.

[**Yang 2010**] Yang, G. H., Jin, M. S., Jin, Y., and Kang, S. (2010), "T-Mobile: Vibrotactile Display Pad with Spatial and Directional Information for Hand-Held Device", *in*: *IEEE/RSJ 2010 International Conference on Intelligent*

Robots and Systems, IROS 2010 - Conference Proceedings, pp. 5245–5250, DOI: 10.1109/iros.2010.5651759.

[**Yang 2019**] Yang, G.-H., Lee, W., and Kang, S. (2019), "Development of Vibrotactile Pedestal With Multiple Actuators and Application of Haptic Illusions for Information Delivery", *in*: *IEEE Transactions on Industrial Informatics* 15.*1*, pp. 591–598, DOI: 10.1109/TII.2018.2850849.

[**Yang 2009**] Yang, G.-H., Ryu, D., and Kang, S. (2009), "Vibrotactile Display for Hand-Held Input Device Providing Spatial and Directional Information", *in*: *World Haptics 2009 - Third Joint EuroHaptics Conference and Symposium on Haptic Interfaces for Virtual Environment and Teleoperator Systems*, pp. 79–84, DOI: 10.1109/WHC.2009.4810831.

[**Yang 2014**] Yang, S., Tippey, K., and Ferris, T. K. (2014), "Exploring the Emergent Perception of Haptic Beats from Paired Vibrotactile Presentation", *in*: *Proceedings of the Human Factors and Ergonomics Society*, vol. 2014-Janua, pp. 1716–1720, DOI: 10.1177/1541931214581358.

[**Yatani 2012**] Yatani, K., Banovic, N., and Truong, K. (2012), "SpaceSense: Representing Geographical Information to Visually Impaired People Using Spatial Tactile Feedback", *in*: *Proceedings of the SIGCHI Conference on Human Factors in Computing Systems*, pp. 415–424, DOI: 10.1145/2207676.2207734.

[**Yatani 2009**] Yatani, K. and Truong, K. N. (2009), "SemFeel: A User Interface with Semantic Tactile Feedback for Mobile Touch-Screen Devices", *in*: *Proceedings of the 22nd Annual ACM Symposium on User Interface Software and Technology*, pp. 111–120, DOI: 10.1145/1622176.1622198.

[**Yin 2023**] Yin, H., Zhang, W., Zhu, L., Meng, F., Liu, J., and Wen, G. (2023), "Review on Lattice Structures for Energy Absorption Properties", *in*: *Composite Structures* 304, p. 116397, DOI: 10.1016/j.compstruct.2022.116397.

[**Yoon 2017**] Yoon, H. U., Anil Kumar, N., and Hur, P. (2017), "Synergistic Effects on the Elderly People's Motor Control by Wearable Skin-Stretch Device Combined with Haptic Joystick", *in*: *Frontiers in Neurorobotics* 11, DOI: 10.3389/fnbot.2017.00031.

[**Zikmund 2019**] Zikmund, P., Macik, M., Dubnicky, L., and Horpatzska, M. (2019), "Comparison of Joystick Guidance Methods", *in*: *2019 10th IEEE International Conference on Cognitive Infocommunications (CogInfoCom)*, pp. 265–270, DOI: 10.1109/CogInfoCom47531.2019.9089978.

APPENDICES

TRAJECTORIES - PEDESTRIAN NAVIGATION

In this appendix are presented the individual trajectories of participants in the pedestrian navigation experiment covered in section 5.1. Participants used the haptic handle with three guidance strategies (`Attractive`, `Repulsive` and `Latent Attractive`) and two rendering schemes (`4Dir` and `8Dir`) which guided them along three target paths (`P1`, `P2` and `P3`).

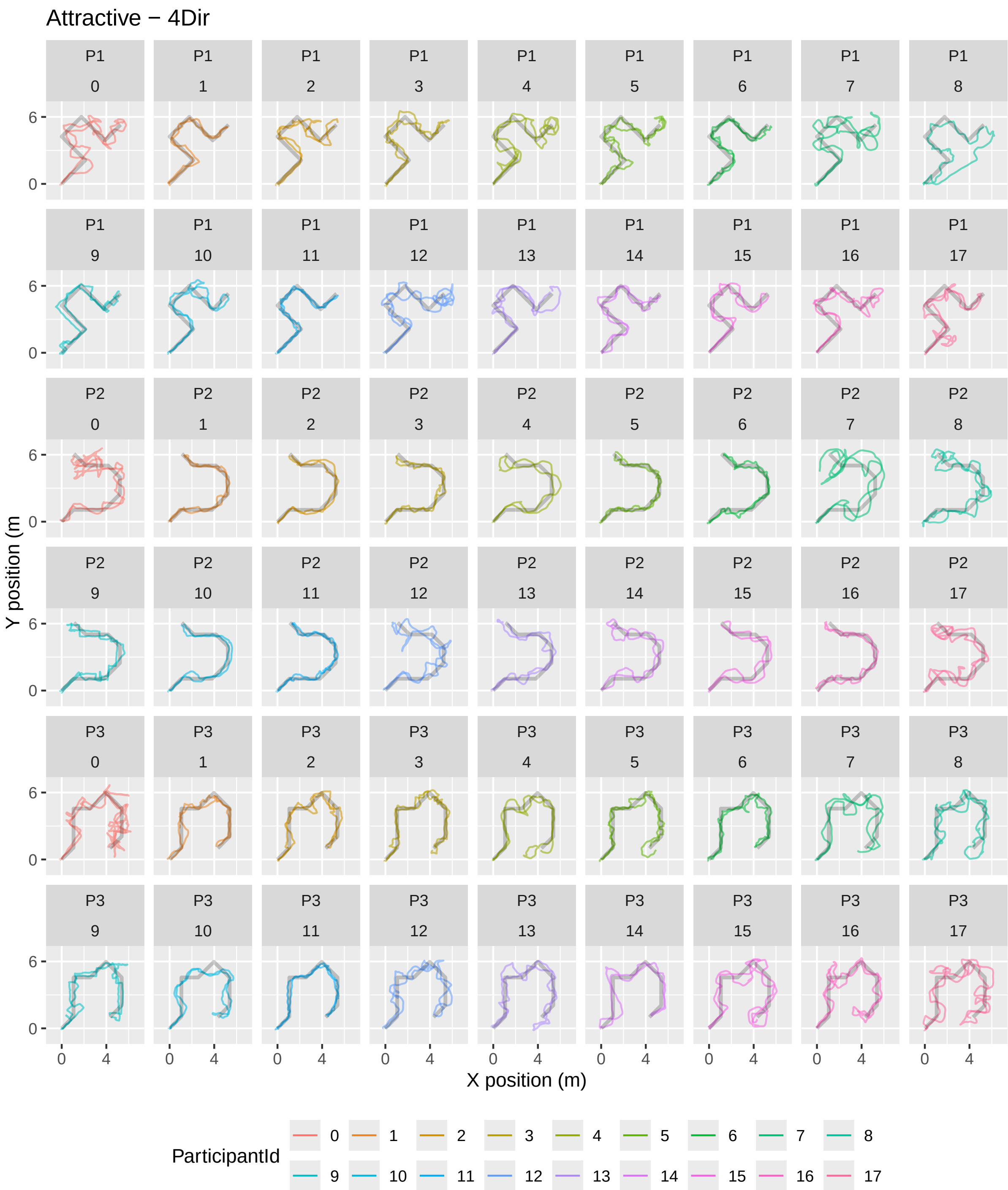

Figure 7.2: Individual trajectories using the `Attractive` strategy and `4Dir`.

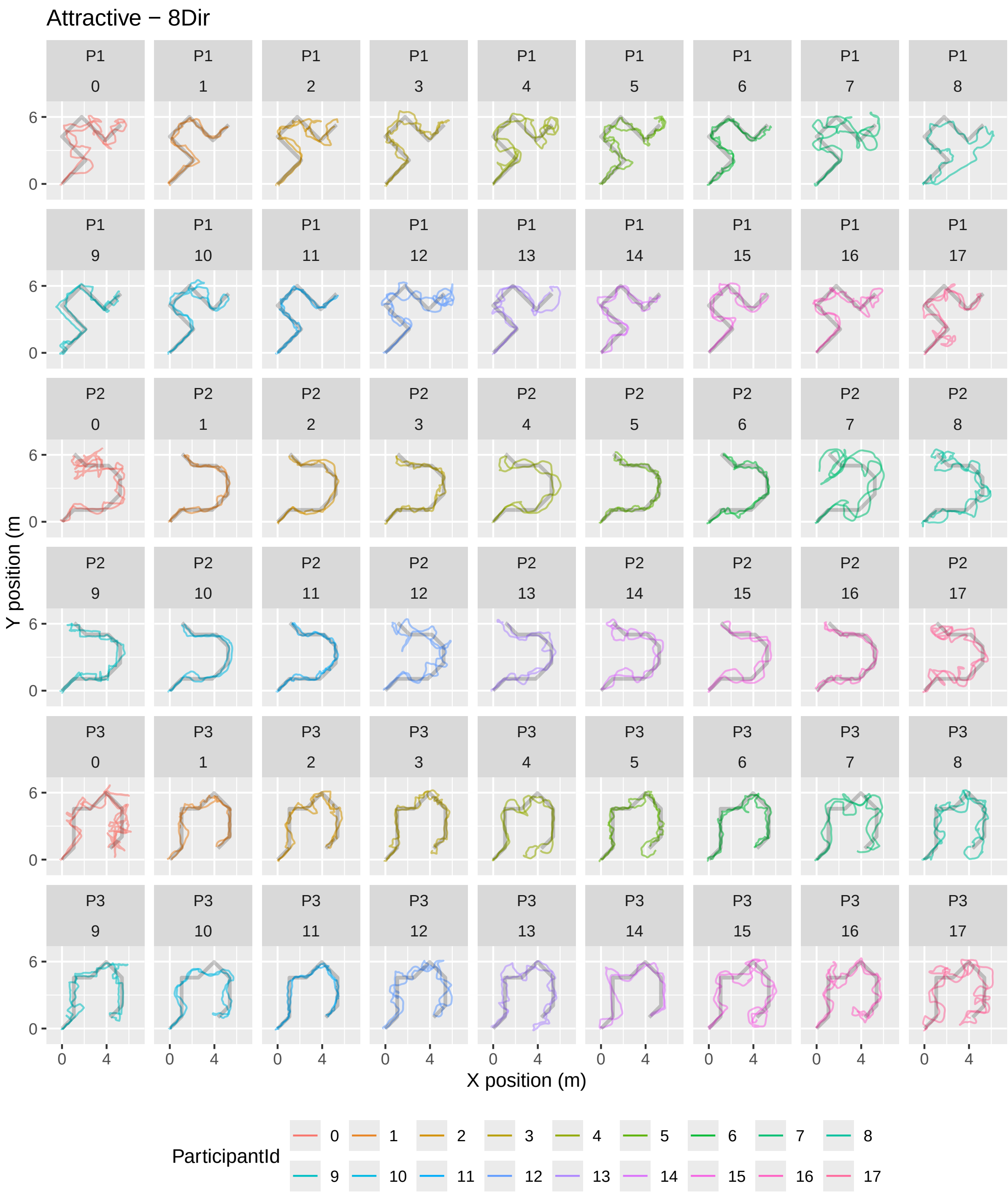

Figure 7.3: Individual trajectories using the `Attractive` strategy and `8Dir`.

Figure 7.4: Individual trajectories using the `Repulsive` strategy and `4Dir`.

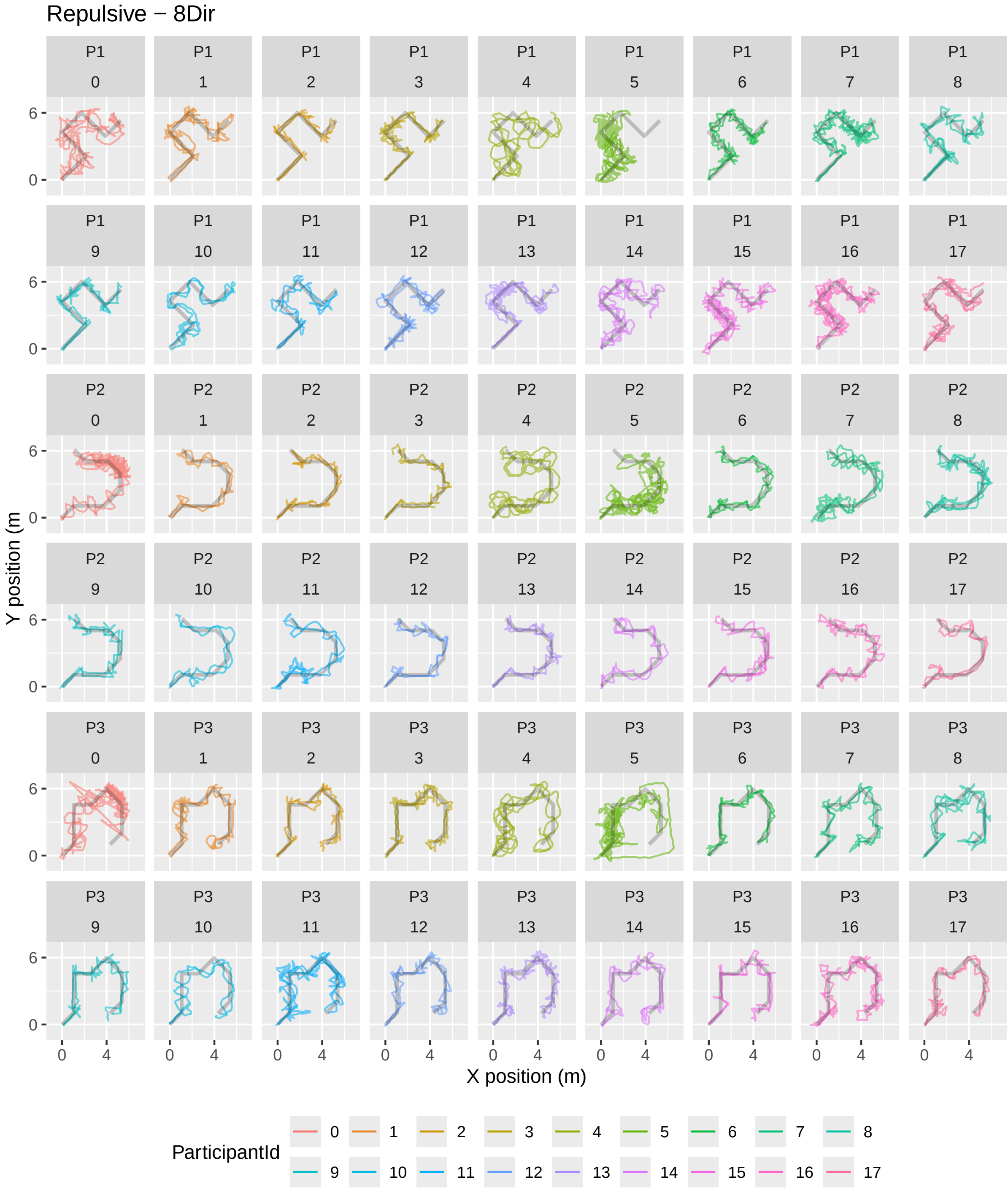

Figure 7.5: Individual trajectories using the `Repulsive` strategy and `8Dir`.

Figure 7.6: Individual trajectories using the `Latent Attractive` strategy and `4Dir`.

Figure 7.7: Individual trajectories using the `Latent Attractive` strategy and `8Dir`.

TRAJECTORIES - EFFECT OF FEEDBACK LOCATION ON POWER WHEELCHAIR NAVIGATION

In this appendix are presented the individual trajectories of participants in the first power wheelchair navigation experiment covered in section 5.2. Participants used the haptic handle with the `Attractive` guidance strategy and two rendering schemes (`4Dir` and `8Dir`) which guided them along three target paths (`P1`, `P2` and `P3`) either with the handle placed on the joystick of the power wheelchair (`CoLoc`) or in their free, non-driving hand (`DeLoc`).

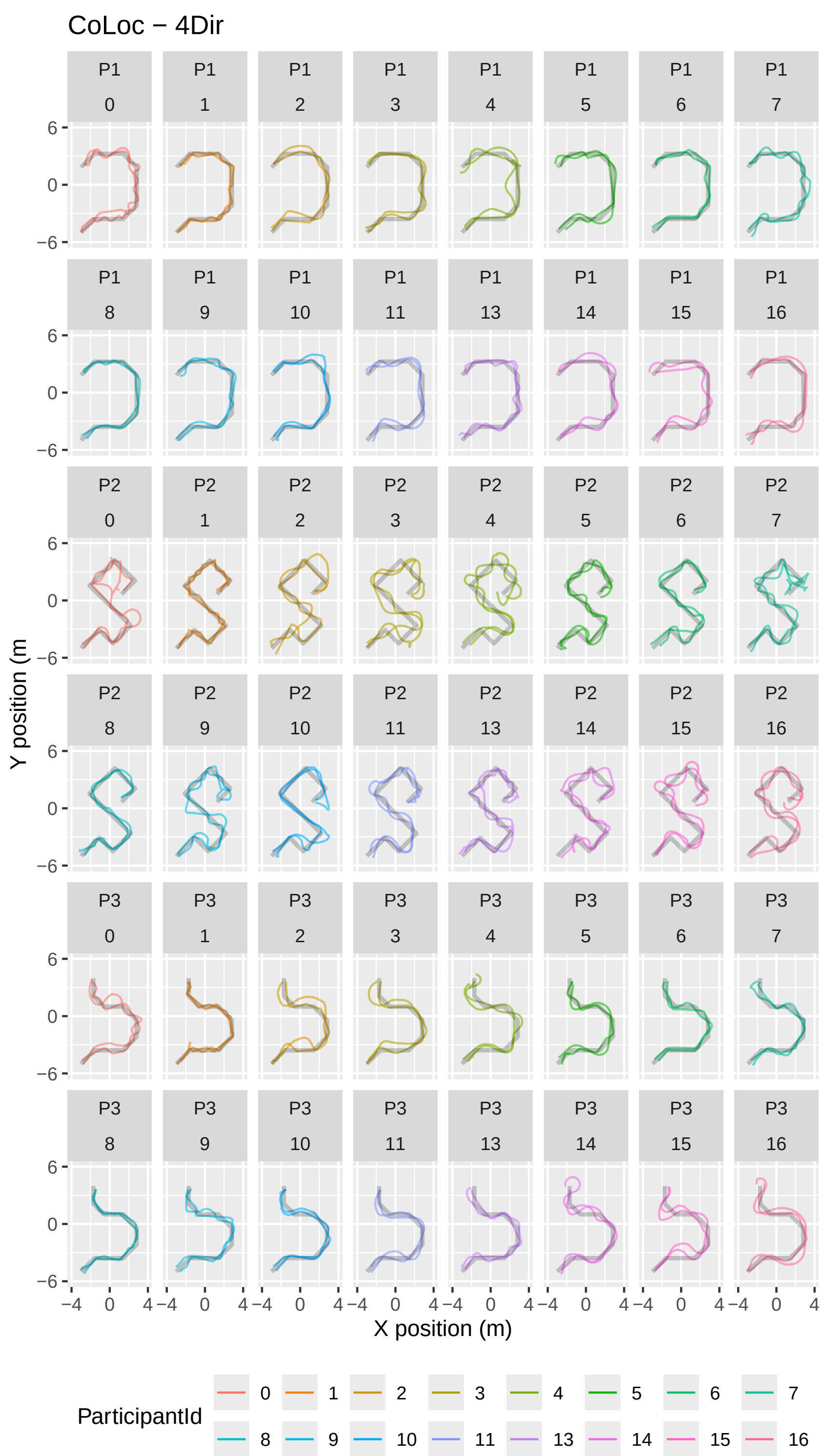

Figure 7.8: Individual trajectories using `4Dir` and `CoLoc`.

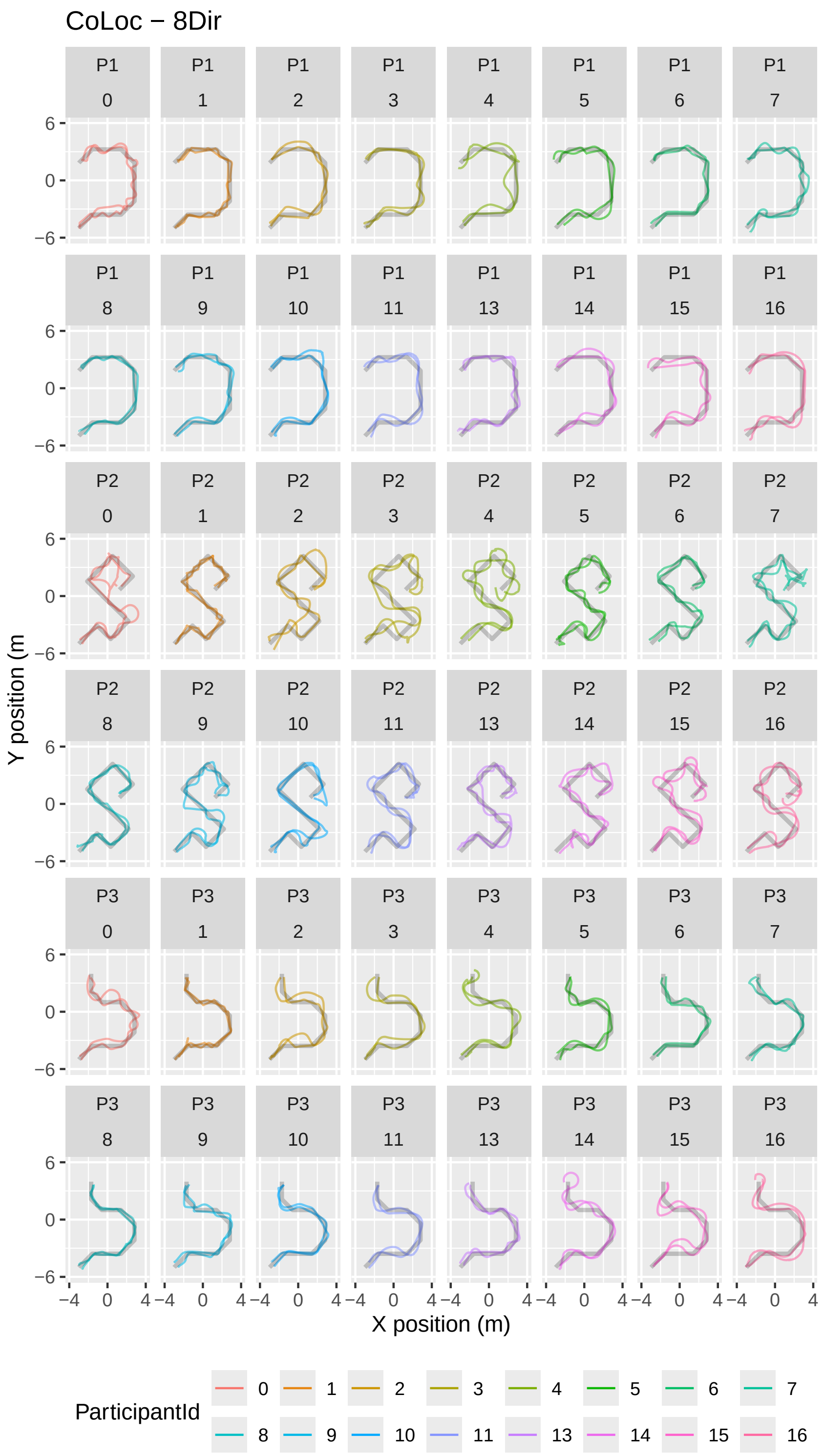

Figure 7.9: Individual trajectories using `8Dir` and `CoLoc`.

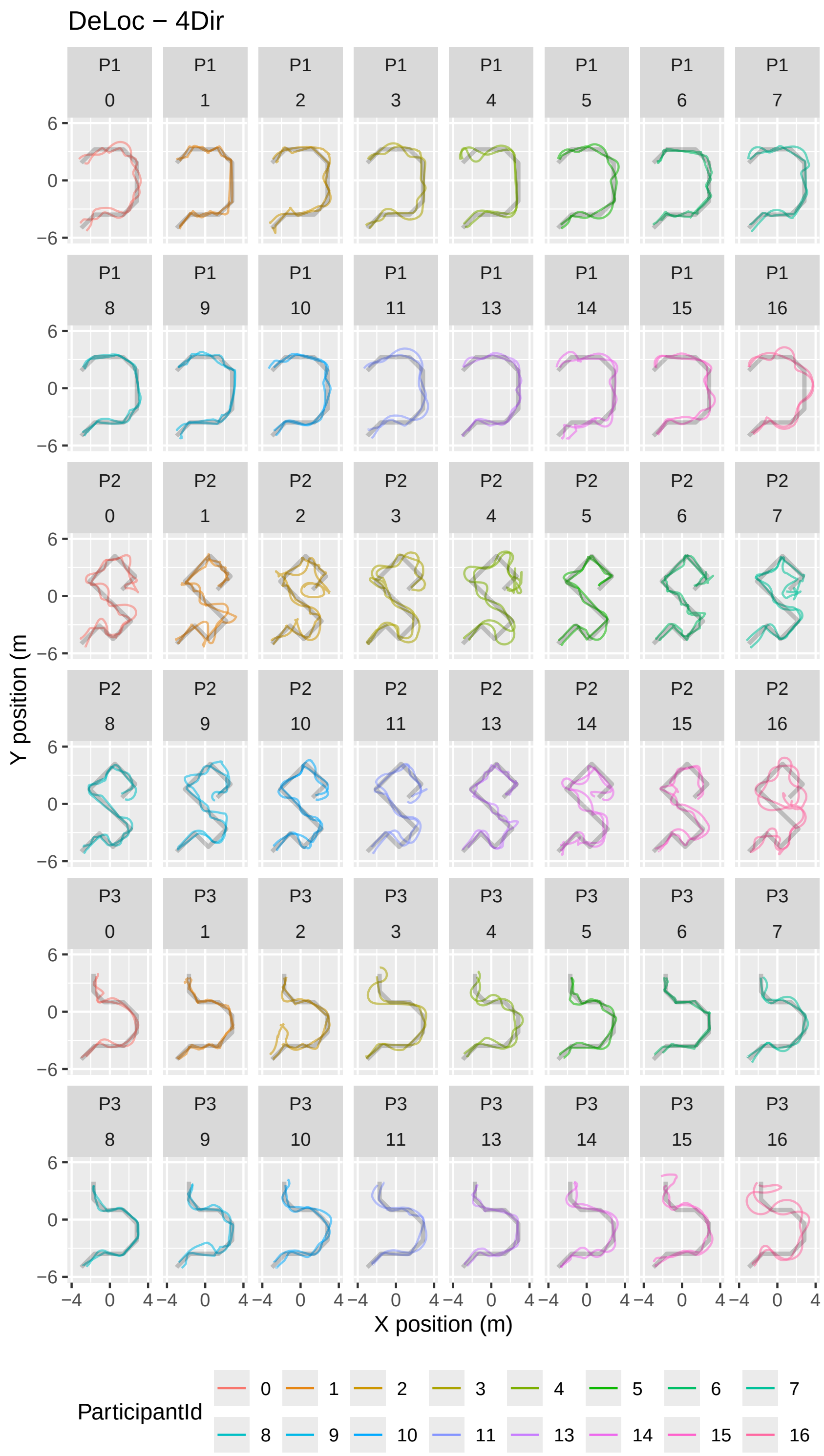

Figure 7.10: Individual trajectories using `4Dir` and `DeLoc`.

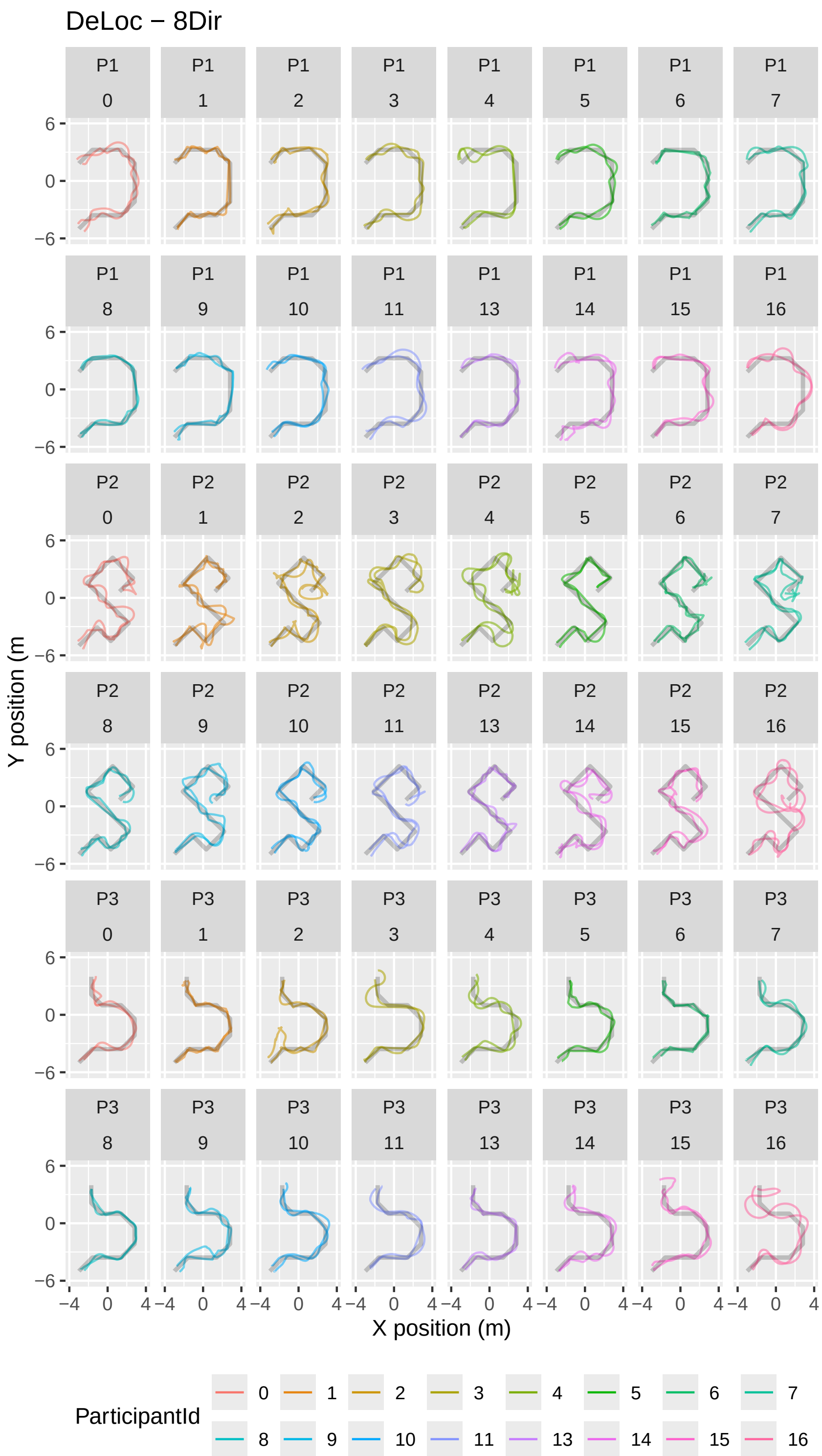

Figure 7.11: Individual trajectories using `8Dir` and `DeLoc`.

TRAJECTORIES - POWER WHEELCHAIR NAVIGATION WITH REGULAR USERS

In this appendix are presented the individual trajectories of participants in the pilot study conducted with regular power wheelchair users covered in chapter 6. Participants used the haptic handle with the `Attractive` guidance strategy and two rendering schemes (`4Dir` and `8Dir`) which guided them along three target paths (`P1`, `P2` and `P3`).

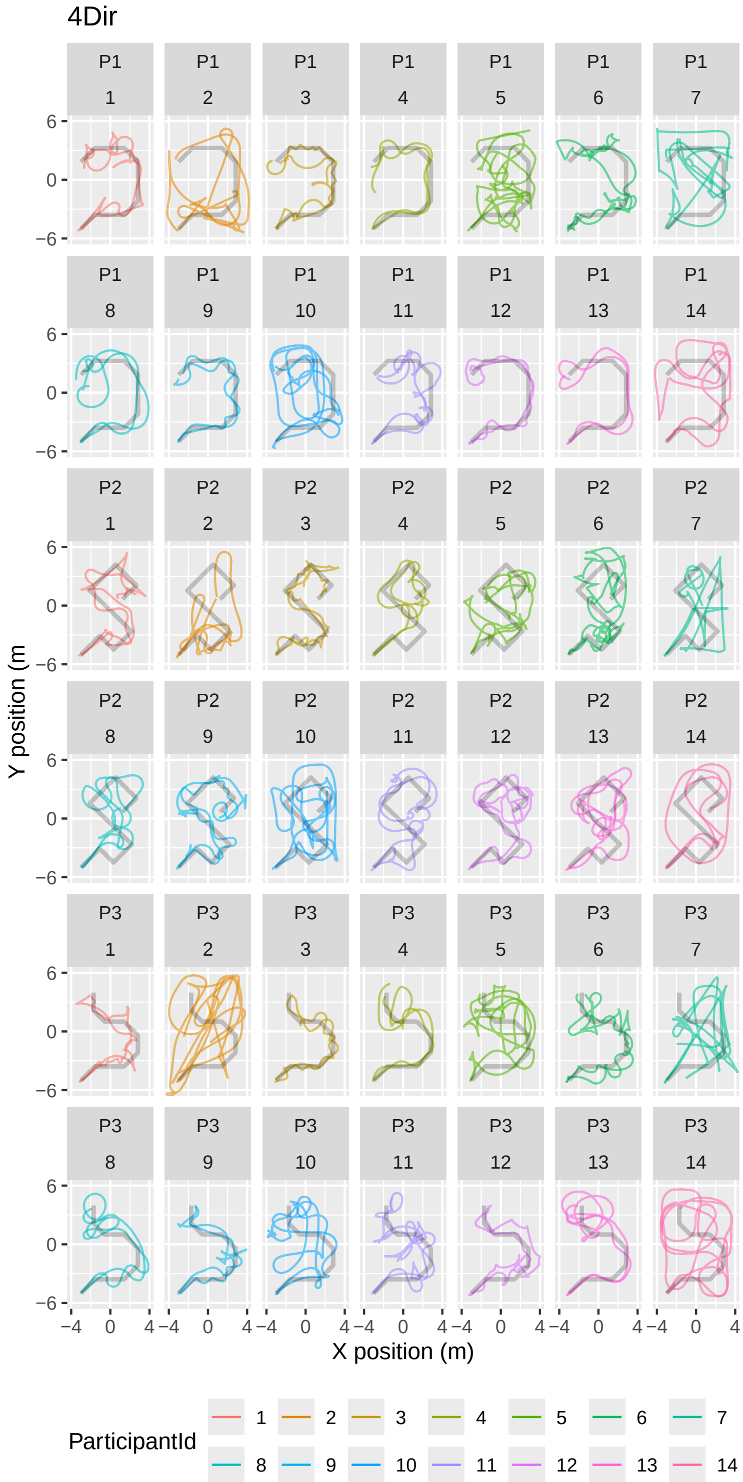

Figure 7.12: Individual trajectories using `4Dir`.

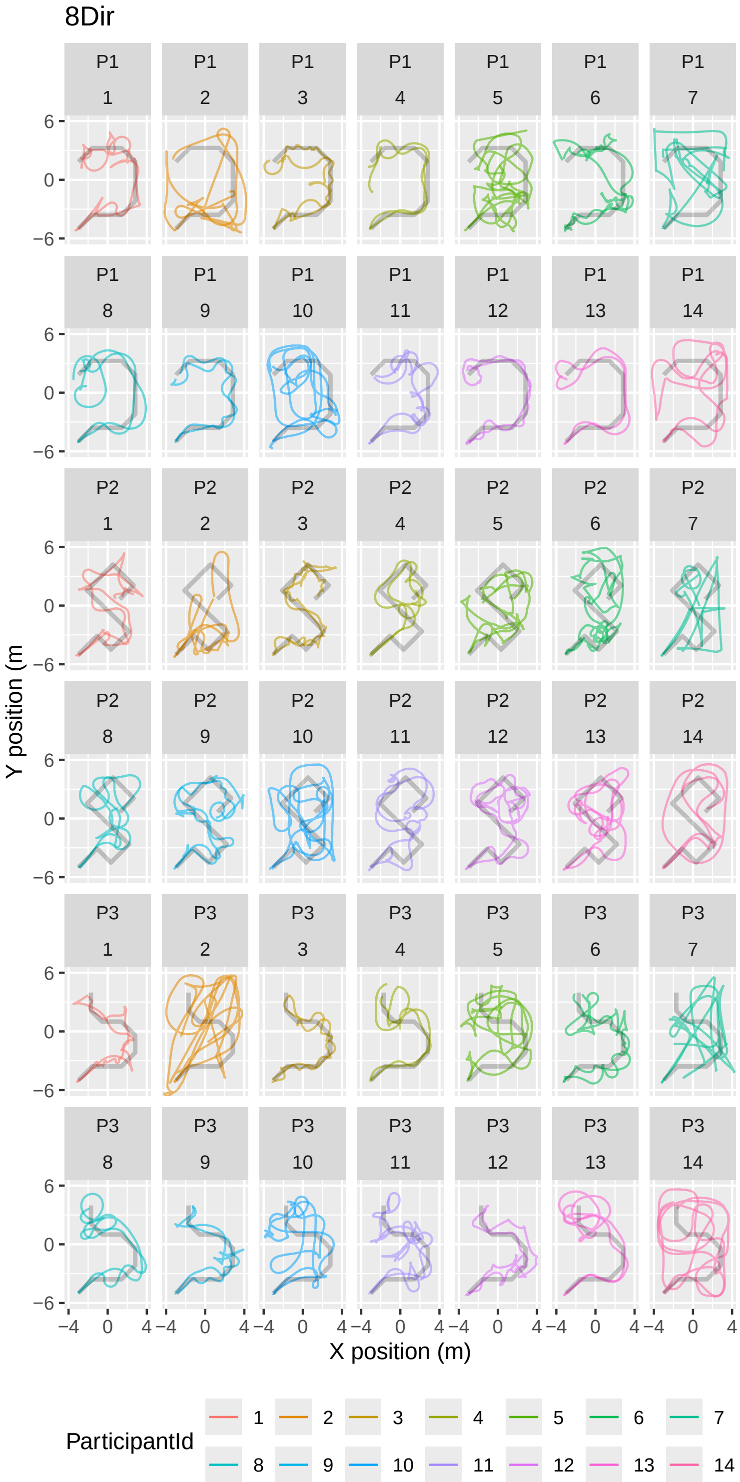

Figure 7.13: Individual trajectories using `8Dir`.

RÉSUMÉ LONG EN FRANÇAIS

Ce manuscrit présente les recherches menées dans le cadre de la thèse de doctorat intitulée « Conception de dispositifs haptiques multi-actionneurs et de méthodes de rendu pour la navigation et les interactions virtuelles ». Cette thèse vise à étudier l'utilisation de l'haptique dans des interfaces portatives comme moyen de fournir aux utilisateurs des sensations plus riches et informatives. En particulier, notre travail se concentre sur les interfaces vibrotactiles multi-actionneurs, conçues pour fournir des sensations localisées. Ces interfaces peuvent être utiles dans des applications telles que l'aide à la navigation et les interactions en réalité virtuelle.

Contexte

Assistance haptique à la navigation

La navigation fait partie de notre vie quotidienne, qu'il s'agisse de s'orienter dans une ville, une rue ou un bâtiment. Il s'agit d'une tâche complexe, mêlant la perception de notre environnement direct pour éviter en toute sécurité les obstacles et les dangers, et une perception plus globale pour planifier un itinéraire efficace vers un objectif. Dans la plupart des cas, il s'agit d'une tâche que les individus peuvent accomplir sans charge cognitive trop élevée.

Cependant, dans des environnements inconnus, nous avons le plus souvent besoin d'aide pour naviguer efficacement. Les systèmes actuels de navigation basés GPS sont les plus courants, que ce soit pour les piétons ou les véhicules. Ces systèmes fournissent généralement un retour d'information visuel et/ou auditif pour guider les utilisateurs. Toutefois, ces solutions peuvent être inadaptées ou inaccessibles dans certaines conditions, notamment pour les personnes souffrant de déficiences visuelles, cognitives ou de mobilité. Ainsi, les modalités visuelles ou sonores peuvent être inappropriées, ou peuvent déjà être utilisées pour d'autres tâches. Dans ce cas, la surcharge de ces canaux sensoriels pourrait être évitée en utilisant une autre modalité de retour d'information. De même, les personnes handicapées ou les utilisateurs de dispositifs d'aide à la mobilité peuvent rencontrer des difficultés pour progresser dans des environnements encombrés ou surpeuplés.

Pour ces raisons, l'utilisation de l'haptique a été proposée comme modalité alternative pour transmettre des informations de navigation. Les interfaces haptiques destinées à ce type d'application se présentent sous différentes formes, chacune avec ses propres avantages. Elles peuvent être intégrées dans des dispositifs existants, tels que des cannes blanches ou des smartphones, être des interfaces portables, comme des gilets ou des bracelets, ou bien des dispositifs portatifs autonomes.

Améliorer le rendu haptique des interactions en réalité virtuelle

La réalité virtuelle peut être définie comme un ensemble de technologies qui permettent de simuler des environnements virtuels dans lesquels les utilisateurs peuvent être immergés et interagir [Fuchs 2006]. Dans le contexte de cette thèse, nous nous concentrons sur l'utilisation de casques de réalité virtuelle, qui sont aujourd'hui le moyen le plus courant de vivre des expériences immersives de réalité virtuelle. Ces écrans fournissent un retour d'information visuel et sonore et ont été combinés à divers dispositifs haptiques au fil des ans. Cependant, le retour haptique en réalité virtuelle est souvent axé sur un nombre limité d'interactions ou de sensations [Culbertson 2018], et la conception de dispositifs capables de produire des sensations riches et réalistes dans une variété d'interactions est un développement relativement récent dans le domaine [Wang 2020].

Les développements de la dernière génération de consoles de jeu vidéo montrent également un intérêt pour un meilleur retour haptique. Par exemple, la Nintendo Switch et la Playstation 5 ont abandonné les actionneurs habituellement utilisés dans les manettes de jeu et ont opté pour l'utilisation d'actionneurs capables de fournir des sensations plus variées, ou sur l'utilisation de multiples actionneurs pour fournir des sensations localisées.

Le projet Dornell

Cette thèse s'inscrit dans le cadre du projet Dornell, financé par l'Inria. Le projet est une collaboration entre des équipes Inria de Rennes, Paris, Bordeaux et Nancy, l'Institut des Systèmes Intelligents et de Robotique (ISIR), l'Institut des jeunes aveugles - Les Charmettes, et le Pôle de Médecine Physique et de Réadaptation St Hélier. Le projet Dornell comporte de multiples objectifs, le but principal étant de créer une poignée haptique multisensorielle et personnalisable pour aider les utilisateurs de dispositifs d'assistance à la mobilité dans leurs tâches de navigation. La poignée pourrait par exemple fournir un guidage ou aider à éviter les obstacles. Pour ce faire, le projet explore l'utilisation de modalités sensorielles multiples pour fournir des informations, en concevant des poignées qui peuvent être adaptées sur différents dispositifs d'aide à la mobilité, comme des fauteuils roulants ou des déambulateurs (voir Figure 7.14). L'utilisation de matériaux innovants et de techniques d'impression 3D est également explorée, afin de créer des poignées personnalisables avec des capteurs intégrés qui pourront détecter les intentions ou le statut des utilisateurs.

Dans le cadre de ce projet, notre recherche porte sur la conception d'une poignée qui fournirait des sensations localisées, et sur les façons dont ces sensations pourraient être utilisées pour fournir des informations de navigation. Pour ce faire, nous utilisons la réalité virtuelle pour expérimenter avec le retour haptique multi-actionneurs, et comme plateforme pour expérimenter avec l'utilisation d'une poignée haptique pour naviguer dans des environnements virtuels.

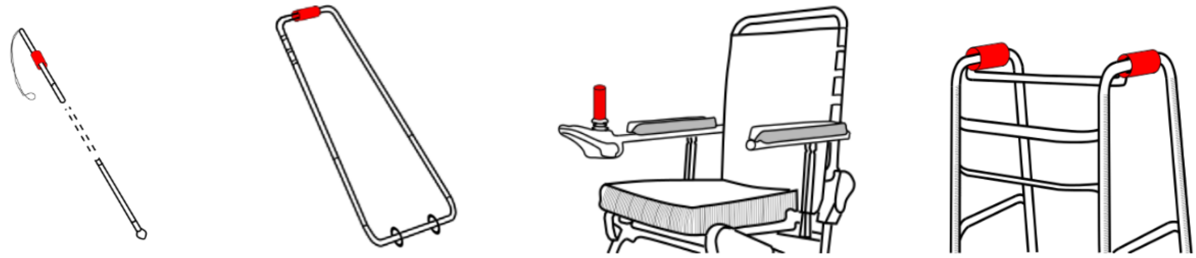

Figure 7.14: L'objectif du projet Dornell est la conception d'une poignée haptique qui pourrait s'adapter à divers dispositifs d'assistance à la mobilité existants, tels qu'une canne blanche, une précanne, un fauteuil roulant électrique ou un déambulateur. Cette poignée offrirait un retour haptique personnalisé pour fournir un ensemble d'informations aidant à la navigation, comme la distance par rapport aux obstacles ou la direction à prendre.

Les objectifs de cette thèse sont les suivants. Premièrement, elle vise à concevoir et à développer des dispositifs capables de fournir des sensations précises et localisées dans la main de l'utilisateur. Deuxièmement, elle cherche à créer de nouvelles méthodes de rendu qui exploitent efficacement ces sensations localisées, permettant un retour d'information plus immersif et plus intuitif dans diverses applications. Enfin, la thèse explore l'application de ces dispositifs pour la navigation, en étudiant la manière dont ils peuvent fournir des informations de guidage ou de détection d'obstacles.

Challenges scientifiques et contributions

Challenges scientifiques

Dans le cadre de cette thèse, nous avons identifié trois défis scientifiques sous-jacents, à l'interface entre l'haptique, la réalité virtuelle et la navigation. Ces défis portent sur la conception d'interfaces portatives offrant des sensations haptiques améliorées. Celles-ci pourraient bénéficier à la fois aux interactions en réalité virtuelle et à l'assistance à la navigation, à condition que des techniques de rendu capables d'exploiter ces sensations soient développées.

I. Offrir un retour haptique amélioré dans les interfaces portatives. Étant donné la complexité et l'étendue du sens du toucher, les interfaces haptiques se concentrent sur la stimulation d'une zone limitée du corps, ainsi que sur un ensemble spécifique de sensations à fournir. Dans le cas des interfaces portatives, elles ciblent une petite zone du corps qui est aussi extrêmement sensible. Offrir des sensations haptiques plus riches constitue un défi pour ce type d'appareil du fait de leur taille limitée. Il existe plusieurs approches pour relever ce défi. Du côté matériel, de nouveaux dispositifs peuvent être créés en explorant des combinaisons d'actionneurs qui fournissent des sensations complémentaires pour un retour multisensoriel, ou en concevant des interfaces haptiques avec une plus grande résolution, avec des actionneurs plus nombreux ou de plus grandes capacités de rendu. Les algorithmes contrôlant ces actionneurs peuvent également tirer parti de notre perception tactile pour créer des sensations plus riches, par exemple en exploitant les illusions sensorielles pour simuler un plus grand nombre de points de stimulation ou pour créer des sensations de mouvement.

II. Concevoir des interactions multisensorielles en réalité virtuelle. Avec le développement de nouveaux dispositifs haptiques, il devient nécessaire de concevoir des techniques de rendu qui exploitent pleinement leurs capacités. Lorsque l'on manipule un objet dans un environnement virtuel, par exemple, des algorithmes doivent être créés pour générer des sensations haptiques basées sur les interactions de l'utilisateur et les propriétés physiques de l'objet. Ces sensations doivent être générées de manière fluide et réaliste pour améliorer l'expérience utilisateur. Pour les interactions multisensorielles, cela est particulièrement difficile, car chaque modalité de retour doit être modélisée de manière appropriée. Dans ce cas, la synchronisation des différentes modalités de retour est également cruciale. Au-delà des interactions physiques, les dispositifs haptiques peuvent également être utilisés pour transmettre des informations plus abstraites. Par exemple, le retour haptique pourrait être utilisé pour guider l'attention de l'utilisateur ou pour communiquer des données complexes de manière innovante. À mesure que de nouvelles méthodes de rendu sont créées, elles doivent aussi être évaluées, que ce soit en termes de réalisme, de performance ou d'immersion. Évaluer leur impact sur l'expérience utilisateur garantira qu'elles apportent des avantages dans des applications pratiques.

III. Développer des solutions d'assistance à la navigation haptique accessibles, intuitives et personnalisées. Des dispositifs de navigation haptique ont été développés au fil des ans, généralement destinés à des groupes spécifiques d'individus. Ces interfaces ont chacune leur propre manière de communiquer des informations via l'haptique, auquel les utilisateurs doivent s'adapter et apprendre à utiliser. Pour être facilement utilisables par un grand nombre d'utilisateurs, les dispositifs de navigation haptique devraient être personnalisables. Premièrement, l'interface devrait s'adapter physiquement aux utilisateurs en tenant compte de leur morphologie (par exemple, la taille ou la forme de la main pour les interfaces portatives) et du contexte d'utilisation, comme lorsqu'elles sont utilisées en combinaison avec des dispositifs d'aide à la mobilité existants. Deuxièmement, les sensations haptiques devraient également s'adapter aux utilisateurs en étant personnalisables, leur permettant de choisir quelles informations sont fournies, ainsi que la manière et le moment où elles le sont. Pour ce faire, la conception de différentes techniques de navigation doit être explorée afin de déterminer lesquelles sont efficaces, si elles peuvent être personnalisées, et dans quelle mesure cela est possible.

Contributions et plan

Notre recherche s'articule autour de trois axes, ciblant des objectifs plus spécifiques en lien avec ces trois défis. Nos principales contributions, qui se situent dans ces axes, sont résumées ici.

Axe 1 : Conception d'une interface portative multi-actionneurs. Dans cet axe, nous explorons l'utilisation de multiples actionneurs vibrotactiles dans les interfaces portatives. Nous commençons par étudier la combinaison d'objets tangibles (c'est-à-dire des objets physiques passifs utilisés pour représenter des objets virtuels) avec un nombre variable d'actionneurs vibrotactiles. Grâce à ces prototypes, nous évaluons la faisabilité et les limites de cette approche, en évaluant combien de points de vibration peuvent être stimulées et avec combien d'actionneurs (C1). La propagation des vibrations limitant la clarté du retour haptique fourni par les interfaces vibrotactiles, nous proposons ensuite d'utiliser l'impression 3D de matériaux souples pour créer une structure isolante dans une poignée (C4).

Axe 2 : Conception d'interactions haptiques en réalité virtuelle basées sur le retour multi-actionneurs. Dans ce deuxième axe, nous explorons l'utilisation des prototypes vibrotactiles multi-actionneurs que nous avons développés afin de fournir des sensations plus riches en réalité virtuelle. Nous examinons les avantages de méthodes de rendu multi-actionneurs en combinaison avec des objets tangibles dans un ensemble de tâches de manipulation en réalité virtuelle (C2). Nous approfondissons également le rendu des impacts, en utilisant des vibrations localisées pour fournir aux utilisateurs des informations plus détaillées sur la direction et la distance d'impacts (C3).

Axe 3 : Navigation à l'aide d'une poignée haptique multi-actionneurs. Dans le cadre de ce troisième axe, nous nous concentrons sur l'utilisation de notre poignée haptique isolée dans des applications de navigation. Nous commençons par étudier son utilisation pour fournir une représentation spatiale des obstacles autour de l'utilisateur dans un environnement virtuel (C5). Nous proposons ensuite un ensemble de techniques de navigation basées sur des vibrotactiles localisés pour guider les utilisateurs en marchant (C6). Dans un effort d'intégration de la poignée avec un fauteuil roulant électrique, nous examinons l'impact de la localisation du retour haptique entre la main dominante utilisée pour conduire et la main non-dominante libre (C7). Enfin, nous menons une étude pilote avec des utilisateurs de fauteuils roulants électriques, évaluant l'impact de notre système de navigation sur la conduite ainsi que sa facilité d'utilisation et son acceptabilité (C8).

Le reste de ce manuscrit s'articule autour de ces contributions.

Le **Chapitre 1** présente d'abord l'état de l'art sur la conception et l'utilisation des dispositifs haptiques pour la réalité virtuelle (VR) et la navigation. Après un aperçu de l'haptique en général, l'utilisation de l'haptique pour la navigation est discutée, en passant en revue une sélection de dispositifs conçus pour cette application, tant pour les piétons que pour les utilisateurs d'aides à la mobilité. Ensuite, nous abordons le retour haptique pour les interactions en réalité virtuelle, en présentant les différentes propriétés ou informations que l'haptique peut fournir dans les environnements virtuels. Enfin, nous approfondissons les dispositifs haptiques multi-actionneurs, en nous concentrant sur la conception d'interface portatives permettant de fournir des sensations localisées.

Les chapitres suivants sont divisés en deux parties. D'abord, la **Partie I** se concentre sur la conception d'interfaces vibrotactiles multi-actionneurs et sur les méthodes de rendu associées.

Dans le **Chapitre 2**, nous explorons la combinaison d'objets tangibles avec un nombre variable d'actionneurs vibrotactiles pour fournir des retours plus riches en réalité virtuelle. Nous étudions l'utilisation de jusqu'à cinq actionneurs dans un objet sphérique pour des tâches de manipulation, en évaluant la capacité des utilisateurs à discriminer les sensations localisées à travers des études utilisateurs. Ensuite, nous proposons un ensemble de méthodes de rendu pour diverses interactions en VR, et évaluons leurs avantages par rapport au retour haptique monolithique habituellement utilisé. Enfin, nous évaluons plus en détail cette approche avec une poignée à deux actionneurs pour fournir de meilleures sensations d'impacts.

Le **Chapitre 3** poursuit notre investigation du retour multi-actionneurs, cette fois avec pour objectif de fournir des vibrations localisées plus nettes et distinctes en main. Après une discussion des itérations de conception du dispositif, nous présentons une structure déformable imprimée en 3D pour isoler les vibrations de quatre moteurs autour d'une poignée. Nous évaluons les avantages de cette conception dans une étude de vibrométrie, en comparant la version proposée à une structure rigide. Deux études de perception sont également réalisées pour évaluer la perception distincte des vibrations par les utilisateurs et le rendu de sensations directionnelles.

La **Partie II** aborde ensuite l'utilisation de notre poignée haptique isolée, en se concentrant sur son utilisation pour la navigation.

Dans le **Chapitre 4**, nous proposons d'augmenter la perception de l'environement de l'utilisateur en réalité virtuelle à l'aide d'une représentation haptique de son environnement proche. À travers deux études utilisateurs, nous évaluons l'utilisation de deux types de sensations haptiques, en évaluant leur capacité à aider l'utilisateur à éviter des obstacles dynamiques, et en mesurant l'influence de cette représentation haptique de l'espace personnel sur l'évitement d'obstacles statiques.

Le **Chapitre 5** présente la conception et l'évaluation expérimentale de techniques de rendu haptique pour la navigation, utilisant les sensations localisés fournis par notre poignée haptique. Nous présentons deux méthodes de rendu haptique combinées à trois stratégies de navigation que nous évaluons dans une étude utilisateur où des participants sont guidés le long de tracés prédéfinis. Dans un effort d'intégration de notre interface haptique avec des aides à la mobilité existantes, nous évaluons son utilisation pour la navigation avec un fauteuil roulant électrique. En particulier, nous étudions l'effet de la colocalisation du retour haptique avec le joystick qui contrôle le fauteuil roulant, en comparant la performance de navigation avec la délocalisation de la poignée haptique dans la main non dominante.

Dans le **Chapitre 6**, nous évaluons l'utilisation et l'acceptation de notre système de guidage haptique lors d'une étude avec des utilisateurs réguliers de fauteuils roulants électriques, en collaboration avec des cliniciens du centre de rééducation du Pôle Saint Hélier à Rennes. Nous évaluons l'utilisation de deux méthodes de rendu dans une série de deux expériences, en évaluant la perception des retours fournis par la poignée haptique dans une tâche statique et leur utilisation dans une tâche de navigation dynamique.

Enfin, le **Chapitre 7** conclut ce manuscrit en résumant nos résultats et en discutant des perspectives pour des travaux futurs.

COLLEGE DOCTORAL BRETAGNE
MATHS, TELECOMS INFORMATIQUE, SIGNAL SYSTEMES, ELECTRONIQUE

INSA INSTITUT NATIONAL DES SCIENCES APPLIQUÉES RENNES

Titre : Conception de dispositifs haptiques multi-actionneurs et de méthodes de rendu pour la navigation et les interactions virtuelles

Mot clés : Haptique, Navigation, Réalité Virtuelle

Résumé : Naviguer dans des environnements complexes ou peu familiers constitue un défi quotidien, en particulier pour les personnes en situation de handicap. Les dispositifs haptiques offrent une solution prometteuse en fournissant un retour sensoriel pour une navigation sûre et efficace. Afin de fournir des informations plus riches et intuitives par le biais du retour haptique, cette thèse s'intéresse aux dispositifs haptiques portables multi-actionneurs, en particulier pour générer des sensations de vibrations localisées. Dans un premier temps, les sensations que de tels dispositifs peuvent procurer sont évaluées en développant des prototypes en réalité virtuelle. Ce faisant, l'utilisation et la pertinence des sensations haptiques localisées pour les interactions en réalité virtuelle sont aussi étudiées. La conception d'une poignée haptique à actionneurs multiples est aussi proposée, utilisant l'impression 3D de matériaux flexibles pour mieux isoler les différentes sources de vibrations. Cette poignée et les sensations localisées qu'elle fournit sont ensuite utilisées pour communiquer diverses informations de navigation, concernant l'environnement des utilisateurs et leur destination. Enfin, l'utilisation de cette poignée en combinaison avec un fauteuil roulant électrique est étudiée, notamment au travers d'études avec des usagers en situations de handicap. Ainsi, cette thèse ouvre des perspectives pour la conception, et peut être l'utilisation future, de nouveau dispositifs d'assistance à la navigation.

Title: Design of multi-actuator haptic devices and rendering methods for navigation and virtual interactions

Keywords: Haptics, Navigation, Virtual Reality

Abstract: Navigating complex or unfamiliar environments presents daily challenges, particularly for individuals with disabilities. Haptic devices offer a promising solution by providing sensory feedback for safe and efficient navigation. In order to provide more rich and intuitive information through haptic feedback, this thesis explores the design and use of handheld multi-actuator haptic devices, in particular to display localized vibration sensations. We first explored the sensations that such devices could provide through the design of prototypes in virtual reality. Doing so, we also investigated the use and relevance of localized haptic sensations for VR interactions. We then looked into the design of a multi-actuator haptic handle, using 3D printing of flexible materials to isolate the different vibration sources. This handle and the localized sensations it provides were then used to communicate various navigational information about the user's environment and destination. Finally, we investigated the use of this handle in combination with a power wheelchair, concluding our work with a pilot study involving regular power wheelchair users. This thesis therefore opens up perspectives for the design, and perhaps future use, of new navigation assistance devices.